STRUCTURE AND BONDING 137

Series Editor D. M. P. Mingos
Volume Editor Peter W. Roesky

Molecular Catalysis of Rare-Earth Elements

Springer

137

Structure and Bonding

Series Editor: D. M. P. Mingos

For further volumes:
http://www.springer.com/series/430

Structure and Bonding

Series Editor: D. M. P. Mingos

Recently Published and Forthcoming Volumes

Molecular Catalysis of Rare-Earth Elements
Volume Editor: Peter W. Roesky
Vol. 137, 2010

Metal-Metal Bonding
Volume Editor: Gerard Parkin
Vol. 136, 2010

Functional Phthalocyanine Molecular Materials
Volume Editor: Jianzhuang Jiang
Vol. 135, 2010

Data Mining in Crystallography
Volume Editors: Hofmann, D. W. M., Kuleshova, L. N.
Vol. 134, 2010

Controlled Assembly and Modification of Inorganic Systems
Volume Editor: Wu, X.- T.
Vol. 133, 2009

Molecular Networks
Volume Editor: Hosseini, M. W.
Vol. 132, 2009

Molecular Thermodynamics of Complex Systems
Volume Editors: Lu, X., Hu, Y.
Vol. 131, 2009

Contemporary Metal Boron Chemistry I
Volume Editors: Marder, T. B., Lin, Z.
Vol. 130, 2008

Recognition of Anions
Volume Editor: Vilar, R.
Vol. 129, 2008

Liquid Crystalline Functional Assemblies and Their Supramolecular Structures
Volume Editor: Kato, T.
Vol. 128, 2008

Organometallic and Coordination Chemistry of the Actinides
Volume Editor: Albrecht-Schmitt, T. E.
Vol. 127, 2008

Halogen Bonding
Fundamentals and Applications
Volume Editors: Metrangolo, P., Resnati, G.
Vol. 126, 2008

High Energy Density Materials
Volume Editor: Klapötke, T. H.
Vol. 125, 2007

Ferro- and Antiferroelectricity
Volume Editors: Dalal, N. S., Bussmann-Holder, A.
Vol. 124, 2007

Photofunctional Transition Metal Complexes
Volume Editor: V. W. W. Yam
Vol. 123, 2007

Single-Molecule Magnets and Related Phenomena
Volume Editor: Winpenny, R.
Vol. 122, 2006

Non-Covalent Multi-Porphyrin Assemblies
Synthesis and Properties
Volume Editor: Alessio, E.
Vol. 121, 2006

Recent Developments in Mercury Science
Volume Editor: Atwood, David A.
Vol. 120, 2006

Layered Double Hydroxides
Volume Editors: Duan, X., Evans, D. G.
Vol. 119, 2005

Molecular Catalysis of Rare-Earth Elements

Volume Editor: Peter W. Roesky

With contributions by

D. Cui · F.T. Edelmann · K.C. Hultzsch · J. Jenter · T. Li · B. Liu · A.L. Reznichenko · P.W. Roesky · B. Wang · Y. Yang · Z. Zhang

Springer

Prof. Dr. Peter W. Roesky
Institute of Inorganic Chemistry
Karlsruhe Institute of Technology (KIT)
Bldg. 30.45, Engesserstr. 15
76131 Karlsruhe
Germany
roesky@kit.edu

ISSN 0081-5993 e-ISSN 1616-8550
ISBN 978-3-642-12810-3 e-ISBN 978-3-642-12811-0
DOI 10.1007/978-3-642-12811-0
Springer Heidelberg Dordrecht London New York

Library of Congress Control Number: 2010930519

Cover design: KünkelLopka GmbH, Heidelberg, Germany

Printed on acid-free paper

Springer is part of Springer Science+Business Media (www.springer.com)

Series Editor

Prof. D. Michael P. Mingos

Principal
St. Edmund Hall
Oxford OX1 4AR, UK
michael.mingos@st-edmund-hall.oxford.ac.uk

Volume Editors

Prof. Dr. Peter W. Roesky

Institute of Inorganic Chemistry
Karlsruhe Institute of Technology (KIT)
Bldg. 30.45, Engesserstr. 15
76131 Karlsruhe
Germany
roesky@kit.edu

Editorial Board

Structure and Bonding
Also Available Electronically

Structure and Bonding is included in Springer's eBook package *Chemistry and Materials Science.* If a library does not opt for the whole package the book series may be bought on a subscription basis. Also, all back volumes are available electronically.

For all customers who have a standing order to the print version of *Structure and Bonding*, we offer the electronic version via SpringerLink free of charge.

If you do not have access, you can still view the table of contents of each volume and the abstract of each article by going to the SpringerLink homepage, clicking on "Chemistry and Materials Science," under Subject Collection, then "Book Series," under Content Type and finally by selecting *Structure and Bonding.*

You will find information about the

– Editorial Board
– Aims and Scope
– Instructions for Authors
– Sample Contribution

at springer.com using the search function by typing in *Structure and Bonding*.

Color figures are published in full color in the electronic version on SpringerLink.

Aims and Scope

The series *Structure and Bonding* publishes critical reviews on topics of research concerned with chemical structure and bonding. The scope of the series spans the entire Periodic Table and addresses structure and bonding issues associated with all of the elements. It also focuses attention on new and developing areas of modern structural and theoretical chemistry such as nanostructures, molecular electronics, designed molecular solids, surfaces, metal clusters and supramolecular structures. Physical and spectroscopic techniques used to determine, examine and model structures fall within the purview of *Structure and Bonding* to the extent that the focus

is on the scientific results obtained and not on specialist information concerning the techniques themselves. Issues associated with the development of bonding models and generalizations that illuminate the reactivity pathways and rates of chemical processes are also relevant.

The individual volumes in the series are thematic. The goal of each volume is to give the reader, whether at a university or in industry, a comprehensive overview of an area where new insights are emerging that are of interest to a larger scientific audience. Thus each review within the volume critically surveys one aspect of that topic and places it within the context of the volume as a whole. The most significant developments of the last 5 to 10 years should be presented using selected examples to illustrate the principles discussed. A description of the physical basis of the experimental techniques that have been used to provide the primary data may also be appropriate, if it has not been covered in detail elsewhere. The coverage need not be exhaustive in data, but should rather be conceptual, concentrating on the new principles being developed that will allow the reader, who is not a specialist in the area covered, to understand the data presented. Discussion of possible future research directions in the area is welcomed.

Review articles for the individual volumes are invited by the volume editors.

In references *Structure and Bonding* is abbreviated *Struct Bond* and is cited as a journal.

Impact Factor in 2008: 6.511; Section “Chemistry, Inorganic & Nuclear”:
Rank 2 of 40; Section “Chemistry, Physical”: Rank 7 of 113

Dedicated to the memory of Professor Herbert Schumann († 2010), a pioneer of organolanthanide chemistry

Preface

This volume reviews the recent developments in the use of molecular rare-earth metal compounds in catalysis. Most of the applications deal with homogenous catalysis but in some cases, heterogeneous systems are also mentioned. The rare-earth elements, which are the lanthanides and their close relatives – scandium and yttrium – have not been in the focus of molecular chemistry for a long time and therefore have also not been considered as homogenous catalysts. Although the first organometallic compounds of the lanthanides, which are tris(cyclopentadienyl) lanthanide complexes, were already prepared in the 1950s, it was only in the late 1970s and early 1980s when a number of research groups began to focus on this class of compounds. One reason for the development was the availability of single crystal X-ray diffraction techniques, which made it possible to characterize these compounds. Moreover, new laboratory techniques to handle highly air and moisture sensitive compounds were developed at the same time. Concomitant with the accessibility of this new class of compounds, the application in homogenous catalysis was investigated. One of the first applications in this field was the use of lanthanide metallocenes for the catalytic polymerization of ethylene in the early 1980s. In the last two or three decades, a huge number of inorganic and organometallic compounds of the rare-earth elements were synthesized and some of them were also used as catalysts. Although early work in homogenous catalysis basically focused only on the hydrogenation and polymerization of olefins, the scope for catalytic application today is much broader. Thus, a large number of catalytic σ-bond metathesis reactions, e.g. hydroamination, have been reported in the recent years.

This book contains four chapters in which part of the recent development of the use of molecular rare-earth metal compounds in catalysis is covered. To keep the book within the given page limit, not all aspects could be reviewed in detail. For example, the use of molecular rare-earth metal complexes as Lewis acidic catalysts is not discussed in this book. The first two chapters review different catalytic conversions, namely the catalytic σ-bond metathesis (Chapter by Reznichenko and Hultzsch) and the polymerization of 1,3-conjugated dienes (Chapter by Zhang et al.). Within these chapters, different catalytic systems and applications are discussed. The final two chapters are more concentrated on recent developments of

catalysts synthesis; but of course catalytic aspects are also mentioned. Therefore, these two chapters are focused on homogeneous catalysis using lanthanide amidinates and guanidinates (Chapter by Edelmann) and the synthesis of rare-earth metal post-metallocene catalysts with chelating amido ligands (Chapter by Li et al.). The organometallic lanthanide catalysts of the first generation, which are the metallocene catalysts of the general composition $[(\eta^5\text{-}C_5Me_5)_2LnR]$ ($R = CH(SiMe_3)_2$, $N(SiMe_3)_2$, H), are mentioned in the first two chapters, but are not covered in a separate synthetic contribution because a number of excellent reviews on this topic have been published over the recent years.

In summary, the present volume of *Structure and Bonding* shows the substantial activity carried out in recent years in the field of synthesis of inorganic and organometallic rare-earth metal compounds and their use as catalysts for a number of different transformations. The future holds great promise for the rapid growth of this field of chemistry and for new spectacular results.

Karlsruhe *Peter W. Roesky*
June 2010

Contents

Struct Bond (2010) 137: 1–48
DOI:10.1007/430_2010_17

Published online: 11 May 2010

Catalytic σ-Bond Metathesis

Alexander L. Reznichenko and Kai C. Hultzsch

Abstract This account summarizes information on recently reported applications of organo-rare-earth metal complexes in various catalytic transformations of small molecules. The σ-bond metathesis at d^0 rare-earth metal centers plays a pivotal role in carbon–carbon and carbon–heteroatom bond forming processes. Relevant mechanistic details are discussed and the focus of the review lies in practical applications of organo-rare-earth metal complexes.

Keywords: C–H activation · Catalysis · Cyclization · Hydroalkoxylation · Hydroamination · Hydroboration · Hydrogenation · Hydrophosphination · Hydrosilylation · Hydrostannation

Contents

A.L. Reznichenko and K.C. Hultzsch (✉)
Department of Chemistry and Chemical Biology, Rutgers, The State University of New Jersey, 610 Taylor Road, Piscataway, NJ 08854-8087, USA
e-mail: hultzsch@rci.rutgers.edu

1 Introduction

The activation of H_2 [1] and C–H bonds [2] by d^0 early transition metal complexes has been discovered more than three decades ago. It became clear at this point that oxidative addition at the metal center, which is common for late transition metals (1) was not a viable mechanism [3]. More detailed investigations of dihydrogen activation by group I [4] and group IV [5] metals as well as rare-earth metal-mediated C–H activation [6] were supportive of an associative mechanism with a highly organized transition state (2). The so-called σ-bond metathesis involves interaction of the activated σ-bond with a *vacant* orbital at the metal center; therefore, it does not involve a formal change of an oxidation state. Subsequent experimental and theoretical studies are supportive of this mechanism [7–14].

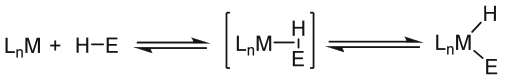

(1)

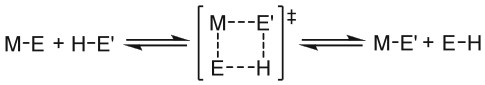

(2)

The reaction in (2) can be seen as a transfer of hydrogen from E′ to E, and the calculation for the degenerative C–H activation exchange of scandocene shows that the four-membered transition state remains kite-shaped [7] with all three groups fully bound to the metal atom (Fig. 1).

As shown in Fig. 2, two different four-membered transition states are possible, giving rise to two sets of products for the same reagents employed. Recent theoretical calculations illustrate that the energy profile of the reaction is sensitive toward the nature of the group being actually transferred. The barrier difference between transfer of H and CH_3 (Fig. 2a) is remarkable (60 kcal mol^{-1}) [15]; however, the silicon group transfer is significantly easier than that of hydrogen (**a**), due to the

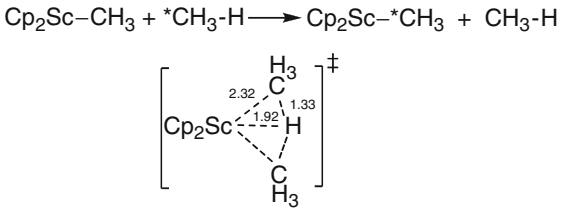

Fig. 1 Methane C–H activation via σ-bond metathesis

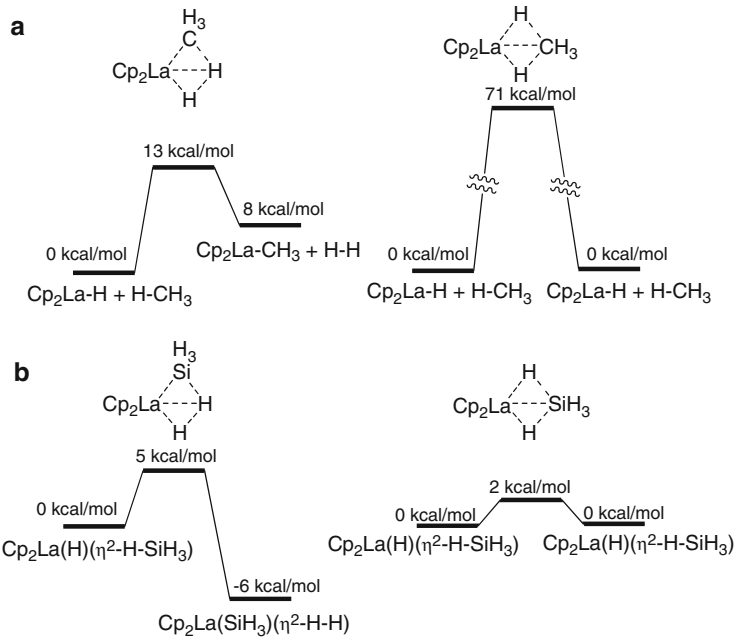

Fig. 2 Free energy (**a**) and relative electronic energies (**b**) for two possible reaction pathways for $Cp_2La\text{-}H + CH_4$ (**a**) and rearrangement of $Cp_2La(H)(H\text{-}SiH_3)$ (**b**) [15, 16]

hypervalent character of silicon (**b**) [16]. In general, activation enthalpies increase when the hydrogen substituents in SiH_4 are successively replaced by alkyl substituents due to the better overlap and polarizability of the hydrogen 1s orbital as compared to the already polarized and directional sp^3 hybrids of CH_3 [17].

The protonation of organo-rare-earth metal species through σ-bond metathesis plays a key role in many catalytic applications described below. The high reactivity of rare-earth metals for insertion of unsaturated carbon–carbon multiple bonds [18], in conjunction with smooth σ-bond metathesis, allows to perform *catalytic* small molecule synthesis. This route is atom efficient, economic, and opens access to nitrogen-, phosphorous-, silicon-, boron-, and other heteroatom-containing molecules. The most important catalytic applications of organo-rare-earth metals involving the σ-bond metathesis process will be discussed in this review.

Catalytic applications of organo-rare-earth metal complexes reported prior to 2002 are summarized in two excellent reviews [19, 20] and, therefore, will not be discussed unless being relevant for understanding of key reaction details. A recent comprehensive review on theoretical analyses of organo-rare-earth metal-mediated catalytic reactions is available [17]. Although σ-bond metathesis plays a pivotal role in many rare-earth metal-catalyzed polymerizations, the discussion of these processes is beyond the scope of this review and the interested reader may consult one of the pertaining reviews [21–24].

2 Catalytic Hydrogenation

Although certain lanthanocenes have demonstrated to be exceptionally reactive in alkene hydrogenation [25], their widespread application was apparently hampered by low functional group tolerance and high air and moisture sensitivity. The general mechanism for a rare-earth metal-catalyzed hydrogenation is shown on Fig. 3.

The key steps of the reaction mechanism are Ln–C bond protonolysis and alkene insertion with the latter being the product-determining step. Turnover frequencies of up to 120,000 h^{-1} were observed (3) [25]. Terminal monosubstituted double bonds generally exhibit higher reactivity and can be reduced selectively even in case of the highly strained norbornene framework (4) [26]. Enantioselective catalytic hydrogenations of a limited set of substrates utilizing C_1-symmetric *ansa*-lanthanocenes (Fig. 4) have been reported to proceed with reasonable enantioselectivities (5) [27]. Hydrogenolysis of a Ln–C bond can be used as a termination step in the well-documented process of catalytic diene carbocyclization [30–32]. Thus, 1,6-heptadienes can be cyclized to afford cyclohexane derivatives using an yttrocene catalyst (6) [31].

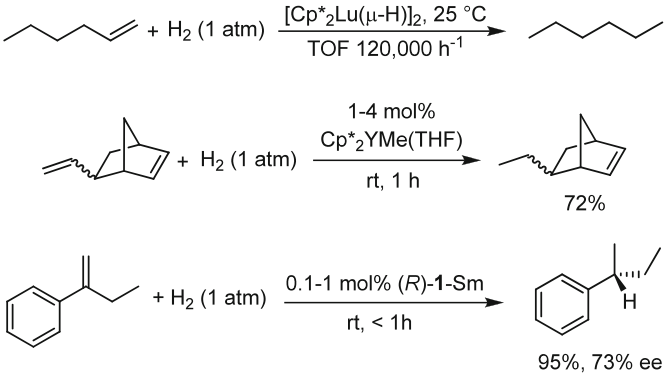

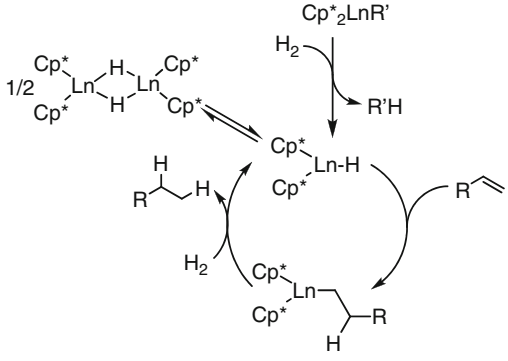

Fig. 3 Organolanthanide-catalyzed alkene hydrogenation

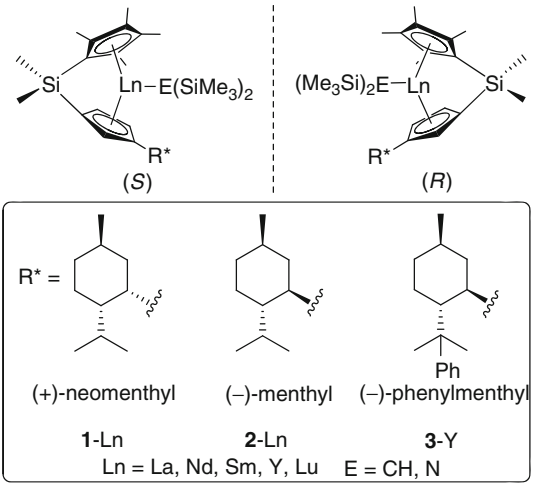

Fig. 4 C_1-symmetric chiral lanthanocene catalysts for asymmetric hydrogenation, hydrosilylation, and hydroamination [27–29]

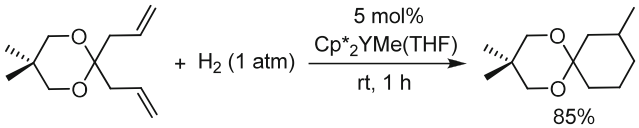

(6)

In general, rare-earth metal-catalyzed hydrogenation has drawn significantly less attention in the last decade; therefore, the interested reader may consult previous reviews for a more comprehensive coverage [19, 20].

3 Catalytic Hydrosilylation

Hydrosilylation, the addition of a Si–H bond across an unsaturated carbon–carbon linkage, is a facile and atom-economical route to organosilanes, which can be functionalized further, for example, using the Tamao or Fleming oxidation protocol [33].

3.1 Hydrosilylation of Alkenes

The mechanism of catalytic hydrosilylation (Fig. 5) is analogous to that of hydrogenation. Key steps are alkene insertion and σ-bond metathesis; with alkene insertion apparently being the product-determining step [29, 34, 35].

Notably, in the absence of the alkene the hydride complex may undergo either degenerative hydrogen scrambling [34] or silylation [36–38], which are competitive processes. Hydrogen exchange is faster; however, silylation is more thermodynamically feasible [16], which opens the route to well-documented rare-earth metal-catalyzed dehydrogenative silane couplings (Fig. 6) [39]. Since the possibility

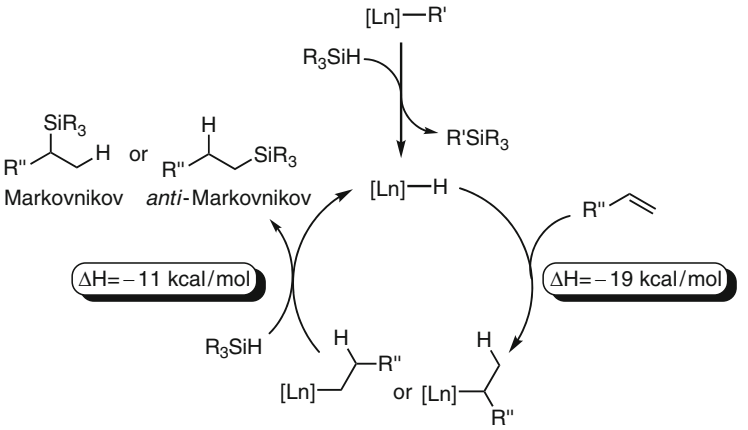

Fig. 5 Catalytic cycle for organo-rare-earth metal-mediated hydrosilylation [29, 34, 35]

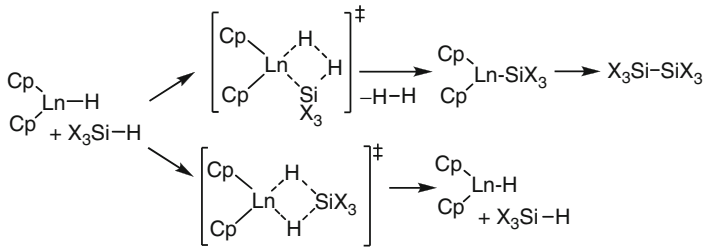

Fig. 6 Hydrogen scrambling (*bottom*) and dehydrogenative silane coupling (*top*) as competing processes between a metal hydride and a silane

of silane dehydrocoupling is not ruled out, the hydrosilylation catalyst should be able to perform both steps, alkene insertion and the desired σ-bond metathesis, fast enough to suppress the unwanted side reaction.

Pioneering preparative reactions have been performed with lanthanocene catalysts [40–43], with yttrium complexes exhibiting the highest reactivities and selectivities in most cases that allow reactions to be performed at ambient temperatures (7) [44].

In general, terminal alkenes typically produce linear silanes with high selectivity (7) and (8), whereas the amount of the branched silane can be increased either by tying the cyclopentadienyl ligands back through an *ansa*-linkage that opens the coordination sphere around the metal center, or by using a larger rare-earth metal [45, 46].

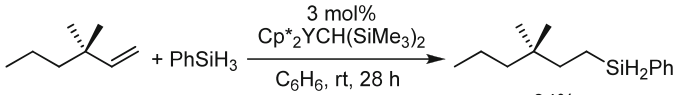

(7)

More substituted double bonds are less reactive, and therefore, regioselective hydrosilylations of dienes are possible (8) and (9) [45]. Yttrocene catalysts are less reactive in case of 1,1-disubstituted alkenes; however, the larger samarocene is better suitable to catalyze this transformation with excellent diastereoselectivity (10) [47].

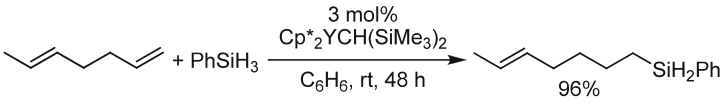

(8)

(9)

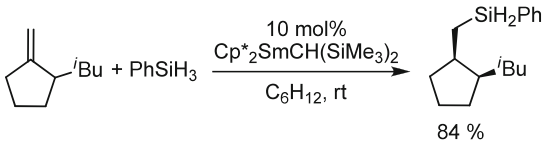

(10)

More recently, postmetallocene catalyst systems, such as constrained-geometry complexes **4–6** (Fig. 7) [48–51], the polymeric (pentamethylcyclopentadienyl)samarium(II) alkyl complex **7** (Fig. 7) [52], and cyclopentadienyl-free

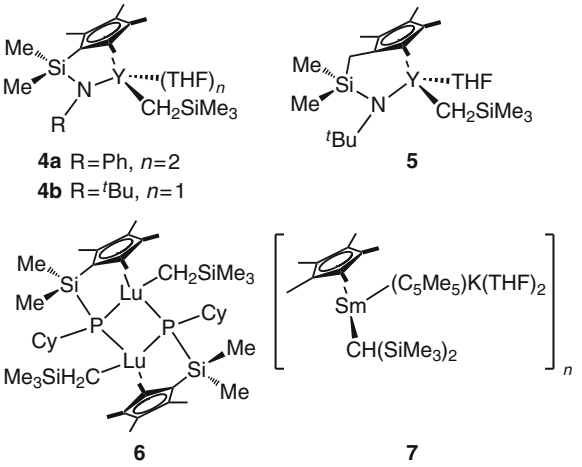

Fig. 7 Cyclopentadienyl-based postmetallocene rare-earth metal-based catalysts for hydrosilylation [48–52]

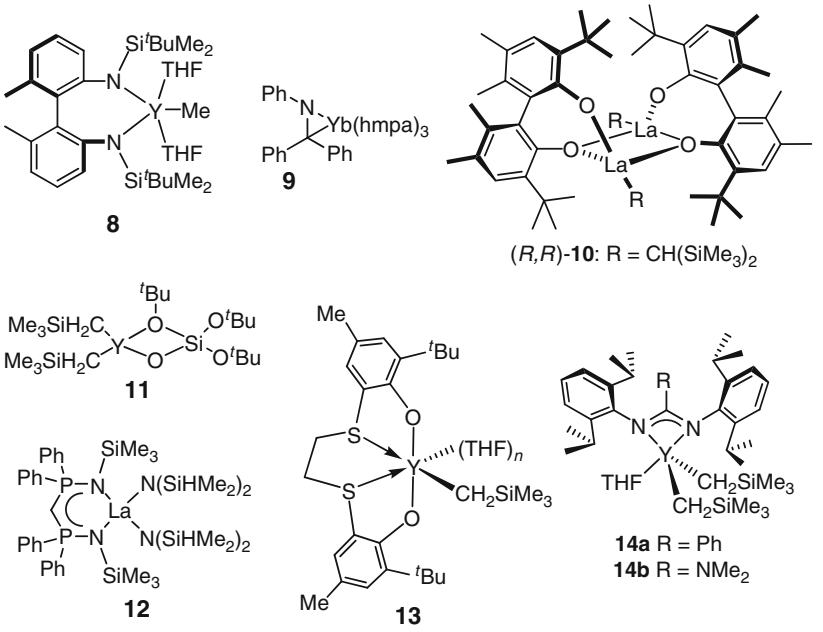

Fig. 8 Cyclopentadienyl-free catalysts for hydrosilylation [53–61]

complexes (Fig. 8) [53–63], have been studied in hydrosilylation reactions, some of which (e.g., **6**, **8**, **14b**) display exceptionally high catalytic activity (Table 1). In general, the postmetallocene catalysts exhibit the same trends as lanthanocenes for reactivity and selectivity in hydrosilylation reactions.

The "less constrained" geometry catalyst **5** displays a higher catalytic activity in the hydrosilylation of 1-decene than the "more constrained" complexes **4** (Table 1) [51]. The reason for this seems to stem from a greater stability of an dimeric hydride intermediate derived from **4**, while the respective dimeric hydride intermediate generated from **5** readily dissociates to form a more reactive monomeric hydride species. However, complex **4b** allows a better regiocontrol than **5** in the hydrosilylation of styrene, as the more open coordination sphere allows more facile 2,1-insertion of styrene. Note, however, that stoichiometric insertion reactions of styrene in the metal–hydride bond give exclusively the 2,1-insertion product [48, 64] due to the aryl-directing effect (see below), indicating that the linear product results from an unobserved 1,2-insertion product.

The readily available homoleptic trisamide complex La{N(SiMe$_3$)$_2$}$_3$ exhibits good reactivity at ambient temperature (11) (Table 1) [62], indicating that sophisticated spectator ligands are not strict requirements to achieve good activity and regioselectivity.

Table 1 Catalytic hydrosilylation of styrene and α-olefins

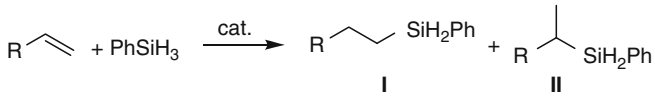

I II

R	Catalyst	[cat.]/[s] (%)	*T* (°C)	*t* (h)	**I:II**	Yield (%) (TOF h^{-1})	References
$^{n}C_8H_{17}$	$Cp^*_2SmR^a$	5	25		11:1	90	[45]
$^{n}C_8H_{17}$	**15**-Sm	5	25		1:2	98	[45]
$^{n}C_4H_9$	$La(NR'_2)_3{}^b$	3	25	40	96:4	98	[62]
$^{n}C_8H_{17}$	**4a**	5	25		100:0	(4.0)	[51]
$^{n}C_8H_{17}$	**4b**	5	25		100:0	(2.9)	[51]
$^{n}C_8H_{17}$	**5**	5	25		100:0	(20.0)	[51]
$^{n}C_8H_{17}$	**6**	2.5	25	0.17	100:0	100	[49]
$^{n}C_8H_{17}$	**7**	2	25	72	95:5	95	[52]
$^{n}C_4H_9$	**8**	5	25	0.17	92:8	80	[53]
$^{n}C_4H_9$	(*R*,*R*)-**10**	2	60	22	38:1	87	[56]
$^{n}C_8H_{17}$	**11**	2.5	25	2	100:0	100	[59]
$^{n}C_4H_9$	**12**	1.5	25	16	99:1	99	[57,58]
$^{n}C_4H_9$	**13**	2.3	60	4	99:1	91	[60]
$^{n}C_4H_9$	**14b**	2	23	0.08	>99:1	100	[61]
Ph	$La(NR'_2)_3{}^b$	3	25	5	<1:99	99	[62]
Ph	**4a**	5	25		37:63	(0.22)	[51]
Ph	**4b**	5	25		12:88	(4.0)	[51]
Ph	**5**	5	25		40:60	(2.5)	[51]
Ph	**6**	2.5	25	0.67	46:54	100	[49]
Ph	**7**	2	25	10	7:93	100	[52]
Ph	**9**	5	−35	20	100:0	85	[54,55]
Ph	(*R*,*R*)-**10**	2	60	2	1:17	95	[56]
Ph	**12**	1.5	25	30	35:65	99	[57,58]
Ph	**13**	2.3	50	19	3:97	75	[60]
Ph	**14b**	2	23	1.17	33:67	100	[61]

[a]R = $CH(SiMe_3)_2$
[b]NR'_2 = $N(SiMe_3)_2$

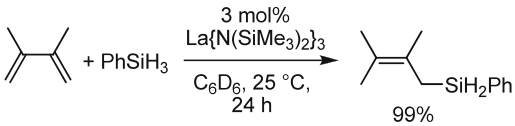

(11)

Contrary to aliphatic-substituted alkenes, catalytic hydrosilylation of vinyl arenes proceeds usually with Markovnikov selectivity to give benzyl silane derivatives. This reversal of regioselectivity may be explained with the alkene insertion step proceeding through the sterically more encumbered transition state which is favored due to attractive metal–arene interactions [29]. Electron-donating substituents in the aromatic ring increase the turnover frequency as well as regioselectivity, which is in agreement to this hypothesis [29]. The selectivity of the hydrosilylation increases with increasing metal ionic radius and opening of the coordination sphere. *Ansa*-metallocenes, such as **15**, are typically the most selective catalysts (12) [29], whereas constrained-geometry [48,49,51], bis(phosphinimino)methanide [57,58],

and guanidinato [61] complexes produce a significant amount of the linear *anti*-Markovnikov isomer (Table 1). The imine complex **9** is an exception, as it forms the linear *anti*-Markovnikov product exclusively [54, 55].

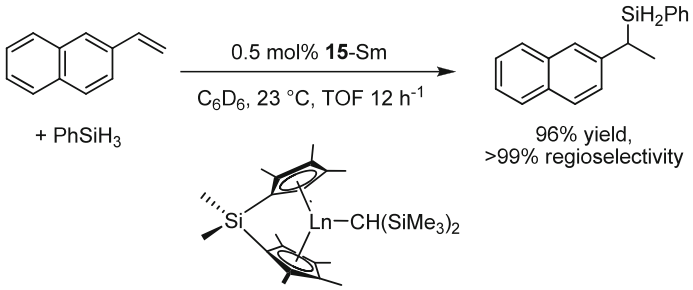

(12)

Few examples of asymmetric hydrosilylations of styrene derivatives with chiral lanthanocene catalysts have been reported (13) [29]. The cyclopentadienyl-free chiral yttrium diamidobiphenyl complex **8** was used for asymmetric hydrosilylation of norbornene with high enantioselectivity (14) [53].

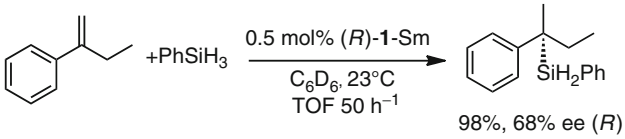

(13)

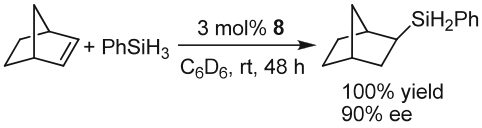

(14)

The yttrium silanolate complex **11** shows good catalytic activity with high *anti*-Markovnikov regioselectivity in the hydrosilylation of 1-decene (Table 1) [59]. Cationic silanolate rare-earth metal alkyl species derived from **11** were either inactive or exhibited significantly diminished activity, possibly as a result of tight binding of the benzene solvent as well as decomposition of the cationic metal hydride intermediate.

The sterically encumbered guanidinato complex **14b** exhibits one of the highest catalytic activities among the cyclopentadienyl-free hydrosilylation catalysts (Table 1) [61]. Weakly coordinating donor groups, for example, thioacetals, in aliphatic alkenes have only a minor effect on regioselectivity (Scheme 1), while alkenes containing stronger donors, for example, acetals, may result in an inversion of regioselectivity. The corresponding benzamidinate complex **14a** is slightly less active, but allows better regiocontrol [61]. Electronically as well as sterically more saturated bis(guanidinate) complexes are significantly less active [63].

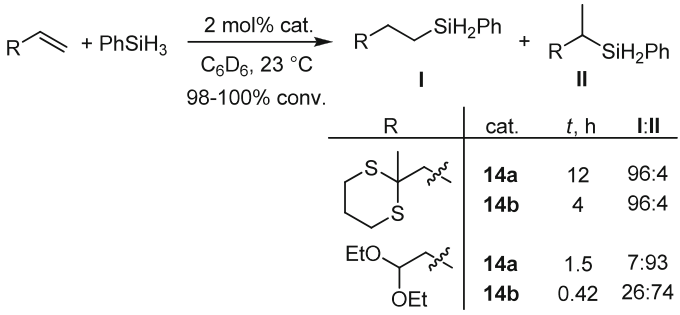

R	cat.	*t*, h	I:II
	14a	12	96:4
	14b	4	96:4
	14a	1.5	7:93
	14b	0.42	26:74

Scheme 1 Regioselectivity in the hydrosilylation of donor-functionalized alkenes

3.2 Hydrosilylation of Alkynes

Terminal alkynes undergo metallation at the Brønsted-acidic sp-hybridized terminal C–H bond with organo-rare-earth metal species rather than hydrosilylation [65,66]. However, internal alkynes undergo hydrosilylation in the presence of an yttrocene catalyst, although the required reaction conditions are typically harsher than the conditions applied in alkene hydrosilylations (15)–(17) [67]. Unsymmetric alkynes give mixtures of regioisomers, both being the products of *syn*-addition of the Si–H moiety to the alkyne, and commonly the less encumbered regioisomer is favored (15) [67]. Increasing steric bulk of the propargyl substituents results in regiospecific addition (16). Note that the alkene remains intact as the reaction proceeds exclusively at the triple bond [68]. The regioselectivity of the transformation may also be driven by electronic factors even if they compete with steric preferences. Thus, hydrosilylation of an alkynylsilane gives predominantly the sterically disfavored product, presumably due to the electronic "silyl-directing" effect of the organosilane group (17) [69]. Aryl groups have been reported to direct the alkyne hydrosilylation in a similar manner [20,70].

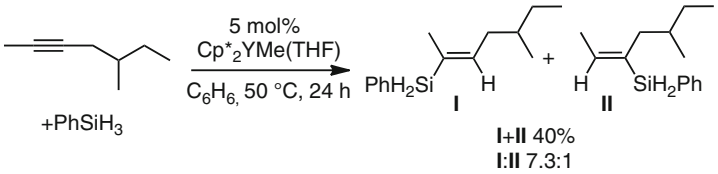

(15)

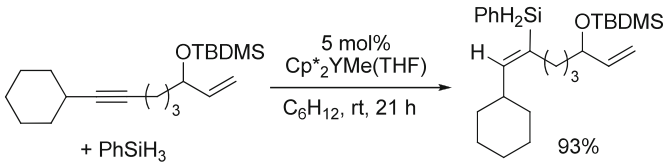

(16)

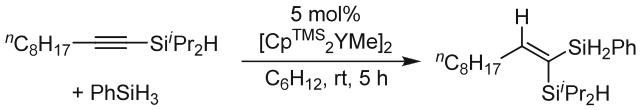

(17)

3.3 Hydrosilylation/Carbocyclization

The ability of organo-rare-earth metal complexes to undergo alkene or alkyne insertion provides the possibility to perform polyene cyclizations, producing metal–alkyl species which can then undergo σ-bond metathesis with an appropriate reagent to produce a cyclic compound. Thus, termination via protonolysis (6) results in cycloalkane derivatives; however, termination via silylation is more desirable as a functionalized cyclic framework is formed (Fig. 9).

Initial studies on the hydrosilylation/carbocyclization of terminal dienes carried out in the early 1990s have demonstrated that five-membered ring formation proceeds smoothly in the presence of lutetocene [40], neodymocene [43], and samarocene [29] catalysts (18).

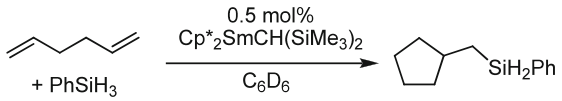

(18)

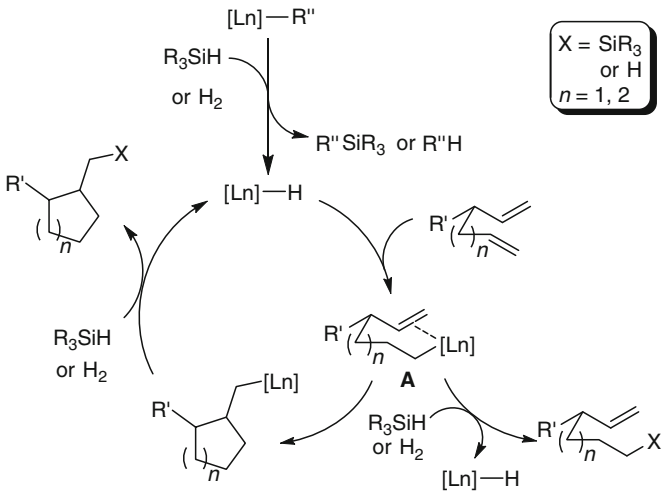

Fig. 9 Mechanism for hydrosilylation/carbocyclization and hydrogenation/carbocyclization

Postmetallocene catalysts can also facilitate this transformation [50, 60, 62], although they are typically less selective and a significant amount of acyclic hydrosilylation product may form if the rate of silylation of the initial alkene insertion product **A** (Fig. 9) is competitive with the rate of carbocyclization.

Molander and coworkers have studied the scope of diene substrates using the yttrocene catalyst $Cp^*_2YMe(THF)$ [71]. As expected, six-membered ring formation appeared to be more challenging [44], however, it can be facilitated with secondary organosilanes R_2SiH_2, which are less prone to side reactions such as formation of silicon-bridged dimers (19) [71].

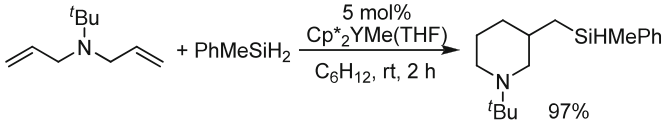

(19)

Rare-earth metal catalysts tolerate a variety of aprotic functional groups; for example, sterically encumbered mesityl sulfonamides sufficiently shield the oxygen from the metal center in order to allow hydrosilylation/carbocyclization, albeit at a reduced rate (20) [72].

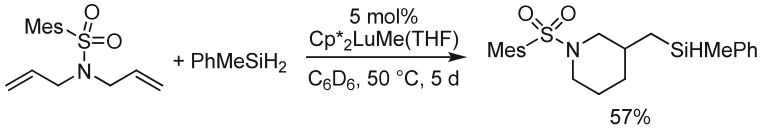

(20)

Diastereoselective cyclizations are possible [73], in particular when the outcome of the stereochemistry is set by the configuration of a cylic ring junction (Fig. 10). The stereochemistry-determining insertion step proceeds via the less encumbered transition state providing a single diastereoisomer.

The reaction is sensitive to steric factors, for example allylic substitution significantly diminishes the reactivity of a double bond, in particular in six-membered ring formation processes. Thus, an impressive regioselectivity can be observed in a cyclization of a triene that features double bonds with different accessibility (21) [73].

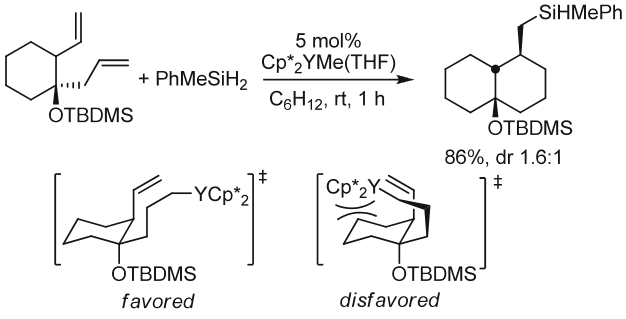

Fig. 10 Diastereospecific decaline formation

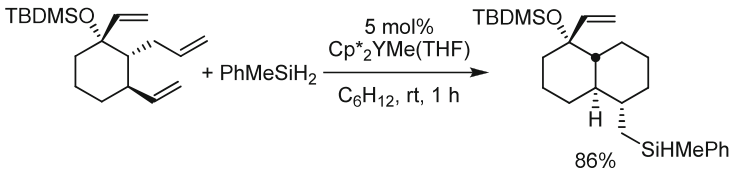

(21)

In case of five-membered rings, allylic-substituted double bonds can also undergo cyclization, which allows the regioselective transformation of an unsymmetric triene involving two consecutive carbocyclizations followed by a silylation step (22) [73].

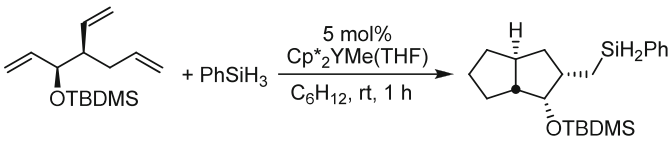

(22)

Hydrosilylation/cyclization of hindered polyenes can be efficiently catalyzed by sterically open *ansa*-lanthanocenes, but trimethylsilylcyclopentadienyl derivatives are particular active and allow cyclization of these challenging substrates at room temperature (23) [74].

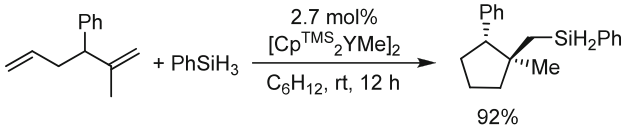

(23)

As mentioned in Sect. 3.2, the carbon–carbon triple bond has a superior reactivity in hydrosilylation compared to a double bond, presumably due to a faster insertion step. This creates an opportunity to perform regio- and chemoselective transformations of enynes [68]. Regioselective transformations of 1,6- and 1,7-enynes proceed via preferred insertion of the triple bond (24).

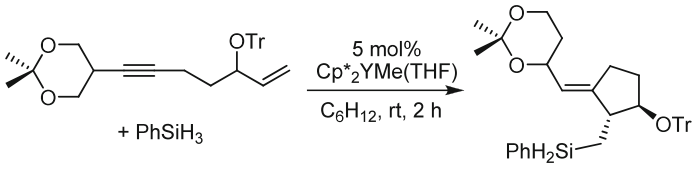

(24)

So far, the only example of an asymmetric hydrosilylation/carbocyclization sequence of α,ω-hexadienes and heptadienes utilize the (*R*)-BINOL-derived yttrocene catalyst **16** to produce cyclopentanes and cyclohexanes in high yields but only low to moderate enantioselectivities of up to 50% ee (25) [75].

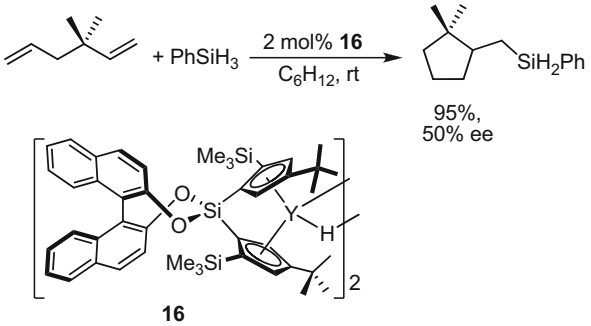

(25)

4 Catalytic Hydrostannation

Organostannanes are important intermediates in preparative organic chemistry and the metal-catalyzed hydrostannation constitutes an attractive atom-economical approach to their synthesis [76]. However, only a single report on organolanthanide-catalyzed hydrostannation has surfaced [77]. The *anti*-Markovnikov hydrostannation of 1-octene is catalyzed by a sterically unobstructed yttrocene catalyst at ambient temperature (26). Although the mechanism of this transformation has not been studied in detail, it apparently resembles that of hydrosilylation. Enhanced reactivity of the tin–hydrogen bond results in a significant amount of distannane side product formed via dehydrogenative σ-bond metathetical coupling.

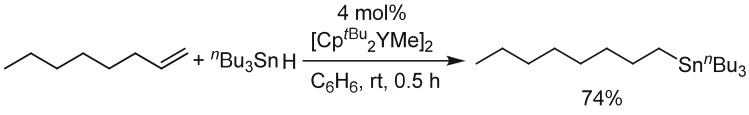

(26)

5 Catalytic Hydroboration

The utility of the well-known hydroboration protocol has been expanded significantly with the advent of metal-catalyzed processes [78, 79]. A few examples of organo-rare-earth metal-catalyzed hydroborations have been reported over the last two decades. In a pioneering study, Marks and coworkers have demonstrated that simple lanthanocene derivatives such as $Cp^*_2LaCH(SiMe_3)_2$ readily catalyze the addition of catecholborane to alkenes at room temperature (27). The proposed mechanism is shown in Fig. 11. High *anti*-Markovnikov regioselectivity (>98%) was reported in all cases including reactions of vinyl arenes. Trace amounts of alkene hydrogenation side product were detected [80]. Elimination of (catechol)$BCH(SiMe_3)_2$ providing an active metal hydride catalyst precedes the catalytic cycle as evidenced by NMR spectroscopic observations. The last step of the

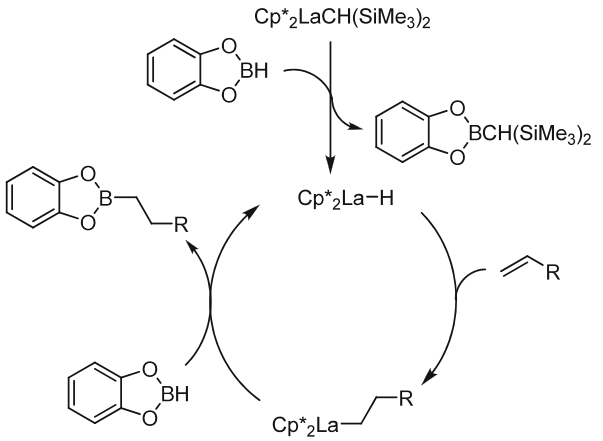

Fig. 11 Proposed mechanism for intermolecular hydroboration of alkenes

catalytic cycle is believed to be rate-determining, as the significant higher reactivity of lanthanum in comparison to yttrium can be attributed to a lower σ-bond metathetical transition state in case of the larger La^{3+} ion [81].

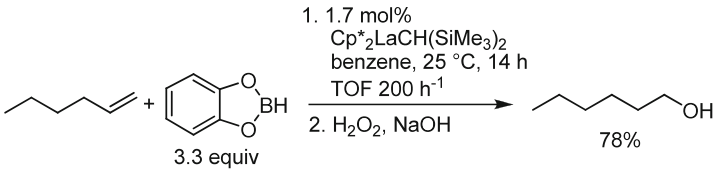

(27)

Subsequent studies have demonstrated that the relatively robust and readily accessible rare-earth trisamide $La\{N(SiMe_3)_2\}_3$ can also be successfully employed to catalyze *anti*-Markovnikov hydroboration of alkenes (28) [82]. The 1,2-addition product in the hydroboration of vinyl arenes constitutes the opposite 2,1-addition products commonly favored in vinyl arene hydrosilylations (Sect. 3.1), although both reactions are believed to proceed via analogous mechanisms. This fact may also be interpreted in terms of uncatalyzed addition of the borane to the alkene being competitive with the catalyzed process in some cases [82, 83].

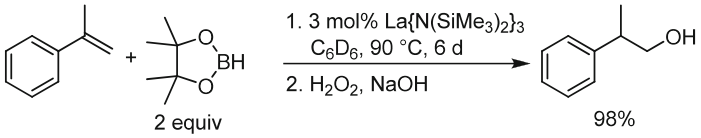

(28)

A tandem carbocyclization/hydroboration sequence has been disclosed by Molander [83]. The carbocyclization of α,ω-dienes proceeds smoothly in the presence of the divalent samarocene $Cp^*_2Sm(THF)$ and the metal–alkyl intermediate is trapped by a 1,3-diaza-2-boracyclopentane to afford the cyclic hydroboration product (29).

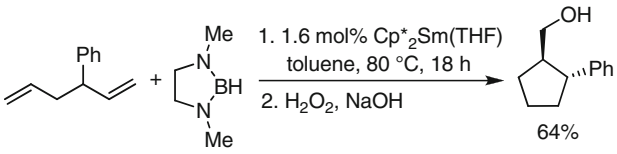

(29)

It should be noted that SmI_3-catalyzed hydroboration of alkenes with catecholborane was reported in 1993 [84]. However, this reaction is unlikely to involve σ-bond metathesis as SmI_3 acts only as a Lewis acid.

6 Catalytic Hydroamination

The metal-catalyzed addition of an amine N–H bond across an unsaturated carbon–carbon linkage – the so-called hydroamination, allows a facile and highly atom-economical access to industrially relevant nitrogen containing basic and fine chemicals. This process has therefore attracted significant attention in the last two decades [85–89]. In particular asymmetric hydroamination, which remains a very challenging area, has flourished tremendously over the last decade [90–96]. Among various transition and main group metal-based hydroamination catalyst systems, rare-earth metal complexes remain one of the most active and selective ones [88, 97]. Due to the large amount of data, we will focus on the most relevant achiral and chiral catalyst systems in this chapter.

6.1 Intramolecular Hydroamination

Rare-earth metal complexes have proven to be very efficient catalysts for *intramolecular* hydroamination reactions involving aminoalkenes, aminoalkynes, aminoallenes, and conjugated aminodienes [88, 97]. They are significantly less efficient in *intermolecular* hydroamination reactions and only a limited number of examples are known [98–102]. The difficulties in intermolecular hydroamination reactions originate primarily from inefficient competition between strongly binding amines and weakly binding alkenes for vacant coordination sites at the catalytically active metal center.

As will be discussed in more detail in the following chapters, the intramolecular hydroamination reaction of aminoalkenes and other substrates involves two key steps in the catalytic cycle. Insertion of the unsaturated carbon–carbon linkage into a rare-earth metal amide bond, followed by protonolysis of the resulting metal alkyl (respectively, allyl or vinyl) species. The insertion step is generally perceived as the rate-determining step of the process, although this may not be true for all substrate classes. The hydroamination/cyclization of aminoalkenes differs significantly from reactions involving aminoalkynes, aminoallenes, and conjugated aminodienes from a thermodynamic point of view. The alkene insertion step of the Ln–amide

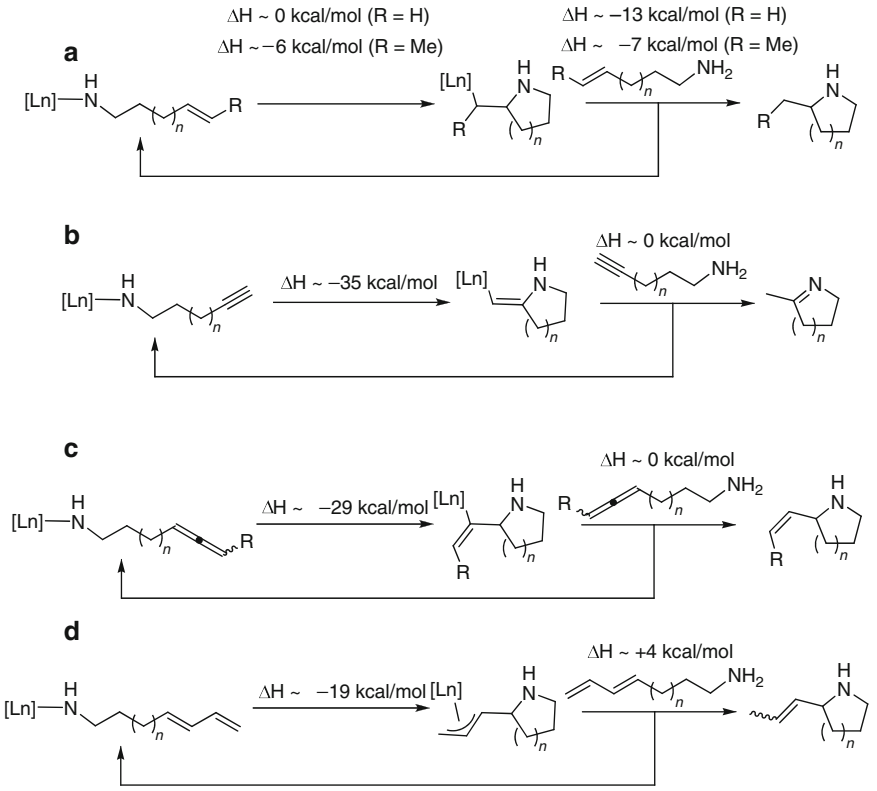

Fig. 12 Thermodynamics of the elementary steps in rare-earth metal-catalyzed hydroamination/cyclization of aminoalkenes (**a**), aminoalkynes (**b**), aminoallenes (**c**), and aminodienes (**d**) ($n = 1$–3) [103–108]

into the carbon–carbon double bond is approximately thermoneutral for terminal aminoalkenes and it is only slightly exothermic for an internal aminoalkene with a 1,2-disubstituted alkene (Fig. 12a) [103, 104]. The subsequent protonolysis of the primary rare-earth metal alkyl species is quite exothermic, to a lesser extent also for the secondary rare-earth metal alkyl species. In marked contrast, insertion of an alkyne, allene, or 1,3-diene into the Ln–amide bond is very exothermic (Fig. 12b–d) [105–108]. Protonolysis of the resulting vinyl (in case of alkynes and allenes) or η^3-allyl (in case of conjugated dienes) rare-earth metal species is about thermoneutral (for the vinylic species) to slightly endothermic (for the allylic species) due to the significant stabilization of these species. Despite these considerable differences, it has been proposed that in all these cyclization reactions, the insertion step is rate-determining [109, 110], followed by a rapid protonolysis step. However, recent DFT analyses of the catalytic cycle of the rare-earth metal-catalyzed hydroamination of dienes and allenes suggest that protonolysis of the rare-earth metal η^3-allyl species (in hydroamination of dienes), respectively, vinylic species (in hydroamination of allenes), is the rate-determining step [111–113].

6.1.1 Cyclization of Aminoalkenes

Pioneering experimental findings by Marks and coworkers [97, 103, 114] followed by theoretical analysis [109] allowed elucidation of the mechanism of aminoalkene hydroamination/cyclization (Fig. 13). The reaction is considered to proceed through a rare-earth metal amido species, which is formed upon protonolysis of a rare-earth metal amido or alkyl bond. As discussed in the previous section, the first step of the catalytic cycle involves insertion of the alkene into the rare-earth metal amido bond with a seven-membered chair-like transition state (for $n = 1$). The roughly thermoneutral [103, 109] insertion step is considered to be rate-determining, giving rise of a zero-order rate dependence on substrate concentration and first-order rate dependence on catalyst concentration.

The resting state of the catalyst is believed to be an amine adduct of the catalytic active Ln–amide. For lanthanocene catalysts such an amido amine species of the type $Cp^*_2Ln(NHR)(NH_2R)$ has been spectroscopically and crystallographically characterized [103]. Amines, coordinating solvents and other external bases may adversely affect the reactivity of the rare-earth metal center, in particular if the metal center is readily accessible. Sterically open *ansa*-lanthanocenes and constrained-geometry catalysts (CGC) [27, 104, 108] and more recently also sterically readily accessible nonmetallocene catalysts [101, 115, 116] have displayed product inhibition (leading to apparent first-order kinetics) or substrate inhibition (resulting in self-acceleration).

On the one hand, coordinative saturation of the metal center through strong amine binding results in reduced electrophilicity and therefore reduced catalytic activity.

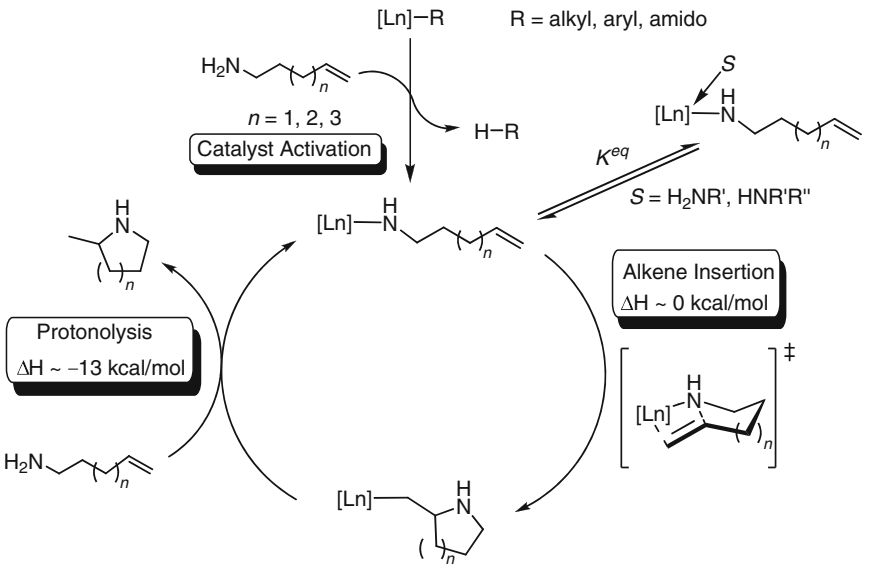

Fig. 13 Simplified catalytic cycle for aminoalkene hydroamination/cyclization [103, 109]

On the other hand, coordination of the amine significantly lowers the reaction barrier for the σ-bond metathetical protonation, as shown in computational studies [109]. The rare-earth metal alkyl species formed in the insertion process is therefore prone to rapid protonolysis with a second amine molecule, regenerating the rare-earth metal amido species, and releasing the heterocyclic product. Surprisingly, kinetic studies using *N*-deuterated aminoalkenes have revealed a large primary kinetic isotope effect with k_H/k_D in the range of 2.3–5.2 [101, 103], although apparently no N–H bond breaking is involved in the rate-determining alkene insertion step. A plausible explanation involves partial proton transfer from a coordinated amine to the α-carbon in the four-membered insertion step (Fig. 14) [103]. However, some experimental data, in particular the observation of sequential hydroamination/carbocyclization sequences (Sect. 6.2) is in conflict with this interpretation, as the latter requires a finite lifetime of the rare-earth metal alkyl intermediate.

Initial studies focused on lanthanocene-based catalyst systems that proofed to be efficient in the *exo*-specific cyclization of terminal aminoalkenes to form five-, six-, and seven-membered azacycles (Scheme 2). The reactions are predictably faster for the formation of smaller five-membered rings and in the presence of *gem*-dialkyl substituents [117]. An increasing metal ionic radius and a more open coordination sphere, for example, in *ansa*-lanthanocenes, are also beneficial for higher cyclization rates [103]. A further increase in catalytic activity is observed when sterically more open and more electrophilic CGC **17** (Fig. 15) are applied [118].

Although lanthanocene catalysts initially developed for aminoalkene hydroamination are highly sensitive and not readily available, their catalytic activity remains unsurpassed as of now and only a few postmetallocene rare-earth metal complexes can reach comparable levels of catalytic efficiency. Besides constrained-geometry (Fig. 15) [118, 119] and other half-sandwich [102, 120, 121] rare-earth metal complexes, a large number of cyclopentadienyl-free catalyst systems have been

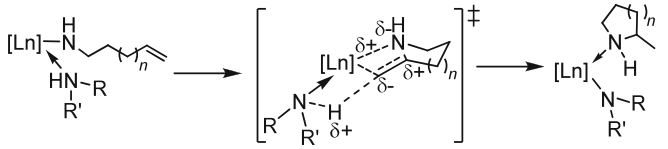

Fig. 14 Proposed amine assisted alkene insertion in hydroamination/cyclization (RR′NH = substrate or hydroamination product)

n	R	T/°C	TOF/h^{-1}
1	H	60	140
1	Me	25	95
2	H	60	5
3	Me	60	0.3

Scheme 2 Lanthanocene-catalyzed intramolecular hydroamination of terminal aminoalkenes

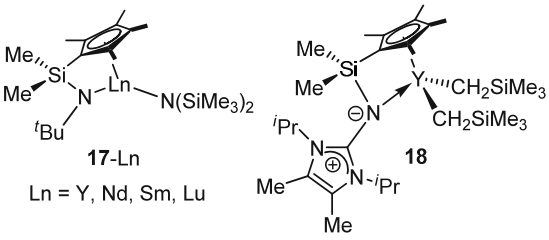

Fig. 15 Constrained-geometry rare-earth metal hydroamination catalysts [118, 119]

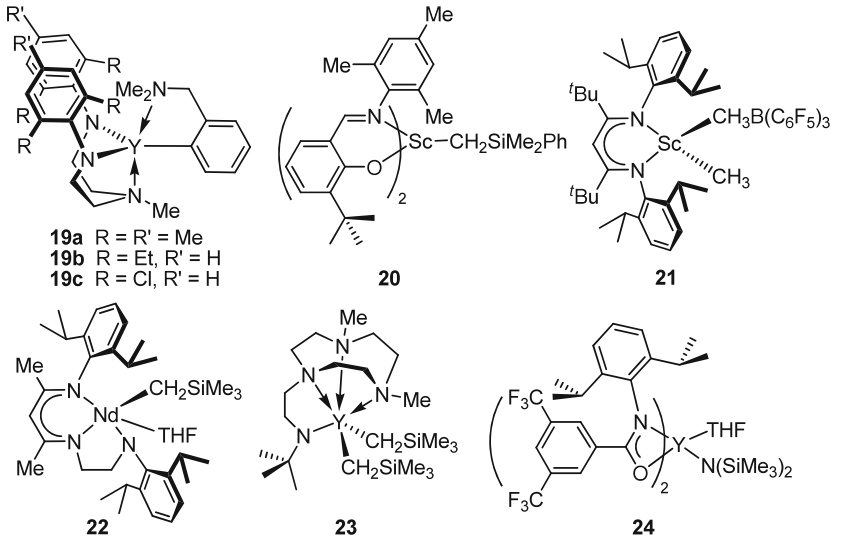

Fig. 16 Selected examples of achiral, nonmetallocene rare-earth metal-based catalysts for hydroamination of aminoalkenes [116, 132–134, 136]

developed over the last decade, ranging from simple trisamides $Ln\{N(SiMe_3)_2\}_3$ [116, 122, 123] or bisamide $Sm\{N(SiMe_3)_2\}_2$ [124] to more elaborate ligand frameworks, such as chelating diamides [123, 125–127], diamidoamine [116], aminotroponiminato [128], bis(phosphinimino)methanide [57, 58, 129–131], salicylaldiminato [132], β-diketiminato [132, 133], triazacyclononane-amide [134], benzamidinate [134], tridentate triamine [135], amidate [136], and tris(oxazolinyl)borato [137] ligands. Some catalyst systems are depicted in Fig. 16 and catalytic results are compiled in Table 2. Additionally, many chiral catalyst systems for *asymmetric* hydroamination reactions have been developed (see Sect. 6.1.5) in order to overcome significant drawbacks of chiral cyclopentadienyl-containing rare-earth metal complexes.

Catalyst systems obtained in situ from rare-earth metal trisamides $Ln\{N(SiMe_3)_2\}_3$ and various chelating diamines (Fig. 17) have shown good activity in the cyclization of aminoalkenes (Schemes 3 and 4) [123, 125–127]. The more challenging cyclization of the chiral aminoalkene **26** can be accomplished with

Table 2 Catalytic hydroamination/cyclization of aminoalkenes

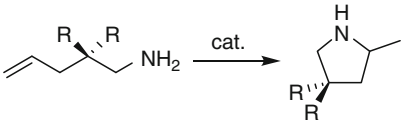

R	Catalyst	[cat.]/[s] (%)	*T* (°C)	*t* (h)	Conv. (%)	References
Me	$Y\{N(SiMe_3)_2\}_3$	2.7	24	6	>95	[123]
Me	**12**	1.3	60	6	Quant.	[58]
Me	**14a**	1	50	0.8	>99	[134]
Me	**19a**	3	25	3.65	95	[116]
Me	**21**	5	65	24	>90	[132]
Me	**22**	0.5	60	1	98	[133]
Me	**23**/$[PhNMe_2H][B(C_6F_5)_4]$	1	50	12	>99	[134]
Me	**24**	10	25	2.5	93	[136]
Ph	**18**	4	RT	0.05	Quant.	[119]
Ph	**20**	10	65	2	>95	[132]
Ph	**21**	5	25	2	>95	[132]
Ph	**24**	10	25	<0.25	93	[136]

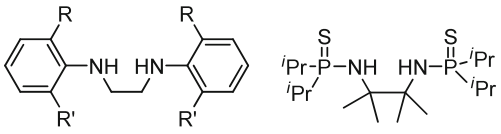

25a R = ^{i}Pr, R' = H
25b R = R' = Et

25c

Fig. 17 Chelating diamines used as ligands for non-metallocene hydroamination catalysts

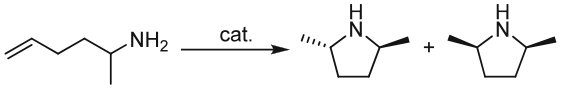

26 *trans*-**27** *cis*-**27**

cat.	conditions	*trans*:*cis*	yield, %
5 mol% $Sc\{N(SiMe_3)_2\}_3$ + 5 mol% **25a**	60 °C, 1.5 h	49:1	>95
3 mol% **19b**	25 °C, 8 h	23:1	89
$La\{N(SiMe_3)_2\}_3$	90 °C, 13 h	4:1	>99

Scheme 3 Diastereoselective cyclization of **26** [116, 127]

high *trans*-diastereoselectivity (up to 49:1) at 60°C [127]. The preferred formation of *trans*-**27** can be explained with minimal 1,3-diaxial interactions in the chair-like cyclization transition state [103, 138]. Unfortunately, the structure of the chelating diamide catalyst system is not known. Structurally characterized diamidoamine complexes **19** have shown slightly higher reactivity that allows the

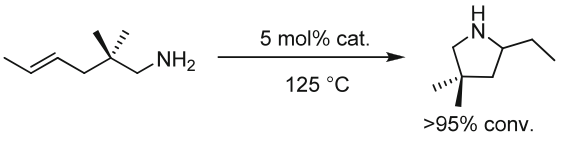

cat.	*t*, h	TOF, h^{-1}
15-Sm	~1	21.6
17-Sm	~5.5	3.59
$Nd\{N(SiMe_3)_2\}_3$ / **25b**	6.5	

Scheme 4 Catalytic hydroamination/cyclization of an aminoalkene with an internal double bond [104, 125]

reaction to proceed at 25°C with up to 23:1 *trans*-selectivity [116]. The formation of seven-membered rings constitute another significant challenge for postmetallocene catalysts, but can be accomplished utilizing the bis(amidate) yttrium catalyst **24** (30) [136].

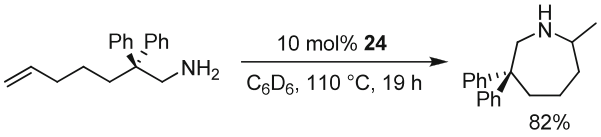

(30)

While most rare-earth metal-based catalyst systems are neutral, only a few cationic catalyst systems have been investigated. For example, the β-diketiminato scandium complex **21** [132] and the triazacyclononane-amide complex **23** when treated with $[PhNMe_2H][B(C_6F_5)_4]$ [134] display improved catalytic activity over their neutral congener. However, this trend is not general, as the opposite result, higher activity for the neutral over the cationic species, was found for the benzamidinate complex **14a** (Fig. 8) [134]. Quite generally, it is expected that the Ln–amide bond is stronger for the more electron deficient species, thus impeding the insertion process of the olefin into the Ln–amide bond. However, the reduced steric strain around the cationic metal center in case of **21** and **23** (after activation with $[PhNMe_2H][B(C_6F_5)_4]$) could compensate for this impediment and result in an overall net rate increase in comparison to the neutral, sterically more congested analogues.

Cyclization of 1,2- and 1,1-disubstituted alkenes [104, 123, 125, 126, 136, 138–140] requires elevated temperatures and sterically more open and more reactive catalysts, such as *ansa*-lanthanocenes $Me_2Si(C_5Me_4)_2LnCH(SiMe_3)_2$ (**15**-Ln), constrained-geometry catalysts $Me_2Si(C_5Me_4)(^tBuN)LnN(SiMe_3)_2$ (**17**-Ln), or nonmetallocene complexes with chelating bis(amides) (Schemes 4 and 5), while trisubstituted alkenes remain challenging.

Scheme 5 Cyclization of a 1,1-disubstituted aminopentene [123, 139]

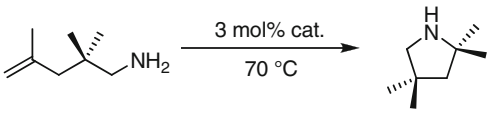

cat.	*t*, h	yield, %
$[Cp^{TMS}{}_2SmMe]_2$	2	93
$Y\{N(SiMe_3)_2\}_3$	8	94

6.1.2 Cyclization of Aminoalkynes

The rare-earth metal-catalyzed hydroamination/cyclization of internal and terminal aminoalkynes is a facile process, as shown by experimental [105, 106] and theoretical [110] studies. In general, the reaction proceeds via the same mechanism as aminoalkene hydroamination (Fig. 13) with some notable difference arising from a different insertive reactivity of the triple bond. The insertion of the C–C triple bond proceeds much faster than that of a double bond due to the exothermic nature of the step (Fig. 12). Overall, the cyclization of an aminoalkyne is commonly 1–2 orders of magnitude faster than that of an analogous terminal aminoalkene. However, the insertion step is still considered to be the rate-determining step, based on aforementioned DFT calculations and experimental observations.

Interestingly, the reactivity pattern in rare-earth metal-catalyzed hydroamination/cyclization reactions of aminoalkynes with respect to ionic radius size and steric demand of the ancillary ligand follows the opposite trend to that observed for aminoalkenes, namely *decreasing* rates of cyclization with *increasing* ionic radius of the rare-earth metal and more open coordination sphere around the metal. This phenomenon can be explained by a negligible sterical sensitivity of a sterically less encumbered triple bond, as sterically less open complexes and smaller metal ions provide more efficient reagent approach distances and charge buildup patterns in the transition state [110].

Selected examples of intramolecular aminoalkyne hydroamination catalyzed by rare-earth metal complexes (see Figs. 8, 16, and 18) are shown in Scheme 6 and Table 3. Formation of five-, six-, and seven-membered cyclic imines has been achieved in excellent yields.

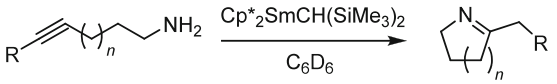

n	R	T /°C	TOF /h^{-1}
1	H	21	580
1	Me	21	96
1	$SiMe_3$	21	>7600
1	Ph	60	2830
2	Ph	60	328
3	Ph	60	0.11

Scheme 6 Samarocene-catalyzed hydroamination/cyclization of aminoalkynes [105, 106]

Table 3 Catalytic hydroamination/cyclization of aminoalkynes

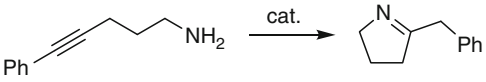

Catalyst	[cat.]/[s] (%)	T (°C)	t (h)	Conv. (%)	References
12	1	60	1	Quant.	[58]
19c	3	60	0.25	93	[116]
20	10	25	0.75	>95	[132]
21	10	25	0.75	>90	[132]
$Y\{N(SiMe_3)_2\}_3$/**25c**	5	60	1.5	96	[141]
28	2	21	100	Quant.	[128]

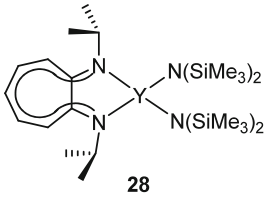

28

Fig. 18 Aminotroponiminato catalyst for hydroamination of aminoalkynes [128]

Catalyst systems derived from $Ln\{N(SiMe_3)_2\}_3$ and chelating diamines (e.g., **25a**, Fig. 17) are also active in the cyclization of aminoalkynes with quite remarkable activity and functional group tolerance (31) [141].

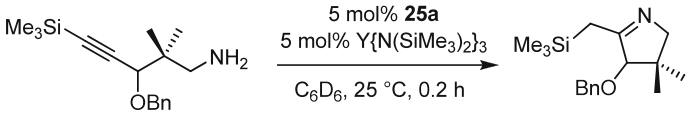

98% (31)

The rare-earth metal-catalyzed cyclization of aminoalkenes, aminoalkynes and aminodienes generally produces exclusively the exocyclic hydroamination products. The only exception was found in the cyclization of homopropargylamines leading to the formation of the endocyclic enamine product via a 5-*endo-dig* hydroamination/cyclization (32) [142], most likely due to steric strain in a potential four-membered ring exocyclic hydroamination product. Interestingly, the 5-*endo-dig* cyclization is still preferred even in the presence of an alkene group that would lead to a 6-*exo* hydroamination product [142].

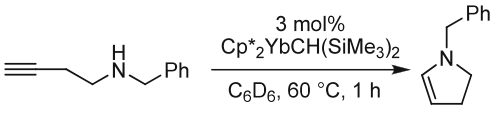

95% (32)

6.1.3 Cyclization of Aminodienes

Hydroamination of 1,3-dienes is a facile process due to the transient formation of an η^3-allyl intermediate, which forms E/Z-vinylpyrrolidines and vinylpiperidines upon protonation, and, under certain conditions, also allyl isomers (Fig. 19 and Scheme 7). Cyclizations with lanthanocenes lead preferentially to the E alkene in up to 98:2 E/Z ratio [107, 108]. For the sterically more congested $Cp^*_2YCH(SiMe_3)_2$ the vinylpiperidine becomes the prevailing product at a dramatically reduced reaction rate. Generally, the reaction rates are higher for aminodienes compared to the corresponding aminoalkenes, despite increased steric encumbrance of the cyclization transition state. High stereo- and regioselectivities apparently result from kinetically impeded protonolysis of the more substituted carbon atom of the stabilized allyl intermediate (Fig. 19), as shown by calculations. It is, noteworthy, that according to DFT calculations the protonolysis step might be rate-determining due to the facile insertion [111]. Hydroamination/cyclization of dienes shows a rate dependence on the Ln^{3+} ionic radius and coordinative unsaturation that is even more pronounced than in case of aminoalkenes [108].

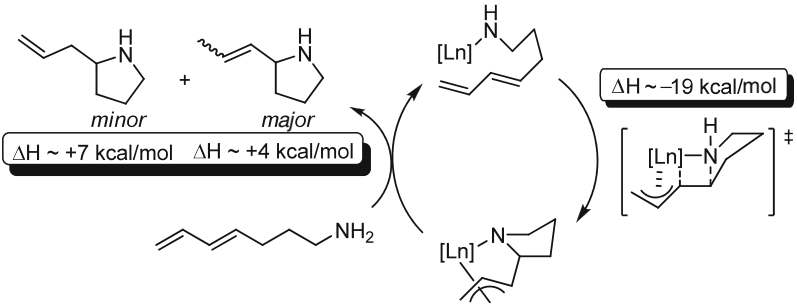

Fig. 19 Mechanism of aminodiene cyclization [107, 108]

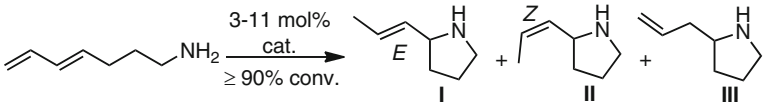

cat.	T/°C	I:II:III	TOF/h^{-1}
$Cp^*_2LaCH(SiMe_3)_2$	25	84:16:0	40
$Cp^*_2YCH(SiMe_3)_2$	60	30:19:51	0.05
2-Sm	23	98:2:0	74
17-Sm	25	59:41:0	3.1
17-Y	25	87:13:0	~0.08

Scheme 7 Cyclization of aminoheptadiene [107, 108]

6.1.4 Cyclization of Aminoallenes

Hydroamination of aminoallenes proceeds faster than cyclization of aminoalkenes but slower than that of aminoalkynes. Two insertion pathways are feasible, as a mixture of *exo*- and *endo*-products are obtained in case of monosubstituted allenes (33) [143, 144]. Cyclization of 1,3-disubstituted allenes on the other hand proceeds exclusively via the *exo* route to generate the allylic amine (34) and α-substituted aminoallenes cyclize with high diastereoselectivities to give the 2,5-*trans*-pyrrolidines exclusively (35). However, in the latter case the *E*/*Z* ratio is lower in comparison to the high selectivities observed for aminodienes. This potential disadvantage becomes irrelevant if the amine is subjected to subsequent hydrogenation, providing an alternative synthetic access to 2-alkyl azacycles instead of a more sluggish cyclization of an aminoalkene with a 1,2-disubstituted double bond [145].

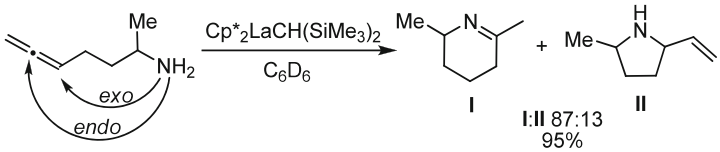

(33)

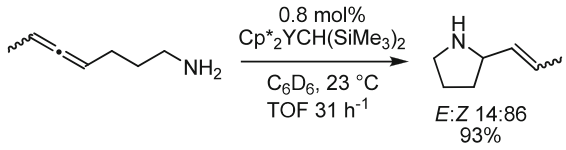

(34)

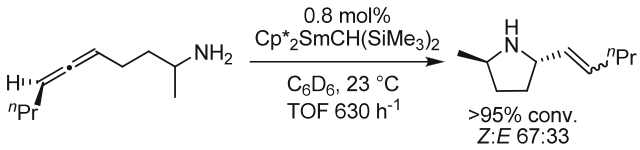

(35)

The kinetic analysis demonstrated an unusual dependence of the cyclization rate on the rare-earth metal ion size, with maximum turnover rates observed for the medium-sized yttrium and slower rates for the larger lanthanum and smaller lutetium [144]. Similar to aminoalkynes, catalysts with more open ligand frameworks are less active. DFT calculations indicate that protonolysis is the rate-determining step of the process [113], although this notion is contrary to some experimental observations [143, 144].

6.1.5 Asymmetric Hydroamination

Chiral C_1-symmetric lanthanocenes (see Fig. 4) have achieved enantioselectivities of up to 74% (36) in various intramolecular hydroamination reactions [27, 146, 147]. While complexes **1–3** are better suitable for the formation of five-membered rings,

the extended wingspan of the octahydrofluorenyl complexes **29** are optimized for six-membered ring formation (37). Unfortunately, the chiral lanthanocenes undergo facile epimerization under the conditions of catalytic hydroamination via reversible protolytic cleavage of the metal cyclopentadienyl bond [27,104,147,148]. Thus, the enantioselectivity of product formation is limited by the catalyst's epimeric ratio in solution and the absolute configuration of the hydroamination product is independent of the diastereomeric purity of the precatalyst.

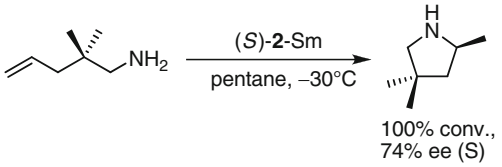

(36)

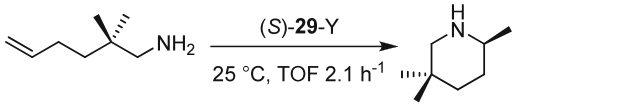

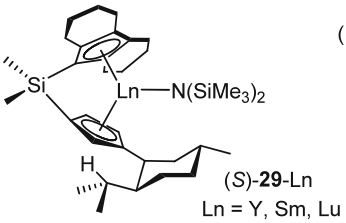

(37)

Many chiral cyclopentadienyl-free catalyst systems designed to overcome this configurational instability have been reported since 2003 [56,101,115,149–170]. Several relevant catalyst systems are shown in Fig. 20 and a brief survey of catalytic results is listed in Table 4.

A variety of bisoxazolinato rare-earth metal complexes such as **30** have been studied with regard to their hydroamination/cyclization catalytic activity [149]. The precatalysts show similar enantioselectivity and only slightly reduced catalytic activity when prepared in situ from $[La\{N(SiMe_3)_2\}_3]$ and the bisoxazoline ligand. In this ligand accelerated catalyst system the highest rates were observed for a 1:1 metal to ligand ratio.

The ate complexes $[Li(THF)_4][Ln\{(R)\text{-}1,1'\text{-}(C_{10}H_6NR)_2\}_2]$ ((*R*)-**31**; Ln = Yb, Y; R = ^{i}Pr (**a**), Cy (**b**), C_5H_9 (**c**)) [153–156,158,160] are unusual hydroamination catalysts as they lack an obvious leaving amido or alkyl group that is replaced during the initiation step by the substrate. It is very likely that at least one of the amido groups is protonated during the catalytic cycle. The best catalytic results were obtained using a small rare-earth metal (Yb) and a large cyclopentyl substituent on the diamidobinaphthyl ligand, but the moderate catalytic activity required the presence of activating *gem*-dialkyl substituents [117] in the aminoalkene substrates.

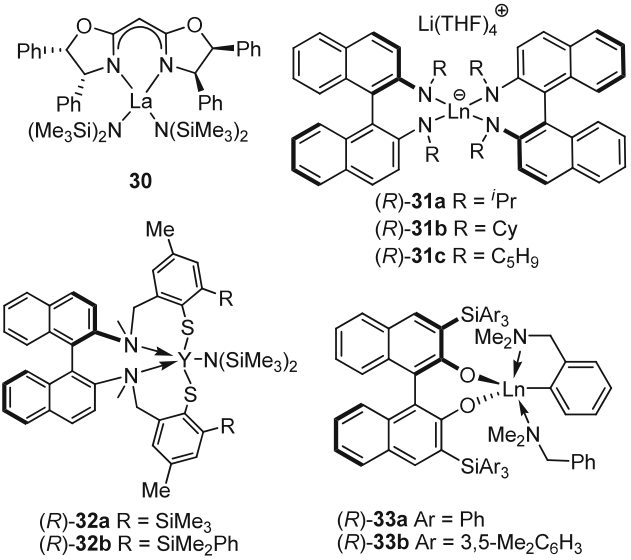

Fig. 20 Important postmetallocene catalysts for asymmetric aminoalkene hydroamination/cyclization [101, 149, 155, 156, 158, 161]

Table 4 Asymmetric intramolecular hydroamination of aminopentenes

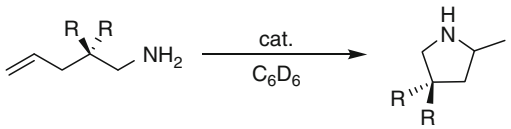

Cat.	*R*, *R*	[cat.]/[s] (%)	*T* (°C)	Time	Yield (%)	% ee	References
30	H, H	5	23	∼9 d	>95	40	[149]
30	Me, Me	5	23	∼1 h	>95	67	[149]
30	Ph, Ph	5	23	∼7 min	>95	34	[149]
(*R*)-**31a**-Y	$-(CH_2)_5-$	7	25	20 h	Quant.	67	[156]
(*R*)-**31b**-Yb	$-(CH_2)_5-$	6	25	18 h	94	65	[155]
(*R*)-**31c**-Yb	$-(CH_2)_5-$	6	25	20 h	90	87	[158]
(*R*)-**32a**	Me, Me	5	30	23 d	95	89	[161]
(*R*)-**32b**	Me, Me	5	60	9 h	95	87	[161]
(*R*)-**32b**	H, H	5	60	8 h	95	81	[161]
(*R*)-**33b**-Sc	H, H	5	22	17 h	93	90	[101]
(*R*)-**33a**-Sc	Me, Me	2	60	6 h	93	73	[101]
(*R*)-**33a**-Sc	Ph, Ph	2	25	0.6 h	94	95	[101]

Good to high enantioselectivities for a wide range of aminoalkene substrates, including internal alkenes or secondary amines, were achieved using the in situ generated aminothiophenolate catalyst system (*R*)-**32** [161]. Variation of the steric demand of the silyl substituent attached to the thiophenolate moiety allowed facile fine-tuning of the enantiomeric excess, providing increasing selectivity with

increasing steric hindrance. While the larger bite angle of the amino(thio)phenolate ligand is believed to improve enantiofacial differentiation as the chiral ligand reaches further around the metal center [150], the multidentate nature of the ligand also electronically saturates the metal center, effectively diminishing catalytic performance. Enantiomeric excess of up to 89% can be achieved at 30°C, though reactions at this temperature require a long period of time to reach completion.

Significantly higher catalytic activities are achievable, when more electron deficient ligand sets are employed. Binaphtholate aryl complexes (*R*)-**33** (Ln = Sc, Y, Lu) [101, 163] with sterically demanding tris(aryl)silyl substituents in the 3- and 3′-position show not only superior catalytic activity at room temperature, comparable in magnitude to lanthanocene catalysts, but also achieve up to 95% ee in hydroamination/cyclization reactions of aminoalkenes, among the highest enantioselectivities observed so far. The sterically demanding tris(aryl)silyl substituents in the diolate complexes play a pivotal role not only to achieve high enantioselectivities, but they are also crucial to prevent undesired complex aggregation [56, 115] and reduce detrimental amine binding of the substrate and product to the catalytic active metal centers [101].

The binaphtholate complexes (*R*)-**33** were successfully applied in the efficient kinetic resolution of chiral aminoalkenes (Table 5) [101, 163, 171]. Racemic aminopentenes can be kinetically resolved with resolution factors f as high as 19. The resolution factor value depends dramatically on the nature of the substituent *R*. Mechanistic studies have revealed that diminished efficiencies in the kinetic resolution of aminoalkenes with aliphatic substituents is caused by an unfavorable state of the Curtin–Hammett pre-equilibrium that favors the mismatching substrate–catalyst complex, whereas in the significantly more efficient kinetic resolutions of aryl-substituted aminoalkenes the matching substrate–catalyst complex predominates the pre-equilibrium [171].

Enantioselective cyclizations of amino-octadiene with chiral lanthanocene catalysts provide a facile access to (+)-coniine with 63% ee after hydrogenolysis of the

Table 5 Catalytic kinetic resolution of chiral aminopentenes [101, 163, 171]

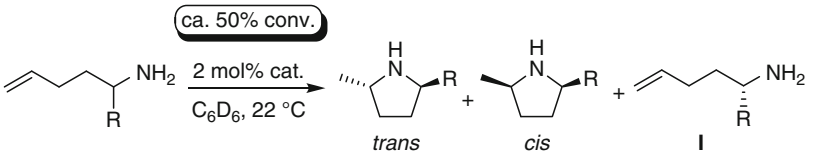

Subst.	Cat.	*t* (h)	Conv. (%)	*trans*:*cis*	% ee of recov. **I**	f [a]	References
Me	(*R*)-**33b**-Y	26	52	13:1	80	16	[101, 163]
Cy	(*R*)-**33a**-Lu	23	47	8:1	51	6.0	[171]
Ph	(*R*)-**33a**-Lu	15[b]	52	≥50:1	83	19	[101]
4-ClC_6H_4	(*R*)-**33b**-Y	10[b]	51	≥50:1	80	19	[171]
4-$MeOC_6H_4$	(*R*)-**33a**-Y	8[b]	50	≥50:1	78	19	[101]

[a] Resolution factor
[b] At 40°C

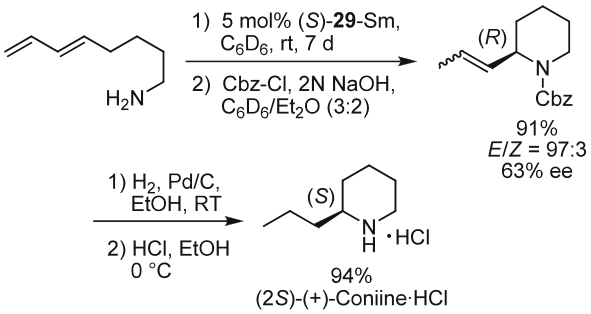

Scheme 8 Synthesis of (+)-coniine·HCl via enantioselective aminodiene hydroamination/cyclization

Cbz-protected vinylpiperidine (Scheme 8) [108]. Cyclization of aminodienes followed by hydrogenation constitutes an alternative to the less facile direct hydroamination of a 1,2-disubstituted aminoalkene (see Sect. 6.1.1).

6.1.6 Tandem Hydroamination/Hydrosilylation

As discussed in the previous sections, hydrosilylation and hydroamination reactions can be catalyzed by essentially the same catalysts under very similar reaction conditions due to the similarity in their reaction mechanisms. Hence, both reactions can be performed in one synthetic procedure as a one-pot sequence. Although less explored than hydrosilylation of C–C multiple bonds, organolanthanide-catalyzed hydrosilylation of imines is a facile straightforward process [172, 173]. Imines, in particular cyclic imines, are readily available via organolanthanide-catalyzed hydroamination of alkynes. Roesky and coworkers have demonstrated that *N*-silylated saturated heterocycles can be smoothly obtained (38) and (39) utilizing the bis(phosphinoamide)methanide complex **12** (Fig. 8) [57, 58]. The higher reactivity of aminoalkynes in the hydroamination process makes this method a valuable alternative to aminoalkene hydroamination.

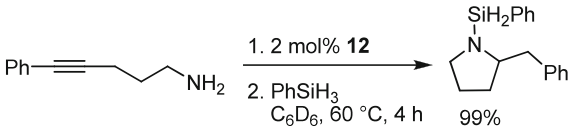

(38)

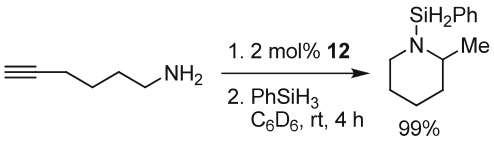

(39)

6.2 Hydroamination/Carbocyclization

Hydroamination/bicyclization of aminodialkenes, aminodialkynes, and aminoalkenynes opens a straightforward route to pyrrolizidines and indolizidines in a tandem C–N and C–C bond forming process. An important prerequisite for the success of this reaction sequence is a sufficient lifetime of the rare-earth metal alkyl intermediate formed in the initial insertion process of the alkene/alkyne in the Ln–amide bond in order to permit the carbocyclization step (Scheme 9) [99, 174].

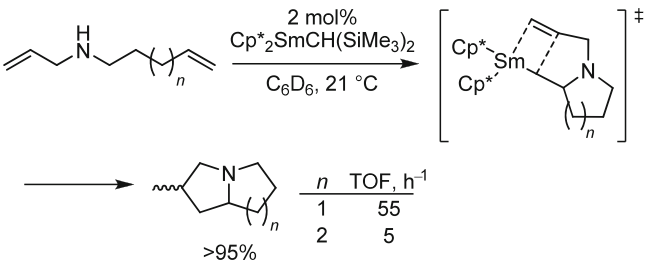

Scheme 9 Synthesis of pyrrolizidines ($n = 1$) and indolizidines ($n = 2$) via hydroamination/carbocyclization [99, 174]

The scope of this process has been extended in a more detailed investigation to the synthesis of quinolizines [175] and the influence of alkyl substituents in various positions of the aminodialkene substrate on product diastereoselectivity was probed. Neodymium-based catalysts are particularly efficient for six-membered ring formation (40). The methodology has found further application in the synthesis of tri- and tetracyclic alkaloidal skeletons (41) [176].

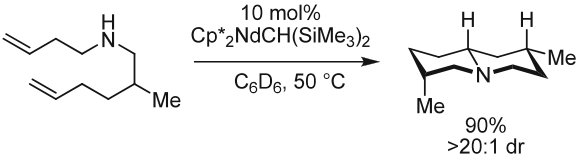

(40)

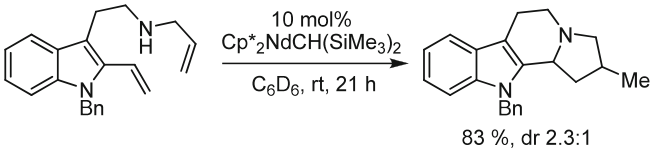

(41)

6.3 Intermolecular Hydroamination

Although *intramolecular* hydroamination reactions are catalyzed very efficiently by rare-earth metal catalysts, *inter*molecular hydroamination reactions are significantly more challenging and only a limited number of reports, utilizing either

lanthanocene [98–100], phenylene-bridged binuclear half-sandwich [102], or binaphtholate [101] catalysts, have been documented in the literature. The reaction of an unactivated alkene requires large excess of the alkene in order to overcome the competition between strongly binding amines and weakly binding alkenes, even if the sterically open *ansa*-lanthanocene $Me_2Si(C_5Me_4)_2NdCH(SiMe_3)_2$ (**15**-Nd) is employed (42) [98].

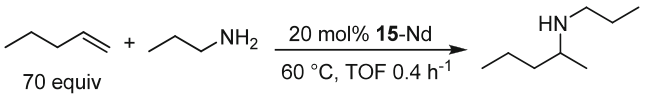

(42)

A sequence of *inter*- and *intramolecular* hydroaminations and carbocyclizations of the aminoalkeneyne **34** substrate allows the facile assembly of the tricyclic polyheterocycle **35** with exclusive *trans*-diastereoselectivity (43) [99].

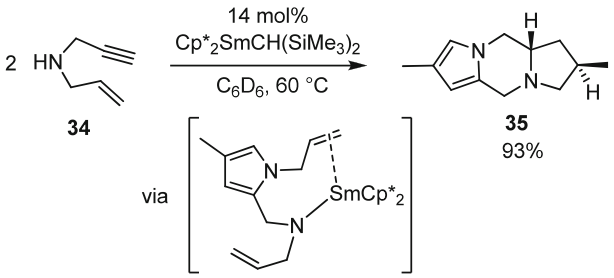

(43)

Hydroamination of vinyl arenes is a more facile process, proceeding exclusively via 2,1 insertion (Fig. 21) [100] obviously resulting from an aryl-directing effect as discussed in Sect. 3.1.

Trivinyl benzene may be utilized in a hydroamination/carbocyclization process that is initiated by an intramolecular *anti*-Markovnikov addition of *n*-propylamine followed by an intramolecular hydroamination and a highly diastereoselective carbocyclization step (44) [100].

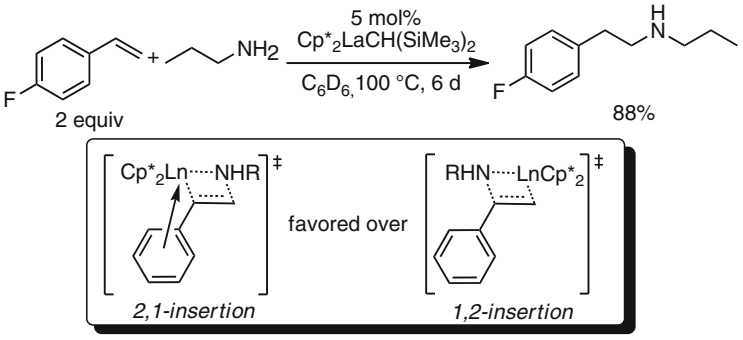

Fig. 21 *Anti*-Markovnikov hydroamination of vinyl arenes [100]

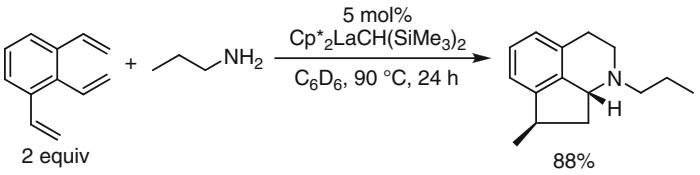

(44)

Another versatile class of unsaturated substrate for intermolecular hydroaminations are methylenecyclopropanes which utilize the ring strain of the cyclopropane ring as the driving force for the reaction. Ring opening of the unsymmetrical phenylmethylenecyclopropane proceeds with high regioselectivity to generate the linear product predominantly (Scheme 10) [100].

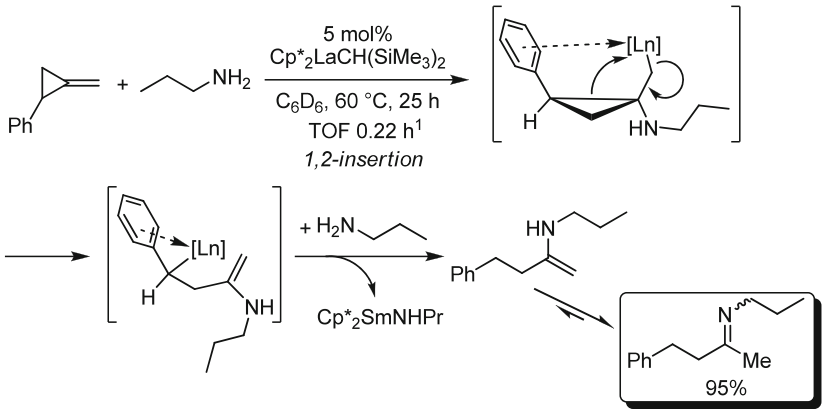

Scheme 10 Intermolecular hydroamination of phenylmethylenecyclopropane [100]

Intermolecular hydroamination of internal alkynes with nonequivalent substituents give the corresponding imines in a regioselective fashion (45) using the *ansa*-lanthanocene $Me_2Si(C_5Me_4)_2NdCH(SiMe_3)_2$ (**15**-Nd) [100].

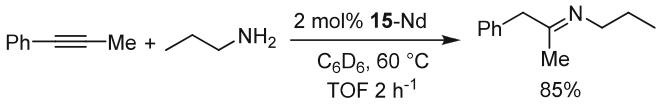

(45)

7 Catalytic Hydrophosphination

Significant progress in organolanthanide-catalyzed hydroamination over the last two decades has sparked the interest in the development of analogous catalytic hydrofunctionalization protocols. Catalytic hydrophosphination of unsaturated carbon–carbon linkages offers an attractive atom-economic route to phosphines [87, 177]. It should be noted that inter- and intramolecular hydrophosphinations are also

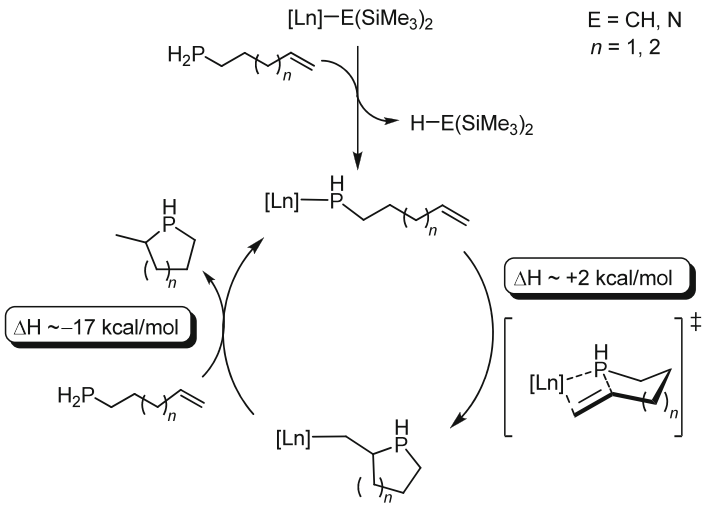

Fig. 22 Mechanism of intramolecular hydrophosphination [179, 181]

catalyzed by Brønsted acids, bases, and free radical initiators, and they can proceed spontaneously in the presence of light. However, the metal-catalyzed hydrophosphination may allow control of the regio- and stereochemistry of this process.

The mechanism and scope of rare-earth metal-catalyzed intramolecular hydrophosphination has been studied in detail by Marks and coworkers [147, 178–181]. The hydrophosphination of phosphinoalkenes is believed to proceed through a mechanism analogous to that of hydroamination. The rate-determining alkene insertion into the Ln–P bond is nearly thermoneutral, while the faster protolytic σ-bond metathesis step is exothermic (Fig. 22) [179, 181]. The experimental observation of a first-order rate dependence on catalyst concentration and zero-order rate dependence on substrate concentration are supportive of this mechanism. A notable feature is a significant product inhibition observed after the first half-life of the reaction. This is apparently caused by a competitive binding of a cyclic phosphine to the metal center that impedes coordination of the phosphinoalkene substrate and, therefore, diminishes catalytic performance [179].

Interestingly, although phosphines are slightly stronger Brønsted acids than amines [182], protonolysis of the precatalyst Ln–N or Ln–C bond with a phosphine proceeds much slower than in case of hydroamination, which is attributed to the softer nature of phosphorous versus nitrogen [179] and a weaker Ln–P bond compared to the Ln–N bond [181, 183]. Thus, in contrast to hydroamination, hydrophosphination is a protonation-controlled process, as shown by calculations [181].

Another interesting aspect is the metal size effect. In general, increasing ionic radii correlate with enhanced catalytic activity in hydroamination/cyclization of aminoalkenes [27, 103, 114]. However, a different trend is observed for phosphinoalkenes. Here, the mid-sized yttrium shows the highest reactivity, followed by lutetium and samarium, while the largest rare-earth metal, lanthanum, is the least active catalyst system [179].

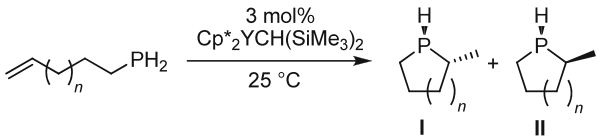

n	I:II	TOF /h^{-1}
1	29:54	50.1
2	89:9	91·3

Scheme 11 Catalytic hydrophosphination of phosphinoalkenes [179]

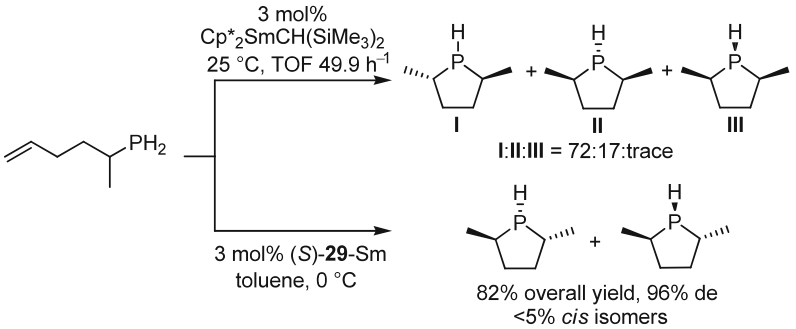

Scheme 12 Diastereoselective hydrophosphination/cyclization of chiral phosphinoalkenes [147, 179]

Typical examples illustrating the scope of catalytic hydrophosphinations of phosphinoalkenes and phosphinoalkynes are shown in Schemes 11 and 12, and (46) and (47). Analogous to the corresponding intramolecular hydroamination reactions, the hydrophosphination generally proceeds as an *exo*-cyclization to afford five- and six-membered phosphacycles, but in contrast to hydroamination formation of seven-membered rings remains a challenge. In general, intramolecular hydrophosphinations are ca. 5–10 times slower than the corresponding hydroaminations [179]. Lanthanocenes [179] and homoleptic rare-earth metal trisalkyls or trisamides (47) [180] have been used as catalysts. An important feature of the process is that an additional P-stereocenter is generated due to slow inversion on phosphorous [184] and mixtures of diastereomeric products are obtained even in case of achiral phosphinoalkenes. The diastereoselectivity was found to be sensitive to both metal and ligand framework [179, 180]. *Trans*-disubstituted phospholanes are formed with high preference (>20:1) over the *cis*-isomer and high diastereoselectivity when the chiral octahydrofluorenyl-based catalyst (*S*)-**29**-Sm is employed (Scheme 12) [147].

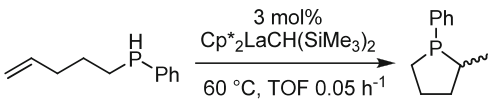

(46)

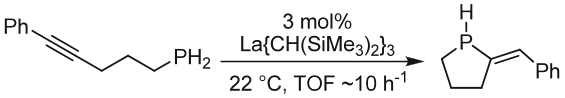

(47)

Organolanthanide-catalyzed *intermolecular* hydrophosphination is a more facile process than *intermolecular* hydroamination. The reaction of alkynes, dienes, and activated alkenes with diphenylphosphine was achieved utilizing the ytterbium imine complex **9** (Fig. 8) as catalyst [185–188]. Unsymmetric internal alkynes react regioselectively, presumably due to an aryl-directing effect (48) [186].

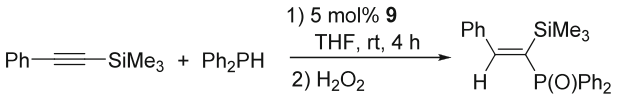

100%, *E*/*Z* 100:0 (48)

The hydrophosphination of 1,3-butadiene with PH_3 catalyzed by Cp_2EuH should proceed predominantly via a 1,4-addition and to a lesser extend through a 1,2-addition pathway based on a computational study [189]. The reaction of isoprene with diphenylphosphine indeed forms both regioisomers (49) [186]. Isolated double bonds are also reactive, as styrene derivatives are almost as reactive as alkynes (50); however, simple unactivated alkenes, such as 1-decene, are unreactive even at elevated temperatures [186].

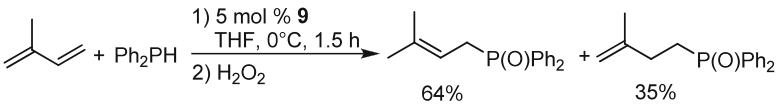

(49)

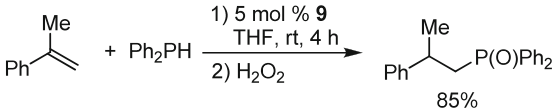

(50)

8 Catalytic Hydroalkoxylation

While the highly versatile rare-earth metal-catalyzed hydrogenation, hydroboration, hydrosilylation, hydroamination, and hydrophosphination has been studied over the last two decades, the rare-earth metal-mediated activation of the hydroxyl O–H bond for an analogous hydroalkoxylation process [87, 190] has been reported only recently. Homoleptic trisamides were reported to catalyze the smooth cyclization of allenyl alcohols [191] and alkynyl alcohols [191, 192] to form the corresponding unsaturated ethers.

Cyclization of penta-3,4-dien-1-ol (**36**) affords a mixture of exocyclic products (51). However, cyclization of the isomeric pent-4-yn-1-ol (**37**) forms methylene tetrahydrofurane exclusively (52) [191]. The reaction can also be applied to

secondary alcohols and the formation of six-membered rings, though significantly harsher reaction conditions are required to produce methylene tetrahydropyrane derivatives (53) [192].

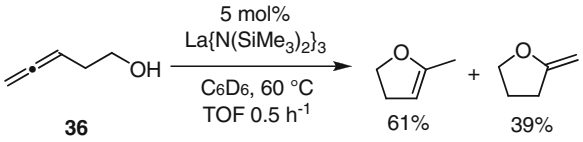

(51)

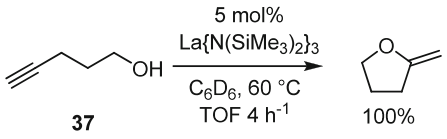

(52)

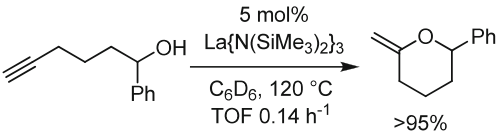

(53)

The reaction is believed to proceed via a mechanism analogous to hydroamination and hydrophosphination. There is experimental evidence for a rate-determining insertion step (Fig. 23). The high oxophilicity of the lanthanide ion results in a high barrier for the olefin insertion and therefore, diminished reactivity of alkenyl alcohols. Rare-earth metal triflates are also capable to catalyze cyclization of alkenyl alcohols in ionic liquids [193], although the mechanism is unlikely to be similar to the σ-bond metathesis mechanism discussed above.

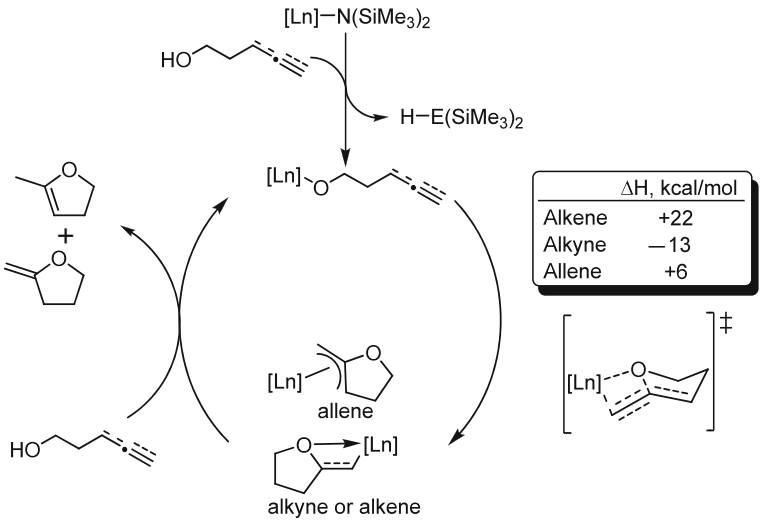

Fig. 23 Proposed mechanism for rare-earth metal-catalyzed hydroalkoxylation [191, 192]

9 Catalytic Alkene and Alkyne Coupling

Carbometallation of multiple carbon–carbon bonds is an atom-economical approach to new organometallic species, which can be subjected to further transformations to complete a catalytic cycle.

An interesting cyclodimerization of internal alkynes is apparently proceeding via metallation in the propargylic position, followed by an insertion of a second alkyne molecule, intramolecular carbometallation and σ-bond metathetical protonolysis (Fig. 24) [65]. The reaction is slow even at elevated temperatures and the insertion is not regioselective in case of unsymmetrical alkynes. More hindered substituents such as ^{t}Bu are not tolerated as the reaction stops at the metallation step. The reaction is more of a fundamental interest, as the cyclization pattern is different from the most common [2 + 2] route of existing protocols of transition-metal (in particular cobalt)-catalyzed alkyne cyclodimerization, which are significantly more versatile and synthetically applicable [194].

The dimerization of terminal alkynes is a straightforward process which is catalyzed by lanthanocenes of scandium [195, 196], yttrium [66, 197], lanthanum

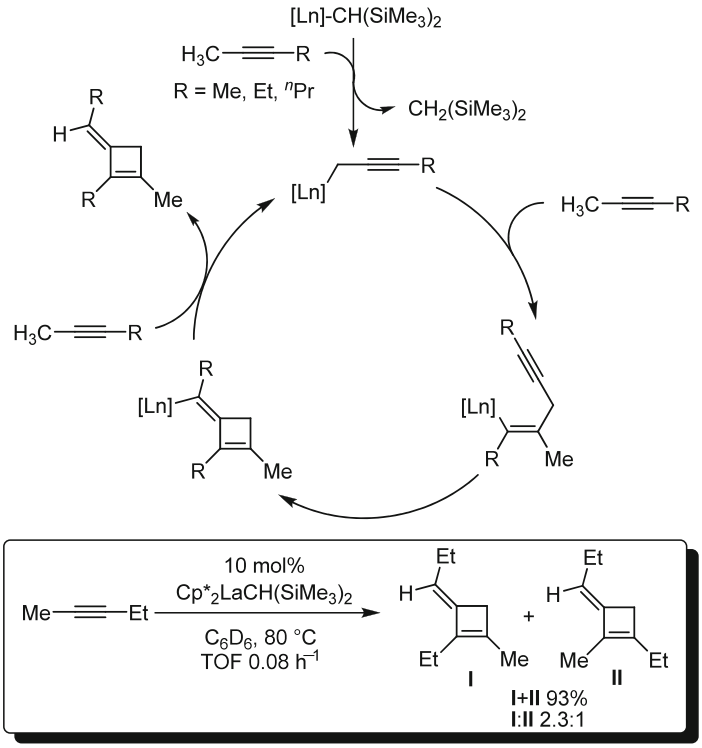

Fig. 24 Catalytic dimerization/cyclization of internal alkynes [65]

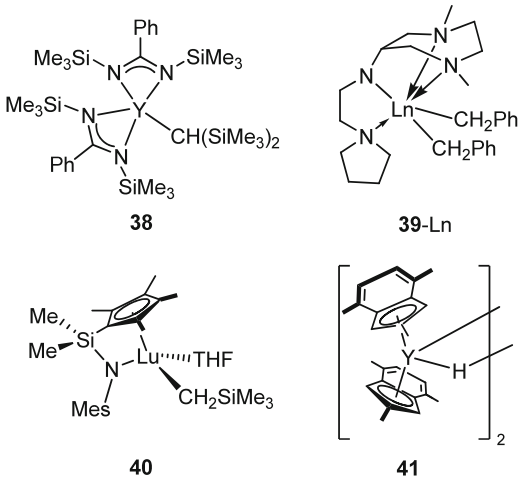

Fig. 25 Rare-earth metal catalysts for alkene and alkyne dimerizations [201–204]

[66, 198], cerium [66, 198], and samarium [199], as well as a half-sandwich aryloxide yttrium complex [200]. The reaction cleanly provides 2,4-disubstituted enynes (54) [195].

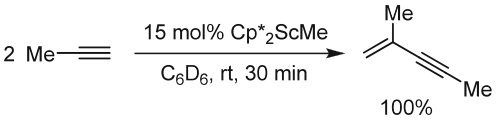

(54)

Postmetallocene catalysts such as the bis(benzamidinato)yttrium alkyl **38** (Fig. 25) [201] have been studied with respect to their activity in these alkyne dimerizations as well (55). However, the catalytic activity is significantly lower in comparison to the lanthanocenes, and the catalyst is not applicable to nonhindered alkynes such as propyne. Larger substituents (e.g., Ph, ^{t}Bu) as well as elevated temperatures are required [201].

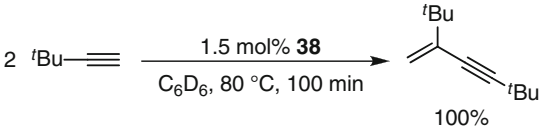

(55)

Neutral and cationic chelating amide complexes [202, 205] exhibit an interesting selectivity pattern producing exclusively tail-to-tail dimers with excellent Z selectivity of the internal double bond (Scheme 13) [202]. In case of the smaller yttrium complex, a higher catalytic activity is observed for the cationic species generated with $[PhNMe_2H][B(C_6F_5)_4]$, while for the larger lanthanum the neutral species is more effective.

The Z-tail-to-tail dimers can also be obtained with high selectivity from aryl-substituted alkynes using the trisamide $Ln\{N(SiMe_3)_2\}_3$ (Ln = Y, La, Sm) [206] or the constrained-geometry catalyst system **40** [203]. The latter system is more

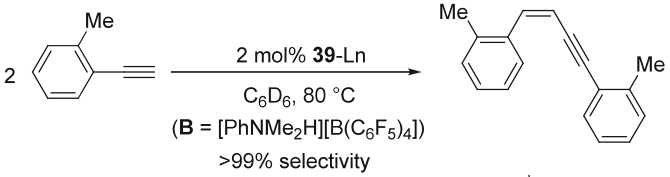

Ln	activator	*t* / min	conv. / %
Y	--	90	--
Y	**B**	30	100
La	--	90	>99
La	**B**	40	<5

Scheme 13 *Z*-selective tail-to-tail dimerization of terminal alkynes [202]

interesting, since it provides the same selectivity for alkyl-substituted alkynes (56) whereas all other catalytic systems tend to give head-to-tail products in this case.

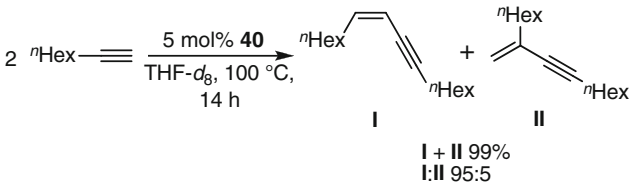

(56)

While rare-earth metals are proven powerful olefin polymerization catalysts [21–24], there are only limited reports on controlled olefin oligomerizations or selective olefin dimerizations utilizing these elements [204, 207, 208]. An *ansa*-scandocene [207] and the bis(indenyl)yttrium complex **41** (Fig. 25) [204] were reported to produce head-to-tail dimers from monosubstituted aliphatic alkenes (57). Complex **41** produces predominantly the tail-to tail adduct with styrene. The codimerization of an aliphatic alkene (including substrates containing various functionalities) with styrene affords *trans*-tail-to-tail dimers, apparently as a result of 1,2-insertion of the α-olefin followed by 2,1-insertion of styrene directed by the phenyl group (58).

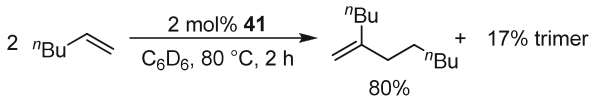

(57)

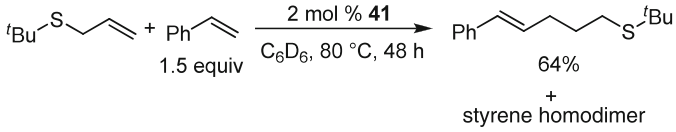

(58)

10 Catalytic C–H Activation

Despite numerous notable advances achieved over the last four decades, selective C–H activation remains a major challenge. Lanthanide complexes capable of activating C–H bonds have been studied intensively over the past 30 years [3, 11, 12, 209–211].

Pioneering work of Watson described the scrambling of $^{13}CH_4$ into soluble rare-earth metal complexes $Cp^*_2LnCH_3$ (Ln = Lu, Y) (59) [212]. The lutetocene system was also shown to activate C–H bonds of arenes and alkyl silanes [6, 213].

$$Cp^*_2Ln{-}CH_3 + {}^{13}CH_4 \longrightarrow Cp^*_2Ln{-}{}^{13}CH_3 + CH_4 \quad (59)$$

Ln = Lu, Y

The C–H activation by a number of related organo-rare-earth and organoactinide complexes has been studied thoroughly experimentally [195, 214] and theoretically [14, 17, 211], and a general σ-bond metathesis mechanism has been envisioned (Fig. 26).

Important experimental observations such as reaction rates that are first order in both reagents, large negative activation entropies, and a pronounced KIE ($k_H/k_D \sim$ 3–6) are strongly supportive of the mechanism shown in Fig. 26. The analysis of the transition state shows that the H transfer can be viewed as proton transfer between two methyl anions ($CH_3{}^{\delta-} \cdots H^{\delta+} \cdots CH_3{}^{\delta-}$) and therefore is thought to be better stabilized by an electrostatic field of early rare-earth metal cations, which indeed exhibit higher reactivity in most cases [10]. An alternative unimolecular tuck-in mechanism was proposed through DFT calculations for the alkyl metathesis of certain lanthanocenes, which can be competitive to the bimolecular process in case of small metals with a small ionic radius, such as scandium [215–217].

Despite the early breakthrough in the area, productive catalytic reactions of methane have not been reported until 2003. Tilley and Sadow have treated Cp^*_2ScMe with 10 equiv diphenylsilane and 150 atm of methane at 80°C [218]. After 1 week, 5 equiv of $MePh_2SiH$ were produced, indicating at least four catalytic turnovers (60). Despite moderate reactivity, this example of methane

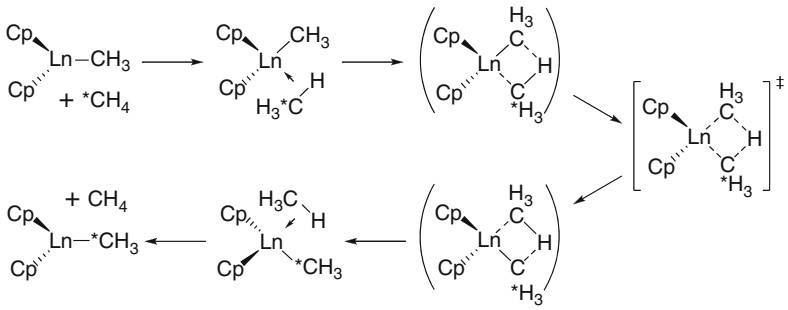

Fig. 26 C–H activation through σ-bond metathesis

dehydrosilylation is promising further developments of catalytic C–H activation reactions via the σ-bond metathesis processes.

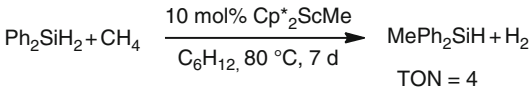

(60)

Permethylscandocene catalyzes also the hydromethylation of propene, but again only three to four turnovers were observed for this nondegenerate methane C–H activation (61) [219].

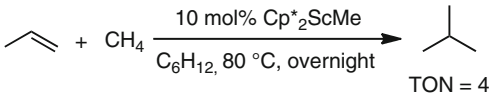

(61)

DFT calculations suggest that the fine interplay of both steric and electronic factors in this transformation account for the unique reactivity of scandium in conjunction with the bulky pentamethylcyclopentadienyl ligand. The larger lutetium [220] or the more open *ansa*-lanthanocene framework [221] results in stronger Lewis acidity of the complex that preferentially binds the alkene over methane and blocks the catalytic cycle.

11 Conclusions

The catalytic application of σ-bond metathesis processes has seen significant progress over the last decade with the development of novel postmetallocene catalysts, in particular in the area of catalytic hydroamination. Several new promising catalytic σ-bond metathesis processes – such as hydrophosphination, hydroalkoxylation, alkane dehydrosilylation, and alkene hydromethylation – have been developed during this time period. These areas leave room for significant catalyst improvements as they have not been explored in great detail. Catalytic hydrosilylation and hydroamination are certainly the processes that have advanced the farthest, although more information on functional group tolerance is necessary in order to allow the application in the synthesis of more complex target molecules. As all catalytic processes studied in this review can be initiated by the very same precatalysts, one can expect that we will see in future studies new synthetically useful single-pot and tandem processes analogous to hydrosilylation/carbocyclization, hydroamination/carbocyclization, and hydroamination/hydrosilylation.

References

1. Wailes PC, Weigold H, Bell AP (1972) J Organomet Chem 43:C32
2. Erker G (1977) J Organomet Chem 134:189
3. Arndtsen BA, Bergman RG, Mobley TA, Peterson TH (1995) Acc Chem Res 28:154

4. Vitale AA, San Filippo J (1982) J Am Chem Soc 104:7341
5. Gell KI, Posin B, Schwartz J, Williams GM (1982) J Am Chem Soc 104:1846
6. Watson PL, Parshall GW (1985) Acc Chem Res 18:51
7. Ziegler T, Folga E, Berces A (1993) J Am Chem Soc 115:636
8. Eisenstein O, Maron L (2002) J Organomet Chem 647:190
9. Sadow AD, Tilley TD (2005) J Am Chem Soc 127:643
10. Barros N, Eisenstein O, Maron L (2006) Dalton Trans:3052
11. Jones WD (2000) Science 287:1942
12. Labinger JA, Bercaw JE (2002) Nature 417:507
13. Lin Z (2007) Coord Chem Rev 251:2280
14. Balcells D, Clot E, Eisenstein O (2010) Chem Rev 110:749
15. Maron L, Perrin L, Eisenstein O (2002) Dalton Trans:534
16. Perrin L, Maron L, Eisenstein O (2002) Inorg Chem 41:4355
17. Hunt PA (2007) Dalton Trans:1743
18. Zhou X, Zhu M (2002) J Organomet Chem 647:28
19. Molander GA, Dowdy ED (1999) Top Organomet Chem 2:119
20. Molander GA, Romero JAC (2002) Chem Rev 102:2161
21. Yasuda H (1999) Top Organomet Chem 2:255
22. Hou Z, Wakatsuki Y (2002) Coord Chem Rev 231:1
23. Gromada J, Carpentier J-F, Mortreux A (2004) Coord Chem Rev 248:397
24. Hou Z, Luo Y, Li X (2006) J Organomet Chem 691:3114
25. Jeske G, Lauke H, Mauermann H, Schumann H, Marks TJ (1985) J Am Chem Soc 107:8111
26. Molander GA, Hoberg JO (1992) J Org Chem 57:3266
27. Giardello MA, Conticello VP, Brard L, Gagné MR, Marks TJ (1994) J Am Chem Soc 116:10241
28. Giardello MA, Conticello VP, Brard L, Sabat M, Rheingold AL, Stern CL, Marks TJ (1994) J Am Chem Soc 116:10212
29. Fu P-F, Brard L, Li Y, Marks TJ (1995) J Am Chem Soc 117:7157
30. Piers WE, Bercaw JE (1990) J Am Chem Soc 112:9406
31. Molander GA, Hoberg JO (1992) J Am Chem Soc 114:3123
32. Haar CM, Stern CL, Marks TJ (1996) Organometallics 15:1765
33. Jones GR, Landais Y (1996) Tetrahedron 52:7599
34. Voskoboynikov AZ, Parshina IN, Shestakova AK, Butin KP, Beletskaya IP, Kuz'mina LG, Howard JAK (1997) Organometallics 16:4041
35. Voskoboynikov AZ, Shestakova AK, Beletskaya IP (2001) Organometallics 20:2794
36. Forsyth CM, Nolan SP, Marks TJ (1991) Organometallics 10:2543
37. Radu NS, Tilley TD, Rheingold AL (1992) J Am Chem Soc 114:8293
38. Radu NS, Tilley TD (1995) J Am Chem Soc 117:5863
39. Tilley TD (1993) Acc Chem Res 26:22
40. Watson PL, Tebbe FN (1990) (du Pont de Nemours, E. I., and Co., USA). US Patent 4,965,386
41. Beletskaya IP, Voskoboinikov AZ, Parshina IN, Magomedov GK-I (1990) Russ Chem Bull 39:613
42. Sakakura T, Lautenschlager H-J, Tanaka M (1991) J Chem Soc Chem Commun:40
43. Onozawa S-Y, Sakakura T, Tanaka M (1994) Tetrahedron Lett 35:8177
44. Molander GA, Julius M (1992) J Org Chem 57:6347
45. Molander GA, Dowdy ED, Noll BC (1998) Organometallics 17:3754
46. Fu P-F (2006) J Mol Catal A Chem 243:253
47. Molander GA, Winterfeld J (1996) J Organomet Chem 524:275
48. Trifonov AA, Spaniol TP, Okuda J (2001) Organometallics 20:4869
49. Tardif O, Nishiura M, Hou Z (2003) Tetrahedron 59:10525
50. Trifonov AA, Spaniol TP, Okuda J (2004) Dalton Trans:2245
51. Robert D, Trifonov AA, Voth P, Okuda J (2006) J Organomet Chem 691:4393
52. Hou Z, Zhang Y, Tardif O, Wakatsuki Y (2001) J Am Chem Soc 123:9216
53. Gountchev TI, Tilley TD (1999) Organometallics 18:5661

54. Takaki K, Sonoda K, Kousaka T, Koshoji G, Shishido T, Takehira K (2001) Tetrahedron Lett 42:9211
55. Takaki K, Komeyama K, Takehira K (2003) Tetrahedron 59:10381
56. Gribkov DV, Hampel F, Hultzsch KC (2004) Eur J Inorg Chem:4091
57. Rastätter M, Zulys A, Roesky PW (2006) Chem Commun:874
58. Rastätter M, Zulys A, Roesky PW (2007) Chem Eur J 13:3606
59. Elvidge BR, Arndt S, Spaniol TP, Okuda J (2006) Dalton Trans:890
60. Konkol M, Kondracka M, Voth P, Spaniol TP, Okuda J (2008) Organometallics 27:3774
61. Ge S, Meetsma A, Hessen B (2008) Organometallics 27:3131
62. Horino Y, Livinghouse T (2004) Organometallics 23:12
63. Lyubov DM, Bubnov AM, Fukin GK, Dolgushin FM, Antipin MY, Pelce O, Schappacher M, Guillaume SM, Trifonov AA (2008) Eur J Inorg Chem:2090
64. Hultzsch KC, Voth P, Beckerle K, Spaniol TP, Okuda J (2000) Organometallics 19:228
65. Heeres HJ, Heeres A, Teuben JH (1990) Organometallics 9:1508
66. Heeres HJ, Teuben JH (1991) Organometallics 10:1980
67. Molander GA, Retsch WH (1995) Organometallics 14:4570
68. Molander GA, Retsch WH (1997) J Am Chem Soc 119:8817
69. Molander GA, Romero JAC, Corrette CP (2002) J Organomet Chem 647:225
70. Retsch WH (1997) PhD thesis, University of Colorado at Boulder
71. Molander GA, Nichols PJ (1995) J Am Chem Soc 117:4415
72. Molander GA, Romero JAC (2005) Tetrahedron 61:2631
73. Molander GA, Nichols PJ, Noll BC (1998) J Org Chem 63:2292
74. Molander GA, Dowdy ED (1998) J Org Chem 63:3386
75. Muci AR, Bercaw JE (2000) Tetrahedron Lett 41:7609
76. Smith ND, Mancuso J, Lautens M (2000) Chem Rev 100:3257
77. Voskoboynikov AZ, Beletskaya IP (1995) New J Chem 19:723
78. Burgess K, Ohlmeyer MJ (1991) Chem Rev 91:1179
79. Miyaura N (2001) In: Togni A, Grützmacher H (eds) Catalytic heterofunctionalization from hydroamination to hydrozirconation. Wiley, Weinheim, p 1
80. Harrison KN, Marks TJ (1992) J Am Chem Soc 114:9220
81. Bijpost EA, Duchateau R, Teuben JH (1995) J Mol Catal A Chem 95:121
82. Horino Y, Livinghouse T, Stan M (2004) Synlett:2639
83. Molander GA, Pfeiffer D (2001) Org Lett 3:361
84. Evans DA, Muci AR, Stuermer R (1993) J Org Chem 58:5307
85. Müller TE, Beller M (1998) Chem Rev 98:675
86. Brunet JJ, Neibecker D (2001) In:Togni A, Grützmacher H (eds) Catalytic heterofunctionalization from hydroamination to hydrozirconation. Wiley, Weinheim, p 91
87. Alonso F, Beletskaya IP, Yus M (2004) Chem Rev 104:3079
88. Müller TE, Hultzsch KC, Yus M, Foubelo F, Tada M (2008) Chem Rev 108:3795
89. Doye S (2009) In: Enders, D (ed) Science of synthesis, vol 40a. Thieme, Stuttgart, p 241
90. Roesky PW, Müller TE (2003) Angew Chem Int Ed 42:2708
91. Hultzsch KC (2005) Adv Synth Catal 347:367
92. Hultzsch KC (2005) Org Biomol Chem 3:1819
93. Aillaud I, Collin J, Hannedouche J, Schulz E (2007) Dalton Trans:5105
94. Zi G (2009) Dalton Trans:9101
95. Chemler SR (2009) Org Biomol Chem 7:3009
96. Reznichenko AL, Hultzsch KC (2010) In: Nugent TC (ed) Chiral amine synthesis: methods, developments and applications. Wiley, Weinheim, p 341
97. Hong S, Marks TJ (2004) Acc Chem Res 37:673
98. Li Y, Marks TJ (1996) Organometallics 15:3770
99. Li Y, Marks TJ (1998) J Am Chem Soc 120:1757
100. Ryu J-S, Li GY, Marks TJ (2003) J Am Chem Soc 125:12584
101. Gribkov DV, Hultzsch KC, Hampel F (2006) J Am Chem Soc 128:3748
102. Yuen HF, Marks TJ (2009) Organometallics 28:2423
103. Gagné MR, Stern CL, Marks TJ (1992) J Am Chem Soc 114:275

104. Ryu J-S, Marks TJ, McDonald FE (2004) J Org Chem 69:1038
105. Li Y, Fu P-F, Marks TJ (1994) Organometallics 13:439
106. Li Y, Marks TJ (1996) J Am Chem Soc 118:9295
107. Hong S, Marks TJ (2002) J Am Chem Soc 124:7886
108. Hong S, Kawaoka AM, Marks TJ (2003) J Am Chem Soc 125:15878
109. Motta A, Lanza G, Fragalà IL, Marks TJ (2004) Organometallics 23:4097
110. Motta A, Fragalà IL, Marks TJ (2006) Organometallics 25:5533
111. Tobisch S (2005) J Am Chem Soc 127:11979
112. Tobisch S (2005) Chem Eur J 11:6372
113. Tobisch S (2006) Chem Eur J 12:2520
114. Gagné MR, Marks TJ (1989) J Am Chem Soc 111:4108
115. Gribkov DV, Hultzsch KC, Hampel F (2003) Chem Eur J 9:4796
116. Hultzsch KC, Hampel F, Wagner T (2004) Organometallics 23:2601
117. Jung ME, Piizzi G (2005) Chem Rev 105:1735
118. Tian S, Arredondo VM, Stern CL, Marks TJ (1999) Organometallics 18:2568
119. Panda TK, Hrib CG, Jones PG, Jenter J, Roesky PW, Tamm M (2008) Eur J Inorg Chem:4270
120. Yuen HF, Marks TJ (2008) Organometallics 27:155
121. Xu X, Chen Y, Feng J, Zou G, Sun J (2010) Organometallics 29:549
122. Bürgstein MR, Berberich H, Roesky PW (2001) Chem Eur J 7:3078
123. Kim YK, Livinghouse T, Bercaw JE (2001) Tetrahedron Lett 42:2933
124. Quinet C, Ates A, Markó IE (2008) Tetrahedron Lett 49:5032
125. Kim YK, Livinghouse T (2002) Angew Chem Int Ed 41:3645
126. Kim YK, Livinghouse T, Horino Y (2003) J Am Chem Soc 125:9560
127. Kim JY, Livinghouse T (2005) Org Lett 7:4391
128. Bürgstein MR, Berberich H, Roesky PW (1998) Organometallics 17:1452
129. Zulys A, Panda TK, Gamer MT, Roesky PW (2004) Chem Commun:2584
130. Panda TK, Zulys A, Gamer MT, Roesky PW (2005) Organometallics 24:2197
131. Panda TK, Zulys A, Gamer MT, Roesky PW (2005) J Organomet Chem 690:5078
132. Lauterwasser F, Hayes PG, Bräse S, Piers WE, Schafer LL (2004) Organometallics 23:2234
133. Lu E, Gan W, Chen Y (2009) Organometallics 28:2318
134. Bambirra S, Tsurugi H, van Leusen D, Hessen B (2006) Dalton Trans:1157
135. Ge S, Meetsma A, Hessen B (2008) Organometallics 27:5339
136. Stanlake LJE, Schafer LL (2009) Organometallics 28:3990
137. Pawlikowski AV, Ellern A, Sadow AD (2009) Inorg Chem 48:8020
138. Ryu J-S, Marks TJ, McDonald FE (2001) Org Lett 3:3091
139. Molander GA, Dowdy ED (1998) J Org Chem 63:8983
140. Molander GA, Dowdy ED (1999) J Org Chem 64:6515
141. Kim H, Livinghouse T, Shim JH, Lee SG, Lee PH (2006) Adv Synth Catal 348:701
142. Molander GA, Hasegawa H (2004) Heterocycles 64:467
143. Arredondo VM, McDonald FE, Marks TJ (1998) J Am Chem Soc 120:4871
144. Arredondo VM, McDonald FE, Marks TJ (1999) Organometallics 18:1949
145. Arredondo VM, Tian S, McDonald FE, Marks TJ (1999) J Am Chem Soc 121:3633
146. Gagné MR, Brard L, Conticello VP, Giardello MA, Stern CL, Marks TJ (1992) Organometallics 11:2003
147. Douglass MR, Ogasawara M, Hong S, Metz MV, Marks TJ (2002) Organometallics 21:283
148. Vitanova DV, Hampel F, Hultzsch KC (2007) J Organomet Chem 692:4690
149. Hong S, Tian S, Metz MV, Marks TJ (2003) J Am Chem Soc 125:14768
150. O'Shaughnessy PN, Knight PD, Morton C, Gillespie KM, Scott P (2003) Chem Commun:1770
151. O'Shaughnessy PN, Scott P (2003) Tetrahedron Asymmetry 14:1979
152. O'Shaughnessy PN, Gillespie KM, Knight PD, Munslow I, Scott P (2004) Dalton Trans:2251
153. Collin J, Daran J-D, Schulz E, Trifonov A (2003) Chem Commun:3048
154. Collin J, Daran J-D, Jacquet O, Schulz E, Trifonov A (2005) Chem Eur J 11:3455
155. Riegert D, Collin J, Meddour A, Schulz E, Trifonov A (2006) J Org Chem 71:2514

156. Riegert D, Collin J, Daran J-D, Fillebeen T, Schulz E, Lyubov D, Fukin G, Trifonov A (2007) Eur J Inorg Chem:1159
157. Hannedouche J, Aillaud I, Collin J, Schulz E, Trifonov A (2008) Chem Commun:3552
158. Aillaud I, Collin J, Duhayon C, Guillot R, Lyubov D, Schulz E, Trifonov A (2008) Chem Eur J 14:2189
159. Aillaud I, Lyubov D, Collin J, Guillot R, Hannedouche J, Schulz E, Trifonov A (2008) Organometallics 27:5929
160. Aillaud I, Wright K, Collin J, Schulz E, Mazaleyrat J-P (2008) Tetrahedron Asymmetry 19:82
161. Kim JY, Livinghouse T (2005) Org Lett 7:1737
162. Kim H, Kim YK, Shim JH, Kim M, Han M, Livinghouse T, Lee PH (2006) Adv Synth Catal 348:2609
163. Gribkov DV, Hultzsch KC (2004) Chem Commun:730
164. Meyer N, Zulys A, Roesky PW (2006) Organometallics 25:4179
165. Yu X, Marks TJ (2007) Organometallics 26:365
166. Heck R, Schulz E, Collin J, Carpentier J-F (2007) J Mol Catal A Chem 268:163
167. Xiang L, Wang Q, Song H, Zi G (2007) Organometallics 26:5323
168. Zi G, Xiang L, Song H (2008) Organometallics 27:1242
169. Wang Q, Xiang L, Song H, Zi G (2008) Inorg Chem 47:4319
170. Wang Q, Xiang L, Song H, Zi G (2009) J Organomet Chem 694:691
171. Reznichenko AL, Hampel F, Hultzsch KC (2009) Chem Eur J 15:12819
172. Obora Y, Ohta T, Stern CL, Marks TJ (1997) J Am Chem Soc 119:3745
173. Takaki K, Kamata T, Miura Y, Shishido T, Takehira K (1999) J Org Chem 64:3891
174. Li Y, Marks TJ (1996) J Am Chem Soc 118:707
175. Molander GA, Pack SK (2003) J Org Chem 68:9214
176. Molander GA, Pack SK (2003) Tetrahedron 59:10581
177. Tanaka M (2004) Top Curr Chem 232:25
178. Douglass MR, Marks TJ (2000) J Am Chem Soc 122:1824
179. Douglass MR, Stern CL, Marks TJ (2001) J Am Chem Soc 123:10221
180. Kawaoka AM, Douglass MR, Marks TJ (2003) Organometallics 22:4630
181. Motta A, Fragalà IL, Marks TJ (2005) Organometallics 24:4995
182. Issleib K, Kümmel R (1965) J Organomet Chem 3:84
183. Nolan SP, Stern, D, Hedden, D, Marks, TJ (1990) ACS Symp Ser 428:159
184. Baechler RD, Mislow K (1970) J Am Chem Soc 92:3090
185. Takaki K, Takeda M, Koshoji G, Shishido T, Takehira K (2001) Tetrahedron Lett 42:6357
186. Takaki K, Koshoji G, Komeyama K, Takeda M, Shishido T, Kitani A, Takehira K (2003) J Org Chem 68:6554
187. Takaki K, Komeyama K, Kobayashi D, Kawabata T, Takehira K (2006) J Alloys Compd: 408–412, 432
188. Komeyama K, Kobayashi D, Yamamoto Y, Takehira K, Takaki K (2006) Tetrahedron 62:2511
189. Mercy M, Maron L (2009) Dalton Trans:3014
190. Tani K, Kataoka Y (2001) In: Togni A, Grützmacher H (eds) Catalytic heterofunctionalization from hydroamination to hydrozirconation. Wiley, Weinheim, p 171
191. Yu X, Seo S, Marks TJ (2007) J Am Chem Soc 129:7244
192. Seo S, Yu X, Marks TJ (2009) J Am Chem Soc 131:263
193. Dzudza A, Marks TJ (2009) Org Lett 11:1523
194. Haber S, Regitz M (1997) In: de Meijere A (ed) Houben-Weyl methods of organic chemistry, vol 17f. Thieme, New York, p 1051
195. Thompson ME, Baxter SM, Bulls AR, Burger BJ, Nolan MC, Santarsiero BD, Schaefer WP, Bercaw JE (1987) J Am Chem Soc 109:203
196. St. Clair M, Schaefer WP, Bercaw JE (1991) Organometallics 10:525
197. Den Haan KH, Wielstra Y, Teuben JH (1987) Organometallics 6:2053
198. Heeres HJ, Nijhoff J, Teuben JH, Rogers RD (1993) Organometallics 12:2609
199. Evans WJ, Keyer RA, Ziller JW (1993) Organometallics 12:2618

200. Schaverien CJ (1994) Organometallics 13:69
201. Duchateau R, van Wee CT, Teuben JH (1996) Organometallics 15:2291
202. Ge S, Meetsma A, Hessen B (2009) Organometallics 28:719
203. Nishiura M, Hou Z, Wakatsuki Y, Yamaki T, Miyamoto T (2003) J Am Chem Soc 125:1184
204. Kretschmer WP, Troyanov SI, Meetsma A, Hessen B, Teuben JH (1998) Organometallics 17:284
205. Tazelaar CGJ, Bambirra S, van Leusen D, Meetsma A, Hessen B, Teuben JH (2004) Organometallics 23:936
206. Komeyama K, Kawabata T, Takehira K, Takaki K (2005) J Org Chem 70:7260
207. Piers WE, Shapiro PJ, Bunel EE, Bercaw JE (1990) Synlett:74
208. Hajela S, Bercaw JE (1994) Organometallics 13:1147
209. Bercaw JE (1990) Pure Appl Chem 62:1151
210. Crabtree RH (2004) J Organomet Chem 689:4083
211. Sakaki S (2005) Top Organomet Chem 12:31
212. Watson PL (1983) J Am Chem Soc 105:6491
213. Watson PL (1983) J Chem Soc Chem Commun:276
214. Fendrick CM, Marks TJ (1986) J Am Chem Soc 108:425
215. Sherer EC, Cramer CJ (2003) Organometallics 22:1682
216. Woodrum NL, Cramer CJ (2006) Organometallics 25:68
217. Lewin JL, Woodrum NL, Cramer CJ (2006) Organometallics 25:5906
218. Sadow AD, Tilley TD (2003) Angew Chem Int Ed 42:803
219. Sadow AD, Tilley TD (2003) J Am Chem Soc 125:7971
220. Barros N, Eisenstein O, Maron L, Tilley TD (2006) Organometallics 25:5699
221. Barros N, Eisenstein O, Maron L, Tilley TD (2008) Organometallics 27:2252

Struct Bond (2010) 137: 49–108
DOI:10.1007/430_2010_16

Published online: 11 May 2010

Polymerization of 1,3-Conjugated Dienes with Rare-Earth Metal Precursors

Zhichao Zhang, Dongmei Cui, Baoli Wang, Bo Liu, and Yi Yang

Abstract This chapter surveys the publications except patents related to *cis*-1,4-, *trans*-1,4-, 3,4-regio-, and stereoselective polymerizations of 1,3-conjugated dienes with rare-earth metal-based catalytic systems during the past decade from 1999 to 2009. The concerned catalyst systems are classified into the conventional Ziegler–Natta catalysts, the modified Ziegler–Natta catalysts, and the single-site cationic systems composed of lanthanocene and noncyclopentadienyl precursors, respectively. For the conventional Ziegler–Natta catalysts of the most promising industry applicable recipe, the multicomponents based on lanthanide carboxylate or phosphate or alkoxide precursors, research works concern mainly about optimizing the catalyst preparation and polymerization techniques. Special emphases are put on the factors that influence the catalyst homogeneority, catalytic activity and efficiency, as well as *cis*-1,4-selectivity. Meanwhile, tailor-made lanthanide aryloxide and amide complexes are designed and fully characterized to mimic the conventional Ziegler–Natta catalysts, anticipated to elucidate the key processes, alkylation and cationization, for generating the active species. Regarding to the single-site catalytic systems generally comprising well-defined complexes containing lanthanide–carbon bonds, investigations cover their versatile catalytic activity and efficiency, and the distinguished regio- and stereoselectivity for both polymerization of dienes and copolymerization of dienes with alkenes. The correlation between the sterics and electronics of ligands and the molecular structures of the complexes and their catalytic performances are highlighted. The isolation of the probable active species in these polymerization processes from the stoichiometric reactions of the precursors with activators will be presented.

Keywords: Diene polymerization · Metallocene · Rare-earth metals · Specific polymerization · Ziegler–Natta

Z. Zhang, D. Cui (✉), B. Wang, B. Liu, and Y. Yang
State Key Laboratory of Polymer Physics and Chemistry, Changchun Institute of Applied Chemistry, Chinese Academy of Sciences, Changchun 130022, China
e-mail: dmcui@ciac.jl.cn

Contents

Abbreviations

Ar	Aryl
BD	Butadiene
BR	Polybutadiene rubber
Bu	Butyl
CN	Coordination number
cot	Cyclooctatetraene
Cp	Cyclopentadienyl
d	Day(s)
DIBAC	Diisobutylaluminum chloride
DIBAH	Diisobutylaluminum hydride
DMAC	Dimethylaluminum chloride
DME	Dimethoxyethane
DMPE	1,2-Bis(dimethylphosphino)ethane
DMSO	Dimethyl sulfoxide
EASC	Ethylaluminum sesquichloride
equiv	Equivalent(s)
Et	Ethyl
Flu	Fluorenyl
FTIR	Fourier transform infrared spectroscopy
h	Hour(s)
Hex	Hexyl
HIBAO	Hexaisobutylaluminoxane
^{i}Bu	Isobutyl
Ind	Indenyl
IP	Isoprene
^{i}Pr	Isopropyl
IR	Polyisoprene rubber
L	Liter(s)
Ln	Rare-earth metal (i.e., Sc, Y, La–Lu)
MAO	Methylaluminoxane
Me	Methyl

Mes	Mesityl
min	Minute(s)
MMA	Methyl methacrylate
MMAO	Modified methylaluminoxane
ND	Neodecanoate
NDH	Neodecanoic acid
NdP	Neodymium bis(2-ethylhexyl)phosphate
NdV	Neodymium versatate
NHC	*N*-heterocyclic carbene
NMR	Nuclear magnetic resonance
NR	Natural rubber
Oct	Octyl
Ph	Phenyl
Phen	1,10-Phenanthroline
Pr	Propyl
Py	Pyridine
RT	Room temperature
SBR	Styrene–butadiene rubbers
SEC	Size exclusion chromatography
TBP	Tributylphosphate
^{t}Bu	Tertbutyl
TEA	Triethylaluminum
THF	Tetrahydrofuran
TIBA	Triisobutylaluminum
TMA	Trimethylaluminum
TNHA	Tri(*n*-hexyl)aluminum
TNOA	Tri(*n*-octyl)aluminum
TON	Turnover number
VT	Variable temperature

1 Introduction

One of the everlasting topics in macromolecule chemistry is to prepare polymers with designated properties through precisely controlling the microstructures of polymer chains. Thus, polymerizations of 1,3-conjugated dienes have been one of the most important processes via which the simple C4–C5 monomers transfer into polymeric materials possessing *cis*-1,4, *trans*-1,4, *iso*-3,4 (or 1,2), *syndio*-3,4 (or 1,2), and *atactic*-3,4 (or 1,2) regularities and versatile properties and wide applications. For instance, the *cis*-1,4-regulated polybutadiene (BR) is high-performance rubber that can blend with other elastomers to make tyres, whilst polyisoprene (IR) when its *cis*-1,4-regularity is over 98% meanwhile has high molecular weight can be applied as an alternative to natural rubber (NR). The *trans*-1,4-regulated polydienes are usually employed as an important component of tires-sides and tread rubbers

as well as shape–memory elastomers, the crystallinity of which is governed by *trans*-1,4-content. The 3,4-(or 1,2-) polydienes have attracted an increasing attention for they can be used to prepare high-value-added rubbers or long-life "green" tires such as those with wet-skid resistance and low-rolling resistance. 3,4-(or 1,2-) Polybutadienes could be amorphous, semicrystalline and crystalline depending on both the 3,4-(or 1,2-) regiospecificity and the iso- or syndiotactic stereoregularity.

Although the 1,3-conjugated dienes could be polymerized via radical and anionic mechanisms, it was the discovery of the Ziegler–Natta catalysts at the middle of 1950s that started the era of coordination polymerizations, which exhibited overwhelming advantages on governing the regio- and stereoregularity to afford polymers with designed properties. Shortly after this event, patents on the use of Ziegler–Natta catalysts for the specific polymerizations of 1,3-conjugated dienes were filed, and Co- and Ti-based catalysts were employed to the large-scale industrial application. The Ziegler–Natta type catalyst systems based on lanthanide (Ln) elements came to the researchers' eyesight in 1964 when the Chinese scientists Shen et al. [1] discovered the binary lanthanide trichlorides combined with aluminum alkyls to initiate the highly *cis*-1,4-selective polymerization of butadiene albeit with low activity. Meanwhile, patents concerning the lanthanide binary catalyst systems and the succedent lanthanide ternary catalyst systems were submitted by Union Carbide Corporation and Goodyear, respectively [2–5]. Since 1980s, research on lanthanide catalysis toward polymerization of dienes had experienced a renaissance and become booming, as their superior performance than the Co-, Ti-, and Ni-based systems with respect to the activity and selectivity, less-gel formation as well as providing polymers with outstanding properties [6, 7]. For instance, *cis*-1,4-polymerization of butadiene with a Ziegler–Natta neodymium system affords polybutadiene, showing excellent abrasion and cracking resistance, raw polymer strength, and high tensile strength of the vulcanizates. Moreover, the residue of the catalysts does not arouse the aging performances except the cerium complexes owing to the stable trivalent oxidation state of lanthanide ions. Therefore, lanthanide η^3-allyls, the homogeneous Ziegler–Natta catalyst systems composed of lanthanide carboxylates, phosphates, or alkoxides and coactivators aluminum alkyls or aluminum alkyl chlorides, have been extensively investigated for their behaviors toward the *cis*-1,4-polymerization of dienes. Some research works relating butadiene polymerization were reviewed by Shen, Kuran, and Obsrecht [6–9], respectively. Meanwhile investigation of the mechanism of Ziegler–Natta catalysts and the molecular structure of the active species were carried out, emphases have been drawn on the interaction between the cocatalysts with the tailor-made and fully characterized lanthanide precursors, part of which was summarized by Anwander [10]. Recently, the single-site cationic catalysts based on lanthanocene, half-sandwich lanthanocene, and lanthanide precursors bearing noncyclopentadienyl (non-Cp) ligands, respectively, have gathered an upsurge in research interests [11–13]. These well-defined precursors have exhibited distinguished high *cis*-1,4-selectivity, well control on molecular weight and molecular weight distribution of the resultant polymers, which are strongly influenced by the sterics and electronics and framework of the ligands attached to the central metal ions. This will be discussed in detail in this contribution.

Regarding *trans*-1,4-selective polymerization of dienes, catalysts showing both high activity and *trans*-1,4-selectivity are rather limited, among which the widely explored systems are based on Ti, V, and Fe metals [14–19], those based on rare-earth metals [20, 21] emerged only recently, which will be highlighted. Similarly, the 3,4-selective polymerization of isoprene (the corresponding 1,2-polymerization of butadiene with lanthanide-based catalysts has been an unexplored area) has also received less attention. The efficient catalyst systems are scarce and restricted to the smaller transition metal-based complexes, and in few cases the 3,4-selectivity is over 90% [22–27]. The landmark constrain-geometry-configuration half-sandwich lanthanocenes, and the *C*2 symmetric non-Cp-ligated rare-earth metal complexes exhibiting high 3,4-selectivity or even stereoselectivity for the polymerization of isoprene, were just reported, which will be particularized. The copolymerization of dienes with alkenes *etc* monomers, providing new structural materials or high-added-value rubbers, has been reported less and usually suffers from the lowered activity and decreased molecular weight as well as broadened molecular weight distribution because of different polymerization mechanisms. Moreover, the amount of alkenes or dienes inserted into the copolymer chain remains low which is generally concomitant with the formation of homopolymers. Some recent breakthroughs in this research area will be presented at the last part of this chapter.

2 *cis*-1,4-Polymerization of 1,3-Conjugated Dienes

cis-1,4-Selective polymerization of diene is a very important process in the chemical industry to afford products among the most significant and widely used rubbers. It has been believed that a slight increase in the *cis*-1,4-regularity of the product leads to a great improvement in elastic properties [28–30]. A direct consequence of high *cis*-1,4-contents is strain-induced crystallization of raw rubbers as well as of the respective vulcanizates. As strain-induced crystallization beneficially influences the tack of raw rubbers as well as tensile strength and resistance of vulcanizates to abrasion and fatigue; therefore, the high *cis*-1,4-content makes Nd–BR particularly useful for tire applications [8].

2.1 Ziegler–Natta Rare-Earth Metal Precursors

2.1.1 Conventional Ziegler–Natta Rare-Earth Metal Precursors

The Ziegler–Natta rare-earth metal catalysts, mainly the binary systems $LnCl_3$–AlR_3 and the ternary systems LnL_3–AlR_3–$HAlR_2$ (or R_2AlX) (Ln = lanthanide including yttrium and scandium, L = carboxylate, phosphate, alkyl(aryl) oxide, allyl, X = halogen), have been the most simple to be prepared, economic, thermal

stable, and less sensitive to moisture and oxygen compared to those of metallocene catalysts. Meanwhile, they provide high *cis*-1,4-selectivity (∼97%) and exhibit high activity at very low catalytic concentration. Therefore, Ziegler–Natta rare-earth metal catalysts have the most promising potentials for industry application. However, there still have problems, for instance, the *cis*-1,4-selectivity drops obviously when the polymerization is performed at a higher temperature such as within 60–80°C, which will reduce the tensile strength of the polymers especially polyisoprene. The other is the less controlled molecular weight and broad molecular weight distribution of the resultant polymers owing to the multisite nature of these systems and their inferior solubility in the industry-used medium cyclohexane or hexane. Moreover, the structures of the catalytic precursors and the active species need to be characterized, and the mechanisms are still not completely understood [6–10]. Therefore, many efforts have been paid to modify the Ziegler–Natta catalysts to settle these problems. To enhance the activity of the binary catalyst systems [31–35], the addition of electron donor ligands such as alcohols, tetrahydrofuran, pyridine, dimethyl sulfoxide, phosphates, and amines to the system have been widely employed which usually does not result in any decrease in stereospecificity [36–40]. Zhang reported that addition of long-chain alcohol could generate soluble binary system $NdCl_3{\cdot}3EHOH$ (2-ethylhexanol) in hexane, which in combination with $AlEt_3$ exhibited higher activity for isoprene polymerization as compared with the typical ternary catalysts $NdCl_3/3^{i}PrOH$ (isopropanol)/TEA($AlEt_3$) and NdV(neodymium versatate)/DEAC($AlEt_2Cl$)/DIBA($Al(^{i}Bu)_2H$). Moreover, the molecular weight of the resultant polyisoprene can be controlled by varying the Al-to-Nd ratio and polymerization temperature and time, showing some degree of living mode, and its microstructure featuring high *cis*-1,4-stereospecificity (ca. 96%) [41]. Jain described the new neodymium chloride tripentanolate catalysts of the general formula $NdCl_3 \times 3L$(L = 1-pentanol, 2-pentanol, and 3-pentanol) prepared by an alcohol interchange reaction between neodymium chloride and the alcohols. The systems were evaluated for the polymerization of butadiene in cyclohexane using TEA as cocatalyst, among which the combination of $NdCl_3$ and 2-pentanol has higher catalytic activity followed by 1-pentanol and 3-pentanol. The conversions were increased with increases in catalyst and cocatalyst concentrations and temperature, and decrease in intrinsic viscosity value. The microstructure was found to have a predominantly *cis*-1,4-structure (99%), which was marginally influenced by variation in cocatalyst concentration and temperature [42]. Boisson employed a soluble arene complex $Nd(\eta^6\text{-}C_6H_5Me)(AlCl_4)_3$, prepared by mixing $NdCl_3$ and $AlCl_3$ in toluene to react in situ with the Lewis-acid MCl_x-masked silica (MCl_x = BCl_3, $AlCl_3$, $TiCl_4$, $ZrCl_4$, $SnCl_4$, $SbCl_5$, $HfCl_4$) (Scheme 1). They found that the resultant supported system based on BCl_3-modified silica was the most active for butadiene polymerization with an activity of 1,188 $g_{polym.}/(g_{cata.}\ h)$ allowing to polymerize butadiene at a very low neodymium concentration of around 10 ppm, and meanwhile the *cis*-1,4 insertion was superior by 99%. This supported catalyst also yielded high molecular weight polyisoprene with a high *cis*-1,4-content of 96.1% (Table 1) [43]. Masuda [44] synthesized directly neodymium isopropoxide $Nd(O^{i}Pr)_3$ which activated by MAO alone exhibited high efficiency

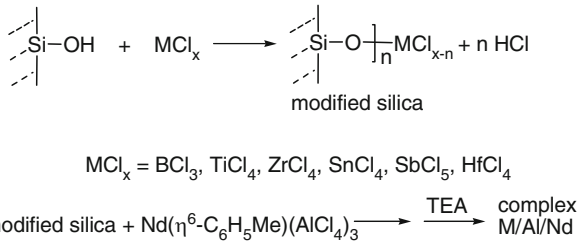

Scheme 1 Synthesis of silica-supported catalysts

Table 1 Polymerization of butadiene with various heterogeneous catalysts [43]

Run	Complex (mg)	Time (min)	Yield (g)	TOF (h^{-1})	η_{inh} (dL g^{-1})	*cis*-1,4 (%)
1[a]	Al/Nd1 (85)	60	1.1	13	3.12	>99
2[b]	Al/Nd2 (85)	30	6.5	153	2.28	>99
3	Ti/Al/Nd (83)	15	11.1	535	2.20	>99
4	Zr/Al/Nd (71)	60	0.8	11	2.25	>99
5	B/Al/Nd (35)	15	10.4	1,188	2.15	>99
6[c]	B/Al/Nd (30)	60	2.8	93	4.0	96.1
7	Sn/Al/Nd (77)	15	9.5	493	5.22	>99
8	Sb/Al/Nd (32)	30	4.0	250	4.39	>99
9	Hf/Al/Nd (108)	20	4.3	119	4.0	>99

[a]Al/Nd1: silica/$AlCl_3$/$NdCl_3$
[b]Al/Nd2: (Al/Nd1)/$AlEt_3$
[c]Polymerization of isoprene: solvent: cyclohexane (120 mL), isoprene (15 mL), DIBAH (3 mmol L^{-1}), 60°C

for isoprene polymerization in heptane even at low [Al]/[Nd] ratios (ca. 30) to give polyisoprene that possessed moderate to high *cis*-1,4-stereoregularity (ca. 90%), high molecular weight ($M_n = 10^5$), and relatively narrow molecular weight distributions (M_w/M_n = 1.9–2.8) without a halogen source although it is generally essential for high activity and high *cis*-1,4-specificity of AlR_3-activated Nd catalysts [45–48]. However, the same catalyst with MMAO resulted in relatively low polymer yield and low molecular weight in toluene and cyclized polyisoprene in dichloromethane, which might be ascribed to the cationic active species derived from MMAO. Addition of chlorine sources (DEAC, ^{t}BuCl, Me_3SiCl) improved the *cis*-1,4-stereoregularity of polymer up to 95% even at a high temperature 60°C albeit sacrificing polymer yield [49]. When dimethylphenylammonium tetrakis(pentafluorophenyl)borate [$HNMe_2Ph$][$B(C_6F_5)_4$]) and TIBA were applied as cocatalysts, the optimal catalyst composition was [Nd]/[borate]/[Al] = 1/1/30, which gave polyisoprene (>97% yield) with high molecular weight ($M_n \sim 2 \times 10^5$) and relatively narrow molecular weight distribution ($M_w/M_n \sim 2.0$) albeit a reduced *cis*-1,4-tacticity (~90%). If [Al]/[Nd] ratio was over 50 or [borate]/[Nd] ratio was not the exact 1, the resultant polymer had low *cis*-1,4-content or showed bimodal peaks in GPC accompanied by low yield, owing to the formation of multiple active species [50]. Boisson investigated the behavior of a new ternary system based

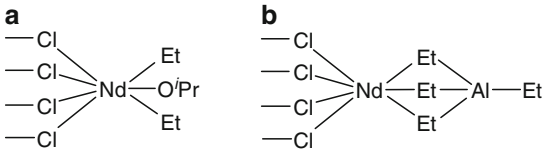

Fig. 1 Possible structures of active centers (**a**) and (**b**)

on an amide compound, $Nd\{N(SiMe_3)_2\}_3$/TIBA/DEAC in the polymerization of butadiene [51], which was at least as efficient as the classical ternary systems [52, 53], and remained highly active at very low neodymium concentrations ($1.35 \times 10^6 g/(mol_{Nd} \cdot h)$). Unlike neodymium alkoxides, the $Nd\{N(SiMe_3)_2\}_3$ was well dispersed in solution and did not form clusters. As commonly reported for lanthanide salts with oxygenated ligands, the catalyst activity depended on the Al-to-Nd ratio. The highest conversion was observed for a ratio between 2 and 2.5; unfortunately, the GPC curves showed a bimodal distribution, indicating the existence of at least two different active centers as shown in Fig. 1. When the ratio increased from 2 to 5, the lowest molecular weight peak (active center **b**) became predominant accompanied by the low *cis*-1,4-stereoregularity. Therefore, the active center which gave the highest molecular weight polymer (active center **a**) was also probably the most stereospecific.

In the meantime, many research works focused on optimizing the composition of the conventional homogeneous ternary Ziegler–Natta catalyst as well as the polymerization conditions. Coutinho et al. investigated a system composed of NdV, *tert*-butyl chloride, and diisobutylaluminum hydride (DIBAH) for butadiene polymerization. They found that increase of the monomer concentration shifted the activity curves to lower polymerization temperatures, meaning that the same activity obtained at higher polymerization temperatures, when higher monomer concentrations were used, can be attained at lower temperatures. This was in consistent with the performance of catalyst systems based on lanthanides with which the reaction rate presented a first-order dependence on the monomer concentration [54]. In contrast, the polymer microstructure was slightly influenced by the monomer concentration in the range of reaction temperature studied; however, a tendency of increasing the *cis*-1,4-unit content with the decrease of monomer concentration was indeed observed. This behavior may be attributed to a lower reaction medium viscosity, which provided higher monomer molecules mobility, thus favoring their complexation to the catalyst sites in appropriate configuration [55]. Obsrecht et al. [56] reported that solvents such as *n*-hexane, *tert*-butylbenzene (TBB), and toluene exerted distinct influence on the polymerization of butadiene by using NdV/DIBAH/EASC (ethylaluminum sesquichloride). From the polymerization kinetics that polymerization rates decreased in the order: *n*-hexane > TBB > toluene there was evidence of competitive coordination between aromatic solvents and butadiene to activate Nd-sites supported by Porri's view [57]. In addition, the conversion-time plot for the polymerization in toluene deviated from the first-order dependency, indicating the presence of the irreversible transfer of benzyl-H-atoms from toluene to active allyl-anionic polymer chains. The evolution of molecular weight distributions with monomer

conversion suggested two active catalyst species present in all three solvents. One of these two species was highly reactive ("hot") and short-lived. This species generated polybutadiene with high molecular weight. The second species had a low reactivity and lived the entire course of the polymerization. In *n*-hexane, the "hot" short-lived species was present only at the start of the polymerization, whereas in TBB and toluene, the "hot" short-lived species became evident at monomer conversion 10% and was constantly (re)generated. However, their finding – that *cis*-1,4-contents determined at final monomer conversion, 94.0% (*n*-hexane), 96.0% (toluene), and 98.0% (TBB) were higher in aromatic solvents than in *n*-hexane – was in contradiction with most other available studies in this field. Coutinho [58] also found that the aliphatic solvents, hexane, cyclohexane, and their mixtures behaved differently toward the NdV/DIBAH/^{t}BuCl-catalyzed butadiene polymerization. Cyclohexane had a solubility parameter (δ) higher than that of hexane and near of polybutadiene. As a consequence with the increase of cyclohexane proportion in the reaction medium, *cis*-1,4-content of the produced polybutadiene increased from 98.2 to 99.1%; however, the molecular weight (M_n from 1.9×10^5 to 0.44×10^5) reduced owing to its higher solvating power, that is, providing more active sites. This supposition was supported by the progressive increase on the molecular weight distribution (from 3.3 to 5.0) as the cyclohexane content increases in the polymerization solvent (Table 2).

Addition of electron donor compounds to binary systems significantly increased the solubility and the consequent higher activity, whereas, addition of which to ternary systems provoked a decrease in *cis*-1,4-units and an increase in *trans*-1, 4-units [59, 60]. This could be explained by Scheme 2 The *trans*-1,4-units are formed via route a_1 or $a_2 \rightarrow a' \rightarrow a''$; meanwhile, the *cis*-1,4-units are formed via route $b \rightarrow b' \rightarrow b''$. Therefore, when electron donors such as amines or ethers (TMEDA or THF) are added to the catalyst system, they are able to occupy a coordination site, forcing the new incoming monomer molecule to coordinate with only one double bond, resulting in *trans*-1,4-repeating units via route a_2 [61].

For multicomponent catalyst systems, the activation degree of the precursor, namely the aging time, influenced the catalytic performances obviously. The catalyst activity increased for a long ageing time, but the stereoselectivity of active catalyst sites seemed not to be affected by aging conditions. Moreover, increase of aging temperature led to a significant drop on polymerization reaction rate [62]. The alkylaluminum played a significant role on governing the

Table 2 Influence of solvent nature on the microstructure of polybutadiene produced by NdV/DIBAH/^{t}BuCl [58]

Composition (% v/v)		PB microstructure (%)			M_n	M_w		Activity
Hexane	Cyclohexane	*cis*-1,4	*trans*-1,4	1,2-vinyl	($\times 10^5$)	($\times 10^5$)	PDI	(g PB)
100	0	98.2	1.3	0.5	1.10	3.68	3.3	30
80	20	98.3	1.2	0.5	1.02	4.11	4.0	29
50	50	98.4	1.1	0.5	0.84	3.73	4.4	30
20	80	98.9	0.5	0.6	0.57	2.89	5.1	30
0	100	99.1	0.4	0.5	0.44	2.23	5.1	29

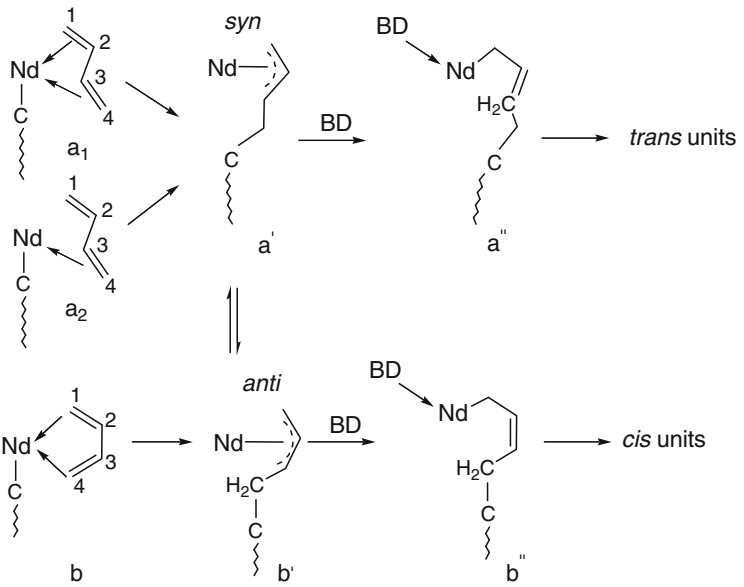

Scheme 2 Regularity of polybutadiene influenced by the coordination mode of butadiene to the metal center

Table 3 Influence of alkylaluminum compounds on the microstructure and molecular weight of polybutadiene afforded by NdV/^{t}BuCl [63]

		Microstructure (%)				
Run	Al cocat.	*trans*-1,4	1,2-vinyl	*cis*-1,4	M_w($\times 10^5$)	PDI
1	DIBAH	0.86	0.39	98.74	4.30	3.54
2	TIBA	1.13	0.65	98.22	7.34	2.82
3	TNHA	1.67	0.68	97.65	8.97	2.55
4	TNOA	1.61	0.79	97.60	10.52	2.54

catalytic performances. Coutinho reported when the long-chain aluminum compounds such as tri(*i*-butyl)aluminum (TIBA), tri(*n*-hexyl)aluminum (TNHA), and tri(*n*-octyl)aluminum (TNOA) were employed, the isolated polybutadiene had the highest molecular weight; however, those with the highest contents of *cis*-1,4-units and the lowest molecular weight were produced when DIBAH was employed. The order observed for catalyst activity obtained with the different types of aluminum compounds was: TNOA > TNHA > TIBA > DIBAH (Table 3) [63]. This might be because the organoaluminum compound changed the kinetic heterogeneity of active sites as reported by Monakov [64]. The heterogeneity of the investigated catalytic systems was shown in the existence of four types of active centers. They were formed at the beginning of the polymerization process and produced macromolecules with lengths that were definite for each type of active center. The nature of the organoaluminum compound greatly influenced the kinetic activity

of the polymerization centers. Thus, the difference in the distributions of kinetic activity and the behavior of active centers of the catalytic system with TEA and the similarity of the behavior of the systems with TIBA, TNHA, and TNOA can be explained by inclination toward association of TEA because of its short carbon chain [63, 64]. Besides as a cocatalyst to activate the lanthanide precursors, the role of aluminum compounds can act as a chain transfer agent to adjust the molecular weight, which was soundly investigated by Obsrecht with NdV/DIBAH/EASC. At low monomer conversions, the molecular weight distribution was distinctly bimodal at the initial process; with the increase of monomer conversion the position of the high molecular weight peak remained constant, while the position of the low molecular weight peak shifted toward lower retention times (high molecular weight). For the highest monomer conversion (=82.5%), the two peaks more or less overlapped resulting in apparently unimodal albeit broad distribution. The system in fact proceeded in a living mode as the molecular weight increased linearly with conversion. However, in contrast to the classical living polymerization, each Nd center generated more than one polymer chain, and the numbers ranged from 2.3 to 15.4 with increasing the [DIBAH]/[Nd] ratio (Table 4). This indicated that aluminum was involved in the generation of polymer chains via chain transfer from Nd onto Al during the course of the polymerization. As Al species attached to isobutyl groups or hydrogen were inert toward the polymerization of butadiene, the chain transfer should be reversible and the polymer chains attached to Al would be back-transferred to Nd and reactivated. Thus, Al with attached polymer chains can be treated as a dormant species. As the molecular weight distributions did not broaden with monomer conversion, it had to be concluded that the reversible transfer of polymer chains between Nd and Al was fast in relation to the speed of polymerization (Scheme 3) [65].

Table 4 Number ($p_{exp.}$) of chains generated by one Nd species of NdV/DIBAH/EASC system at different n_{DIBAH}/n_{Nd} ratios [65]

n_{DIBAH}/n_{Nd}	10	20	30	50
$\overline{DP}_{n,theo.}$[a]	9,250	9,250	9,250	9,250
$\overline{DP}_{n,exp.}$[b]	4,020	1,970	1,100	600
$p_{exp.}$	2.3	4.7	8.4	15.4

[a]For $x = 1$ (100% conversion) and 1 chain per Nd ($p = 1$)
[b]For $x = 1$ (100% conversion)

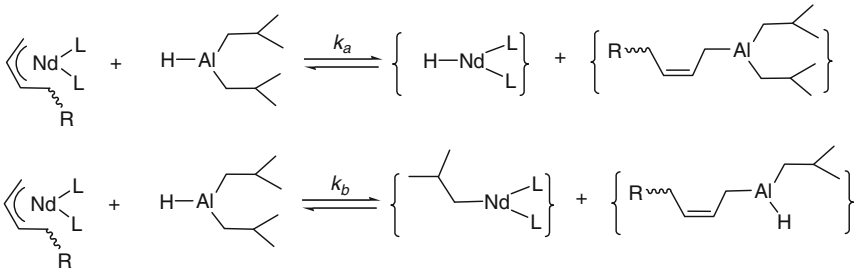

Scheme 3 Interchange of alkyl between Nd and Al

TIBA was used to compare with DIBAH. Within a broad range of Al-to-Nd ratios for both aluminum compounds, the features of a living polymerization with a reversible exchange of the living polybutadienyl chains between neodymium (Nd) and aluminum were observed differentiating at the equilibrium position for TIBA and DIBAH. For instance at the same molar loadings, DIBAH resulted in polybutadiene with molecular weights which were one eighth of those obtained in the presence of TIBA. This was explained by a more facile substitution of a hydride moiety from DIBAH than an isobutyl group from either DIBAH or TIBA by a living polybutadienyl chain, indicating that DIBAH was eight times more effective in molecular weight control than TIBA [66]. The molecular weight control could be also achieved by addition of diethyl zinc ($ZnEt_2$) to the ternary catalyst system of NdV/DIBAH/EASC, which had a negligible impact on polymerization rates. In addition to the reduction of molecular weight, $ZnEt_2$ also reduced the polydispersity (PDI) but unfortunately led to a decrease of the *cis*-1,4-content [67]. Fixing the cocatalysts to DIBAH and EASC, the catalyst system based on NdV (Cl-to-Nd ratio of 2 and H-to-Nd ratio of 30) was found highest polymerization activity for the polymerization of butadiene, whilst that comprising NdA catalyst system was less active as compared with NdV and NdP (neodymium bis(2-ethylhexyl)phosphate) systems [68]. When $SiCl_4$ was used as a chloride source to replace EASC, at the optimum concentration ratio of $NdV/SiCl_4/DIBAH = 1{:}1{:}25$, *cis*-1,4-contents were consistently high (about 97%) for all polymerizations [69]. The effects of the concentrations of cocatalysts and water and versatic acid were reported by Quirk. Using in situ catalyst activation, the optimum concentration ratios of NdV/EASC/DIBAH = 1:1:25 at a catalyst concentration of 0.11 mmol Nd/100 g BD was established and used to determine the influence of water and excess versatic acid on polymerization performance. It was found that unless $[H_2O]/[Nd] = 0.11$, higher and lower amounts of water as well as excess versatic acid above [versatic acid]/[Nd] = 0.22 resulted in lower conversions, broader molecular weight distributions, and higher molecular weights. In contrast, the *cis*-1,4-contents of the polybutadiene were consistently high (ca. 98%) and independent of the water content and excess acid level [70]. The role of the carboxylic acid in the Ziegler–Natta catalyst systems was elucidated by Kwag, when they studied the system $Nd(neodecanoate)_3$(ND)/DEAC/TIBA that was ultrahighly *cis*-1,4-selective for the polymerization of butadiene but very low active with unknown reason. By means of MALDI–TOF mass spectroscopic analysis, they found that ND was a mixture of various oligomeric and hydrated compounds (Scheme 4). The hydrated oligomeric structure would considerably lower the catalytic activity. To prove this, they designed a ND · NDH (neodecanoic acid) catalyst which was prepared through a ligand-exchange method and identified as monomeric structure, satisfying eight-coordination nature and did not contain water, bases, and salts (Scheme 5). In the polymerization of 1,3-butadiene, NDH showed a very high activity of 2.5×10^6 g/(mol_{Nd} h) and produced polybutadiene with over 98% *cis*-1,4-content without gel [71]. The microstructure of polybutadiene was controlled by chain transfer with ND · NDH, catalyst composition, and phosphine compounds. With increase in Nd concentration, increase in branch and decrease in cold flow were observed (Table 5). Addition of phosphine additives helped to

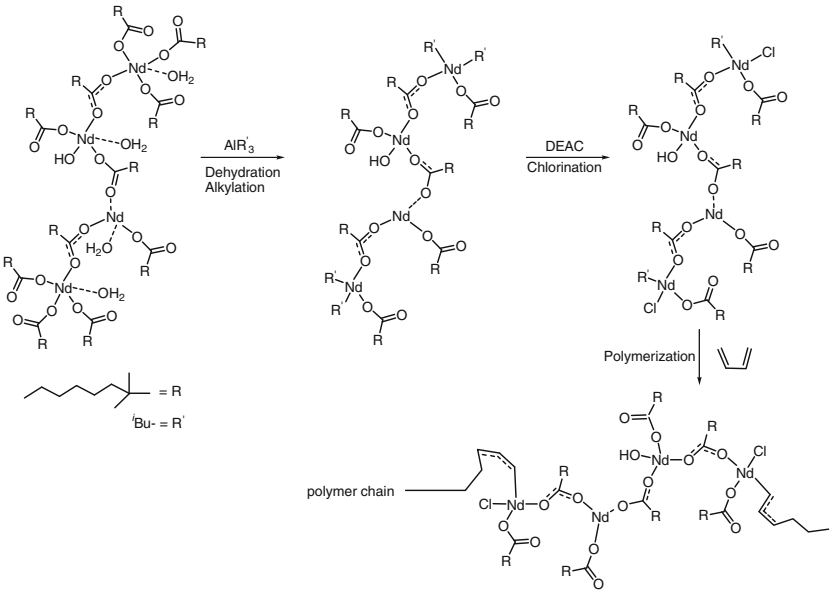

Scheme 4 The mechanism of catalyst activation and chain propagation of ND

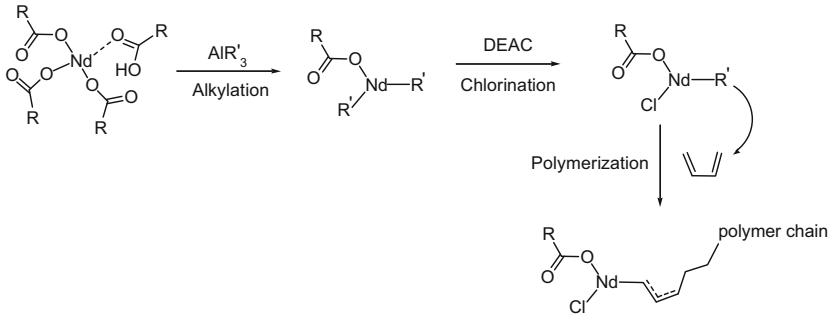

Scheme 5 The mechanism of catalyst activation and chain propagation of NDH

Table 5 Polymerization of 1,3-butadiene by Nd(neodecanoate)$_3$ (neodecanoic acid)/DEAC/TIBA and the analysis of microstructure and cold flow [72]

Run	Cat. ratio[a]	Nd conc. ($\times 10^{-4}$ mol)	Conv.[b] (%)	*cis* (%)	ML (1+4, 100°C)	C/F[c] (mg min^{-1})	M_w ($\times 10^4$)	PDI
1	1/95/2/2.5	0.4	90	98.7	45.2	5.5	59.2	2.55
2	1/30/13/2.5	0.6	91	98.5	44.0	3.6	57.1	2.65
3	1/12/8/2.5	1.0	93	97.5	44.3	1.8	54.8	2.88
4	1/12/10/2.5	1.1	97	97.5	47.6	1.9	59.5	2.97
5	1/15/5/2.5	1.3	100	96.8	41.0	1.3	61.7	3.32
6	1/95/2/2.5	0.4	55	94.5	65.6	2.1	95.6	4.25

[a]Cat. Ratio = Nd/TIBA/DIBAL/DIAE
[b]2 h
[c]C/F = cold flow

enhance the *cis*-1,4-selectivity, for instance, when *tris*(*para*-fluorophenyl) phosphine was used polybutadiene with over 99% *cis*-1,4-content was produced, which was in contrast to the previous reports that the addition of the electron donor decreased the *cis*-selectivity of the system owing to the monomeric nature of the active species. More significantly, they established the correlation between the properties and the microstructure of polybutadiene [72]. The linear high *cis*-1,4-regulated and narrow molecular weight-distribution polybutadiene showed excellent tensile and dynamic properties such as low heat build-up and high abrasion resistance but poor processability in view of high compound viscosity and hardness. Whilst the slightly branched, low *cis*-1,4-regulated polybutadiene with broad molecular weight distribution generated with increase in Nd concentration, exhibited improved processability for better mixing and milling with filler and other polymers in terms of low compound viscosity, and good tensile and dynamic properties such as hardness because of increased miscibility with carbon black [73–76]. The polybutadiene prepared by Ni-based catalyst showed a very low cold flow because of a broad MWD, indicating the good processability, however, low tensile and dynamic properties, especially high heat build-up (34.3°C) and abrasion (17.0 mg) owing to branching [75, 77].

An important kind of Ziegler–Natta catalyst precursors reported by Taube were the allyl neodymium chloride complexes such as $Nd(C_3H_5)_2Cl{\cdot}1.5THF$ and $Nd(C_3H_5)_2Cl{\cdot}2THF$, which could be activated by adding MAO or HIBAO to produce *cis*-1,4-polybutadiene. At the ratio of Al/Nd = 30, a turnover frequency (TOF) of about $1.08 \times 10^6 g/(mol_{Nd}\, h)$ and *cis*-selectivity of 95–97% in moderate yields were achieved under standard conditions (Table 6). Molecular weight determinations indicated a low polydispersity (M_w/M_n = 1–1.5), the formation of only one polymer chain per neodymium and the linear increase of the polymerization degree with the conversion, as observed for living polymerization. From the proven dependence of the polymerization rate (first order in neodymium, second order in butadiene concentration), it followed that two butadiene molecules might take part in the insertion reaction in the transition state of the allyl neodymium complex; the formation of an η^3-butenyl-bis(η^4-butadiene)neodymium(III) complex of the composition $[Nd(\eta^3\text{-}RC_3H_4)(\eta^4\text{-}C_4H_6)_2(X - \{AlOR\}_n)_2]$ ($X^- = Cl^-$ or $C_3H_5^-$) was assumed to be the true active species for the chain propagation (Scheme 6) [78]. When 2 equiv. $AlMe_2Cl$ (DMAC) were used to replace MAO, the resultant combination was highly active for the polymerization of butadiene with an activity doubled compared with MAO, $1.9 \times 10^6 g/(mol_{Nd} \cdot h)$ and narrower than 1.3 polydispersity albeit low *cis*-1,4-selectivity (of 90%). A chloro complex at the Nd(III) center as a consequence of allyl anion transfer to Al(III) (Scheme 7) was proposed to be the active species, in which the coordination of two butadiene monomers was requisite by the coordination number of 8 of Nd(III) [79]. However, employing AlR_3 to activate the solvated $Nd(C_3H_5)_2Cl{\cdot}1,4$-dioxane and $Nd(C_3H_5)Cl_2{\cdot}2(THF)$ or solvent-free $Nd(C_3H_4R)_3$ ($R = (C_4H_6)_nC_3H_5$), respectively, low activity and *cis*-1,4-selectivity were obtained, which might be attributed to the formation of probable chloride-bridged dimeric structure of the mono- or dichloride allyl precursors or the formation of the chloride cluster of resultant active species for the triallyl precursors.

Table 6 Polymerization of butadiene by employing $Nd(C_3H_5)_2Cl{\cdot}1.5THF/HIBAO$[a] [78]

Run	m_K (mg)	[Nd] (mol L^{-1})	$[BD]_0$/[Nd]	Time (min)	Yield (%)	TOF	*cis*/*trans*/1,2 (%)	$M_n \times 10^{-4}$ (LS)	$M_n \times 10^{-4}$ (V)	$M_w \times 10^{-4}$ (LS)	PDI	M_n (LS)/M_n (V)
1	27.3	1×10^{-3}	2,000	4	64	19,400	95/4/1	11.1	6.8	12.5	1.13	1.02
2	28.4	1×10^{-3}	2,000	4	60	17,800	95/4/1	10.4	6.5	11.6	1.12	0.99
3	22.4	8×10^{-4}	2,500	4	57	21,300	95/4/1	12.4	7.7	14.0	1.13	1.00
4	20.3	8×10^{-4}	2,500	4.5	58	19,700	95/4/1	12.7	8.4	14.2	1.12	0.94
5	18.5	6×10^{-4}	3,350	6	58	19,100	96/3/1	14.2	9.4	17.8	1.25	1.10
6	18.2	6×10^{-4}	3,350	6	60	19,900	95/4/1	15.8	9.2	18.9	1.19	1.17
7	14.2	4×10^{-4}	5,000	10	52	15,900	95/4/1	21.9	13.6	27.9	1.27	1.04
8	11.5	4×10^{-4}	5,000	7	52	22,200	96/3/1	23.6	14.0	28.9	1.22	1.00
9	8.9	2×10^{-4}	10,000	10	41	24,600	97/2/1	42.7	21.3	57.2	1.34	1.04
10	6.8	1.5×10^{-4}	13,300	12	29	19,300	98/1/1	57.2	21.5	83.7	1.46	0.97

m_K amount of the neodymium complex; $[BD]_0$ initial butadiene concentration; *TOF* turnover frequency, mol BD/(mol Nd h); M_n determined by light scattering (LS) or viscosimetrically (V)

[a]Performed in toluene, 35°C $[BD]_0 = 2.0\,mol\,L^{-1}$, [Al]/[Nd] = 30

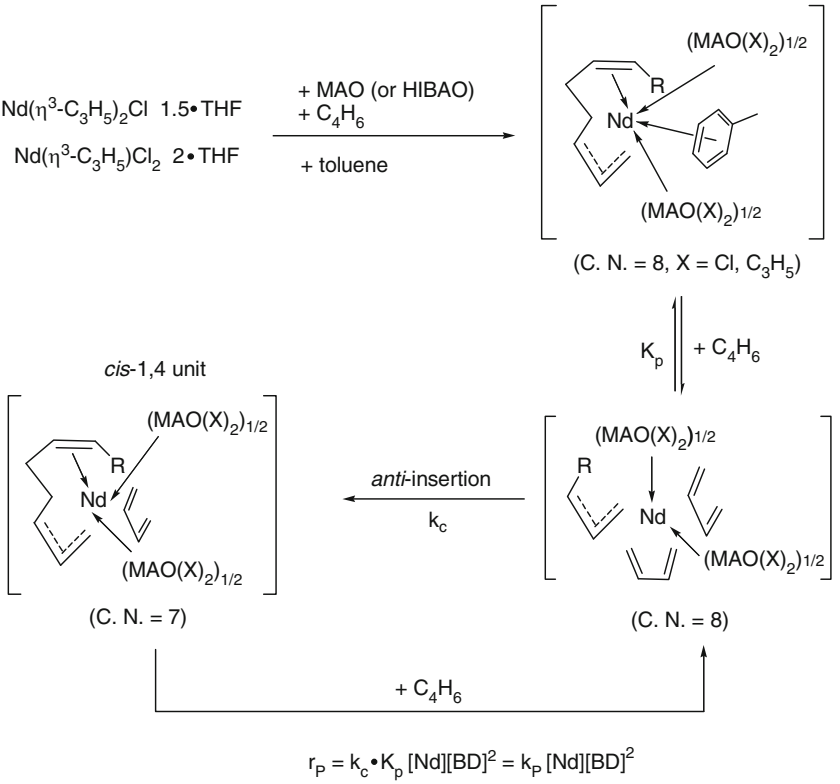

Scheme 6 Formation of catalytically active species and pathway of butadiene insertion (*CN* coordination number)

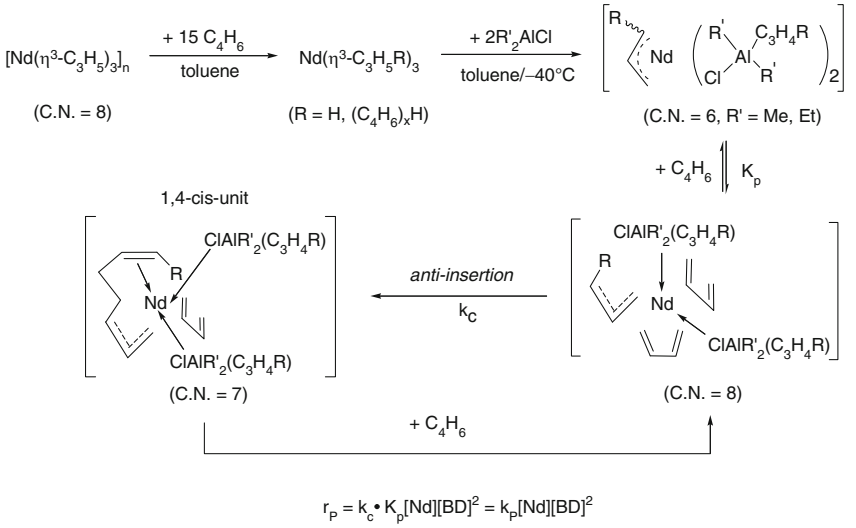

Scheme 7 Formation of allyl neodymium/aluminum complex

2.1.2 Modified Ziegler–Natta Rare-Earth Metal Precursors

The conventional Ziegler–Natta catalyst recipe contains both binary and ternary systems comprising 10–30-fold excess of aluminum trialkyl reagents except the single-component divalent lanthanide iodides [80], even though stoichiometric TIBA is sufficient with the fully defined carboxylate precursors [81]. And in all cases, chloride is included, which is generally believed to be crucial to the success of the polymerization [81–91]. Therefore, although heterobimetallic complexes with alkylated rare-earth metal centers have been proposed to promote 1,3-diene polymerization via an allyl insertion mechanism, details of the polymerization mechanism and the structure of the catalytically active center(s) are still elusive [92]; hence, improvement and optimization of the catalytic system have been achieved only empirically [93–95]. The interaction of the "cationizing" chloride-donating reagent with alkylated rare-earth metal centers is not well understood [96–98]. To mimic these conventional Ziegler–Natta catalytic precursors, the research works have been directed to the tailor-made and well-defined rare-earth metal carboxylates as models for diene polymerization catalysts. Evans designed the neodymium and lanthanum carboxylates $\{Nd[O_2CC(CH_3)_2CH_2CH_3]_3\}_n$ (**1**) and $\{La[O_2CC(CH_3)_2CH_2CH_3]_3\}_n$ (**2**) combined with DEAC and DIBAH to initiate the high *cis*-1,4-isoprene polymerization with high activity. Although the attempt to isolate the active intermediate of the process by crystallization of the reaction product of **1** with DEAC was unsuccessful by giving base-adduct $LnCl_3$, the probable active species were recognized to contain minimally the lanthanide and aluminum as well as halide and ethyl ligands in a formula $Ln_2AlCl_5(Et_2(O_2CR)$ [81–91]. When the cyclopentadienyl ligand was introduced into the carboxyl complexes, some reaction intermediates had been successfully isolated. For instance, by treatment of $[(C_5Me_5)_2Sm(O_2CC_6H_5)]_2$ (**3**) with R_2AlCl(R = Me, Et, ^{i}Bu) a dichloro complex $(C_5Me_5)Sm\text{-}(\mu\text{-}Cl)_2AlR_2$ (**4**) was successfully obtained where carboxylate ligands were replaced indeed by chloride in the reaction (Scheme 8). A divalent precursor $(C_5Me_5)_2Sm(THF)_2$ (**5**) reacted with DEAC, TMA, and TEA, respectively, afforded **4**, and the corresponding aluminates $[(C_5Me_5)_2Sm(AlMe_4)]_2$(**6**) and $(C_5Me_5)_2Sm(THF)\text{-}(\mu\text{-}\eta^2\text{-}Et)AlEt_3$ (**7**). The mixed chloride/alkyl-bridged complexes $(C_5Me_5)_2Ln\text{-}(\mu\text{-}Cl)(\mu\text{-}R)AlR_2$ (**9**), the mimic intermediates, could be prepared by treatment of $(C_5Me_5)_2Y(\mu\text{-}Cl)YCl(C_5Me_5)_2$ (**8**) with aluminum compounds [96]. Complexes **9** were usually monomeric but adopted dimeric structure when TMA was used (Scheme 9). These studies proved at least that the well-defined coordination environment provided by two Cp ligands; R_2AlCl reagents reacted with a lanthanide carboxylate ligand to deliver chloride indeed. The product was not a simple chloride carboxylate exchange product, however, a mixed metal complex containing aluminum bridged by two chloride ligands, $[(C_5Me_5)_2\text{-}Ln(\mu\text{-}Cl)_2AlR_2]$ (**10**). The isolation and identification of the mimic intermediates and the probable active species in the polymerization of dienes by Ziegler–Natta catalysts systems were realized by Anwander, who utilized the substituted homoleptic rare-earth metal carboxylate complexes $\{Ln(O_2CC_6H_2R_3\text{-}2,4,6)_3\}_n$ (**11**) (R = Me,^{i}Pr,^{t}Bu, Ln = Y,

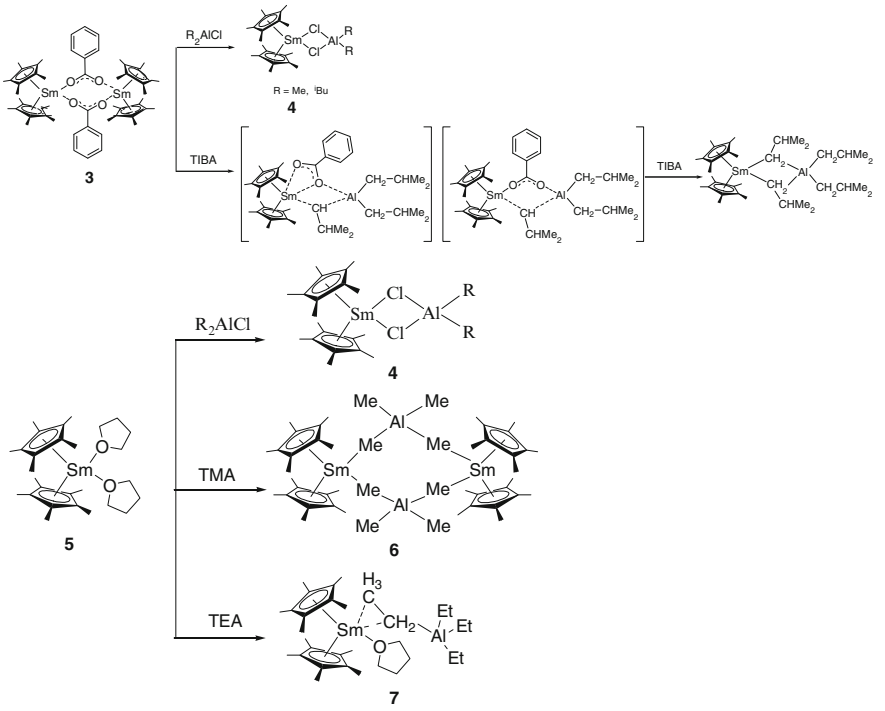

Scheme 8 Synthesis of chloride- and alkyl-bridged Sm–Al bimetallic complexes

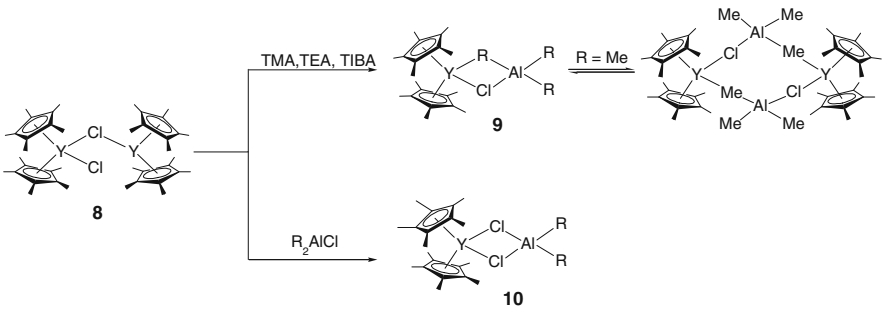

Scheme 9 Activation of **8** with different aluminum compounds

La, Nd, Gd, Lu) and $\{Ln(O_2CC_6H_3R_2\text{-}2,6)_3(THF)\}_n$ (**12**) (R = Ph, Mes, Ln = Y, La) without a Cp ligand to react with stoichiometric amount of AlR_3 (R = Me, Et). The resultant hexane-soluble complexes **13**–**15** featuring a η^2-coordinating tetraalkylaluminate ligand and a novel ancillary $AlMe_2$-bridged bis(carboxylate) ligand, were coordinated by mono- or di-tetraalkylaluminate ligands depending on the steric demand of the benzoate moieties and aluminum alkyls (Scheme 10). Upon activation with 1–2 equiv. DEAC, the resultant Ziegler–Natta catalyst

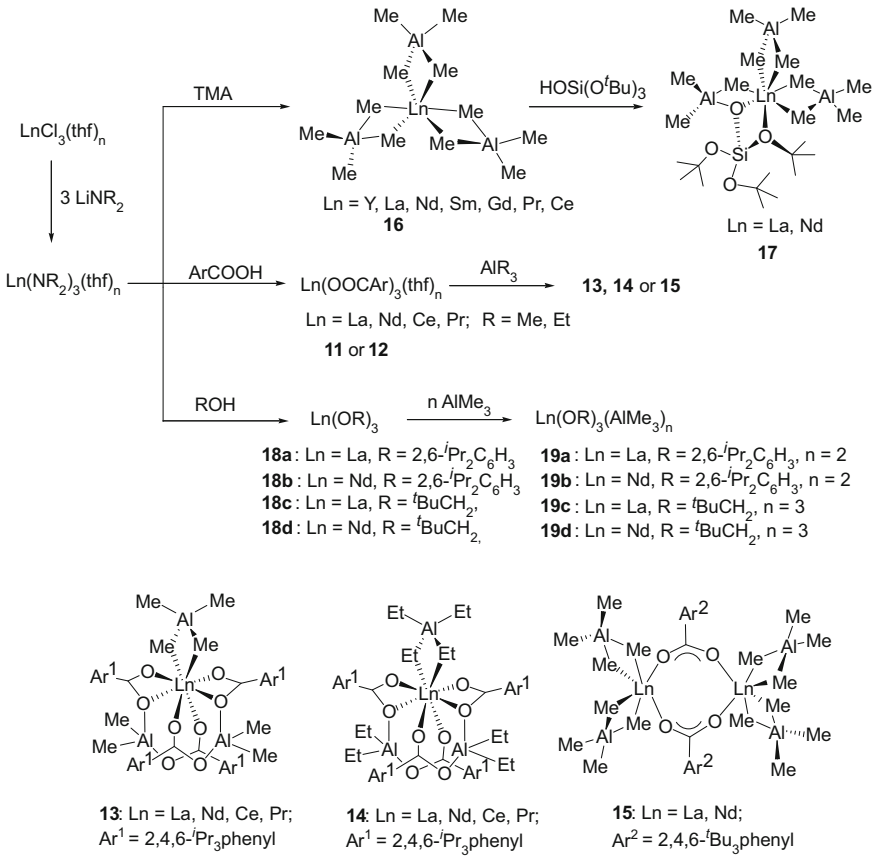

Scheme 10 Syntheses of heterobimetallic complexes

systems efficiently polymerized isoprene (*cis*-1,4 > 99%, Table 7), the performance of which depended significantly on the metal center (Nd > Gd > La) and the degree of alkylation ("$Ln(AlMe_4)_2$" > "$Ln(AlMe_4)$"). Equimolar reaction of $[Me_2Al(O_2CC_6H_2{}^{i}Pr_3\text{-}2,4,6)_2]_2Ln[(\mu\text{-}Me)_2AlMe_2]$ (**14**) with R_2AlCl (R = Me, Et) quantitatively produced $[Me_2Al(O_2CC_6H_2{}^{i}Pr_3\text{-}2,4,6)]_2$ and the proposing initiating species "Me_2LnCl." When the lanthanide aryloxide complexes $Ln(OR)_3$ were employed, the degree of preactivation by TMA influenced the initiating capability distinctly. The heterobimetallic bis-TMA adducts $Ln(OAr^{i}Pr)_3(TMA)_2$ and *tris*-TMA adducts $Ln(OCH_2{}^{t}Bu)_3(TMA)_3$ (Ln = La, Nd) under the activation of DEAC (Cl-to-Ln ratio of 2) produced the same highly reactive and stereoselective (*cis*-1,4 > 99%) initiators $[Me_2LnCl]$, whereas the mono-TMA adducts $Ln(OAr^{t}Bu)_3(TMA)$ were catalytically inert. The alkoxide-based *tris*-TMA adducts gave narrower molecular weight distributions than the aryloxide-based bis-TMA adduct complexes (M_w/M_n = 1.74–2.37 vs. 2.03–4.26) [102]. Homoleptic $Ln(AlMe_4)_3$ (**16**) was spotted as a crucial reaction intermediate

Table 7 Polymerization of isoprene with different lanthanide precatalyst[a]

Run	Precatalyst	Yield (%)	*cis*-1,4 (%)	M_n ($\times 10^3$)	M_w ($\times 10^3$)	PDI	References
1	$LaCl_3(thf)_n/3LiNR_2/3Ar^1COOH/6TMA$	70	98.1	180	816	4.52	[99]
2	$NdCl_3(thf)_n/3LiNR_2/3Ar^1COOH/6TMA$	>99	98.6	271	621	2.29	[99]
3	$CeCl_3(thf)_n/3LiNR_2/3Ar^1COOH/6TMA$	>99	>98	149	532	3.59	[99]
4	$PrCl_3(thf)_n/3LiNR_2/3Ar^1COOH/6TMA$	>99	>98	158	650	4.11	[99]
5	$LaCl_3(thf)_n/3LiNR_2/3Ar^1COOH/6TEA$	>99	96.6	91	454	4.98	[99]
6	$NdCl_3(thf)_n/3LiNR_2/3Ar^1COOH/6TEA$	>99	95.6	92	266	2.88	[99]
7	$LaCl_3(thf)_n/3LiNR_2/3Ar^2COOH/6TMA$	>99	>99	175	564	3.23	[99]
8	$NdCl_3(thf)_n/3LiNR_2/3Ar^2COOH/6TMA$	>99	>99	250	705	2.82	[99]
9	$YCl_3(thf)_n/3LiNR_2/8TMA$	97	75.9	101	400	3.95	[100]
10	$LaCl_3(thf)_n/3LiNR_2/8TMA$	99	>99	184	600	3.26	[100]
11	$NdCl_3(thf)_n/3LiNR_2/8TMA$	>99	>99	117	326	2.78	[100]
12	$SmCl_3(thf)_n/3LiNR_2/8TMA$	7	>99	ND	ND	ND	[100]
13	$GdCl_3(thf)_n/3LiNR_2/8TMA$	>99	>99	146	377	2.58	[100]
14	$CeCl_3(thf)_n/3LiNR_2/8TMA$	>99	>98	152	469	3.08	[100]
15	$PrCl_3(thf)_n/3LiNR_2/8TMA$	>99	>98	320	735	2.30	[100]
17	$NdCl_3(thf)_n/3LiNR_2/8TMA/^tBu_3OSiOH$	>99	>99	116	233	2.00	[101]
18	$CeCl_3(thf)_n/3LiNR_2/8TMA/^tBu_3OSiOH$	>99	>98	535	807	1.51	[80]
19	$PrCl_3(thf)_n/3LiNR_2/8TMA/^tBu_3OSiOH$	>99	>98	446	762	1.71	[101]
21	$LaCl_3(thf)_n/3LiNR_2/3Ar^3OH/2TMA$	54	>99	390	870	2.23	[102]
22	$NdCl_3(thf)_n/3LiNR_2/3Ar^3OH/2TMA$	>99	>99	223	453	2.03	[102]
23	$LaCl_3(thf)_n/3LiNR_2/3NpOH/3TMA$	>99	>99	517	954	1.85	[102]
24	$NdCl_3(thf)_n/3LiNR_2/3NpOH/3TMA$	>99	>99	384	670	1.74	[102]

ND not determined, Ar^1=2,4,6-^{i}Pr$_3$(C$_6$H$_2$), Ar^2=2,4,6-^{t}Bu$_3$(C$_6$H$_2$), Ar^3=2,6-^{i}Pr$_2$(C$_6$H$_3$), *Np* neopentyl

[a]Polymerization procedure: 0.02 µmol precatalyst, 8 mL hexane, 0.04 µmol DEAC (2 equiv.), 20 mmol isoprene; 24 h, 40°C

and was used for the high-yield synthesis of the various alkylated carboxylate complexes according to a novel "tetraalkylaluminate" route. Upon activation with 1–3 equiv. of DEAC, complexes **16** initiated the polymerization of isoprene in quite an efficient manner to yield highly stereospecific *cis*-1,4 > 99% polymers within 24 h [99–101]. The aforementioned Ln/Al heterobimetallic complexes such as $[LnAl_3Me_8(O_2CC_6H_2{}^iPr_3\text{-}2,4,6)_4]$, $[Ln(OR)_3(AlMe_3)_n]$ (R = neopentyl, 2,6-^{t}Bu$_2$C$_6$H$_3$, 2,6-^{i}Pr$_2$C$_6$H$_3$), and $[Ln(AlMe_4)_3]$ can be considered as the alkylated intermediates which, upon further activation with DEAC (or immobilized with MCM-48 [103]), gave similar highly efficient initiators for isoprene polymerization. The actual initiating active species were proposed to be $[Me_2LnCl]_n$ and $[MeLnCl_2]_n$, which were generated by sequential alkylation–chlorination scenario. This was confirmed by their recent result utilizing lanthanide trichlorides as the starting reagent, which were treated with $LiN(SiHMe_2)_2$ to yield a mixture of homoleptic $Ln\{N(SiHMe_2)_2\}_3(thf)_n]$ and a monoamido derivatives

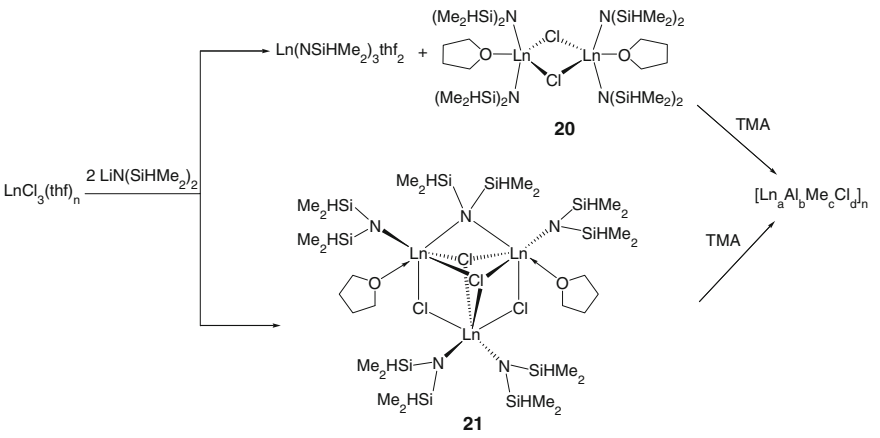

Scheme 11 Formation of chloro-bridged lanthanide amide complexes

$[Ln\{N(SiHMe_2)_2\}Cl_2(thf)_n]$ (**20**) and a dimeric species $[\{Ln\{N(SiHMe_2)_2\}_2(\mu\text{-}Cl)(thf)\}_2]$ (**21**) (Scheme 11). Further addition of excess TMA to the above mixture gave $[Ln_aAl_bMe_cCl_d]_n$ ($a + b = 1, a > b$; $c + d = 3, c > d$; determined by elemental analysis and magic-angle-spinning NMR technique) of single component catalyst (Ln = Nd) that provided an over 99% *cis*-1,4-selectivity with moderate to high activity (24 h, 40°C, >99% yield) [103]. The intrinsic Nd effect was observed in all these systems.

2.2 The Cationic Catalytic System

As the homogeneous catalyst system can provide more controlled polymerization especially the molecular weight of the resulting polydiene products, and the precursor of these systems are usually well defined that facilitate the investigation of the polymerization intermediate as well as the mechanism, thus the single-site homogeneous catalysts have attracted increasing attention. In these systems the organoborates are usually used to activate the precursors to give the cationic active species.

2.2.1 Lanthanocene Precursors

For the (modified) Ziegler–Natta systems although the structures of the precatalysts are still elusive, it is commonly accepted that the active center involves the formation of the Ln–alkyl or Ln–H species and cationization via Al-to-Ln chloride transfer. Therefore, well-defined Ln–C bond-containing complexes have attracted an increasing attention, among which the lanthanocene derivatives occupy notable positions. Coming to the first are samarocene divalent or trivalent complexes such as $(C_5Me_5)_2Sm(THF)_2$ (**5**) or $(C_5Me_5)_2LnR$(R = H or alkyl) which

are known to be efficient catalysts or precatalysts for polymerization of ethylene and methyl methacrylate in a living way to give monodispersed high molecular weight polymers in good yields [104–109]. However, they are almost inert for polymerization of dienes due to easy formation of stable η^3-allyl intermediates that seem to be somewhat of a thermodynamic sink [105]. Strikingly, Kaita discovered that in combination with a cocatalyst such as MMAO, these complexes could efficiently initiate the polymerization of butadiene with an over 98% *cis*-1,4-regularity and high molecular weight and narrow molecular weight distribution (PDI = 1.69). TIBA/$[Ph_3C][B(C_6F_5)_4]$ can also be used as cocatalysts in stead of MMAO. The resultant three-component catalyst system could initiate smooth polymerization of butadiene in a "living" mode to a large extent to provide polybutadiene with high *cis*-1,4-content (94.2–95.0%) and narrow molecular weight distribution (PDI = 1.31–1.39). When the polymerization was carried out at low temperature (−20°C), a dramatic increase in the *cis*-1,4-content of polybutadiene had been obtained (>99.5%) [105–109]. The pronounced enhancements both in activity and in *cis*-1,4-selectivity were brought in by introducing bulky substituents on the Cp ligand or reducing the ionic radius of the central metal ions. For instance, complexes $(C_5Me_4R)_2Sm(THF)_x$ (**22**–**26**, Fig. 2) under the activation with MMAO showed catalytic activity for the polymerization of butadiene depending on the R group; when it was ^{i}Pr, the highest activity was obtained [110]. $(C_5Me_5)_2Ln[(\mu\text{-Me})AlMe_2(\mu\text{-Me})]_2Ln(C_5Me_5)_2$ (**27**, Scheme 12), in situ generated from the reaction of $(C_5Me_5)_2LnTHF_x$ with 8 equiv. TMA, when treated with $[Ph_3C][B(C_6F_5)_4]$/TIBA, showed catalytic activity in a trend of Gd ≫ Nd ≫ Pr and

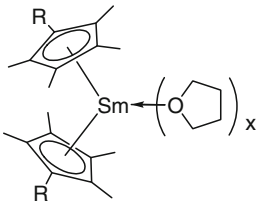

22: R = Me, X = 2, $(C_5Me_5)_2Sm(THF)_2$
23: R = Et, X = 2, $(C_5Me_4Et)_2Sm(THF)_2$
24: R = ^{i}Pr, X = 1, $(C_5Me_4{}^iPr)_2Sm(THF)$
25: R = ^{n}Bu, X = 1, $(C_5Me_4{}^nBu)_2Sm(THF)$
26: R = TMS, X = 1, $(C_5Me_4TMS)_2Sm(THF)$

TMS : trimethylsilyl

Fig. 2 Divalent samarocene complexes

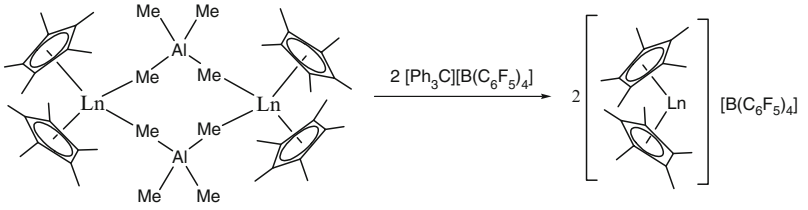

27 : Ln = Pr (**a**), Nd (**b**), Gd (**c**), Ce (**d**), Lu (**e**), Tb (**f**), Dy (**g**), Ho (**h**), Tm (**i**), Yb (**j**)

28 : Ln = Pr (**a**), Nd (**b**), Gd (**c**), Ce (**d**),

Scheme 12 Activation of complex **27** with organoborate

the regularity of the resulting polymer following the similar trend Gd(97.5%) > Nd (91.3%) > Pr (90.2%) (*cis*-1,4-selectivity at 50°C), which were inverse of the size of metal ion. The activity of the Gd complex/TIBA system was so high that the polymerization could be performed fluently at low temperature −78°C to give perfect *cis*-1,4-stereospecific (>99.9%) polybutadiene with sharp molecular weight distribution ($M_w/M_n = 1.45$) under reasonable yields [111].

In contrast, the system based on Ce precursor **27d** with almost similar cocatalysts, TIBA/$[Ph_3C][B(C_6F_5)_4]$, yielded polybutadiene with a low *cis*-1,4-content (38.8%, Table 8). Switching to TMA/$[Ph_3C][B(C_6F_5)_4]$, surprisingly, highly *trans*-1,4-polybutadiene was obtained (93.8%, Table 9), suggesting that the type of the cocatalysts have also dramatic influence on the catalytic performances. Moreover,

Table 8 Polymerization of 1,3-butadiene with **27** and **6** in the presence of TIBA and $[Ph_3C][B(C_6F_5)_4]$[a] [112]

			Microstructure (%)				
Run	Cat.	Yield (%)	1,4-*cis*	1,4-*trans*	1,2-	M_n ($\times 10^3$)	M_w/M_n
1	**27a**	28	55.3	43.9	0.8	22.8	1.27
2	**27b**	63	65.9	32.5	1.6	40.1	1.24
3	**27c**	~100	97.3	2.0	0.7	82.5	1.32
4	**27d**	15	38.8	59.8	1.4	12.8	1.24
5	**27e**	54	87.7	2.5	9.8	95.8	1.66
6	**27f**	~100	96.2	3.0	0.8	96.4	1.39
7	**27g**	~100	95.3	2.9	1.8	94.6	1.53
8	**27h**	~100	96.6	1.6	1.8	108.9	1.32
9	**27i**	~100	87.5	4.7	7.8	98.7	1.58
10	**27j**	0					
11	**27c**	~100	>99.9			113.7	1.70
12[b]	**6**	~100	86.0	13.2	0.8	59.8	1.36

[a]Conditions: toluene: 20 mL, 25°C; 15 min; butadiene $= 1 \times 10^{-2}$ mol; Ln $= 5 \times 10^{-5}$ mol; $[TIBA]_0/[Ln]_0 = 5$; $[Ph_3C][B(C_6F_5)_4]\}_0/[Ln]_0 = 1$

[b]−40°C, 5 h

Table 9 Polymerization 1,3-butadiene with **27** and **6** in the presence of $AlMe_3$ and $[Ph_3C][B(C_6F_5)_4]$[a]

			Microstructure (%)				
Run	Cat.	Yield (%)	1,4-*cis*	1,4-*trans*	1,2-	M_n ($\times 10^3$)	M_w/M_n
1	**27a**	72	9.6	89.6	0.8	56.0	1.25
2	**27b**	87	13.8	85.2	1.0	65.0	1.25
3	**27c**	76	59.7	38.8	1.5	111.5	1.59
4	**27d**	35	4.9	93.8	1.3	38.0	1.41
5	**27e**	24	40.9	50.0	9.1	43.4	1.82
6	**27f**	43	72.4	26.6	1.4	91.2	1.84
7	**27g**	69	56.0	41.1	2.9	144.2	1.88
8	**27h**	48	64.8	32.5	2.7	72.0	1.60
9	**27i**	4	47.8	46.8	5.4	29.5	1.60
10	**27j**	0					
11[b]	**6**	80	33.2	65.2	1.6	71.6	1.46

[a]Conditions: toluene: 20 mL, 25°C, 30 min; butadiene $= 1 \times 10^{-2}$ mol; Ln $= 5 \times 10^{-5}$ mol; $[TMA]_0/[Ln]_0 = 3$; $\{[Ph_3C][B(C_6F_5)_4]\}_0/[Ln]_0 = 1$

[b]24 h

when the Al/Ln ratio was 3–5, the alkylaluminum worked as an activator; the polymerization systems showed somewhat living-like nature to afford polybutadiene with the M_n proportional to monomer consumption whilst the molecular weight distribution stayed constant. In the presence of excess amount of alkylaluminum, it worked as a chain transfer agent to adjust the molecular weight of polybutadiene conveniently [112, 113]. These lanthanocene catalyst systems showed lower activity for isoprene polymerization as compared with butadiene (Table 10). The monomer reactivity ratios by applying the Fineman–Ross method, $r_{butadiene} = 4.7$ and $r_{isoprene} = 0.02$, indicated that isoprene is two orders of magnitude less reactive than butadiene and also low specific regularity (*cis*-1,4-content of butadiene unit 98.4–96.9%, 1,4-content of isoprene unit 54.2–51.5%) [114]. As shown above in striking contrast to the intrinsic "Nd effect" of the conventional Ziegler–Natta catalysts, the catalytic performances of these cationic lanthanocene-based systems were governed significantly by the concerted effects of the specific environment around the reaction centers, the types of lanthanide ions and cocatalysts.

Tardif reported recently that the cationic half-sandwich lanthanide amido complexes $[(Ind)Ln\{N(SiMe_3)_2\}][B(C_6F_5)_4]$ (**29**, Fig. 3) were also highly efficient and *cis*-1,4-selective for butadiene polymerization [115]. Meanwhile, Visseaux demonstrated that the half-sandwich scandium borohydride complex $Cp^*Sc(BH_4)_2(THF)$ (**30**, Fig. 3) combined with $[Ph_3C][B(C_6F_5)_4]$ and TIBA led to the very active and highly stereoselective isoprene polymerization (>90% *cis*-1,4, Table 11) as well as styrene (>99.9% syndio, Table 12). Improvement of the control of the polymerization was performed at lower temperature at −10°C that the *cis*-1,4-ratio increased up to 97.2% followed by the decrease of PDI down to 1.7 [116]. This

Table 10 Polymerization isoprene with **27c**/$[Ph_3C][B(C_6F_5)_4]$/TIBA[a] [114]

Run	Temp (°C)	$[TIBA]_0/[Gd]_0$	Time	Yield (%)	Microstructure (%)			M_w ($\times 10^3$)	M_n ($\times 10^3$)	M_w/M_n	T_g(°C)
					1,4-*cis*	1,4-*trans*	3,4-				
1	RT		2 h	97	32.6	18.8	48.6	370.9	179.1	2.07	−31.7
2	−20		6 days	22	44.9	3.0	52.2	114.6	114.6	10.01	−25.9
3	RT	10	1 h	~10	50.8	12.7	36.5	112.7	65.3	1.73	−51.2
4	0	20	5 h	93	98.7	0.0	1.3	902.0	461.5	1.95	−67.5
5	−20	50	10 h	88	>99.99			1,494.5	675.0	2.21	−68.4

[a]Conditions: in toluene; isoprene: 0.03 mol; **27c**: 2×10^{-5} mol

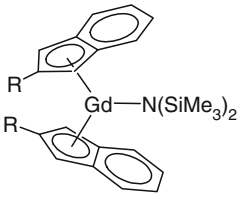

29: R = H (**a**), Me (**b**), Ph (**c**)

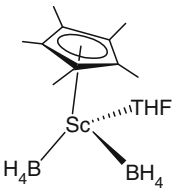

30

Fig. 3 Structures of lanthanide complexes **29** and **30**

Table 11 *cis*-1,4-Polymerization of isoprene (IP) using **30**/$[Ph_3C][B(C_6F_5)_4]$/TIBA [116]

Run	[IP]/[Sc]	[B]/[Sc]	TIBA	Temp (°C)	Time (min)	Yield (%)	Activity (kg (mol h)$^{-1}$)	M_n ($\times 10^3$)	PDI	*cis*-1,4 (%)
1	1,000	1	10	20	9	39	177	36.7	4.1	90.7
2	1,000	2	10	20	7	76	443	92.6	2.7	94.2
3	1,000	2	20	0	25	55	90	96.4	2.4	97.0
4	1,000	2	20	−10	35	41	48	39.9	1.7	97.2
5	3,000	2	10	20	1	38	4,651	166.7	2.2	96.3
6	3,000	2	20	20	15	41	334	115.3	2.6	96.4
7	1,000	1	10	20	10	44	179	36.4	3.9	90.2
8	410	1	10	20	1,440	92	1.1	–	–	94.6

Table 12 Syndiospecific polymerization of styrene (ST) using **30**/$[Ph_3C][B(C_6F_5)_4]$/TIBA[a] [116]

Run	[ST]/[Sc]	Time	Yield (%)	Activity (kg (mol h)$^{-1}$)	M_n ($\times 10^3$)	PDI	sPS (%)	T_f (°C)
1	100	1 min	32	200	24.3	3.68	>99.9	269
2[b]	200	17 h	80	1.0	6.0	3.64	>99.9	265
3	500	3 h 30 min	21	3.1	8.5	2.68	>99.9	270
4[c]	500	18 h	25	0.7	–	–	>99.9	268
5[d]	200	2 h 30 min	62	5.1	86.6	3.83	95[f]	267
6[e]	400	1 h 30 min	88	24.4	3.0	3.29	Atactic	–

[a]Conditions: T = 50°C, [TIBA]/[Sc]/$[Ph_3C][B(C_6F_5)_4]$ = 10/1/1, toluene/monomer = 1
[b]T = 20°C
[c]Toluene/monomer = 5
[d]Synthesized in situ
[e]In the absence of TIBA
[f]Corresponds to 95% pure sPS along with an atactic fraction as evidenced by the high melting point

distinguished performances might be attributed to the introduction of the bulky Cp^* ligand, because the analogous $Sc(BH_4)_3(THF)_{1.5}$/$[Ph_3C][B(C_6F_5)_4]$/(10TIBA) in toluene afforded polyisoprene quantitatively in 10 min at 20°C albeit with less controlled microstructure (mixture of *cis*-1,4-, *trans*-1,4-, and 3,4-units), whereas its neodymium analogue, the in situ-generated ternary catalytic system $Nd(BH_4)_3(THF)_3$/$[HNMe_2Ph][B(C_6F_5)_4]$/TIBA, exhibited better performances with a 92% *cis*-1,4-selectivity together with good control of M_n and PDI [117, 118].

2.2.2 Noncyclopentadienyl Lanthanide Precursors

Non-Cp ligands [119–127] those containing heteroatom compounds have been extensively explored as spectator ligands by virtue of their strong metal–heteroatom bonds and exceptional and tunable steric and electronic features required for compensating coordinative unsaturation of metal centers and for catalytic activity toward polymerization. The elegant non-Cp-ligated cationic yttrium aluminate species applied in the polymerization of 1,3-dienes was reported by Okuda. Both the yttrium aluminates (**31a**) and their lithium ate complexes (**31b**) upon activation

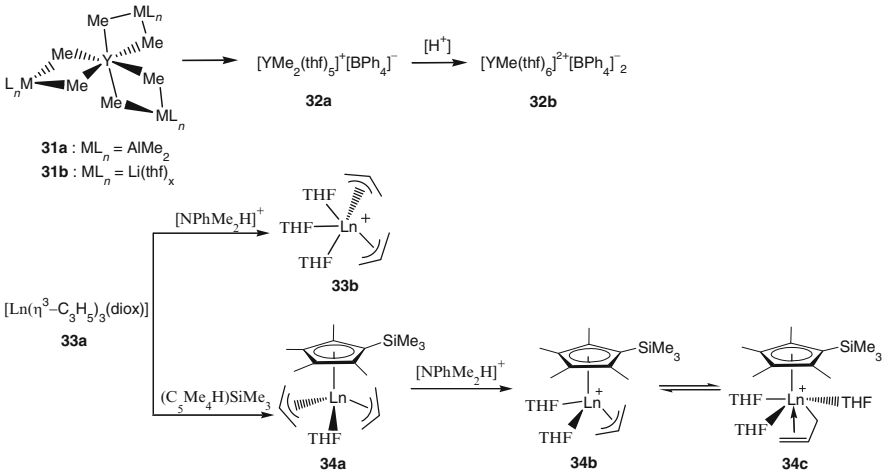

Scheme 13 Synthesis of the mono- and dicationic yttrium methyl complexes **33** and **34** from yttrium aluminate **31** or hexamethyl yttrium **32**

with $[PhNHMe_2][B(C_6F_5)_4]$ catalyzed the polymerization of 1,3-dienes albeit at low activity and gave crosslinked product. The in situ-generated monocation $[YMe_2(solv)_x]^+$ (**32a**) produced polybutadiene in only 90% *cis*-1,4-tacticity and had a significantly lower polymerization activity (no polybutadiene was obtained after 30 min) than the dications (18–26% conversion). Under the presence of TIBA, the activity increased and *cis*-1,4-enriched polybutadienes were produced. Remarkably, the in situ-generated dication $[YMe(thf)_x]^{2+}$ (**32b**) gave *cis*-1,4-polybutadiene in up to 97% tacticity at 100% conversion after 14 h. In addition the molecular weight of the resultant polybutadiene by dicationic species was as high as that obtained with the monocation, indicating either a dication with one growing chain or a monocation with two growing chains (Scheme 13, Table 13) [128]. Very recently, the same group successfully isolated the yttrium bisally monocationic and yttrium monoallyl dicationic complexes (**33b**, **34**), which could initiate polymerization of butadiene with about 90% *cis*-1,4-selectivity [129].

Cui successfully isolated the non-Cp pyrrolyl aldiminate-ligated rare-earth metal bis(alkyl)s (**35**, Fig. 4), which combined with aluminum *tris*(alkyl)s and borate, initiated the polymerization of isoprene with *cis*-1,4-enriched regularity [130]. Increasing the ligand steric bulkiness, the indolyl-stabilized counterpart (**36**, Fig. 4) provided higher *cis*-1,4-selectivity and polyisoprene with more controllable molecular weight and narrow molecular weight distribution. The concerted influence of the environmental hindrance around central metals arising from the bulky substituents (^{i}Pr vs. Me) of the ligands as well as the sterically demanding aluminum *tris*(alkyl)s, and the Lewis-acidic rare-earth metal ion, endowed the scandium combination **36d**/$[Ph_3C][B(C_6F_5)_4]$/TIBA the highest activity and the regioselectivity ($M_n = 2.65 \times 10^5$, $M_w/M_n = 1.07$, *cis*-1,4 = 98.2%, −60°C) [131].

Table 13 1,3-Diene polymerization by **31** activated by $[PhNHMe_2][B(C_6F_5)_4]$[a] [128]

Run	B:Y		Time (min)	Conversion (%)	Selectivity[b]	M_n^c ($\times 10^3$)	M_w/M_n
1,3-Butadiene polymerization							
1[d]	1		30	<5			
2[e]	1		240	73		186	4.4
3	1	TIBA	840	100	90:8:2	50	2.6
4	2		30	26	95:3:2	140	2.0
5[e]	2		240	93		312	2.6
6	2	TIBA	30	18	95:3:2	61	1.7
7	2	TIBA	840	100	97:2:1	100	2.1
Isoprene polymerization							
8	1		10	56	60:26:14	117	1.6
9	1	TIBA	10	86	89:0:11	315	2.1
10	2		10	65	67:13:20	260	1.5
11	2	TIBA	10	78	90:0:10	133	2.9

[a]Conditions: **31**: 5 µmol, 25°C. 1,3-Butadiene polymerization: $V_{butadiene} = 7.5$ mL (14 wt% in toluene); $V_{total} = 30$ mL. Isoprene polymerization: $V_{isoprene} = 1$ mL; $V_{total} = 30$ mL
[b]Ratio *cis*:*trans*: 1,2 for 1,3-butadiene; ratio *cis*: *trans*: 3,4 for isoprene
[c]Determined by GPC
[d]Not determined
[e]Microstructure not determined because of crosslinking; molecular weight determined for the soluble fraction

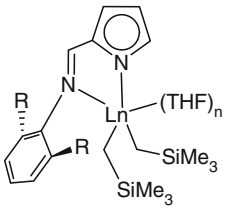

35a: Ln = Lu, R = Me, n = 2
35b: Ln = Sc, R = Me, n = 1
35c: Ln = Lu, R = ^{i}Pr, n = 2
35d: Ln = Sc, R = ^{i}Pr, n = 1

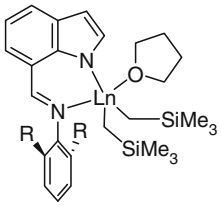

36a: Ln = Lu, R = Me
36b: Ln = Sc, R = Me
36c: Ln = Lu, R = ^{i}Pr
36d: Ln = Sc, R = ^{i}Pr

Fig. 4 Pyrrolyl- and indenyl-stabilized dialkyl lanthanide complexes

The fascinating homogeneous catalysts based on rare-earth metal bis(alkyl) complexes (**37**) bearing bis(phosphinophenyl)amido (PNP) ancillary ligand were reported by Hou. The cationic alkyl species were generated in situ by treatment of **37** with equimolar $[PhMe_2NH][B(C_6F_5)_4]$ in C_6D_5Cl (Scheme 14), among which the yttrium complex **37b** showed extremely high *cis*-1,4-selectivity (99%) and excellent livingness ($M_w/M_n = 1.05$–1.13) for the polymerization of isoprene and butadiene without addition of an aluminum additive (Table 14). The similar catalytic activity was observed for the Sc and Lu analogues, albeit with slightly lower *cis*-1,4-selectivity (96.5–97.1%). The excellent *cis*-selectivity was slightly influenced by increasing polymerization temperature up to 80°C, indicating that the active species were thermal stable. In addition a cationic alkyl lutetium complex

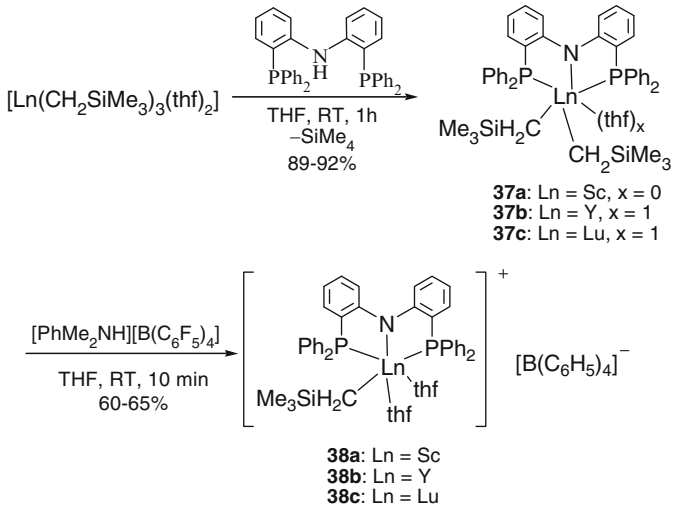

Scheme 14 Synthesis of neutral and cationic rare-earth metal alkyl complexes bearing a bis(2-diphenylphosphinophenyl)amido (PNP ^{Ph})ligand

Table 14 Living *cis*-1,4-polymerization of isoprene (IP) initiated by **37** and borate (or borane)[a] [132]

Run	Cat.	Temp (°C)	Time (min)	Yield (%)	M_n[b] ($\times 10^5$)	M_w/M_n[b]	Microstructure[c] *cis*-1,4-	3,4-	T_g[d] (°C)	Eff.[e] (%)
1	**37**	RT	60	0						
2	**37a/A**[f]	RT	60	100	1.6	1.10	96.5	3.5	−66	26
3	**37b/A**[f]	RT	60	100	2.3	1.10	99.3	0.7	−69	18
4	**37c/A**[f]	RT	60	100	1.9	1.09	97.1	2.9	−67	22
5	**37b/B**[f]	RT	60	79	3.2	1.11	99.3	0.7	−69	10
6	**37b/C**[f]	RT	60	0						
7	**37b/A**[g]	RT	10	40	0.5	1.05	99.3	0.7	−69	33
8	**37b/A**[g]	RT	15	90	1.0	1.05	99.3	0.7	−69	37
9	**37b/A**[g]	RT	20	100	1.2	1.07	99.3	0.7	−69	34
10	**37b/A**[g,h]	RT	40	150	1.8	1.08	99.3	0.7	−69	34
11	**37b/A**[g,h]	RT	60	200	2.3	1.08	99.3	0.7	−69	36
12	**37b/A**[g]	0	180	100	1.3	1.06	99.6	0.4	−69	31
13	**37b/A**[i]	50	10	90	0.7	1.05	98.7	1.3	−68	53
14	**37b/A**[i,j]	50	20	188	1.4	1.05	98.7	1.3	−68	55
15	**37b/A**[i]	80	2	66	0.6	1.05	98.5	1.5	−68	45
16	**37b/A**[i]	80	5	100	0.8	1.05	98.5	1.5	−68	51

[a]Conditions: C_6H_5Cl (10 mL); Ln (25 μmol); $[IP]_0/[Ln]_0 = 600$; $[Ln]_0/[activator]_0 = 1{:}1$ (activator = $[PhMe_2NH][B(C_6F_5)_4]$ (**A**), $[Ph_3C][B(C_6F_5)_4]$ (**B**), $B(C_6F_5)_3$ (**C**))
[b]Determined by GPC
[c]Determined by ^1H and ^{13}C NMR spectroscopy
[d]Measured by DSC
[e]Catalyst efficiency
[f]In runs 2–6, IP was added to **37b**/activator
[g]In runs 7–12, **A** was added to complex/IP
[h]Another equivalent of IP was added
[i]In runs 13–16, **37b** and IP in C_6H_5Cl (3 mL) was added to **A**
[j]$[IP]_0/[\mathbf{37b}]_0 = 1{,}200$

38c was successfully isolated and characterized, which represented in some degree a structural model for the true active species and for the mechanistic understanding of the polymerization process [132]. When PNP ligand was replaced by *N*,*N*′-bis(2,6-diisopropylphenyl)benzamidine ($NCN^{dipp}H$), the corresponding mono(amidinate) bis(aminobenzyl) complex **39** behaved quite differently. In the presence of 1 equiv. $[Ph_3C][B(C_6F_5)_4]$, it converted isoprene quantitatively into polyisoprene with high 3,4-regioselectivity (91%) and some degree of isotacticity (*mm* = 50%). When the polymerization was carried out at low temperature (−10°C), an even higher regio- and stereoselectivity was achieved and almost perfect isotactic 3,4-polyisoprene was obtained (3,4-selectivity up to 99.5%, *mmmm* up to 99%). The addition of TIBA or TEA had little effect on the polymerization; however, addition of 3 equiv. TMA, the resultant system changed the regio- and stereoselectivity of the polymerization dramatically from 3,4-isospecific to *cis*-1,4-selective that increased to as high as 98% at 5 equiv. TMA at −10°C or below. They explained that the steric hindrance and C_2 symmetry of the $(NCN^{dipp})Y$ unit made isoprene coordinate to the Y center preferably in a 3,4-η^2 fashion, leading to the formation of isotactic 3,4-polyisoprene (Scheme 15); when 5 equiv. TMA was added, the resultant heterotrinuclear Y/Al complex **40** preferred the coordination of isoprene in a μ-*cis*-1,4-η^4 fashion by replacement of an TMA unit. The 1,4-addition of a methyl group to the coordinated isoprene gave a μ-π-*anti*-allyl species and its equilibrium isomer μ-σ-allyl species, leading to *cis*-1,4-polyisoprene eventually (Scheme 16) [133].

To date, the characteristic of the mentioned systems are based on lanthanide alkyl complexes, and showed intrinsic Nd or Sm or Gd or Y effects. The Ti, Co, Ni, and Nd metal chlorides, on the other hand, the first innovated to initiate the

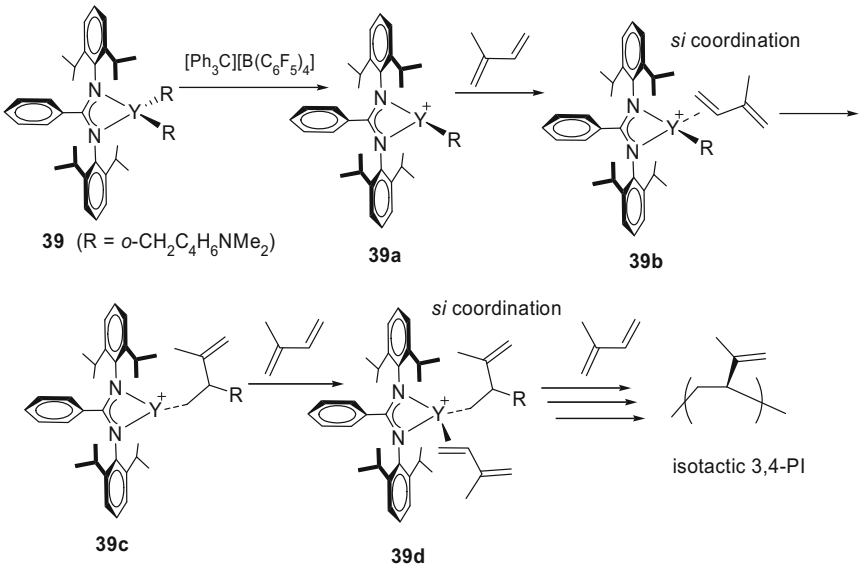

Scheme 15 Possible mechanism for 1,4-selective polymerization of isoprene with **39**

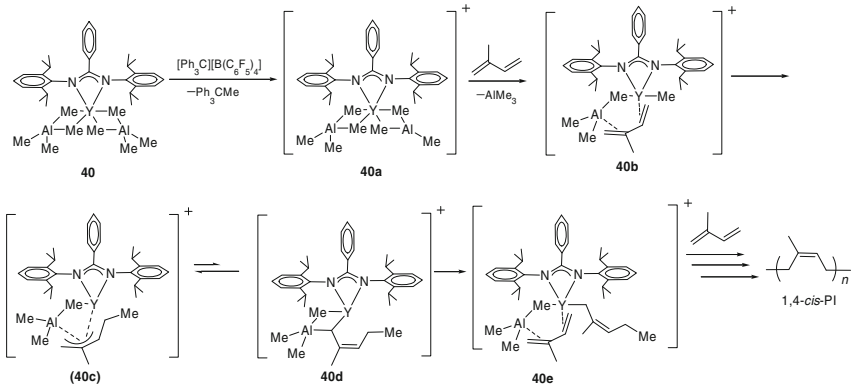

Scheme 16 Possible mechanism for the *cis*-1,4-polymerization with **40**

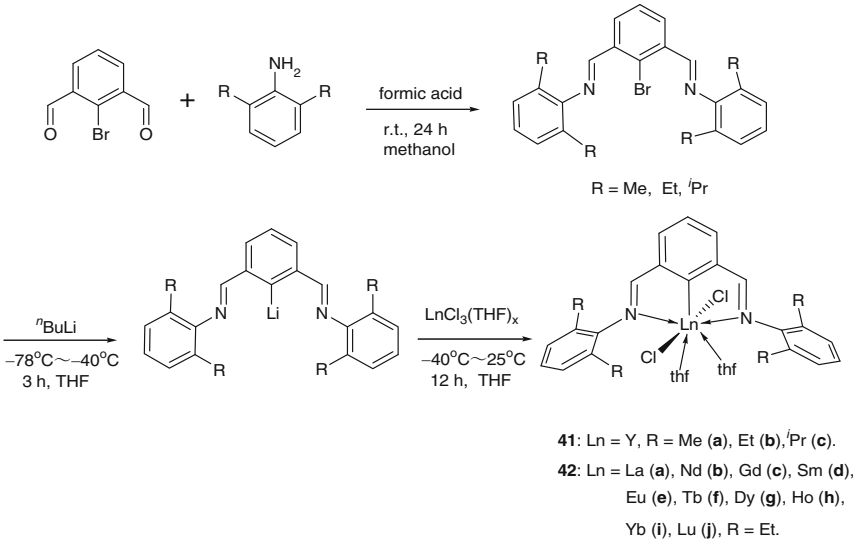

Scheme 17 Synthesis of pincer-type lanthanide dichloride

polymerization of butadiene in the early 1960s, are highly active to give polymers with 98% *cis*-1,4-selectivity but heterogeneous, leading to gel formation [134,135]. The addition of an electron donor to lanthanide trichlorides improves the catalytic activity and selectivity slightly, whereas the system is still heterogeneous [37]. Modifying the lanthanide chloride species with Cp or *ansa*-Cp and Flu moieties generated an inert system for the polymerization of butadiene, although which was active for copolymerization with ethylene, affording *trans*-1,4-butenyl units [136]. Cui's group successfully introduced the aryldiimino NCN-pincer ligand into rare-earth metal chloride compounds via covalent bond to afford complexes **41** and **42** (Scheme 17) [137]. These complexes in combination with aluminum alkyls

Table 15 Polymerization of butadiene induced by $(NCN)LnCl_2THF_2/TIBA/[Ph_3C][B(C_6F_5)_4]$[a] [137]

Run	Complex	[BD]/[Ln]	Temp (°C)	Time (min)	Yield (%)	M_n^b ($\times 10^4$)	M_w/M_n^b	Microstructure (%)[c]		
								cis-1,4-	*trans*-1,4-	1,2-
1	**41a**	500	25	60	80	3.96	1.47	98.5	1.3	0.2
2	**41b**	500	25	60	100	8.60	2.23	99.7	0.3	–
3	**41c**	500	25	60	68	2.63	1.31	95.3	4.2	0.5
4	**42a**	500	25	60	87	7.01	1.59	99.3	0.5	0.2
5	**42b**	500	25	15	100	18.00	2.08	99.5	0.4	0.1
6	**42c**	500	25	10	100	32.21	2.18	99.7	0.3	–
7	**42d**	500	25	120	0					
8	**42e**	500	25	120	0					
9	**42f**	500	25	10	100	21.00	2.43	99.7	0.3	–
10	**42g**	500	25	10	100	26.00	2.24	99.4	0.6	–
11	**42h**	500	25	15	100	14.22	2.44	99.4	0.6	–
12	**42i**	500	25	120	0					
13	**42j**	500	25	60	90	9.75	2.48	99.3	0.6	0.1
14	**41b**	1,000	25	60	100	18.63	2.31	99.3	0.7	
15[d]	**41b**	2,000	25	60	93	39.50	2.40	99.4	0.6	–
16[e]	**41b**	4,000	25	180	90	79.20	2.13	99.7	0.3	–
17[f]	**41b**	5,000	25	180	85	133.00	1.79	99.9	0.1	–
18[g]	**41b**	500	25	60	43	31.88	2.11	66.5	31.7	1.8
19[h]	**41b**	500	25	60	65	17.40	1.68	51.5	47.5	1.0
20	**42c**	500	0	30	85	33.10	1.89	100		
21	**42c**	500	40	5	100	21.35	2.03	99.3	0.7	–
22	**42c**	500	60	5	100	11.70	1.87	97.6	2.1	0.3
23	**42c**	500	80	5	80	10.23	1.95	96.9	3.0	0.5

[a] C_6H_5Cl (5 mL), complex (20 μmol), $[Ln]_0/[TIBA]_0/[B]_0 = 1:20:1$ (B = $[Ph_3C][B(C_6F_5)_4]$
[b] Determined by GPC
[c] Determined by ^{13}C NMR spectrum
[d] C_6H_5Cl (15 mL)
[e] C_6H_5Cl (20 mL)
[f] C_6H_5Cl (30 mL)
[g] $[Y]_0/[TMA]_0/[B]_0 = 1:20:1$
[h] $[Y]_0/[TEA]_0/[B]_0 = 1:20:1$

and organoborate generated a new type of homogeneous Ziegler–Natta catalyst systems that displayed high activities and distinguished *cis*-1,4-selectivities for the polymerizations of butadiene and isoprene (Table 15). These excellent catalytic performances did not show obvious metal-type dependence except the inert Yb, Sm, and Eu counterparts but were influenced significantly by the spatial sterics of the auxiliary ligand and the sterically demanding alkylaluminum. The *cis*-selectivity of this system was found to be influenced by the *ortho*-substituents of the *N*-aryl ring of the ligands, reaching as high as 99.7% for **41b** bearing *o*-ethyl, which dropped slightly for **41a** bearing *o*-methyl (98.5%) and even more in the case of **41c** with the bulky *o*-isopropyl (95.3%). This might be ascribed to the different steric environment of the center metal that was pinched by the two *ortho*-substituted *N*-aryl rings. The dihedral angle formed by the aryl rings was 118.56(13)° in **41a**, 109.9° in **41b**, and 133.28(15)° in **41c**, respectively. The smaller the dihedral angle is, the

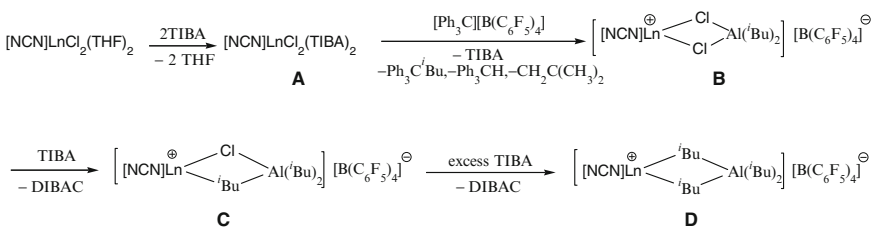

Scheme 18 Probable mechanism for diene polymerization

bulkier the metal center is, the higher *cis*-1,4-selectivity is. Remarkably, the high *cis*-1,4-selectivity remained at elevated polymerization temperatures up to 80°C. These results were in striking contrast to the conventional Ziegler–Natta systems in the specific selective polymerization of dienes. The identification of the active species was depicted in Scheme 18. The pincer yttrium dichloride (**41b**) was first treated with TIBA in C_6D_5Cl. The alkylation did not take place at room temperature within 12 h, suggesting that the Ln–Cl bond in **41b** was strengthened by the chelating NCN-pincer donor as compared to $LnCl_3$. Instead, an intermediate **A** [NCN]$LnCl_2$(TIBA)$_2$, the TIBA adduct of **41b**, was generated. It was reasonable that **A** could not induce the polymerization of butadiene at room temperature. When activated with $[Ph_3C][B(C_6F_5)_4]$, **A** was swiftly transformed into the ion pair **B**. **B** was still inert to the polymerization. When adding one more equivalent of TIBA to **B**, a heteroleptic alkyl/chloride-bridged bimetallic intermediate **C**, [NCN]Ln[(μ-Cl)(μ-^{i}Bu)(Al-(^{i}Bu)$_2$)][$B(C_6F_5)_4$], was given. Under the presence of excess TIBA, **C** initiated the polymerization of butadiene (isoprene) immediately [137]. This result strongly suggested that the intermediate or active species generated by different catalyst systems might be different even though they showed the same high *cis*-1,4-selectivity toward the diene polymerizations. Onward Gambarotta [138] reported the 2,6-diiminopyridine ligand-stabilized rare-earth metal dichloride lithium ate complexes 2,6-[2,6-(^{i}Pr)$_2C_6H_3$]N=C(CH_3)$_2$(C_5H_3N)Nd(THF)(μ-Cl)$_2$[Li(THF)$_2$]·0.5(hexane) (**43a**), and its analogues **43b–d** (Fig. 5). Addition of a solution of **43a** in cyclohexane to a cyclohexane solution of butadiene containing excess MMAO at 50°C started a polymerization affording polybutadiene with 95–97% *cis*-1,4-configuration in good yield (about 70%). Such high stereoselectivity in addition to the high catalyst activity, the high molecular weight, the relatively narrow polydispersity, and other desirable rheological properties placed this catalyst above other transition metal-based catalysts [139–142] and $NdCl_3(THF)_2$ [5], but below the remarkably performing $Cp^*_2Sm(THF)_2$ [105] and the aryldiimino NCN-pincer-ligated rare-earth metal dichlorides (2,6-(2,6-$C_6H_3R_2N$=CH)$_2$−C_6H_3)$LnCl_2(THF)_2$ [137]. The mixed alkyl/chloride complex **43d** showed similar catalytic performances to **43a**, suggesting that partial alkylation occurred during the treatment of **43a** with MMAO. Meanwhile, the complex **43c** was also a potent polymerization catalyst when activated by alkylaluminum derivatives. Although the activity was somewhat lower than **43a**, the molecular weight of the polymer produced by **43c** was higher (Table 16).

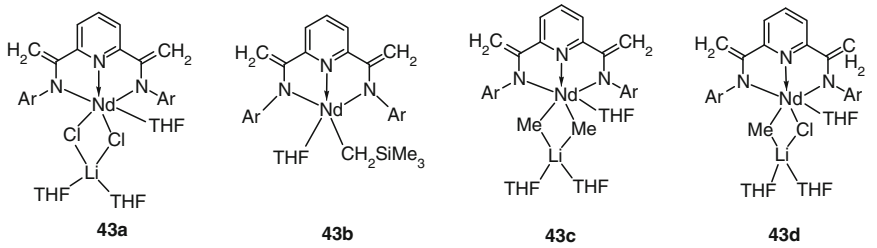

Fig. 5 Structures of complexes **43**

Table 16 Polymerization of butadiene catalyzed by **43** and MMAO [138]

Run	Complex	Time (min)	Activity (kg (mmol h)$^{-1}$)	Yield (%)	*cis*-1,4 (%)	*trans*-1,4 (%)	1,2-(%)	M_w ($\times 10^4$)	M_n ($\times 10^4$)	M_z ($\times 10^4$)	M_w/M_n
1	**43d**	15	0.74	77.3	97.0	2.5	0.5	65.9	26.3	122.0	2.5
2	**43d**	15	0.12(5)	67.5	95.0	4.5	0.5	38.0	16.4	71.5	2.31
3	**43d**	15	0.034(5)	84.8	96.1	4.5	3.4	38.5	16.4	72.7	2.34
4	**43a**	10	0.71	78.6	97.0	2.3	0.7	72.5	26.2	144.0	2.8
5	**43c**	15	0.40	17.2	95.9	3.3	0.8	91.0	15.5	220.0	4.9
6	**43b**	30	0.048	75.0	61.8	36.4	1.8	9.6	4.4	23.5	2.18

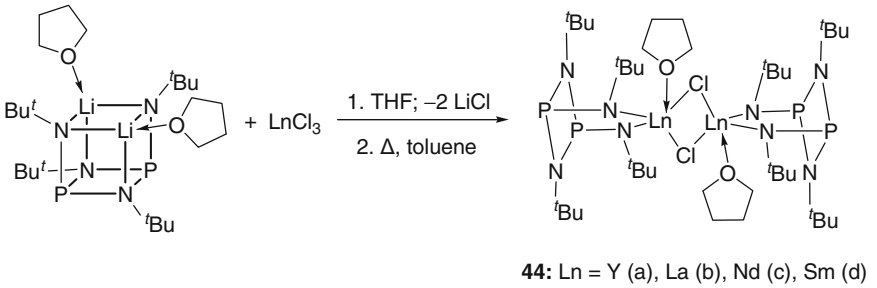

Scheme 19 Synthesis of complexes **44**

Recently Roesky et al. [143] demonstrated the synthesis of dimeric lanthanide chloro complexes featuring bis(amido)cyclodiphosph(III)azane (**44**) through salt metathesis methodology (Scheme 19). In the presence of MMAO, the neodymium complex **44c** displayed considerably high activity (TOF $\approx$ 17,000 h^{-1}) for polymerization of butadiene with 94% *cis*-1,4-selectivity. The number-average molecular weight of the afforded polybutadiene reached to 287,000 g mol^{-1} and the molecular weight distribution was narrow (PDI = 2.1). When the cocatalyst MMAO was replaced by organoborate [R$_2$(Ph)NH][B(C$_6$F$_5$)$_4$](R = octadecyl) and AlMe$_3$, the resultant ternary catalyst system exhibited nearly six times higher activity whilst the molecular weight and molecular weight distribution remained almost unchanged.

3 *trans*-1,4-Polymerization of 1,3-Conjugated Dienes

trans-1,4-Polydienes [144, 145], and particularly *trans*-1,4-polyisoprene produced naturally as gutta-percha rubber, appear well suited for the elaboration of high-performance tires [146], and have found application in the fabrication of golf ball and insulating materials. Moreover, *trans*-polymerization may also allow incorporation of α-olefin into a polydiene chain, affording high-value-added copolymers [147–149]. Therefore, *trans*-1,4-selective polymerization of dienes has attracted an increasing attention. In the investigation of active centers (ACs) with $NdCl_3$ based catalyst system for butadiene polymerization by Monakov, six kinds of ACs were proposed to relate the microstructures of polybutadiene (Fig. 6). The first five involved a π-allyl binding of the terminal unit of the growing polymer chain, which was deemed to be responsible for the *cis*-regulated polybutadiene, whilst only the last one characterized as a σ-alkyl structure led to *trans*-regulated polybutadiene [150]. Thus, the reports on the production of *trans*-1,4-polymers by rare-earth metal complexes remain less owing to few suitable active centers compared with the *cis*-1,4-polymerization.

Visseaux reported that neodymium borohydrido complexes were very efficient catalysts toward isoprene polymerization. Upon activation with alkylaluminum or MAO, these borohydrido complexes yielded polydienes rich in *cis*-1,4-units, whereas *trans*-1,4-polydienes with very high stereoregularity were produced in the presence of dialkyl magnesium activator [150–156]. Although the mechanism was still unclear and no obvious regularity could be drawn, the selectivity was dependent on the metal center [154]. For instance, $Nd(BH_4)_3THF_3$ (**45a**) displayed high activity and selectivity while Sm and Y congeners (**45b**, **45c**) were totally inactive (Table 17). Unlike trialkylaluminum additives which can remarkably change the regioselectivity, varying dialkyl magnesium exhibited no evident effect on the *trans*-1,4-selectivity. Higher activity was realized at elevated temperature albeit sacrificing the selectivity and molecular weight distribution. The used solvent also affected the activity and selectivity. Noncoordinating solvents such as toluene or aliphatic hydrocarbon had no influence on the selectivity, but low activity was observed in

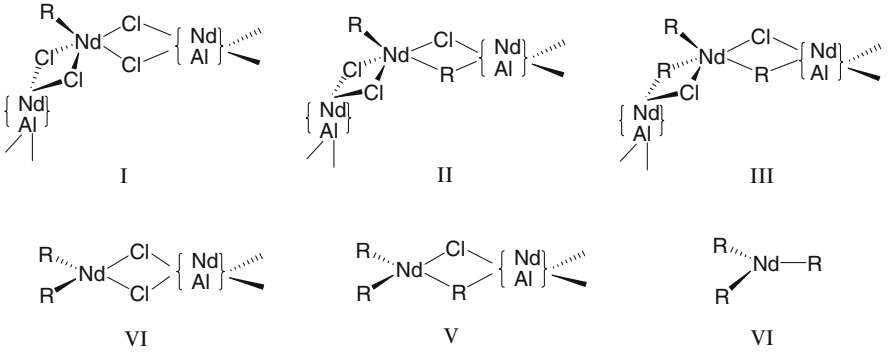

Fig. 6 The probable six kinds of active centers

Table 17 Polymerization of isoprene with borohydride complexes and magnesium activator

Run	Precatalyst[a]	[IP]/[Ln]	Solvent	Temp (°C)	Time (h)	Yield (%)	*trans*-1,4[b] (%)	M_n[c] ($\times 10^3$)	PDI[c]	References
1	**45a**/1 MgBuEt	1,000	Toluene	50	3	92	96.4	43.2	1.37	[154]
2	**45a**/1 $Mg(Hex)_2$	1,000	Toluene	50	3	80	96.2	42.2	1.75	[154]
3	**45a**/1 $MgBu_2$	1,000	Toluene	50	3	85	94.5	46.5	1.59	[154]
4	**45a**/1 $Mg(CH_2TMS)_2$	1,000	Toluene	50	1	50	86.1	82.7	1.61	[154]
5	**45a**/1 $Mg(C_3H_5)_2$	1,000	Toluene	50	1	80	96.3	35.1	1.34	[154]
6	**45b**/1 MgBuEt	1,000	Toluene	50	24	0				[154]
7	**45c**/1 MgBuEt	1,000	Toluene	50	24	0				[154]
8	**45a**/0.5 MgBuEt	1,000	Toluene	50	2	67	93.0	61.5	1.40	[154]
9	**45a**/1 MgBuEt	1,000	Toluene	50	2	87	95.5	52.1	1.35	[154]
10	**45a**/2 MgBuEt	1,000	Toluene	50	2	66	93.9	27.8	1.55	[154]
11	**45a**/3 MgBuEt	1,000	Toluene	50	24	0				[154]
12	**45a**/3 MgBuEt	1,000	Toluene	50	48	30	60.7	15.0	2.05	[154]
13	**45a**/3 MgBuEt	1,000	Toluene	90	24	58	64.8	8.6	3.20	[154]
14	**45a**/5 MgBuEt	1,000	Toluene	50	24	0				[154]
15	**45a**/1 MgBuEt	1,000	Toluene	50	2	87	95.5	NG	1.35	[154]
16	**45a**/1 MgBuEt	1,000	Cyclohexene	50	2	52	95.2	NG	1.48	[154]
17	**45a**/1 MgBuEt	1,000	Pentane	50	2	54	95.8	NG	1.52	[154]
18	**45a**/1 MgBuEt	1,000	Toluene/ THF	50	2	33	96.5	NG	1.60	[154]
19[d]	**45a**/1 MgBuEt	1,000	THF	50	24	0				[154]
20	**45a**/1 MgBuEt	1,000	CH_2Cl_2	50	6	18	87.8	NG	2.18	[154]
21	**45a**/1 MgBuEt	1,000	Toluene	50	3	66	96.4	NG	1.82	[154]
22[e]	**45a**/1 MgBuEt	1,000	Toluene	50	24	94	94.2	NG	1.82	[154]
23[e]	**45a**/1 MgBuEt	1,000	Toluene	20	3	31	97.7	21.5	1.35	[154]
24	**45a**/1 MgBuEt	1,000	Toluene	50	3	92	95.5	63.6	1.37	[154]
25	**45a**/1 MgBuEt	1,000	Toluene	70	3	92	93.7	63.3	1.82	[154]
26	**45a**/1 MgBuEt	1,000	Toluene	80	3	93	93.2	59.0	2.22	[154]
27	**46**/1 $MgBu_2$	600	Toluene	50	22	60	98.4	15.4	2.01	[153]
28[d]	**47**/0.9 $MgBu_2$	120	Toluene	50	2.75	>99	98.5	9.5	1.15	[153]
29	**47**/52 $MgBu_2$	120	Toluene	50	20	60	57.7	ND	ND	[153]
30	**48**/1.2 $MgBu_2$	160	Toluene	50	NG	NG	98.2	9.7	1.22	[153]
31	**48**/1 MgBuEt	1,000	Toluene	50	2	80	97.4	52.3	1.18	[153]
32	**49**/1 MgBuEt	1,000	Toluene	50	2	84	98.2	58.2	1.16	[155]
33	**50**/1 MgBuEt	1,000	Toluene	50	2	41	95.2	31.6	1.57	[155]
34	**51**/1 MgBuEt	1,000	Toluene	50	2	59	96.2	35.5	1.32	[155]

NG not given, *ND* not determined

[a]Precatalyst: 10 µmol solvent: 1 mL

[b]Determined by ^{1}H NMR

[c]Determined by GPC

[d][thf]/Ln] = 3

[e]Toluene: 3 mL

the latter, probably due to the poor solubility of the thus formed polymer. In contrast, the coordinating THF or CH_2Cl_2 were deleterious, owing to their competitive coordination to active sites with dienes. The *trans*-selectivity could be improved by means of enhancing the steric hindrance at the metal center. Thus, the bulky half-metallocene derivatives **46–51** provided more than 98% *trans*-1,4-polyisoprene [152, 153] (Fig. 7, Table 17) as compared with the combination of the homoleptic $Nd(BH_4)_3(THF)_3$ and $MgBu_2$ (96%) [156]. Obviously, *trans*-stereospecific character of these catalysts was tentatively attributed to the concerted effects arising from both Nd and Mg ions, evidenced by the formation of $Nd(\mu\text{-}BH_4)Mg$ bridging

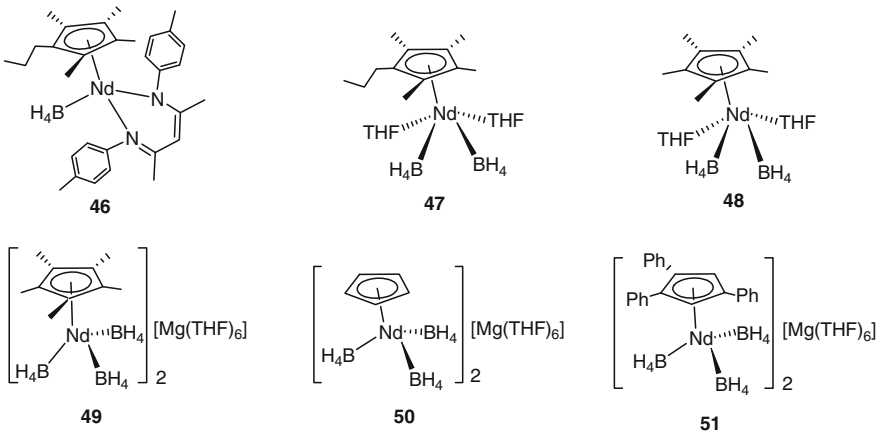

Fig. 7 Structures of half-sandwich neodymium borohydrido complexes **46–51**

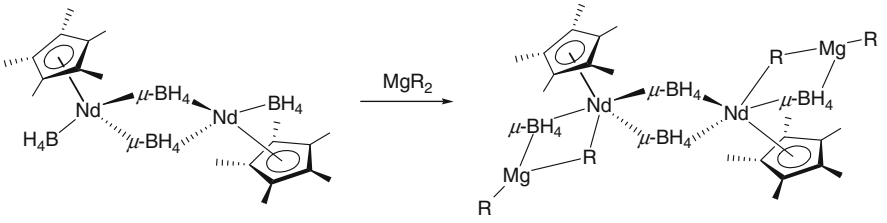

Scheme 20 Probable heterobimetallic active species

active species according to ^{1}H NMR analysis (Scheme 20) [154,155]. Therefore, introducing a long-chain *n*-butyl ethyl magnesium, a living *trans*-1,4-polymerization of isoprene could be achieved [156,157]. The surplus amount of dialkyl magnesium, however, resulted in a lowered *trans*-selectivity with the increase of 3,4-units in the afforded polymer. Surprisingly, when BuLi was used instead of MgR_2, the combination with $(C_5H^iPr_4)Ln(BH_4)_2(THF)$(Ln = Sm, Nd), or $(C_5H^iPr_4)U(BH_4)_3$ enabled not only the *trans*-1,4 (95%) polymerization of isoprene to give high molecular weight product (M_n = 590,000, IP = 1.5, 5 h, 50°C) but also syndioselective (75%) polymerization of styrene (16 h, 50°C, yield 90%, M_n = 530,000, IP = 1.6) [158].

Half-sandwich lanthanide aluminate (**52**) with the activation of organoborate or borane displaying good to excellent activities for the *trans*-1,4-polymerization of isoprene was reported by Anwander [159]. They found that neutral borane $B(C_6F_5)_3$ exhibited superior performance as compared with organoborate, and the larger the rare-earth metal was, the higher the selectivity was. Thus, polyisoprene with very high *trans*-1,4-content (99.5%) and very narrow molecular weight distributions ($M_w/M_n = 1.18$) could be obtained from a combination of $Cp^*La(AlMe_4)_2$ and $[Ph_3C][B(C_6F_5)_3]$ (**53b**), suggesting a living catalyst system (Table 18). Remarkably, a cationic and well-characterized complex **53d** isolated from the reaction between $Cp^*La(AlMe_4)_2$ and $B(C_6F_5)_3$ (Scheme 21) could serve as a single-component catalyst to produce the *trans*-polymer with almost the same properties, which also provided the structure model of the true active center in this

Table 18 Polymerization of isoprene catalyzed by heterobimetallic complexes and borate (or borane)

Run	Precat.	Cocat.	M_n ($\times 10^4$)	M_w/M_n	*trans*-1,4/*cis*-1,4	References
1	**52a**	**A**	2	8.95	20.6/60.5	[159]
2	**52a**	**B**	6	1.59	28.7/43.5	[159]
3	**52a**	**C**	9	1.78	93.6/1.9	[159]
4	**52c**	**A**	3	2.87	69.7/14.0	[159]
5	**52c**	**B**	4	1.16	79.9/6.9	[159]
6	**52c**	**C**	13	1.35	92.4/3.8	[159]
7	**52b**	**A**	7	1.28	87.0/3.5	[159]
8	**52b**	**B**	6	1.22	79.5/3.4	[159]
9	**52b**	**C**	24	1.18	99.5/–	[159]
10	**53d**	–	23	1.19	99.0/0.2	[159]
11	**54a**	**A**	19	2.18	9.0/60.0	[160]
12	**54a**	**B**	12	1.77	4.0/63.0	[160]
13	**54a**	**C**	27	1.74	40.0/52.0	[160]
14	**54b**	**A**	6	1.28	80.3/14.5	[160]
15	**54b**	**B**	6	1.22	79.4/15.3	[160]
16	**54b**	**C**	33	1.52	89.3/–	[160]
17	**55a**	**A**	1	24.41	26.4/38.1	[160]
18	**55a**	**B**	3	1.74	34.6/38.3	[160]
19	**55a**	**C**	5	1.73	80.8/3.4	[160]
20	**55b**	**A**	9	1.45	81.4/3.4	[160]
21	**55b**	**B**	6	1.20	87.7/10.5	[160]
22	**55b**	**C**	20	1.26	95.6/2.2	[160]
23	**56a**	**A**	8	1.67	21.2/45.5	[160]
24	**56a**	**B**	9	1.25	19.0/53.0	[160]
25	**56a**	**C**	5	1.50	56.0/31.0	[160]
26	**56b**	**A**	8	1.41	60.0/20.0	[160]
27	**56b**	**B**	8	1.22	50.0/30.0	[160]
28	**56b**	**C**	11	1.41	90.0/6.0	[160]

A: $[Ph_3C][B(C_6F_5)_4]$, **B**: $[PhNMe_2H][B(C_6F_5)_4]$, **C**: $B(C_6F_5)_3$

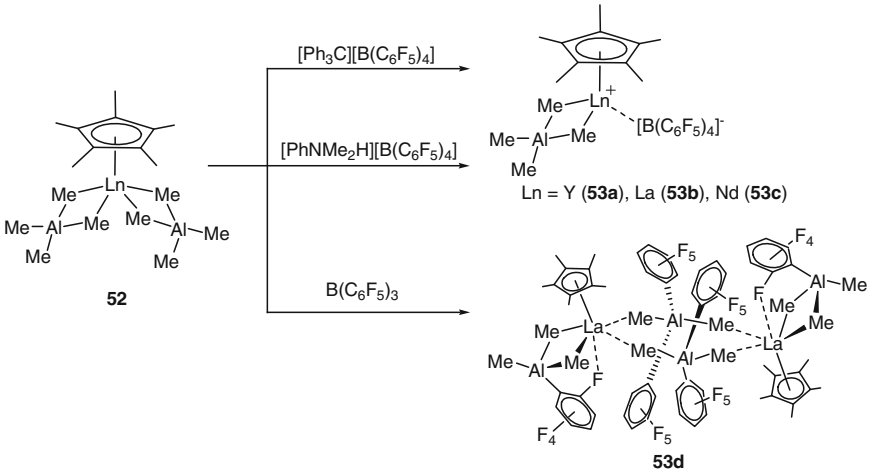

Scheme 21 Activation of Ln/Al complex with different organoborate or borane

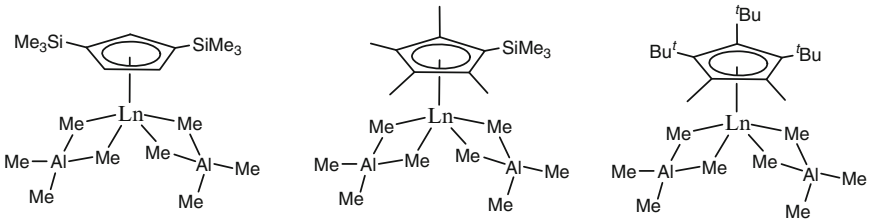

54: Ln = Y (**a**), La (**b**), Nd (**c**) **55:** Ln = Y (**a**), La (**b**) **56:** Ln = Nd (**a**), La (**b**)

Fig. 8 Structures of half-sandwich heterobimetallic lanthanide/aluminum complexes **54–56**

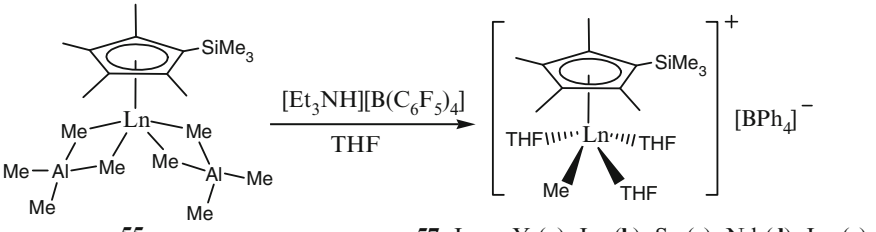

55 **57**: Ln = Y (**a**), La (**b**), Sm(**c**), Nd (**d**), Lu (**e**)

Scheme 22 Isolation of ion pair complex from **55** and organoborate

polymerization process. The regioselectivity could be improved with the complexes (**54–56**, Fig. 8) bearing the ancillary ligands that stabilized the cationic species generated in situ from reaction of catalyst precursor and borane as was disclosed by online NMR technique, although there seemed no correlation between the degree of steric shielding of the ancillary ligand with the catalytic activity and the selectivity [160].

Meanwhile, Okuda investigated the catalytic behavior for the polymerization of butadiene with the same half-sandwich rare-earth metal tetramethylaluminate complexes [Ln(η^5-$C_5Me_4SiMe_3$){(μ-Me)$_2$($AlMe_2$)}$_2$] (**55**, Ln = Y, La, Nd, Sm, Gd, Lu) [161]. Upon activation with $[NEt_3H]^+[B(C_6F_5)_4]^-$, the resultant cationic species enabled the polymerization of butadiene in the presence of TIBA to give *trans*-1,4-polybutadiene with narrow polydispersities ($M_w/M_n = 1.05$–1.09). Different from Anwander's result where heterobimetallic species was isolated, mononuclear ion pair was obtained from the reaction with borate (Scheme 22). Unfortunately, no catalytic data of **57** were given by the authors.

Nd(η^3-C_3H_5)$_3$ and its derivatives were also evaluated as catalysts toward the polymerization of butadiene by Taube [162, 163]. Polymers with *trans*-1,4-unit around 85% were formed by using Nd(η^3-C_3H_5)$_3$ in toluene at 50°C. Detailed study revealed that the M_n of the polymer increased linearly with the conversion and the polydispersity remained narrow. For the solvated precursor Nd(η^3-C_3H_5)$_3$($C_4H_8O_2$), higher *trans*-1,4-selectivity of 94% was achieved. Interestingly, the *trans*-1,4-selectivity can be switched to *cis*-1,4 by addition of trialkylaluminum or MAO. Introducing a Cp ligand, the resultant half-

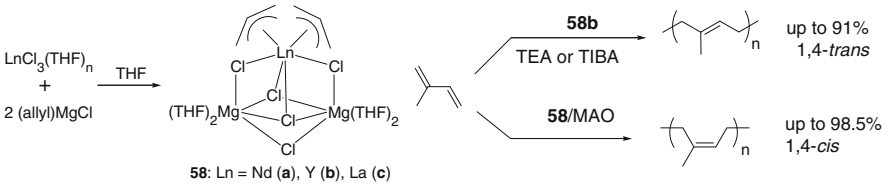

Scheme 23 Polymerization of isoprene initiated by **58** with alkylaluminum activator

Table 19 Polymerization of conjugated dienes by lanthanide precatalyst and different activator

Run	Catalyst	Monomer	Temp (°C)	M_n ($\times 10^3$)	M_w/M_n	1,4-*cis*/1,4-*trans*(%)	References
1	**58a**/MAO	Isoprene	20	78	1.38	96.0/2.3	[164]
2	**58b**/MAO	Isoprene	20	33	6.5	75.2/22.8	[164]
3	**58b**/TEA	Isoprene	20	12	8.6	8.3/90.7	[164]
4	**58b**/TIBA	Isoprene	20	12	6.7	8.8/90.0	[164]
5	**59a**/MAO	Butadiene	25	NG	NG	0/>99	[165]
6	**59a**/$Mg(Bu)_2$/$B(C_6F_5)_3$	Butadiene	25	NG	NG	20/80	[165]
7	**59b**/MAO	Butadiene	25	NG	NG	76/17	[165]
8	**59a**/$Mg(Bu)_2$/$B(C_6F_5)_3$	Butadiene	25	NG	NG	30/70	[165]
9	**59c**/MAO	Butadiene	25	NG	NG	65/35	[165]
10	**59c**/$Mg(Bu)_2$/$B(C_6F_5)_3$	Butadiene	25	NG	NG	0/>99	[165]

NG not given

sandwich allyl complex $Cp^*Nd(\eta^3\text{-}C_3H_5)_2(0.7C_4H_8O_2)$, unfortunately, was inactive for the polymerization of butadiene, which in conjunction with MAO became extremely active albeit without selectivity. It was interesting to find that the central metal ion played a significant role in determining the selectivity of the system. Carpentier reported that the bimetallic neodymium–magnesium $Nd(allyl)_2Cl(MgCl_2)_2(THF)_4$ (**58a**, Scheme 23) combined with TEA or TIBA was highly active and *cis*-1,4-selective for the polymerization of isoprene (average TOFs up to ca. 5×10^4 mol (mol h)$^{-1}$ at 20°C). Whereas the yttrium analogue **58b**/MAO displaying lower activity enabled the formation of either *cis*-1,4-enriched (75%) or *trans*-1,4-enriched (91%) polyisoprenes, simply replacing the MAO activator by TEA or TIBA, respectively (Table 19) [164].

The strong dependence of the catalytic performances on the lanthanide metal ions and the trialkylaluminum compounds were also found in the systems based on lanthanocenes reported by Kaita et al. Lanthanocene complexes **27** in the presence of trialkylaluminum and $[Ph_3C][B(C_6F_5)_4]$ could initiate the living polymerization of butadiene [112]. The most active gadolinium system gave perfectly *cis*-1,4-regulated polybutadiene at −40°C, whilst the analogous cerium complex and TMA and $[Ph_3C][B(C_6F_5)_4]$ displayed high *trans*-1,4-selectivity (93.8%) toward the polymerization of butadiene in a quasiliving mode (Table 9).

The linked half-sandwich ligand brought about obvious improvement in *trans*-1,4-selectivity for the attached active metal center as reported by Napoli [165]. The yttrium complex **59a** (Fig. 9) in conjunction with MAO produced polybutadiene

with >99% *cis*-1,4-regularity, whereas the samarium (**59b**) and neodymium (**59c**) analogues were *cis*-1,4-selective enriched. Replacing MAO by $MgBu_2$ and $B(C_6F_5)_3$, in contrast, **59c** exhibited an as high as *trans*-1,4 > 99% selectivity, whereas *trans*-1,4-selectivity of **59a** system reduced to 80% (Table 19). This proved further that the active species in the *trans*-polymerization of dienes were probably bimetallic.

Up to date, all these complexes showing high *trans*-1,4-selectivity for the polymerization of dienes are rare-earth metal complexes bearing a Cp ligand by virtue of their steric hindrance. Cui's group recently reported the first rare-earth metal bis(alkyl) complexes featuring a non-Cp N,N'-bidentate auxiliary ligand $(L^{1-3})Ln(CH_2SiMe_3)_2(THF)_n$ (**60–62**, Scheme 24), which, in combination with AlR_3 and borate, showed medium activity and good *trans*-1,4-selectivity for the polymerization of butadiene. The resultant polymer had moderate molecular weight ($M_n = 10{,}000$–$18{,}000$) with narrow molecular weight distribution ($M_w/M_n < 1.6$) and *trans*-1,4-regularity varying from 49.2% up to 91.3%. The catalyst performances were strongly dependent on the *ortho*-substituent of the *N*-aryl ring, the type of aluminum alkyls and the lanthanide metal used. Higher

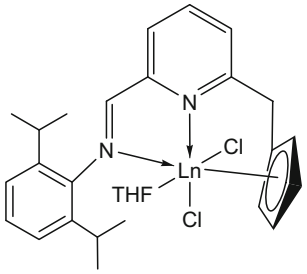

59 : Ln = Y (**a**), Sm (**b**), Nd (**c**)

Fig. 9 Linked half-metallocene complexes of lanthanide

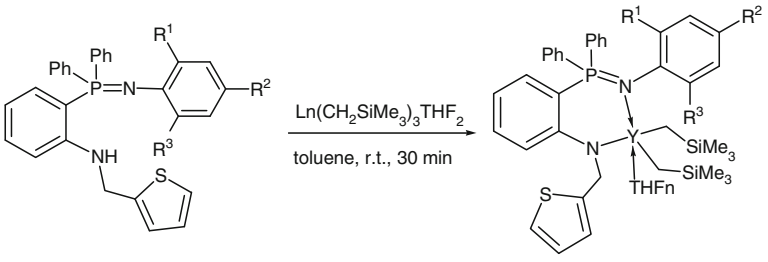

HL^1: $R^1 = R^2 = R^3 = Me$
HL^2: $R^1 = R^3 = Et$, $R^2 = H$
HL^3: $R^1 = R^3 = {}^iPr$, $R^2 = H$

60a: Ln = Sc, n = 1, $R^1 = R^2 = R^3 = Me$
60b: Ln = Lu, n = 1, $R^1 = R^2 = R^3 = Me$
61a: Ln = Sc, n = 1, $R^1 = R^3 = Et$, $R^2 = H$
61b: Ln = Lu, n = 1, $R^1 = R^3 = Et$, $R^2 = H$
61c: Ln = Y, n = 1, $R^1 = R^3 = Et$, $R^2 = H$
62a: Ln = Sc, n = 0, $R^1 = R^3 = {}^iPr$, $R^2 = H$

Scheme 24 Synthesis of dialkyl lanthanide complexes bearing anilido-phosphoimino ligand

trans-1,4-selectivity could be reached with bulky substituents or by employing smaller metal. Furthermore, the introduction of a pendant moiety capable of coordinating to the metal center benefited the *trans*-1,4-regularity [166, 167].

4 3,4-Polymerization of Isoprene

As compared with the explosive number of reports on 1,4-polymerization of dienes, 3,4-selective polymerization of isoprene has remained less explored, although 3,4-regulated polyisoprene is an important component of high-performance rubbers such as those with wet-skid resistance or low-rolling resistance tread [168, 169]. Early researches revealed that diene monomers insert into active lanthanide center to generate Ln-η^3-allyl transition state (Scheme 2). As a consequence of the strong lanthanide allyl bond and higher ionic charge on the lanthanide, the negative charges shifted to C1 atom from C3 atom. Thus, the nucleophilicity of the C3 atom was lessened, suppressing the formation of 3,4-unit by the nucleophilic attack of the diene via C3 atom. Therefore the 3,4-polymerization of isoprene is more impossible. The first efficient 3,4-selective systems were the patented organolithium and ferric acetylacetate [170–172] and the transition metal complexes such as $AlEt_3$–$Ti(OR)_4$ [22], $(dmpe)_2CrCl_2$–MAO [23], and ferric complexes chelated by nitrogen ligands [22–25]. Medium to high 3,4-regularity or strain-crystalline polyisoprene could be obtained by lowering the polymerization temperature. The catalyst systems based on rare-earth metals were achieved only recently by Hou's group using a dimeric yttrium monoalkyl complex **63a** (Fig. 10) bearing bulky linked half-sandwich ligand and a cocatalyst $[Ph_3C][B(C_6F_5)_4]$. The polymerization of isoprene proceeded rapidly to yield 3,4-polyisoprene (99%) with isotactic-rich stereotacticity (*mm* = 80%, *mmmm* = 30%) and a relatively narrow molecular weight distribution ($M_w/M_n = 1.8$, Table 20). When polymerization was carried out at −20°C, a polyisoprene with almost perfect isotactic 3,4-microstructure (3,4-selectivity 100%, *mmmm* > 99%) was obtained. The active species were unstable, easily decomposed, or changed to other species; thus, bimodal molecular weight

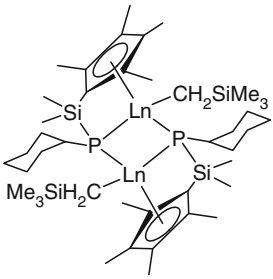

63: Ln = Y (**a**), Lu (**b**)

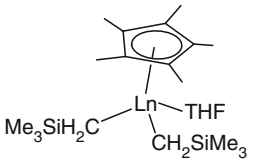

64: Ln = Y (**a**), Sc (**b**)

Fig. 10 Structures of half-metallocenes of lanthanide alkyl complexes

Table 20 Polymerization of isoprene under various conditions lanthanide alkyl complexes[a] [173]

Run	Cat.	Temp (°C)	Time (h)	Yield (%)	M_n[b] ($\times 10^5$)	PDI[b]	Microstructure (%)			T_g/T_m[d]
							3,4-	*mm*	*mmmm*	
1	**63a**	25	2	0						
2	**A**	25	2	80	0.3	7.9	<5[e]			ND
3	**B**	25	2	0						
4	**C**	25	2	0						
5	**63a**+**A**	25	2	92	1.0	1.8	99	80	30	42/–
6	**63a**+**A**	−10	16	41	4.3; 0.3	1.6; 1.4	100	96	80	28/148
7	**63a**+**A**	−20	48	50	3.2; 0.3	1.7; 1.4	100	100	>99	30/154
8	**63a**+**A**	25	2	100	1.2	1.3	99	80	30	41/–
9	**63a**+**A**	−10	16	60	3.7	1.6	100	96	80	31/138
10	**63a**+**A**	−20	48	87	5.0	1.6	100	100	>99	33/162
11[f]	**63a**+**A**	25	2	65	0.8	1.6	99	25		38/–
12	**63a**+**B**	25	2	85	1.4	1.3	99	40		ND
13	**63a**+**C**	25	2	63	1.1	1.4	99	38		ND
14	**63a**+**A**	25	2	17	1.3	1.6	89			ND
15	**64a**+**A**	25	2	100	0.9	1.06	66[g]			ND

ND not determined

[a]Conditions: C_6H_5Cl, 10 mL; neutral complex, 2.5×10^{-5} mol; $[isoprene]_0/[complex]_0 = 600$, $[complex]_0/[activator]_0 = 1{:}1$, **A** = $[Ph_3C][B(C_6F_5)_4]$, **B** = $[PhMe_2NH][B(C_6F_5)_4]$, **C** = $B(C_6F_5)_3$. In runs 5–7, isoprene was added to **63a** and **A**. In runs 8–15, an activator was added to neutral complex and isoprene

[b]Determined by GPC against polystyrene standard

[c]Determined by ^1H and ^{13}C NMR

[d]Determined by DSC

[e]The *trans*-1,4-unit is a major component

[f]In toluene

[g]1,4-unit: 34%

distribution was observed. To avoid this isoprene should be added to the reaction mixture prior to the activator to stabilize the formed active species. By means of DFT calculation, the mechanism was supposed as shown in Scheme 25. It seemed that the steric environment enforced isoprene to adopt η^2-coordination to the active metal center; meanwhile, the agostic interaction of the silymethyl or vinyl chain-end groups with metal ion contributed to the isotacticity. For comparison, the unlinked half-sandwich yttrium dialkyl complex **64a** was employed for the isoprene polymerization to give 66% 3,4-selectivity. This confirmed further that a more steric environment around the metal center benefited 3,4-selectivity [173].

Cui's group successfully synthesized indenyl- and fluorenyl-modified *N*-heterocyclic carbene, a new kind of linked half-sandwich ligand, attached rare-earth metal bis(alkyl) complexes (**65**, **66**) (Fig. 11). In the presence of TIBA and $[Ph_3C][B(C_6F_5)_4]$, complexes **65b–65d** exhibited high activity, medium syndio but remarkably high 3,4-regioselectivity. More strikingly, this system realized for the first time the livingness mode for the 3,4-polymerization of isoprene. Moreover, such distinguished catalytic performances could be maintained under various monomer-to-initiator ratios (500–5,000) and broad range of polymerization temperatures (25–80°C) (Table 21). The resultant polymers are crystalline, having syndiotactic enriched (racemic enchainment triad *rr* = 50%, pentad *rrrr* = 30%)

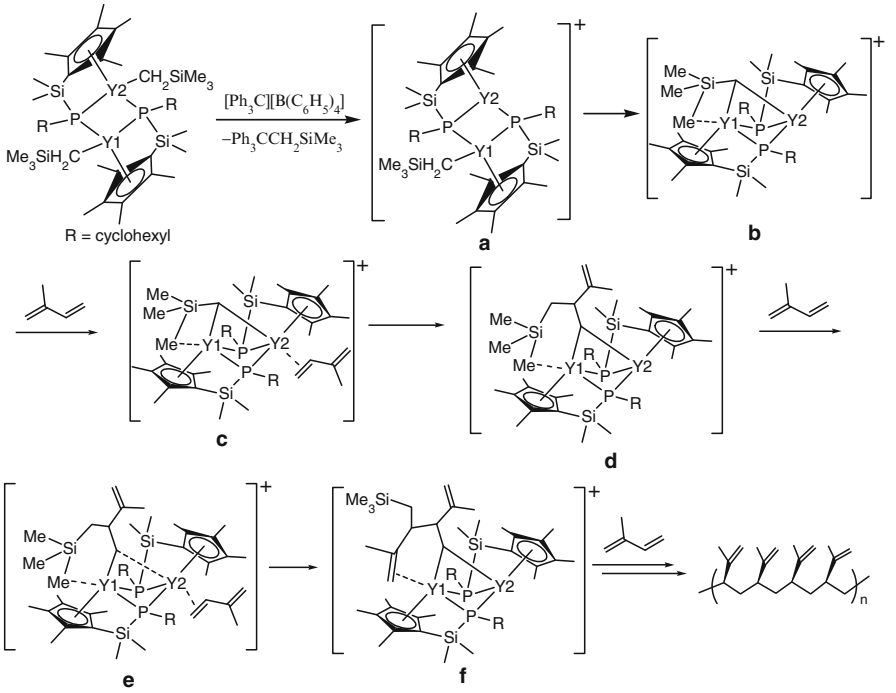

Scheme 25 Possible polymerization mechanism

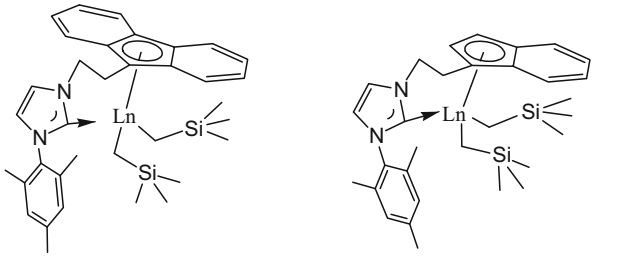

Fig. 11 Fluorenyl- and indenyl-functionalized carbene lanthanide dialkyl complexes

3,4-regulated (99%) microstructure and high glass transition temperatures (40–49°C). In contrast, complex **65a** was almost inert, probably resulting from the overcrowded environment induced by a smaller radius of scandium. For the less sterically hindered carbene–indenyl complexes **66a–66d**, low activity or selectivity was observed. This is in agreement with the assumption that tuning the spatial hindrance at the metal centers effectively changes the regioselectivity [174, 175].

Sequentially, the same group developed a variety of rare-earth metal bis(alkyl) complexes featuring NPN ligands (Scheme 26). Under the assistance of borate

Table 21 Polymerization of isoprene by using rare-earth metal precursors **65a–d** and **66a–d** and $[Ph_3C][B(C_6F_5)_4]$ and TIBA[a] [174]

Run	Cat.	[IP]/[Ln]	Temp (°C)	Time (h)	Yield (%)	3,4- (%)	M_n ($\times 10^4$)	M_w/M_n	T_g (°C)	Eff. (%)
1	**65a**	500	25	6	Trace	ND	ND	ND	ND	ND
2	**65b**	500	25	4	100	98.2	4.72	1.06	41	72.2
3	**65c**	500	25	3	100	98.3	3.94	1.07	43	86.4
4	**65d**	500	25	6	100	99.0	4.08	1.05	45	83.5
5	**65d**	1,000	25	12	100	98.6	8.61	1.11	45	79.1
6	**65d**	2,000	25	24	100	96.6	16.7	1.12	48	81.6
7	**65d**	3,000	25	36	100	96.7	25.1	1.22	48	81.4
8	**65d**	4,000	25	48	100	96.5	32.9	1.27	48	82.8
9	**65d**	5,000	25	72	93	95.2	39.4	1.29	47	80.4
10	**65d**	500	40	5	100	97.4	3.90	1.22	49	87.3
11	**65d**	500	50	4	100	97.3	3.73	1.27	48	91.3
12	**65d**	500	60	3	100	95.4	3.85	1.19	47	88.5
13	**65d**	500	70	3	100	95.4	4.02	1.19	46	84.7
14	**65d**	500	80	2	100	94.5	3.91	1.22	46	87.1
15	**65d**[b]	500	25	12	100	98.1	3.86	1.38	40	88.2
16	**65d**[c]	500	25	2	100	98.2	4.26	1.10	45	80.0
17	**66a**	500	25	6	Trace	ND	ND	ND	ND	ND
18	**66b**	500	25	6	50	89.4	2.03	1.36	23	83.9
19	**66c**	500	25	6	93	76.1	3.81	1.40	3	83.1
20	**66d**	500	25	6	15	91.0	ND	ND	ND	ND

ND not determined

[a]Conditions: toluene (3.0 mL); Ln (10 μmol); $[Ph_3C][B(C_6F_5)_4]$ (10 μmol); TIBA (100 μmol)

[b]Hexane as solvent

[c]Chlorobenzene as solvent

and trialkylaluminum, these complexes displayed extremely high activity and 3,4-selectivity for the polymerization of isoprene [176, 177] which represented the first non-Cp-ligated rare-earth metal-based catalyst system possessing such distinguished performances. Systematic study revealed that the complexes bearing alkyl substituents in the aryl rings of the ligands exhibited higher activity than those bearing electron-withdrawing substituents, irrespective of the central metal type (Table 22). Meanwhile, the sterics and electronics of the ligands played significant roles in governing the 3,4-selectivity of the complexes. With the increase of bulkiness of the *ortho*-substituents of the aryl rings of the ligands as well as reducing the size of the metal ion, the resultant complexes provided an increasing 3,4-selectivity, as the steric shielding around metal center led to isoprene η^2-coordination. The complexes bearing electron-donating ligands showed higher 3,4-selectivity, as the space-filled and electronegative metal center facilitated isoprene η^2-coordination. In contrast, an electrophilic metal center attached by ligands with electron-withdrawing groups favored isoprene η^4-coordination, resulting in moderate 3,4-regulated or even *cis*-1,4-enriched polyisoprene. These results elucidated for the first time the correlation of molecular structures of complexes and catalytic behaviors in 3,4-selective isoprene polymerization.

Similarly, yttrium dialkyl complexes **39**, **39a**, and **40** bearing amidinate ligand, a geometry analogue of NPN-imidophosphine amido ligand, in combination with $[Ph_3C][B(C_6F_5)_4]$, established cationic species for the polymerization of isoprene,

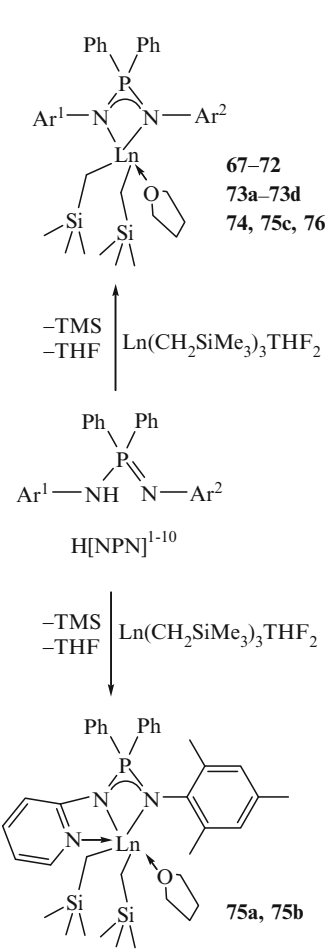

	Ligand	Ar^1	Ar^2	Ln
67	H[NPN]^1			Lu
68	H[NPN]^2			Lu
69	H[NPN]^3			Lu
70	H[NPN]^4			Lu
71	H[NPN]^5			Lu
72	H[NPN]^6			Lu
73a	H[NPN]^7			Lu
73b	H[NPN]^7			Y
73c	H[NPN]^7			Sc
73d	H[NPN]^7			Er
74	H[NPN]^8			Lu
75a	H[NPN]^9	N		Lu
75b	H[NPN]^9	N		Y
75c	H[NPN]^9	N		Sc
76	H[NPN]^{10}	F		Lu

Scheme 26 Synthesis of NPN-ligated lanthanide dialkyl complexes

giving isotactic 3,4-polyisoprene (Scheme 15) [133]. Meanwhile, Kempe reported 2-amidopyridine-ligated scandium dialkyl complexes **77a–d** (Fig. 12) where the ligand could be formally viewed as a variation of amidinate and coordinated to scandium in a *N*, *N′*-η^2-mode. These complexes were activated with organoborate or borane to show more than 95% 3,4-selectivity at room temperature. Further investigation of the monomer-to-initiator ratio with **77a**/$[C_6H_5NH(CH_3)_2][B(C_6F_5)_4]$ disclosed that the number of polymer chain was proportional to that of the metal precatalyst, suggesting a controlled polymerization. In contrast to the previous reports the addition of aluminum alkyl additives was detrimental to the polymerization, resulting in a decreased 3,4-selectivity or broadening of the molecular weight distribution. Although organoscandium cations could be isolated by treatment of **77a–77c**

Table 22 Polymerization of isoprene catalyzed by NPN-ligated lanthanide dialkyl complexes[a] [177]

Run	Cat.	Temp (°C)	Time (min)	Yield (%)	Microstructures (%)			M_n ($\times 10^4$)	M_w/M_n	Eff. (%)
					3,4-	*cis*-1,4	*trans*-1,4			
1	**67**	20	15	100	81.6	17.5	0.9	5.44	1.8	1.25
2	**68**	20	15	100	82.0	17.3	0.7	6.92	1.7	0.98
3	**69**	20	15	100	95.1	4.2	0.7	7.53	1.7	0.90
4	**70**	20	15	100	96.6	3.0	0.4	6.50	1.8	1.05
5	**71**	20	15	100	95.1	4.3	0.6	6.57	2.0	1.04
6	**72**	20	15	100	96.8	3.0	0.2	6.07	1.9	1.12
7	**73a**	20	15	100	97.8	2.0	0.2	7.43	1.9	0.92
8	**73b**	20	15	100	92.3	6.9	0.8	8.74	1.2	0.78
9	**73c**	20	15	100	98.1	1.8	0.1	6.48	1.2	1.05
10	**73d**	20	15	100	93.8	5.9	0.3	10.97	1.3	0.62
11	**73c**	40	10	100	91.6	8.2	0.2	5.03	1.4	1.35
12	**73c**	0	30	89	98.5	1.4	0.1	11.49	1.4	0.59
13	**73c**	−20	360	81	99.4	0.6	0	14.90	1.5	0.46
14	**74**	20	15	100	84.4	15.1	0.5	6.45	1.9	1.05
15	**75a**	20	60	100	85.0	14.6	0.4	4.28	1.8	1.59
16	**75b**	20	15	100	85.5	14.0	0.5	14.60	1.8	0.47
17	**75c**	20	360	80	33.3	65.9	0.8	15.90	1.9	0.43
18	**76**	20	15	100	77.5	21.6	0.9	3.94	1.6	1.73

[a]Conditions: toluene 5 mL, complex 10 μmol, $[Ph_3C][B(C_6F_5)_4]$ 10 μmol, TIBA 100 μmol, $[IP]_0:[Ln]_0 = 1{,}000$

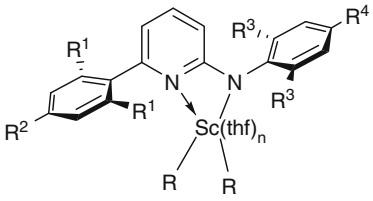

77a: $R^1 = R^2 = R^3 = {}^i$Pr, R^4 = H, R = CH_2SiMe_3, n = 1
77b: $R^1 = R^2 = {}^i$Pr, $R^3 = R^4$ = Me, R = CH_2SiMe_3, n = 1
77c: R^1 = Me, R^2 = H, $R^3 = {}^i$Pr, R^4 = H, R = CH_2SiMe_3, n = 1
77d: $R^1 = R^2 = R^3 = {}^i$Pr, R^4 = H, R = CH_2Ph, n = 1
77e: $R^1 = R^2 = R^3 = {}^i$Pr, R^4 = H, R = $N(SiHMe_2)_2$, n = 0

Fig. 12 Amidopyridine scandium dialkyl and diamide complexes

with borate, their inability to initiate polymerization of isoprene suggested a different pathway from that proposed by Hou [178]. Interestingly, the scandium diamide analogue **77e** produced *cis*-1,4-polyisoprenes (selectivity = 96%) in the presence of borate and trialkylaluminum, which might be attributed to the ligand transfer from scandium to aluminum [179].

5 Copolymerization of Conjugated Dienes with Alkenes

The copolymerization of dienes with alkenes provides a methodology to prepare high-performance rubbers, however, it usually encounters problems of low activity owing to different mechanisms. Recently, some breakthroughs have been achieved by virtue of the fast development of organolanthanide chemistry. Boisson et al. reported the copolymerization of ethylene with butadiene using a series of neodymocene catalysts (Fig. 13), the performances of which were significantly influenced by the ligand framework, the anionic counterion as well as the activator. The lanthanocene chloride complexes **78–80** initiated the copolymerization of ethylene with butadiene in the presence of BuLi/DIBAH to afford random copolymer containing a small ratio of butadiene [178]. The silylene-bridged bis-Flu neodymium chloride and borohydride complexes **81–89** were able to catalyze the copolymerization of ethylene with butadiene but behaved quite differently (Table 23) [149, 180–182], among which **81** could produce a copolymer with high incorporation of butadiene units up to 62 mol% with the increase of butadiene feed ratio. However, in contrast, the yttrium and samarium counterparts **82** and **83** displayed an inferior activity by giving a copolymer with lower butadiene content (13.6%) [149]. An interesting catalytic performance was found for the *ansa*-Flu neodymium complex **84** (or **87**) in the presence of alkylating reagents to afford polymer with *trans*-1,2-cyclohexane rings in the backbone of macromolecular chains. This system could randomly

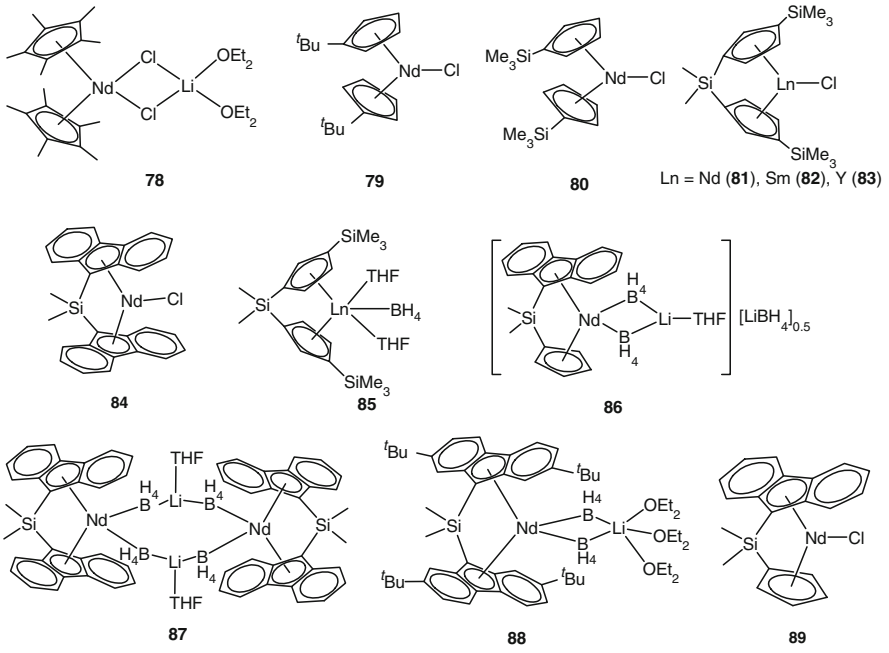

Fig. 13 Structures of lanthanide metallocene catalysts **78–89**

Table 23 Copolymerization of ethylene with butadiene with **84**, **87**, and **88** in the presence of BuMg(Oct)

Run	Catalyst	BD% in polymer	*trans*-1,4	Vinyl	*trans*-1,2-cyclohexane	*cis*-1,2-cyclohexane	*trans*-1,4-cyclohexane	T_g (°C)	References
1	**84** + 2 equiv. Mg	13.3	27.1	20.1	52.8			−31	[180]
2	**84** + 2 equiv. Mg	15.0	25.8	22.9	51.3			−34	[180]
3	**84** + 2 equiv. Mg	19.3	27.6	28.4	44.0			−37	[180]
4	**87** + 5 equiv. Mg	26.7	31.8	35.2	33.0			−36.0	[181]
5	**87** + 2 equiv. Mg	25.3	31.9	31.9	36.1			−33.0	[181]
6	**87** + 2 equiv. Mg	19.3	27.6	28.4	44.0			−37.0	[181]
7	**87** + 10 equiv. Mg	28	32.3	38.9	28.8			−35.3	[181]
8	**87** + 2 equiv. Mg	12.9	25.3	39.6	35.1			−36.0	[181]
9	**87** + 2 equiv. Mg	30.8	29.6	50.3	20.2			−45.6	[181]
10	**88** + 5 equiv. Mg	12.8	17.5	20.2	41.9	5.5	14.7	−33.6	[181]
11	**88** + 5 equiv. Mg	21.6	19.2	32.8	34.3	4.2	9.6	−35.7	[181]
12	**88** + 5 equiv. Mg	32.1	21.5	57.5	19.0	2.0	ND	−28.3	[181]
13	**88** + 5 equiv. Mg	10.2	25.4	7.6	45.9	5.2	15.9	ND	[181]

incorporate 30 mol% of α-olefin into two *trans*-1,4-butadiene units [180, 181, 183]. When an ate complex **88** bearing the steric ^{t}Bu substituents was employed, both *cis*-1,2-cyclohexane and *trans*-1,4-cyclohexane rings were formed along the macromolecular chains in addition to *trans*-1,2-cyclohexane units [181]. Remarkably, alternating copolymerization of ethylene with butadiene was realized by **89** combined with butyloctylmagnesium in a higher activity than that of homopolymerization of each monomer [137]. A possible mechanism of 2,1-insertion was proposed as Scheme 27.

Bochmann [184] developed a heterogeneous catalyst system of silica-supported neodymium amides (Scheme 28) that in conjunction of TIBA displayed activity for the copolymerization of ethylene and butadiene to give copolymer with relatively broad molecular weight distribution and *trans*-1,4-regulated butadiene sequences.

Barbier-Baudry [147, 148, 185–188] studied in detail the *ansa*-samarocene allyl and chloride complexes **91–93** (Fig. 14) as the single-component catalysts for the copolymerization of a series of α-olefins with conjugated dienes. The resultant copolymers contained about 6% linear α-olefins. Each olefin unit randomly inserted between two *trans*-1,4-isoprenes. It was worth noting that the afforded copolymers with different precatalysts were characterized with almost the same properties, denoting the same catalytic active species formed during polymerization [147, 186]. In addition, these catalysts were able to copolymerize isoprene with ε-caprolactone to form diblock copolymers [186, 187] and triblock copolymer poly[isoprene-*co*-

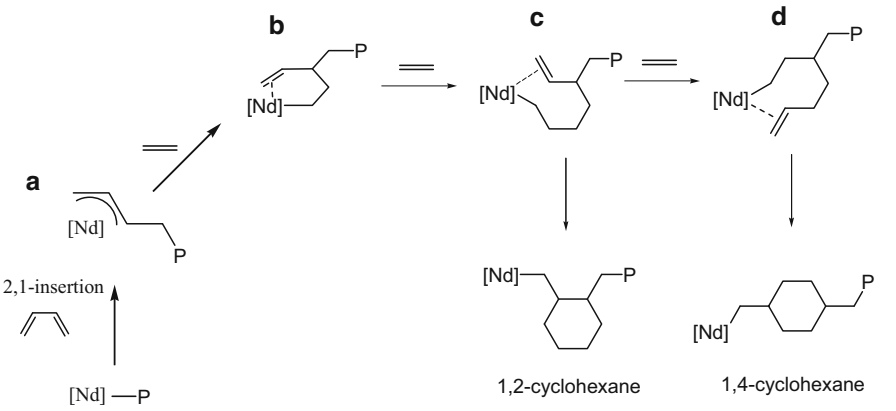

Scheme 27 Possible mechanism for the formation of 1,2- or 1,4-cyclohexane unit

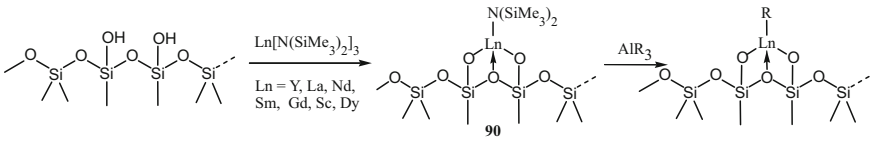

Scheme 28 Silica-supported lanthanide compound

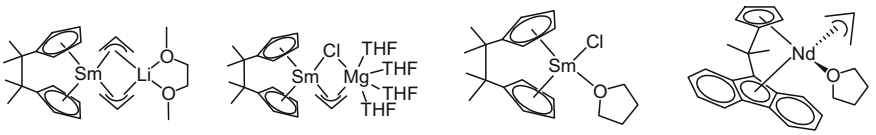

91 92 93 94

Fig. 14 Structures of *ansa*-metallocenes of samarium and neodymium

Table 24 Isoprene/α, ω-diene co-(ter-) polymerization catalyzed by **92**/Li(allyl)(1,4-dioxane) [148]

Run[a]	Monomers	Toluene (mL)	Sm (μmol)	$[M]_0/[Sm]$[b]	Time (h)	Yield (%)	Comonomer content (%)[c]	M_n[d] ($\times 10^3$)	PDI[d]	T_g[e] (°C)
1	1/1/0		6.9	720	20	73	8.2	50	1.3	−60
2	1/0.5/0		7.4	900	20	98	4.5	[f]	[f]	[f]
3	0.5/1/0		6.9	480	40	99	5.4	38	1.6	−58
4	1/1/0	4	1.4	720	27	80	4	[f]	[f]	[f]
5	0.5/0.5/0.5		6.5	520	17	28	4.6[g], 6.3[h]	39.5	1.5	−62
6	1/1/0		6.9	720	19	93[i]	[i]	[f]	[f]	−45
7	0.9/0.9/0	1.8	3.8	650	20	97[i]	[i]	[f]	[f]	[f]
8	0.5/0.5/0	1	5.5	450	63	64	6.5	50	1.8	−69
9	0.5/0.5/0	2	4.6	360	17	79	4.3	[f]	[f]	[f]
10	0.5/1/0	2	4.7	300	21	24	10	[f]	[f]	[f]
11	0.25/0.5/0.25		11.1	450	16	58[i]	[i]	[f]	[f]	[f]
12	0.5/0.4/0.1		11.1	450	5	87[i]	[i]	[f]	[f]	[f]
13	0.5/0.1/0.4		11.1	450	17	82	4[j], 4.8[h]	41.4	2.0	−66

[a]Isoprene/hexa-1,5-diene (runs 1–5), isoprene/octa-1,7-diene/hex-1-ene (runs 6–13), volumes in mL
[b]Initial concentration of isoprene
[c]On the basis of ^{1}H NMR integration
[d]Determined by SEC
[e]Determined by DSC
[f]Not given
[g]Hexa-1,5-diene
[h]Hex-1-ene
[i]Crosslinked: does not take octa-1,7-diene into account
[j]Octa-1,7-diene

(hexene)]-*b*-poly(ε-caprolactone) with narrow molecular weight distribution [187]. Moreover, the copolymerization of isoprene with α, ω-dienes was achieved albeit with low incorporation of nonconjugated dienes (ca. 4–10%) (Table 24) [148, 187]. For instance the copolymerization of isoprene with 1,5-hexadiene resulted in the formation of five-membered ring in the polymer backbone, whilst with 1,7-octadiene afforded vinyl pendent copolymers, indicating that only one double bond was involved in the reaction with isoprene (Fig. 15).

Copolymerization of styrene and conjugated dienes is another attractive subject which provides the most commonly used styrene–butadiene rubbers (SBRs). Boisson reported that by using neodymium amide $Nd\{N(SiMe_3)_2\}_3$ and TIBA and DEAC, SBRs with 10–15 mol% of styrene were produced [189], although drops in both activity and molecular weight were observed as compared with those of

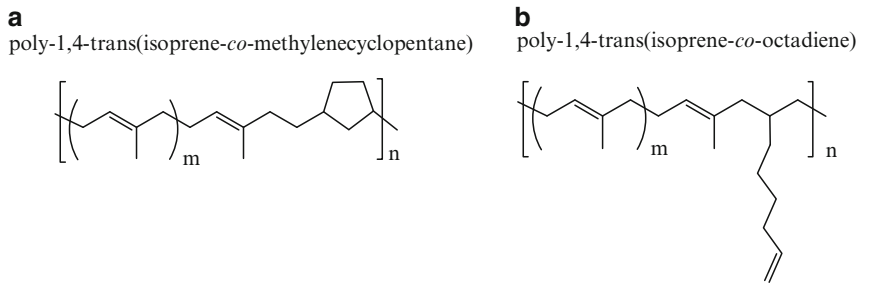

Fig. 15 Structures of copolymers of isoprene/hexa-1,5-diene (**a**) and isoprene/octa-1,7-diene (**b**)

homopolymerizations. ^{13}C NMR analysis disclosed that the microstructure of the butadiene units adopted *cis*-1,4-configuration domain, whereas 95% butadiene units inserted after the styrene unit was *trans*-1,4-regulated. The addition of organoborate to the system showed similar results. By employing conventional Ziegler–Natta catalyst system $Nd(naph)_3$/TIBA/DIBAC Shen et al. successfully synthesized SBRs with varying content of styrene, in which the inserted butadiene was highly *cis*-1,4-tactic (93%); however, this stereoregularity dropped with the increase of the styrene content [190–192]. By using the same catalyst, Wu et al. conducted the polymerization of styrene in $CHCl_3$ at 70°C followed by adding butadiene at low temperature to obtain diblock SBRs with high molecular weight albeit with wide molecular weight distribution, in which the butadiene block was highly *cis*-1,4-regulated (∼97%), almost independent of the content of styrene units [193].

It is noteworthy that when magnesium alkyls were used as activators, the resultant systems provided SBRs possessing usually *trans*-1,4-butadiene units. Mortreux and Carpentier reported catalyst system $Nd(O\text{-}2,6\text{-}^tBu_2\text{-}4\text{-}Me\text{-}C_6H_2)_3(THF)$/$Mg(n\text{-}Hex)_2$ that gave SBRs containing 8–13 mol% styrene. Each sytrene unit was inserted into *trans*-1,4-polybutadiene blocks [194]. Visseaux et al. [195] investigated the combination of $Nd(BH_4)_3THF_3$/BuMgEt that could effectively incorporate styrene into polyisoprene. Introducing Cp^* ligand to neodymium borohydride led to a higher uptake of styrene (30%) and a narrower molecular weight distribution. The polyisoprene backbone was highly *trans*-1,4-regulated up to 98% and the styrene units randomly inserted into two *trans*-1,4-isoprene blocks (Table 25).

Carpentier et al. used a marvelous single-component catalyst the *ansa*-neodymocene allyl complex $(CpCMe_2Flu)Nd(C_3H_5)(THF)$ (**94**) to achieve the copolymerization of isoprene and styrene [196]. The resultant copolymers had high molecular weight and narrow molecular weight distributions in which the polystyrene units were syndiotactic separated by discrete isoprene unit (Table 26). Strikingly, this system enabled the copolymerization of styrene/ethylene/isoprene to afford terpolymers with different T_m and T_g values varying with the initial monomer feed ratios (Table 27).

Hou and Wakatsuki [197] reported a cationic ternary system composed of samarocene aluminate $Cp^*_2Sm(\mu\text{-}Me)_2AlMe_2$ (**95**) and TIBA and $[Ph_3C][B(C_6F_5)_4]$, showing living mode for the copolymerization of butadiene and styrene

Table 25 Copolymerization of styrene and isoprene by borohydrido lanthanide complex and MgBuEt[a] [195]

Run	Catalyst	St in feed	St in polymer	*trans*-1,4-PI	*cis*-1,4-PI	3,4-PI	M_n ($\times 10^3$)	PDI	T_g (°C)
1	$Nd(BH_4)_3THF_3$	0	–	96	2	2	72	2.0	−66
2	$Nd(BH_4)_3THF_3$	20	5	98	<0.5	2	65	1.6	−61
3	$Nd(BH_4)_3THF_3$	50	15	97	1	2	43	1.8	−54
4	$La(BH_4)_3THF_3$	50	11	94	4	2	15	1.5	−63
5	$Nd(BH_4)_3THF_3$	80	27	98	2	<0.5	23	1.8	−40
6	$Nd(BH_4)_3THF_3$	100	–	–	–	–	10	1.6	ND
7	$Cp^*Nd(BH_4)_2THF_2$	0	–	98	0	2	67	1.8	−66
8	$Cp^*Nd(BH_4)_2THF_2$	20	5	97	0	3	66	1.6	−66
9	$Cp^*Nd(BH_4)_2THF_2$	50	16	98	0	2	47	1.4	−51
10	$Cp^*Nd(BH_4)_2THF_2$	80	32	96	<0.5	4	27	1.4	−30
11	$Cp^*Nd(BH_4)_2THF_2$	100	–	–	–	–	8	1.5	ND

[a] 2 h reaction at 50°C in 0.5 mL of toluene; molar ratio monomer/Nd/Mg: 2,000/1/1

Table 26 Copolymerization of styrene–isoprene complex **94**[a] [196]

Entry	[St]/[Nd]	[St]	[IP]	Temp (°C)	Time (min)	Yield (%)	Activity (kg (mol h)$^{-1}$)	St content	M_n ($\times 10^3$)	PDI	T_m (°C)	T_g^b (°C)	T_g^c (°C)
1	600	8.7	–	60	5	2.3	1,710	100	54	1.73	264	–	ND
2	600	0	10	60	35	2.0	122	0	27	1.09	49	–	ND
3	600	4.7	4.0	60	6	2.4	550	70	55	1.54	–	–	63
4	600	6.0	3.0	60	15	3.8	165	85	91	1.25	–	62	67
5	600	7.9	0.9	60	10	9.6	380	94	63	1.62	218	77	ND
6	600	8.3	0.5	60	4	9.2	957	97 ± 2	12	3.25	228	77	84
7	600	8.3	0.5	80	3.5	8.8	1,025	97 ± 2	20	2.95	227	83	91
8	1,700	8.3	0.5	60	7	1.8	309	97 ± 2	73	1.33	245	–	112

[a]General conditions: 0.05–0.15 mmol Ln; total volume 10 mL; reactions were conducted in neat monomers

[b]Melting and glass transition temperatures determined by DSC

[c]Glass transition determined by DMA

(Fig. 16). Thus, block copolymers were produced with highly *cis*-1,4-regulated butadiene fragments (99%) and up to 33.2% styrene content. Meanwhile, the random copolymers with various styrene contents (4.6–33.2 mol%), highly *cis*-1, 4-selective polybutadiene sequences (95.1–80.3%), and high molecular weights ($M_n = 1.01 \times 10^5$–2.34×10^4, PDI = 1.42) were obtained when the polymerization was performed at 50°C. Noteworthy was that the molecular weight distribution became wider and the *cis*-1,4-regularity declined with the increase of styrene content (Table 28). These results were in consistent with Boisson's results that a butadiene inserted after a styrene unit adopted *trans*-1,4-configuration.

The cationic system based on half-sandwich scandium borohydrides $Cp^*Sc(BH_4)_2THF/[Ph_3C][B(C_6F_5)_4]$/TIBA was found by Visseaux et al. to be active toward the copolymerization of isoprene and styrene, although low styrene incorporation and drop of *cis*-1,4-microstructure of isoprene units were observed as compared with the homopolyisoprene obtained using the same system (94% vs. 97%) [116]. The cationic system based on the half-sandwich scandium alkyl complex $(C_5Me_4SiMe_3)Sc(CH_2SiMe_3)_2(THF)$ (**96**, Fig. 16) and $[Ph_3C][B(C_6F_5)_4]$

Table 27 Styrene–ethylene–isoprene terpolymerization catalyzed by complex **94**[a] [196]

Entry	[St]/[Nd]	[St]	[IP]	P (bar)	Temp (°C)	Time (min)	Yield (%)	Activity (kg (mol h)$^{-1}$)	St (mol%)	IP (mol%)	Et (mol%)	M_n ($\times 10^3$)	PDI	T_m (°C)	T_g[b] (°C)	T_g[c] (°C)
1	1,800	–	10	4	60	15	11.4	138	–	76	24	112	1.61	–	–	ND
2	600	2.2	2.2	5	60	60	7.2	33	41	34	25	73	2.41	–	–	35
3	600	7.9	0.9	1	60	15	8.9	244	96 ± 2	3	<1	41	2.84	204	76	ND
4	600	4.1	0.5	4	60	15	25.6	235	71	6	23	83	1.18	219	56	55
5	600	4.1	0.5	4	80	15	40.5	375	71	6	23	ND	ND	ND	ND	ND
6	600	4.1	0.5	1	60	30	18.7	86	81	3	16	ND	ND	–	60	84

[a] General conditions: 0.02–0.35 mmol Ln; total volume 1–60 mL

[b] Melting and glass transition temperatures determined by DSC

[c] Glass transition determined by DMA

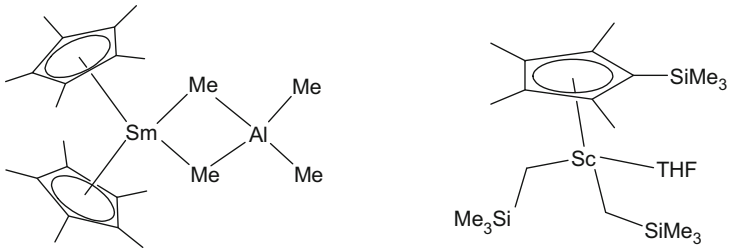

95 **96**

Fig. 16 Structures of half-sandwich lanthanide aluminate and bis(alkyl) complexes **95** and **96**

Table 28 Random copolymerization of butadiene and styrene initiated by **95**/TIBA/$[Ph_3C][B(C_6F_5)_4]$[a] [197]

Run	Styrene in feed (mol%)	Time (h)	Yield (%)	Microstructure (%) *cis*-1,4	*trans*-1,4	1,2-	Styrene content (mol%)	M_n ($\times 10^3$)	PDI
1	40	0.5	21	94.6	4.4	1.0	4.6	101	1.41
2	50	1	22	95.1	3.9	1.0	7.2	78.6	1.59
3	60	6	20	91.7	7.2	1.1	11.4	73.9	1.69
4	70	12	23	87.4	11.7	0.9	19.1	38.7	1.75
5	80	50	21	80.3	18.7	1.0	33.2	23.4	2.23

[a]Polymerization conditions: in toluene; $T_g = 50°C$; $[\text{butadiene}]_0 + [\text{styrene}]_0 = 6.0\,M$ (3.0×10^{-2} mol); $[\mathbf{95}]_0 = 0.006\,M$ (3.0×10^{-5} mol); $[\text{TIBA}]_0/[\text{cat}]_0 = 3$; $\{[Ph_3C][B(C_6F_5)_4]\}_0/[\mathbf{95}]_0 = 1$

reported by Hou et al. has demonstrated distinguished catalytic activity and selectivity for the copolymerization of isoprene and styrene [198]. The system behaved in a living fashion to give diblock and triblock copolymers of AB and ABA, respectively, in which the styrene fragments were perfectly syndiotactic whilst the isoprene blocks were random. Moreover, the random copolymerization could also be realized without detectable formation of homopolyisoprene or atactic polystyrene in the process; meanwhile, the amount of inserted styrene can be adjusted by varying the initial feed ratio. More recently, Hou et al. investigated in detail the catalytic performances of the cationic system based on the half-sandwich scandium alkyl complexes **97–102** analogous to **96** but bearing different substituents (Fig. 17) [199]. By varying the substituents on the Cp ring, the catalytic activity for the polymerization of styrene and isoprene could be adjusted; the highest active system belonged to complex **100**. These variations of the ligands also influenced the selectivity; therefore, copolymers with polyisoprene sequences containing *cis*-1, 4-contents varying from 85 to 92% were obtained. More remarkably, almost perfect alternating copolymerization of ethylene with isoprene was achieved.

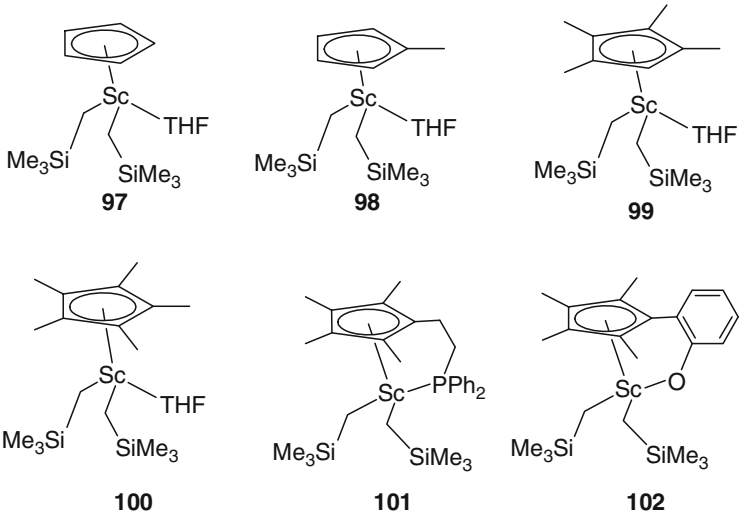

Fig. 17 Structures of half-sandwich scandium alkyl complexes **97** to **102**

6 Conclusions and Perspective

There is no doubt that the rapid development of rare-earth metal coordination catalysts has significantly advanced the syntheses of polydienes and the copolymers with precisely controlled microstructures that in turn determine their unique properties and versatile applications. The homogeneous single-site catalyst systems based on well-defined rare-earth metal complexes offer a decisive enhancement on catalytic activity and *cis*-1,4-, *trans*-1,4-, and 3,4-regioselectivity, and 3,4-stereoselectivity, which can be achieved by tuning the sterics and electronics of the ancillary ligands and the geometry of the ligand frameworks, as well as the types of cocatalysts such as aluminum or magnesium *etc* metal compounds or addition of organoborate cationization agents. In addition, successful isolation of some probable reaction intermediates facilitates further investigation of mechanism and guides the design of new catalysts. Meanwhile, modifying the conventional Ziegler–Natta catalyst systems focusing on increase of their catalytic activity, efficiency, and specific selectivity, control of the molecular weight and molecular weight distribution and identification of the active species, has gained obvious improvements by optimizing the catalyst recipe and polymerization conditions, and by employing the mimic tailor-made Ziegler–Natta catalyst systems.

Despite these encouraging progresses in this area, there still have many problems to be solved. The single-site lanthanide catalysts containing metal carbon bond are generally complicated in preparation, high cost, extremely sensitive to moisture and oxygen, and therefore less thermally stable, which hinder large-scale production. The cationic systems are usually heterogeneous in the industry-used aliphatic alkane medium owing to the addition of borates. The selectivity is not satisfactory

at room temperature or higher for most of present systems. The catalyst systems of highly active and selective for *trans*-1,4- and 3,4-polymerization of dienes still remain scarce, and those initiate copolymerization of dienes with alkene still need further investigation. Moreover, the successful copolymerization of dienes and alkenes goes along with an increase of 1,2- and *trans*-1,4-configuration. Sometimes, even 1,2-cyclohexane units are formed. For various applications, copolymers with a high *cis*-content are of high interest. It is not clear neither from experimental nor from theoretical point of view whether copolymers with a *cis*-1,4-content are feasible and how the respective catalysts have to be modified in order to meet this requirement. More importantly, the mechanism of polymerization is not clear at present and the correlation between structure of catalyst and stereoregularity as well as activity has not been established yet, which impede the search of potent catalysts for diene polymerization and their copolymerization with olefins or polar monomers.

Acknowledgements This work was partly supported by The National Natural Science Foundation of China for project No. 20934006. The Ministry of Science and Technology of China for projects Nos. 2005CB623802; 2009AA03Z501.

References

1. Shen Z, Gong ZY, Zhong ZQ, Ouyang J (1964) Sci Sin (Engl Transl) 13:1339
2. Von Dohlen WC, Wilson TP, Caflisch EG (1964) Belg Patent 644291
3. Von Dohlen WC, Wilson TP, Caflisch EG (1965) Chem Abstr 63:32659
4. Throckmorton MC (1969) Kautsch Gummi Kunstst 22:293
5. Yang JH, Tsutsui M, Chen Z, Bergbreiter DE (1982) Macromolecules 15:230
6. Shen Z (1987) Inorg Chim Acta 140:7
7. Kuran W (2001) Principle of coordination polymerisation. Wiley, West Sussex
8. Shen Z, Ouyang J (1987) Handbook on the physics and chemistry of rare earth. Elsevier, Dordrecht
9. Friebe L, Nuyken O, Obsrecht W (2006) Adv Polym Sci 204:1 and references therein
10. Fischbach A, Anwander R (2006) Adv Polym Sci 204:155 and references therein
11. The synthesis and catalysis of cationic rare-earth metal complexes, see review: Hou Z, Wakatsuki Y (2002) Coord Chem Rev 231:1
12. Arndt S, Okuda J (2001) Chem Rev 102:1953
13. Zeimentz PM, Arndt S, Elvidge BR, Okuda J (2006) Chem Rev 106:2404
14. Natta G, Porri L, Carbonaro A (1964) Makromol Chem 77:126
15. Milione S, Cuomo C, Capacchione C, Zannoni C, Grassi A, Proto A (2007) Macromolecules 40:5638
16. Natta G, Porri L, Corradini P, Morero D (1958) Chim Ind 40:263
17. Natta G, Porri L, Mazzei A (1959) Chim Ind 41:116
18. Colamarco E, Milione S, Cuomo C, Grassi A (2004) Macromol Rapid Commun 25:450
19. Nakayama Y, Baba Y, Yasuda H, Kawakita K, Ueyama N (2003) Macromolecules 36:7953
20. Jenkins DK (1985) Polymer 26:147
21. Baudry-Barbier D, Andre N, Dormond A, Pardes C, Richard P, Visseaux M, Zhu CJ (1998) Eur J Inorg Chem, p 1721
22. Gronski W, Murayama N, Cantow HJ, Miyamoto T (1976) Polymer 17:358
23. Ricci G, Battistella M, Porri L (2001) Macromolecules 34:5766
24. Sun Q, Wang F (1988) Acta Polym Sin 2:145

25. Bazzini C, Giarrusso A, Porri L (2002) Macromol Rapid Commun 23:922
26. Nakayama Y, Baba Y, Yasuda H, Kawakita K, Ueyama N (2003) Macromolecules 36:7953
27. Bazzini C, Giarrusso A, Porri L, Pirozzi B, Napolitano R (2004) Polymer 45:2871
28. Marina NG, Monakov YB, Sabirov ZM, Tolstikov GA, (1991) Polym Sci USSR (Engl. Trans.) 33:387
29. Monakov YB, Marina NG, Sabirov ZM (1994) Polym Sci USSR (Engl. Trans.) 36:1404
30. Taube R, Sylvester G, (1996) Stereospecific polymerization of butadiene or isoprene. In: Cornils B, Herrmann WA (eds) Applied homogeneous catalysis with organometallic compounds, vol. 1 VCH, Weinheim, p 280
31. Iovu H, Hubea G, Racoti D, Hurst JS (1999) Eur Polym J 35:335
32. Porri L, Ricci G, Shubin N (1988) Macromol Symp 128:53
33. Kobayashi E, Hayashi N, Aoshima S, Furukawa J (1998) J Polym Sci Part A Polym Chem 36:241
34. Mello IL, Coutinho FMB. (2008) Eur Polym J 44:2893
35. Mello IL, Coutinho FMB, Nunes DSS, Soares BG, Costa MAS, Maria LCS (2004) Quim Nova 27:277
36. Yang J, Hu J, Fang S, Pan E, Xie D, Zhong CG, Ouyang J (1980) Sci Sin 23:734
37. Srinivasa Rao GS, Upadhyay VK, Jain RC (1997) Angew Makromol Chem 251:193
38. Gallazzi MC, Bianchi F, Depero L, Zocchi M (1988) Polymer 29:1516
39. Rafikov SR, Monakov YB, Marina NG, Duvakina NV, Tolstikov GA, Krivonogov VP, Nurmukhametov FN, Kovalev NF, Tikhomirova GA (1980) USSR Pat. 730,710. Chem Abstr 1980, 93:96152V
40. Monakov YB, Rafikov SR, Bezgina AS, Tolstikov GA, Duvakina NV, Marina NG, Murinov YI, Nikitin YE, Berg AA (1980) USSR Pat. 726, 110. Chem Abstr 1980, 93:72926Z
41. Ren C, Li G, Dong W, Jiang L, Zhang X, Wang F (2007) Polymer 48:2470
42. Srinivasa Rao GS, Upadhyay VK, Jain RC (1999) J Appl Polym Sci 71:595
43. Barbotin F, Spitz R, Boisson C (2001) Macromol Rapid Commun 22:1411
44. Dong W, Masuda T (2002) J Polym Sci Part A Polym Chem 40:1838
45. Ricci G, Italia S, Comitani C, Porri L (1991) Polym Commun 32:514
46. Endo K, Masaki K, Uchida Y (1997) Polym J 29:583
47. Wilson DJ (1996) Polym Int 39:235
48. Cui L, Ba X, Teng H, Ying L, Li K, Jin Y (1998) Polym Bull 40:729
49. Dong W, Masuda T (2003) Polymer 44:1561
50. Taniguchi Y, Dong W, Katsumata T, Shiotsuki M, Masuda T (2005) Polym Bull 54:173
51. Boisson C, Barbotin F, Boisson RS (1999) Macromol Chem Phys 200:1163
52. Oehme A, Gebauer U, Gehrke K (1993) J Mol Catal 82:83
53. Kaita S, Kobayashi E, Sakakibara S, Aoshima S, Furukawa J (1996) J Polym Sci A Polym Chem 34:3431
54. Hsieh HL, Yeh HC (1985) Rubber Chem Technol 58:117
55. Pires NMT, Coutinho FMB, Costa MAS (2004) Eur Polym J 40:2599
56. Friebe L, Müller JM, Nuyken O, Obsrecht W (2006) J Macromol Sci A Pure Appl Chem 43:841
57. Porri L, Giannini U, Pino P (1987) Encyclopedia of polymer science and engineering, vol 8. Identification to lignin, 2nd edn. Wiley, New York
58. Mello IL, Coutinho FMB, Nunes DSS, Soares BG, Costa MAS, Luiz Claudio de Santa Maria (2004) Eur Polym J 40:635
59. Coutinho FMB, Rocha TCJ, Mello IL, Nunes, DSS, Soares BG, Costa MAS (2005) J Appl Polym Sci 98:2539
60. Gallazzi MC, Giarrusso A, Porri L (1981) Makromol Chem Rapid Commun 2:59
61. Porri L, Gallazzi MC (1983) Makromol Chem Rapid Commun 4:485
62. Mello IL, Coutinho FMB (2009) J Appl Polym Sci 112:1496
63. Rocha TCJ, Coutinho FMB, Soares BG (2009) Polym Bull 62:1
64. Sigaeva NN, Usmanov TS, Zaikov GE, Monakov YB (2003) J Appl Polym Sci 89:674
65. Friebe L, Nuyken O, Windisch H, Obsrecht W (2002) Macromol Chem Phys 203:1055

66. Friebe L, Windisch H, Nuyken O, Obsrecht W (2004) J Macromol Sci A Pure Appl Chem 41:245
67. Friebe L, Müller JM, Nuyken O, Obsrecht W (2006) J Macromol Sci A Pure Appl Chem 43:11
68. Friebe L, Nuyken O, Obsrecht W (2005) J Macromol Sci A Pure Appl Chem 42:839
69. Quirk RP, Kells AM (2000) Polym Int 49:751
70. Quirk RP, Kells AM, Yunlub K, Cuif J-P (2000) Polymer 41:5903
71. Kwag G (2002) Macromolecules 35:4875
72. Kwag G, Kim P, Han S, Choi H (2005) Polymer 46:3782
73. James DI (1967) Abrasion of rubber. Maclarren, London
74. Erma B, Mark JE (1998) Macromolecules 31:3099
75. Su T-K, Mark JE (1993) Macromolecules 26:7161
76. Mark JE (2003) Macromol Symp 201:77
77. Merwe MJ, Gradwell MHS, McGill WJ (2001) J Appl Polym Sci 81:2587
78. Maiwald S, Sommer C, Müller G, Taube R (2001) Macromol Chem Phys 202:1446
79. Maiwald S, Sommer C, Müller G, Taube R (2002) Macromol Chem Phys 203:1029
80. Evans WJ, Giarikos DG, Allen NT (2003) Macromolecules 36:4256
81. Evans WJ, Giarikos DG, Ziller JW (2001) Organometallics 20:5751
82. Quirk R, Kells A, Yunlu KM, Cuif J-P (2000) Polymer 41:5903
83. Oehme A, Gebauer U, Gehrke K, Lechner MD (1996) Angew Makromol Chem 235:121
84. Kwag G, Lee H, Kim S (2001) Macromolecules 34:5367
85. Koboyashi E, Hayashi N, Aoshima S, Furukaya J (1998) J Polym Sci Polym Chem 36:1707
86. Pross A, Marquardt P, Reichert K-H, Nentwig W, Knauf T (1993) Angew Makromol Chem 211:89
87. Ricci G, Italia S, Cabassi F, Porri L (1987) Polym Commun 28:223
88. Iovu H, Hubca G, Racoti D, Hurst JS (1999) Eur Polym J 35:335
89. Dimonie M, Hubca G, Badea E, Simionescu E, Iovu H, Vasile I, Stan S (1991) Rev Roum Chim 40:83 and references therein
90. Boisson C, Barbotin F, Spitz R (1999) Macromol Chem Phys 200:1163
91. Evans WJ, Giarikos DG (2004) Macromolecules 37:5130
92. Fischbach A, Perdih F, Sirsch P, Scherer W, Anwander R (2002) Organometallics 21:4569
93. Fink G, Mühlhaupt R, Brintzinger H-H (eds) (1995) Ziegler catalysts. Springer, Berlin
94. Mühlhaupt R (2003) Macromol Chem Phys 204:289
95. Böhm LL (2003) Angew Chem Int Ed 42:5010
96. Evans WJ, Champagne TM, Giarikos DG, Ziller JW (2005) Organometallics 24:570
97. Evans WJ, Champagne TM, Ziller JW (2005) Organometallics 24:4882
98. Evans WJ, Champagne, TM, Ziller JW (2005) Chem Commun, p 5925
99. Fischbach A, Perdih F, Herdtweck E, Anwander R (2006) Organometallics 25:1626
100. Fischbach A, Klimpel MG, Widenmeyer M, Herdtweck E, Scherer W, Anwander R (2004) Angew Chem Int Ed 43:2234
101. Zimmermann M, Froystein NA, Fischbach A, Sirsch P, Martin Dietrich H, Tönroos KW, Herdtweck E, Anwander R (2007) Chem Eur J 13:8784
102. Fischbach A, Meermann C, Eickerling G, Scherer W, Anwander R (2006) Macromolecules 39:6811
103. Meermann C, Törnroos KW, Nerdal W, Anwander R (2007) Angew Chem Int Ed 46:6508
104. Kaita S, Hou Z, Wakatsuki Y (1999) Macromolecules 32:9078
105. Schumann H, Marks TJ (1985) J Am Chem Soc 107:8091
106. Jeske G, Schock LE, Swepston PN, Schumann H, Marks TJ (1985) J Am Chem Soc 107:8103
107. Yasuda H, Yamamoto H, Yokota K, Miyake S, Nakamura A (1992) J Am Chem Soc 114:4908
108. Yasuda H, Furo M, Yamamoto H, Miyake S, Kibino N (1992) Macromolecules 25:5115
109. Yamashita M, Ihara E, Yasuda H (1995) Macromolecules 29:1798
110. Kaita S, Takeguchi Y, Hou Z, Nishiura M, Doi Y, Wakatsuki Y (2003) Macromolecules 36:7923
111. Kaita S, Hou Z, Nishiura M, Doi Y, Kurazumi J, Akira C, Horiuchi AC, Wakatsuki Y (2003) Macromol Rapid Commun 24:179

112. Kaita S, Yamanaka M, Horiuchi AC, Wakatsuki Y (2006) Macromolecules 39:1359
113. Yang Y, Liu B, Lv K, Gao W, Cui D, Chen X, Jing X (2007) Organometallics 26:4575
114. Kaita S, Doi Y, Kaneko K, Horiuchi AC, Wakatsuki Y (2004) Macromolecules 37:5860
115. Tardif O, Kaita S (2008) Dalton Trans, p 2531
116. Bonnet F, Violante CDC, Roussel P, Mortreux A, Visseaux M (2009) Chem Commun, p 3380
117. Visseaux M, Mainil M, Terrier M, Mortreux A, Roussel P, Mathivet T, Destarac M (2008) Dalton Trans, p 4558
118. Zinck P, Barbier-Baudry D, Loupy A (2005) Macromol Rapid Commun 26:46
119. Bijpost EA, Duchateau R, Teuben JH (1995) J Mol Catal A Chem 95:121
120. Duchateau R, van Wee CT, J. H. Teuben, (1996) Organometallics 15:2291
121. Aubrecht KB, Chang K, Hillmyer MA, Tolman WB (2001) J Polym Sci A Polym Chem 39:284
122. Duchateau R, van Wee CT, Meetsma A, Teuben JH (1993) J Am Chem Soc 115:4931
123. Bailey PJ, Pace S (2001) Coord Chem Rev 214:91
124. Giesbrecht GR, Whitener GD, Arnold J (2001) J Chem Soc Dalton Trans, p 923
125. Lu Z, Yap GPA, Richeson DS (2001) Organometallics 20:706
126. Hayes PG, Piers WE, Lee LWM, Knight LK, Parvez M, Elsegood MRJ, Clegg W (2001) Organometallics 20:2533
127. Emslie DJH, Piers WE, McDonald R (2002) J Chem Soc Dalton Trans, p 293
128. Arndt S, Beckerle K, Zeimentz PM, Spaniol TP, Okuda J (2005) Angew Chem Int Ed 44:7473
129. Robert D, Abinet E, Spaniol TP, Okuda J (2009) Chem Eur J 15:11937
130. Yang Y, Liu B, Lv K, Gao W, Cui D, Chen X, Jing X (2007) Organometallics 26:4575
131. Yang Y, Wang Q, Cui D (2008) J Polym Sci A Polymer Chem 46:5251
132. Zhang L, Suzuki T, Luo Y, Nishiura M, Hou Z (2007) Angew Chem Int Ed 46:1909
133. Zhang L, Nishiura M, Yuki M, Luo Y, Hou Z (2008) Angew Chem Int Ed 47:2642
134. Allen G (1989) Comprehensive polymer science, vol 4. Pergamon, Oxford, pp 53–108
135. Longiave C, Castelli R (1963) J Polym Sci C Polym Symp 4:387
136. Thuilliez J, Monteil V, Spitz R, Boisson C (2005) Angew Chem Int Ed 44:2593
137. Gao W, Cui D (2008) J Am Chem Soc 130:4984
138. Sugiyama H, Gambarotta S, Yap GPA, Wilson DR, Thiele SKH (2004) Organometallics 23:5054
139. Gehrke K, Harwart M (1993) Plast Kautsch 40:356
140. Anzai S, Irako K, Onishi A, Furukawa J (1969) Kogyo Kagaku Zasshi 72:2081
141. Oehme A, Gebauer U, Gehrke K (1995) Macromol Rapid Commun 16:563
142. Zambelli A, Proto A, Longo P, Oliva P (1994) Macromol Chem Phys 195:2623
143. Rastätter M, Muterle RB, Roesky PW, Thiele SKH (2009) Chem Eur J 15:474
144. Halasa AF, Hsu WL, Austin LE, Jasiunas CA (2002) U.S. Patent 183469
145. Halasa AF, Hsu WL, Austin LE, Jasiunas CA, Goodyear (2002) Chem Abstr 138:14610
146. Song JS, Huang BC, Yu DS (2001) J Appl Polym Sci 82:81
147. Visseaux M, Barbier-Baudry D, Bonnet F, Dormond A (2001) Macromol Chem Phys 202:2485
148. Bonnet F, Visseaux M, Barbier-Baudry D, Dormond A (2002) Macromolecules 35:1143
149. Boisson C, Monteil V, Ribour D, Spitz R, Barbotin F (2003) Macromol Chem Phys 204:1747
150. Urazbaev VN, Efimov VP, Sabirov ZM, Monakov YB (2003) J Appl Polym Sci 89:601
151. Bonnet F, Visseaux M, Pereira A, Bouyer F, Barbier-Baudry D (2004) Macromol Rapid Commun 25:873
152. Bonnet F, Visseaux M, Barbier-Baudry D, Vigier E, Marek M, Kubicki MK (2004) Chem Eur J 10:2428
153. Bonnet F, Visseaux M, Pereira A, Barbier-Baudry D (2005) Macromolecules 38:3162
154. Terrier M, Visseaux M, Chenal T, Mortreux A (2007) J Polym Sci A Polym Chem 45:2400
155. Visseaux M, Terrier M, Mortreux A, Roussel P (2007) C R Chimie 10:1195
156. Visseaux M, Zinck P, Terrier M, Mortreux A, Roussel P (2008) J Alloys Compd 451:352
157. Valente A, Zinck P, Mortreux A, Visseaux M (2009) Macromol Rapid Commun 30:528
158. Barbier-Baudry D, Blacque O, Hafid A, Nyassi A, Sitzmann H, Visseaux M (2000) Eur J Inorg Chem, p 2333

159. Zimmermann M, Törnroos KW, Anwander R (2008) Angew Chem Int Ed 47:775
160. Zimmermann M, Törnroos KW, Sitzmann H, Anwander R (2008) Chem Eur J 14:7266
161. Robert D, Spaniol TP, Okuda J (2008) Eur J Inorg Chem, p 2801
162. Taube R, Maiwald S, Sieler J (2001) J Organomet Chem 621:327
163. Maiwald S, Weißenborn H, Sommer C, Müller G, Taube R (2001) J Organomet Chem 640:1
164. Ajellal N, Furlan L, Thomas CM, Casagrande OL, Jr Carpentier J-F (2006) Macromol Rapid Commun 27:338
165. Paolucci G, Zanella A, Bortoluzzi M, Sostero S, Longoc P, Napoli M (2007) J Mol Catal A Chem 272:258
166. Wang D, Li S, Liu X, Gao W, Cui D (2008) Organometallics 27:6531
167. Monakov Y B, Duvakina NV, Ionova IA (2008) Polym Sci Ser B 50:134
168. Wolpers J (1992) US Patent 5,104,941
169. Jonny DM (1994) US Patent 5,356,997
170. Duddey J (2002) US Patent 6,390,163
171. Yamasita K, Murachi M, Sugiyama M (1999) US Patent 5,906,959
172. Hsu W, Halasa A (1993) US Patent 5,239,023
173. Zhang L, Luo Y, Hou Z (2005) J Am Chem Soc 127:14562
174. Wang B, Cui D, Lv K (2008) Macromolecules 41:1983
175. Wang B, Wang D, Cui D, Gao W, Tang T, Chen X, Jing X (2007) Organometallics 26:3167
176. Li S, Miao W, Tang T, Dong W, Zhang X, Cui D (2008) Organometallics 27:718
177. Li S, Cui D, Li D, Hou Z (2009) Organometallics 28:4814
178. Barbotin F, Monteil V, Llauro M, Boisson C, Spitz R. (2000) Macromolecules 33:8521
179. Döring C, Kretschmer WP, Bauer T, Kempe R (2009) Eur J Inorg Chem, p 4255
180. Monteil V, Spitz R, Barbotin F, Boisson C (2004) Macromol Chem Phys 205:737
181. Thuilliez J, Ricard L, Nief F, Boisson F, Boisson C (2009) Macromolecules 42:3774
182. Thuilliez J, Spitz R, Boisson C (2006) Macromol Chem Phys 207:1727
183. Boisson C, Monteil V, Thuilliez J, Spitz R, Monnet C, Llauro MF, Barbotin F, Robert P (2005) Macromol Symp 226:17
184. Woodman TJ, Sarazin Y, Fink G, Hauschild K, Manfred Bochmann M (2005) Macromolecules 38:3060
185. Barbier-Baudry D, Bonnet F, Dormond A, Hafid A, Nyassi A, Visseaux M (2001) J Alloys Compd 323–324:592
186. Barbier-Baudry D, Bonnet F, Domenichini B, Dormond A, Visseaux M. (2002) J Organomet Chem 647:167
187. Bonnet F, Barbier-Baudry D, Dormond A, Visseaux M (2002) Polym Int 51:986
188. Barbier-Baudry D, Bonnet F, Dormond A, Finot E, Visseaux M (2002) Macromol Chem Phys 203:1194
189. Monteil V, Spitz R, Boisson C (2004) Polym Int 53:576
190. Zhang Q, Li W, Shen Z (2002) Eur Polym J 38:869
191. Zhang Q, Ni X, Shen Z (2002) Polym Int 51:208
192. Zhang Q, Ni X, Shen Z (2004) J Macromol Sci A Pure Appl Chem 41:39
193. Zhu H, Wu Y-X, Zhao J-W, Guo Q-L, Huang Q-G, Wu G-Y (2007) J Appl Polym Sci 106:103
194. Gromada J, Pichon LL, Mortreux A, Leising F, Carpentier J-F (2003) J Organomet Chem 683:44
195. Zinck P, Terrier M, Mortreux A, Valente A, Visseaux M (2007) Macromol Chem Phys 208:973
196. Rodrigues A-S, Kirillov E, Vuillemin B, Razavi A, Carpentier J-F (2008) Polymer 49:2039
197. Kaita S, Hou Z, Wakatsuki Y (2001) Macromolecules 34:1539
198. Zhang H, Luo Y, Hou Z (2008) Macromolecules 41:1064
199. Li X, Nishiura M, Hu L, Mori K, Hou Z (2009) J Am Chem Soc 131:13870

Struct Bond (2010) 137: 109–163
DOI:10.1007/430_2010_19

Published online: 11 May 2010

Homogeneous Catalysis Using Lanthanide Amidinates and Guanidinates

Frank T. Edelmann

Dedicated to the memory of Professor Herbert Schumann († 2010), a pioneer of organolanthanide chemistry and a friend

Abstract For decades, the organometallic chemistry of the rare earth elements was largely dominated by the cyclopentadienyl ligand and its ring-substituted derivatives. A hot topic in current organolanthanide chemistry is the search for alternative ligand sets which are able to satisfy the coordination requirements of the large lanthanide cations. Among the most successful approaches in this field is the use of amidinate ligands of the general type $[RC(NR')_2]^-$ (R = H, alkyl, aryl; R′ = alkyl, cycloalkyl, aryl, $SiMe_3$) which can be regarded as steric cyclopentadienyl equivalents. Closely related are the guanidinate anions of the general type $[R_2NC(NR')_2]^-$ (R = alkyl, $SiMe_3$; R′ = alkyl, cycloalkyl, aryl, $SiMe_3$). Two amidinate or guanidinate ligands can coordinate to a lanthanide ion to form a metallocene-like coordination environment which allows the isolation and characterization of stable though very reactive amide, alkyl, and hydride species. Mono- and trisubstituted lanthanide amidinate and guanidinate complexes are also readily available. Various rare earth amidinates and guanidinates have turned out to be very efficient homogeneous catalysts, for example, for ring-opening polymerization reactions. This article covers the success story of lanthanide amidinates and guanidinates and their transition from mere laboratory curiosities to efficient homogeneous catalysts.

Keywords: Amidinates · Guanidinates · Lanthanides · Organolanthanide chemistry · Polymerization catalysis

F.T. Edelmann (✉)
Chemisches Institut der Otto-von-Guericke-Universität Magdeburg, Universitätsplatz 2, 39106 Magdeburg, Germany
e-mail: frank.edelmann@ovgu.de

Contents

Abbreviations

AN	Acrylonitrile
CL	ε-Caprolactone
Cp	η^5-Cyclopentadienyl
Cp′	η^5-(Trimethylsilyl)cyclopentadienyl
Cp*	η^5-Pentamethylcyclopentadienyl
Cy	Cyclohexyl
Dipp	2,6-Di(isopropyl)phenyl, $C_6H_3Pr^i_2$–2,6
DippForm	$[HC(NDipp)_2]^-$
EBI	Ethylene-bis(η^5-indenyl)
Giso	$[Cy_2NC(NR)_2]^-$ (R = $C_6H_3Pr^i_2$–2,6)
HSAB	Hard and soft acids and bases
Mes	Mesityl, $C_6H_3Me_3$–2,4,6
MMA	Methylmethacrylate
PHB	Poly(hydroxy-3-butyrate)
PMMA	Poly(methylmethacrylate)
ROP	Ring-opening polymerization
THF	Tetrahydrofuran
TIBAO	Isobutyl alumoxane
TMC	Trimethylene carbonate
TMEDA	*N,N,N′,N′*-tetramethylethylenediamine
TMS	Trimethylsilyl

1 Introduction

The very beginning of organolanthanide chemistry dates back to the year 1954, when Birmingham and Wilkinson reported the synthesis of the first tris(cyclopentadienyl) lanthanide complexes, Cp_3Ln [1]. However, a major drawback encountered in this young field of organometallic chemistry was the intrinsic instability of certain classes of organolanthanide complexes combined with their often extreme sensitivity towards traces of air and moisture. Thus, until about 30 years ago organometallic compounds of the rare earth metals remained a curiosity. This situation changed slowly in the late 1970s and the early 1980s when more sophisticated preparative and analytical techniques became more generally available [2]. Especially the use of dry-boxes and access to single crystal X-ray diffraction techniques made it possible to safely handle and characterize these compounds and to understand the structural features of these fascinating complexes. The area developed even faster in the late 1980s, largely stimulated by the discovery of the high potential of these compounds as reagents in organic synthesis and as very active homogeneous catalysts [3].

It should be emphasized at this point that the organometallic chemistry of the lanthanide (and actinide) elements differs significantly in several ways from that of the *d*-transition metals [4, 5]. Generally accepted principles of organo-*d*-transition metal chemistry do not apply to organolanthanide compounds, including the well-known "18-electron rule," σ-donor/π-acceptor metal ligand bonding, the formation of stable carbonyls and olefin, alkyne, carbene or carbyne complexes, as well as the formation of stable M=O, M=N, or M≡N multiple bonds. In fact, even direct metal–metal bonds, a common phenomenon observed in *d*-transition metal chemistry, are virtually nonexistent in organo-*f*-element chemistry. This is due to several intrinsic properties of the lanthanide ions imparting unique electronic and steric features to rare earth organometallics. The rare earth metals (=Ln) generally comprise the lanthanides La–Lu as well as the Group 3 metals scandium and yttrium. The 14 elements of the lanthanide series represent the largest subgroup in the Periodic Table. All lanthanide metals are highly electropositive, comparable to the alkali and alkaline earth metals, so that metal-to-ligand bonding can be considered as predominantly ionic. Therefore, the spectroscopic and magnetic properties of lanthanide coordination compounds are largely uninfluenced by the ligands. According to the hard and soft acids and bases (=HSAB) concept, lanthanide ions are considered as hard acids. This hard acid character combined with the largely ionic bonding is the origin of the pronounced oxophilicity of the lanthanide ions which can be quantified in terms of the dissociation energy of LnO. This oxophilic nature of the metal centers strongly influences the reactivity of lanthanide compounds and leads to a preference of hard oxygen- or nitrogen-based ligands while coordination of softer ligands containing, for example, phosphorus or sulfur donor atoms is generally disfavored. In all cases, Ln^{3+} is the most stable oxidation state, especially in aqueous solution. The most easily accessible exceptions from the uniform Ln(III) oxidation state are tetravalent cerium as well as the reduced Ln^{2+} state for samarium, europium, and ytterbium. When crossing the series from La to Lu, a steady

decrease in the Ln^{3+} ionic radii is observed. This phenomenon is well known as the lanthanide contraction which is basically caused by shielding of the $4f$ electrons by the $5s^2$ and $5p^6$ orbitals [4,5]. The lanthanide contraction causes the lanthanide ions to have similar, but not identical, properties and is the main reason why separation of the lanthanides can be achieved.

Lanthanide amidinates and guanidinates comprise a relatively young class of rare earth metal complexes containing *N*-chelating ligands. Such compounds are known for about 20 years. When first reported around 1990, no practical uses were envisaged for lanthanide amidinates. Since then, amidinates (and the closely related guanidinates) of the rare earth elements have turned out to be highly promising with respect to applications in homogeneous catalysis, especially polymerization reactions. This review tries to cover the whole success story of lanthanide amidinates and guanidinates and their transition from mere laboratory curiosities to efficient homogeneous catalysts. References in this article are restricted mainly to publications illustrating the historic development of the field as well as review articles and the most recent original papers. A recently published review article entitled "Advances in the Coordination Chemistry of Amidinate and Guanidinate Ligands" provides rapid access to all original literature covered in this article up to 2008 [6]. The subject was also recently covered in a *Chemical Society Reviews* tutorial review entitled "Lanthanide amidinates and guanidinates: from laboratory curiosities to efficient homogeneous catalysts and precursors for rare-earth oxide thin films" [7].

2 Amidinate Anions: Highly Versatile Cyclopentadienyl-Alternatives

Following the early discovery of the tris(cyclopentadienyl) complexes of the lanthanide elements by Wilkinson and Birmingham [1], most of the organolanthanide compounds studied were sandwich-type complexes containing unsubstituted or ring-substituted cyclopentadienyl ligands [3]. Their relatively high stability against moisture and (to a lesser extent) air motivated numerous research groups to develop the area of lanthanocene chemistry during the last 3 decades. A main drawback encountered with using unsubstituted Cp was certainly the difficulty in obtaining anything else than Cp_3Ln, the chemistry of which is rather limited. With the introduction of pentamethylcyclopentadienyl (=Cp^*) ligands into organolanthanide chemistry more versatile compounds of the Cp^*_2LnX type became more easily available and this opening of the coordination sphere led to the development of a much more diverse derivative chemistry. Subsequently, it was demonstrated that various lanthanocene complexes exhibit highly efficient catalytic activity for olefin transformations including hydrogenation, polymerization, hydroboration, hydrosilylation, hydroamination, and hydrophosphination [8, 9]. However, in this chemistry, the steric saturation of the coordination sphere around the large *f*-element ions is much more important than the number of valence electrons. Thus, current research in this area is increasingly focussed on the development of alternative ligand

Scheme 1

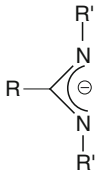

R = H, alkyl, aryl
R' = H, alkyl, cycloalkyl, aryl, trimethylsilyl

Scheme 2

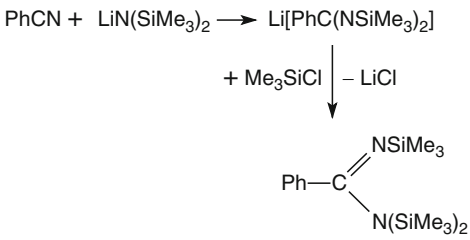

sets. Amidinate and guanidinate anions play a central role in this area of research. An early account of lanthanide amidinate chemistry can be found in a 1995 review article entitled "Cyclopentadienyl-free Organolanthanide Chemistry" [10–13].

Amidinate anions of the general formula $[RC(NR')_2]^-$ (Scheme 1) are nitrogen analogs of the carboxylate anions. They have been widely employed as spectator ligands in main group and transition metal coordination chemistry, with the latter encompassing both early and late transition metals as well as the lanthanides and actinides. As illustrated in Scheme 1, all three substituents at the heteroallylic N–C–N unit can be varied in order to meet a large range of steric (and, to a lesser degree, electronic) requirements.

In addition to the substituents listed in Scheme 1, chiral groups may be introduced, and unsymmetrically substituted amidinate anions are also possible. The amidinate anions may also contain additional functional groups, or two such anions can be linked with or without a suitable spacer unit. Yet another variety comprises the amidinate unit being part of an organic ring system [6, 7].

Historically, the amidinate story begins with the discovery of *N,N,N′*-tris (trimethylsilyl)benzamidine, $PhC(=NSiMe_3)[N(SiMe_3)_2]$, by Sanger et al. [14]. The compound was prepared by the reaction of benzonitrile with $LiN(SiMe_3)_2$ followed by treatment with chlorotrimethylsilane (Scheme 2).

The method was later improved by Oakley et al. [15]. In their 1987 paper these authors also reported a series of *p*-substituted derivatives. In the following years these *N*-silylated ligands were extensively employed in main group as well as transition metal chemistry, and the first review article covering the field was published by Dehnicke in 1990 [16]. Since 1994, an incredible variety of differently substituted amidinate ligands has been developed and employed in the coordination of various elements throughout the Periodic Table [17–19]. The main advantages of these ligands are twofold. Amidinate anions are generally readily accessible using

commercially available or easily prepared starting materials. Furthermore, their steric and electronic properties can be readily modified in a wide range through variation of the substituents on the carbon and nitrogen atoms. These properties combined make the amidinate anions clearly almost as versatile as the ubiquitous cyclopentadienyl ligands.

Metal amidinato complexes are principally accessible through several synthetic routes. The most prevalent of them include:

(a) Insertion of carbodiimides, R–N=C=N–R, into an existing metal-carbon bond;
(b) Deprotonation of an amidine using a metal alkyl;
(c) Salt metathesis reactions between a metal halide substrate and an alkali metal amidinate (with the latter normally being generated by one of the routes (a) or (b)); and
(d) Reaction of metal halides with *N,N,N′*-tris(trimethylsilyl)amidines.

It should be noted here that not all these synthetic routes are equally well applicable to the rare earth elements. Route (b) is severely restricted by the paucity of simple lanthanide alkyls, while route (d) is unsuitable in the lanthanide case as lanthanide trihalides are generally unreactive towards *N,N,N′*-tris(trimethylsilyl)amidines. Deprotonation of amidines by metal amides should also be possible synthetic pathway since the delocalized structure of the resulting anion will increase the acidity. However, this route has apparently not yet been tried.

Closely related to the amidinate anions are the guanidinate ligands (Scheme 3) which differ only in that they contain a tertiary amino group at the central carbon atom of the NCN unit. The beginning of their coordination chemistry dates back to the year 1970, when Lappert et al. reported the first transition metal guanidinate complexes [20]. Like the amidinates, these anions too make attractive ligands because of the similar steric and electronic tunability through systematic variations of the substituents at the carbon and nitrogen atoms. The general synthetic methods for preparing metal amidinato complexes can in part be applied to the corresponding guanidinates and include the following:

(1) Insertion of carbodiimides into an existing metal–nitrogen bond;
(2) Deprotonation of a guanidine using a metal alkyl; and
(3) Salt metathesis reactions between a metal halide substrate and an alkali metal guanidinate (with the latter normally being generated by one of the routes (a) or (b)).

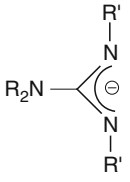

R = alkyl, trimethylsilyl
R' = H, alkyl, cycloalkyl, aryl, trimethylsilyl

Scheme 3

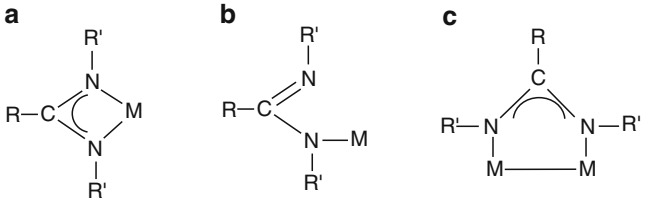

Scheme 4

Here too the same restrictions apply for the preparation of lanthanide guanidinates. This means that especially route (b) is not generally applicable due to the very limited access to simple lanthanide alkyls.

The general coordination modes of amidinate and guanidinate ($R = NR'_2$) ligands are shown in Scheme 4. Both ligands display a rich coordination chemistry in which both chelating and bridging coordination modes can be achieved. By far, the most common coordination mode is the chelating type **A**. In contrast, there are only rare examples of monodentate metal coordination (**B**). This type of bonding can be the result of severe steric crowding in certain amidinate or guanidinate ligands containing very bulky substituents. Also very common in transition metal chemistry is the bridging coordination mode **C**. The bridging coordination mode is often found in dinuclear transition metal complexes with short metal–metal distances, that is, multiple bonding between the metal atoms. The majority of these complexes belong to the class of "paddlewheel"-type compounds with the general formula M_2(amidinate)$_4$ or M_2(guanidinate)$_4$. The fascinating chemistry of these complexes has been extensively investigated mainly by Cotton and Murillo et al. [6, 7]. However, this coordination mode, which is so characteristic for various *d*-transition metals, is completely unknown in lanthanide chemistry. The synthesis of dinuclear complexes comprising any type of direct Ln–Ln bonding (either single or multiple bonding) remains one of the big challenges in organolanthanide chemistry today. Even well-defined complexes containing an unsupported Ln–M bond (M = *d*-transition metal) are extremely rare [21].

The factors governing the formation of either chelating or bridging coordination modes in amidinate and guanidinate complexes have been analyzed in detail. Perhaps the greatest advantage of these ligands besides their easy availability is the possibility of tuning their steric requirements in a wide range by variation of the substituents at carbon and nitrogen. To some extent, the electronic properties can also be influenced by introduction of suitable substituents such as $SiMe_3$ or 2,4,6-$C_6H_2(CF_3)_3$ [18]. Amidinate and guanidinate ligands have small N–M–N bite angles which are typically in the range of 63–65°. Tuning of the steric demand of the ligand by varying the substituents at nitrogen can also influence the coordination geometry of the metal center in bis(amidinato) complexes. Steric hindrance imparted by substituents on the nitrogen atoms has its main effects mainly within the heteroallylic N–M–N plane. Terphenyl substituents on the amidinate carbon atom have been successfully employed to effect steric shielding above and below the N–M–N plane, although this shielding is fairly remote from the metal center. Another

approach to provide steric protection of the N–M–N coordination plane is the use of *ortho*-disubstituted aryl substituents on the nitrogen atoms. Especially useful in this respect is the 2,6-diisopropylphenyl group. Also, a very important point to be noted is that in *N,N′*-bis(trimethylsilyl)benzamidinates and related ligands the orientation of the phenyl ring on the central carbon atom with respect to the N–C–N unit is normally nearly perpendicular. This conformation accounts for the fact that such amidinate anions are not "flat" ligands such as the isoelectronic carboxylate anions, but also extend above and below the N–C–N plane. It was first pointed out by us that these ligands can be regarded as "steric cyclopentadienyl equivalents" [22]. The concept of "steric cyclopentadienyl equivalents" was developed by Wolczanski et al. in connection with a series of tri-*t*-butylmethoxide ("tritox") complexes [23]. The sterically demanding tri-*t*-butylmethoxide ligand forms a steric cone about a metal, similar to bis(trimethylsilyl)amide or cyclopentadienyl. With 125° the cone angle of tritox approaches that of cyclopentadienyl (136°). Amidinate and guanidinate ligands, too, are monoanionic ligands, and their steric demand is tunable in a wide range similar to the transition from unsubstituted cyclopentadienyl to very bulky ring-substituted cyclopentadienyl ligands.

3 Synthesis and Characterization of Lanthanide Amidinates and Guanidinates

3.1 Lanthanide(II) Amidinates and Guanidinates

In (organo)lanthanide chemistry, the divalent oxidation state is most readily accessible under normal conditions for samarium, europium, and ytterbium. Compounds of these elements in the +2 oxidation state are stronger reducing agents and undergo a large variety of interesting redox reactions [3]. Just as in cyclopentadienyllanthanide chemistry, stable divalent species were of particular interest in amidinate and guanidinate interest due to their anticipated high reactivity. In fact, soluble and very reactive ytterbium(II) benzamidinates containing $[RC_6H_4C(NSiMe_3)_2]^-$ ligands were reported as early as 1990 [18]. As shown in Scheme 5, these compounds were readily prepared by treating freshly prepared YbI_2 in tetrahydrofuran (THF) solution with two equivalents of sodium *N,N′*-bis(trimethylsilyl)amidinates and isolated as dark red, highly air-sensitive materials. X-ray diffraction studies revealed the *trans*-coordination with two chelating amidinate ligands. A notable structural feature, characteristic also for many other complexes containing these ligands, is the large dihedral angle (77.3° for R=H) between the phenyl rings and the amidinate N–C–N units which precludes any conjugation between the two π-systems and is responsible for the cone-like overall shape of the amidinate ligands [18].

As expected, the ytterbium(II) benzamidinates shown in Scheme 5 were found to be strong reducing agents and to undergo various redox reactions, for example, with alkyl halides and dichalcogenides REER (E = S, Se, Te). For example, the S–S

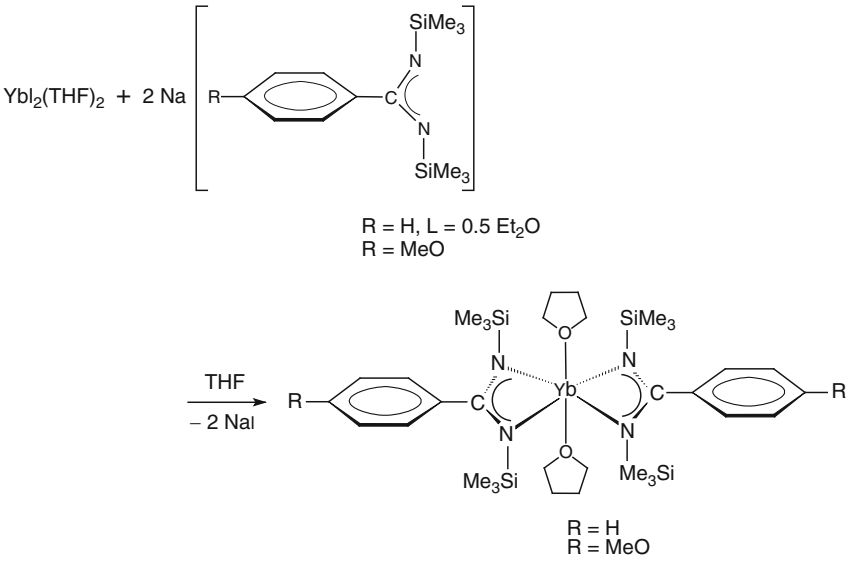

Scheme 5

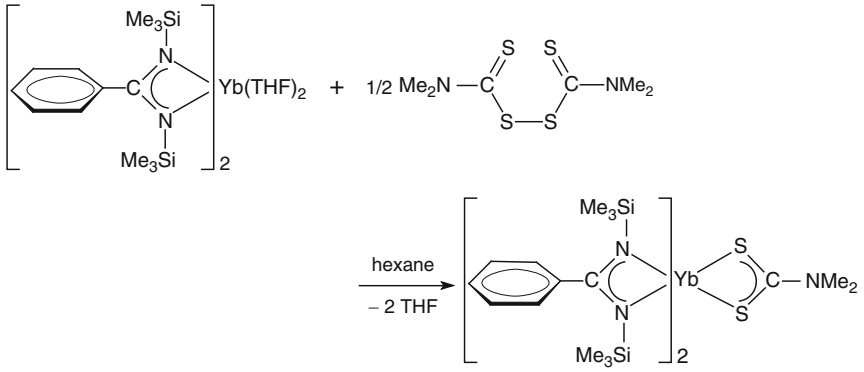

Scheme 6

bond in tetramethylthiuramdisulfide, $[Me_2NC(S)S]_2$, is readily cleaved to form an ytterbium(III) dithiocarbamate complex (Scheme 6) [18].

Facile cleavage of E–E bonds (E = Se, Te) was also observed (Scheme 7) giving rise to stable ytterbium(III) amidinate complexes comprising Yb–Se and Yb–Te bonds [18].

While ytterbium(II) benzamidinate complexes have been known for many years, the synthesis of the first divalent samarium bis(amidinate) required the use of a sterically hindered amidinate ligand, $[HC(NDipp)_2]^-$ (Dipp = $C_6H_3Pr^i_2$–2,6). The dark green samarium(II) bis(amidinate) $Sm(DippForm)_2(THF)_2$ (DippForm = $[HC(NDipp)_2]^-$) can be prepared by three different synthetic routes (Scheme 8). The trivalent diiodo samarate complex $[Na(THF)_5][SmI_2(DippForm)_2(THF)_2]$

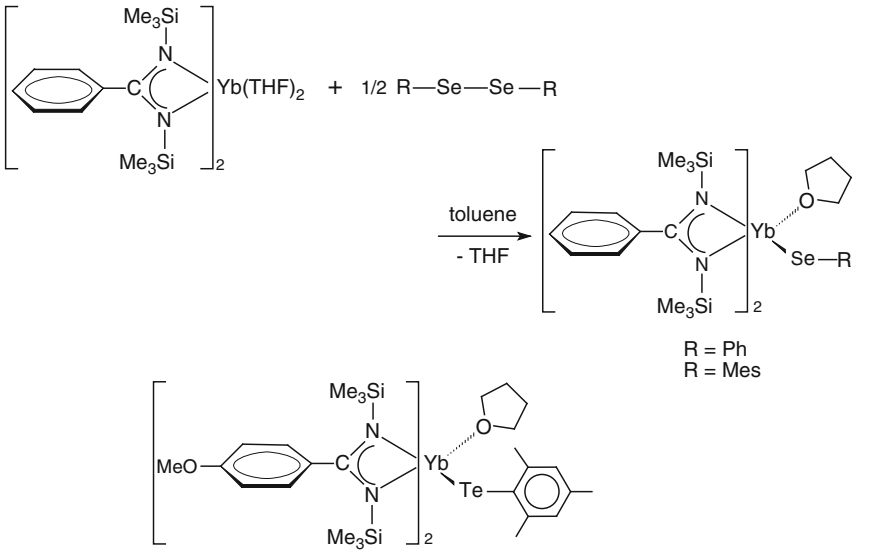

Scheme 7

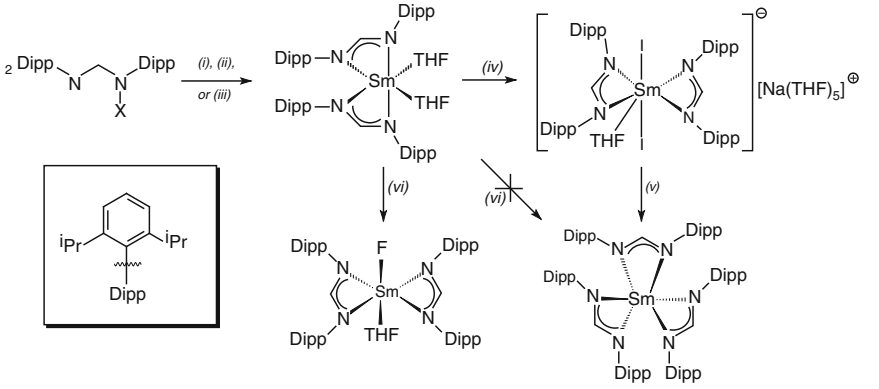

(i) X = Na, $SmI_2(THF)_2$; *(ii)* X = H, $Sm/Hg(C_6F_5)_2$; *(iii)* X = H, $Sm[N(SiMe_3)_2]_2(THF)_2$; *(iv)* $SmI_2(THF)_2$/NaI; *(v)* hexane; *(vi)* DippFormH, $Hg(C_6F_5)_2$

Scheme 8

was isolated in small quantities as a colorless byproduct. Dissolution of this compound in hexane led to ligand redistribution to give $Sm(DippForm)_3$ with concomitant precipitation of NaI and $SmI_3(THF)_{3.5}$. The monofluoro-bis(amidinate) $SmF(DippForm)_2(THF)$ could also be isolated from $Sm(DippForm)_2(THF)_2$ via treatment with $Hg(C_6F_5)_2$. These results clearly show that carefully selected amidinate ligands are capable of stabilizing even the most strongly reducing "classical" lanthanide(II) ion, that is, divalent samarium. Future investigations will show if similar complexes can also be synthesized with "nonclassical" divalent lanthanide

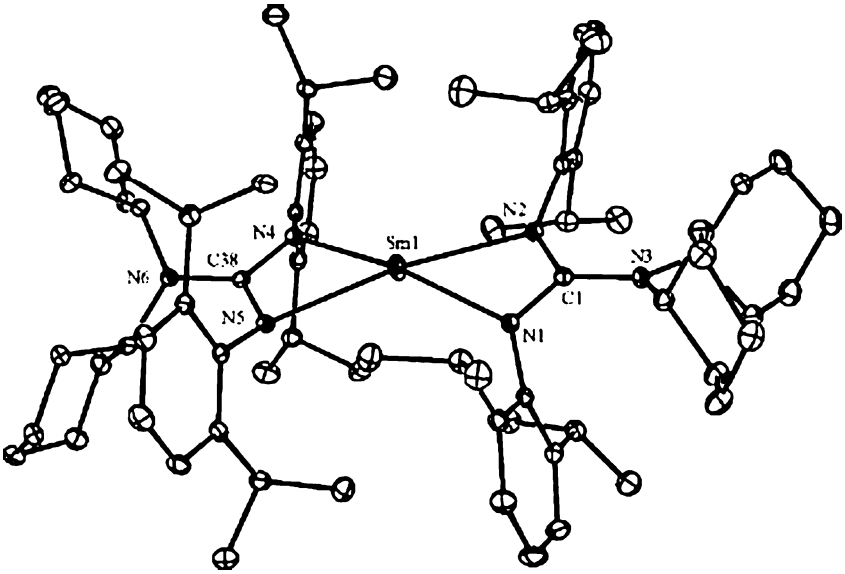

Fig. 1 Molecular structure of $Sm(Giso)_2$ (Giso = $Cy_2NC(NAr)_2$; Ar = $C_6H_3Pr^i_2$–2, 6) [24]

ions such as Tm^{2+}, Nd^{2+} or Dy^{2+}. Apparently, analogous europium(II) amidinates too have not yet been reported, although they should be readily accessible through standard metathetical routes [6, 7].

In 2007, the first homoleptic lanthanide(II) guanidinate complexes, $Ln(Giso)_2$ (Ln = Sm, Eu, Yb; Giso = $Cy_2NC(NAr)_2$; Ar = $C_6H_3Pr^i_2$–2,6), were reported and shown to have differing coordination geometries (including unprecedented examples of planar 4-coordination) [24]. In particular, X-ray studies revealed planar four-coordinate coordination geometries for Sm and Eu derivatives (Fig. 1), while the ytterbium(II) species is distorted tetrahedral. In the case of Yb, two iodo-bridged dimeric lanthanide(II) guanidinate complexes were also isolated from the reaction mixtures (Fig. 2) [24].

The reaction of equimolar amounts of $Na[(Me_3Si)_2NC(NCy)_2]$ (which was prepared in situ from $NaN(SiMe_3)_2$ and *N,N′*-dicyclohexylcarbodiimide), and $YbI_2(THF)_2$ gave the closely related ytterbium(II) guanidinate complex $[\{(Me_3Si)_2NC(NCy)_2\}Yb(\mu\text{-}I)(THF)_2]_2$ with bridging iodo ligands [6, 7, 24]. However, a bis(guanidinato)ytterbium(II) complex stabilized by *N,N,N′,N′*-tetramethylethylenediamine (=TMEDA) was found to be accessible by two different synthetic routes illustrated in Scheme 9. Entry to $[(Me_3Si)_2NC(NCy)_2]_2Yb(TMEDA)$ was provided by either reduction of $[(Me_3Si)_2NC(NCy)_2]_2Yb(\mu\text{-}Cl)_2Li(TMEDA)$ with Na/K alloy or by direct reaction of YbI_2 with the $[(Me_3Si)_2NC(NCy)_2]^-$ anion. In the first case, the solvated complex $[(Me_3Si)_2NC(NCy)_2]_2$ Yb(TMEDA) was generated directly due to the presence of TMEDA in the starting material. Both preparations were found to proceed in excellent yields. The diamagnetic nature of divalent Yb allowed definitive characterization of these materials by NMR spectroscopy [25].

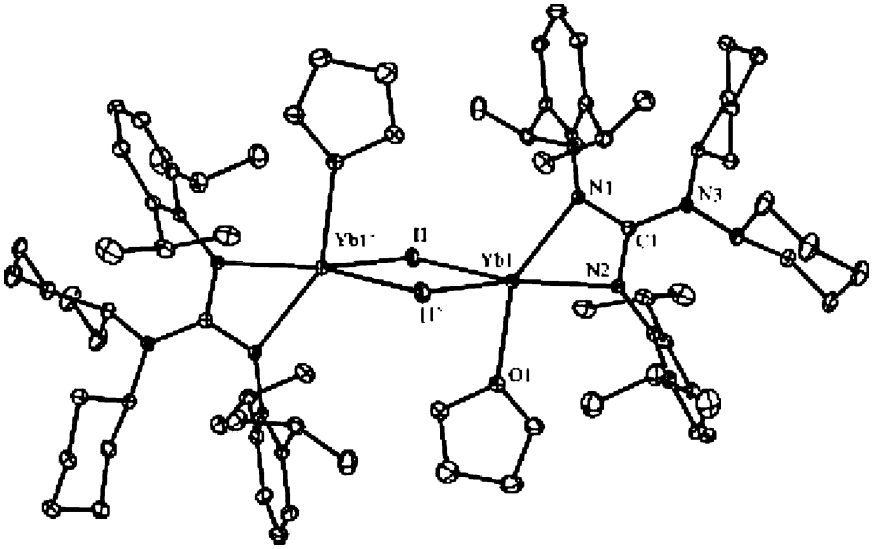

Fig. 2 Molecular structure of $[(Giso)Yb(THF)(\mu\text{-}I)]_2$ (Giso = $Cy_2NC(NAr)_2$; Ar = $C_6H_3Pr^i_2$–2,6) [24]

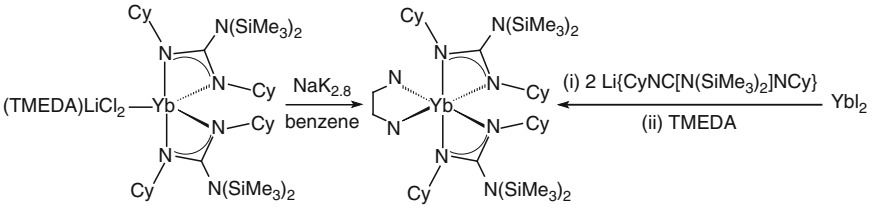

Scheme 9

3.2 Lanthanide(III) Amidinates and Guanidinates

3.2.1 Homoleptic Lanthanide(III) Tris(Amidinates) and Tris(Guanidinates)

Homoleptic lanthanide(III) tris(amidinates) and -guanidinates are among the longest known lanthanide complexes containing these chelating ligands. The first lanthanide amidinate complexes ever reported in the literature were homoleptic tris(amidinates) of the type $[RC_6H_4C(NSiMe_3)_2]_3Ln$ (Scheme 10) which can be regarded as the amidinate analogs of the homoleptic lanthanide tris(cyclopentadienyl) complexes Cp_3Ln [6, 7, 22].

A large number of such complexes was synthesized and fully characterized in the course of the early studies. However, at that time these compounds were mere laboratory curiosities without any apparent practical use. It also turned out that the derivative chemistry of these complexes was rather limited, resembling that of

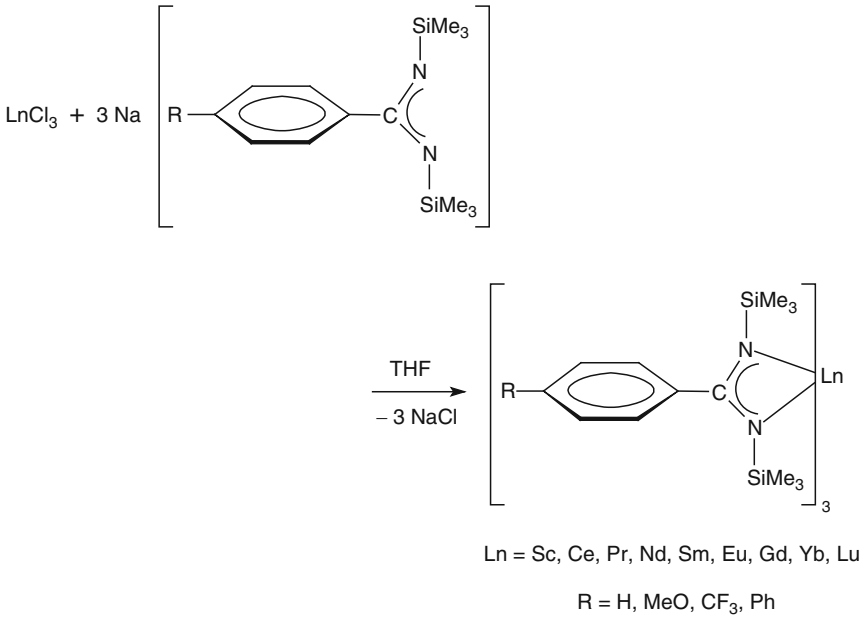

Scheme 10

the parent Cp_3Ln complexes. It took many years until the promising catalytic activities of these compounds were discovered (cf., Sect. 4) [6, 7, 18].

In a similar manner, treatment of anhydrous rare earth chlorides with three equivalents of lithium 1,3-di-*tert*-butylacetamidinate (prepared in situ from di-*tert*-butylcarbodiimide, Bu^t–N=C=N–Bu^t, and methyllithium) afforded $Ln[MeC(NBu^t)_2]_3$ (Ln = Y, La, Ce, Nd, Eu, Er, Lu) in 57–72% isolated yields [6, 7, 26]. X-ray crystal structures of these complexes demonstrated monomeric formulations with distorted octahedral geometry around the lanthanide(III) ions (Fig. 3, Ln = La). The new complexes are thermally stable at >300°C, and sublime without decomposition between 180–220°C/0.05 Torr. Other series of homoleptic lanthanide tris(amidinates) include the *N*-cyclohexyl-substituted derivatives $[RC(NCy)_2]_3Ln(THF)_n$ (R = Me, Ln = Nd, Gd, Yb, n = 0; R = Ph, Ln = Nd, Y, Yb, *n* = 2). A sterically hindered homoleptic samarium(III) tris(amidinate), $Sm[HC(NC_6H_3Pr^i_2\text{–}2,6)_2]_3$, was obtained by oxidation of the corresponding Sm(II) precursor (cf., Scheme 8) [6, 7].

In this area, the carbodiimide insertion route is usually not applicable, because simple, well-defined lanthanide tris(alkyls) and tris(dialkylamides) are not readily available [3–5]. A notable exception is the formation of homoleptic lanthanide guanidinates from anionic lanthanide amido complexes and carbodiimides (Scheme 11) [6, 7, 27, 28]. In the structurally characterized ytterbium derivative $[Ph_2NC(NCy)_2]_3Yb{\cdot}2PhCH_3$ (yellow crystals, 78% yield) the coordination geometry around the lanthanide ion can be best described as a distorted trigonal prism [27]. The same molecular geometry was found for the neodymium and samarium derivatives $[Ph_2NC(NCy)_2]_3Ln{\cdot}2PhCH_3$ (Ln = Nd, Sm) [28].

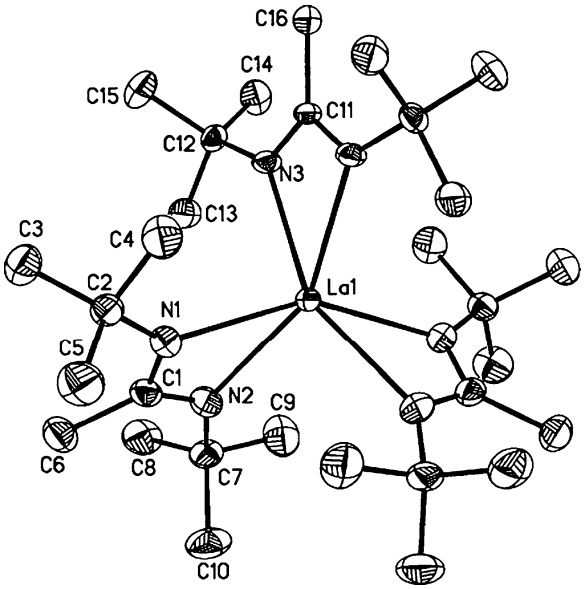

Fig. 3 Molecular structure of $[MeC(NBu^t)_2]_3La$

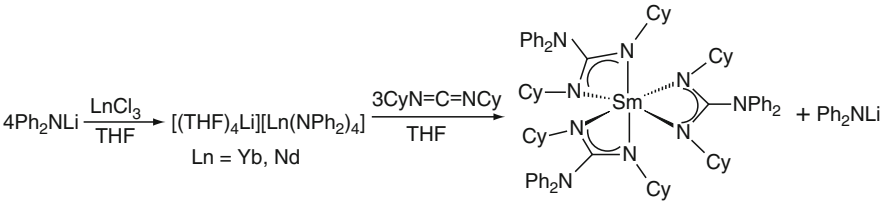

Scheme 11

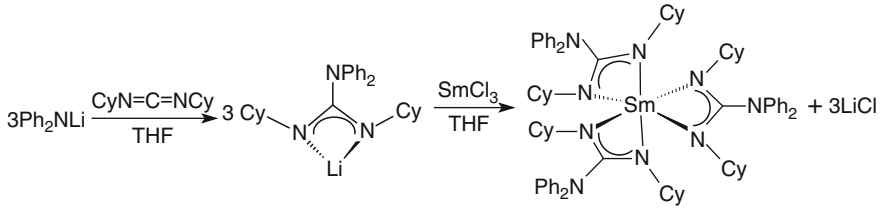

Scheme 12

The major synthetic route leading to homoleptic lanthanide tris(amidinates) and -guanidinates, however, is the metathetical reaction between anhydrous lanthanide trichlorides and preformed lithium amidinates or guanidinates, respectively, in a molar ratio of 1:3 (Scheme 12) [6, 7].

Using this synthetic route, eight novel homoleptic tris(guanidinato) lanthanide complexes $[R_2NC(NPr^i)_2]_3Ln$ [Ln = Y, Gd, Dy; R = Me, Et, Pr^i] have recently

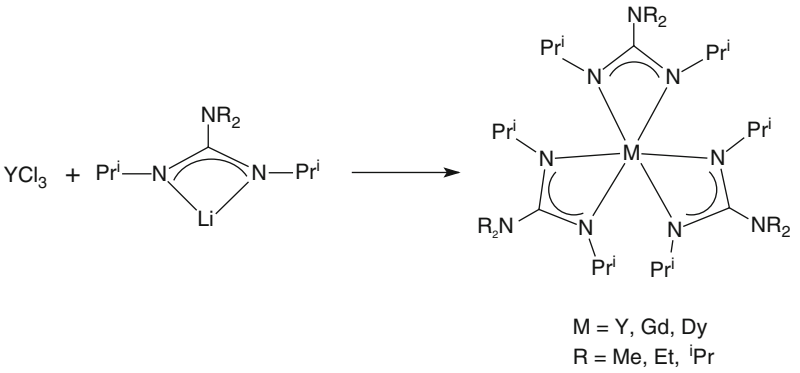

Scheme 13

been prepared according to Scheme 13 and characterized by NMR, CHN analysis and IR spectroscopy. Single crystal X-ray structure analyses revealed that all these compounds are monomers with the rare earth metal center coordinated to the three chelating guanidinate ligands in a distorted trigonal prismatic geometry [29].

The structurally characterized homoleptic lanthanide tris(guanidinate) complex $[(CH_2)_5NC(NPr^i)_2]_3Yb$ was synthesized analogously by the metathesis reaction of the preformed lithium guanidinate with anhydrous $YbCl_3$ in a 3:1 molar ratio in THF [30]. A series of new lanthanide tris(guanidinate) complexes including the first THF-solvated tris(guanidinate) lanthanum complexes were synthesized according to Scheme 14 and fully characterized [31].

The six-coordinate tris(benzamidinates) $[PhC(NSiMe_3)_2]_3Ln$ also form 1:1 adducts with donor ligands such as THF, MeCN, or PhCN. In the case of benzonitrile, it was possible to isolate and structurally characterize two of these seven-coordinated nitrile-adducts. They are most readily isolated when the original preparation is directly carried out in the presence of one equivalent of benzonitrile (Scheme 15). The facile adduct formation with small donor molecules is yet another analogy between the tris(amidinates) and the tris(cyclopentadienyl) complexes, for which similar adducts with, for example, THF, nitriles or isonitriles are well established [6, 7, 17].

In recent years, homoleptic lanthanide(III) tris(amidinates) and -guanidinates have been demonstrated to exhibit extremely high activity for the ROP of polar monomers such as ε-caprolactone (CL) and trimethylene carbonate (TMC) (cf., Sect. 4.2) [6, 7].

3.2.2 Lanthanide(III) Bis(Amidinates) and Bis(Guanidinates): Metallocene Analogs

Bulky heteroallylic ligands such as the benzamidinate anions $[RC_6H_4C(NSiMe_3)_2]^-$ soon became well established as useful alternatives to the cyclopentadienyl ligands.

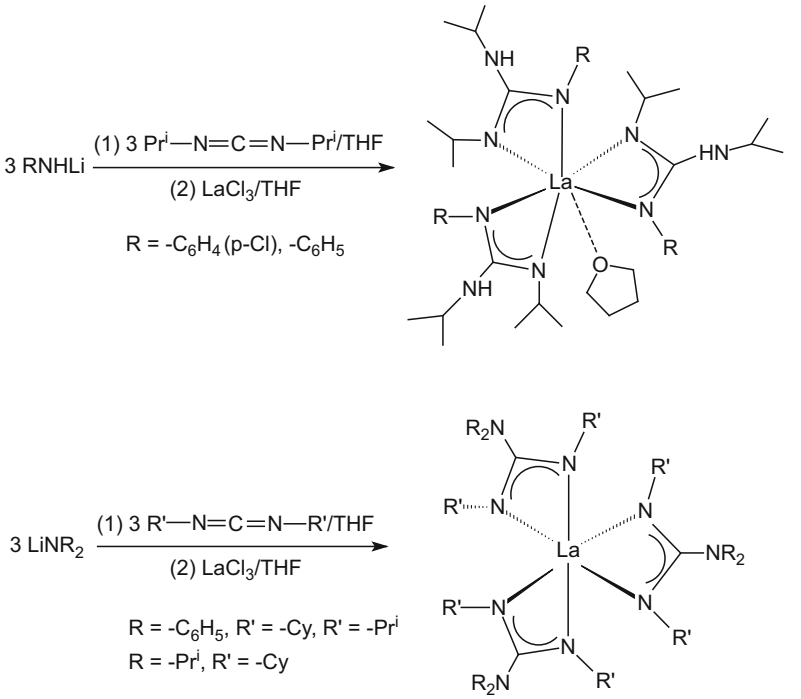

Scheme 14

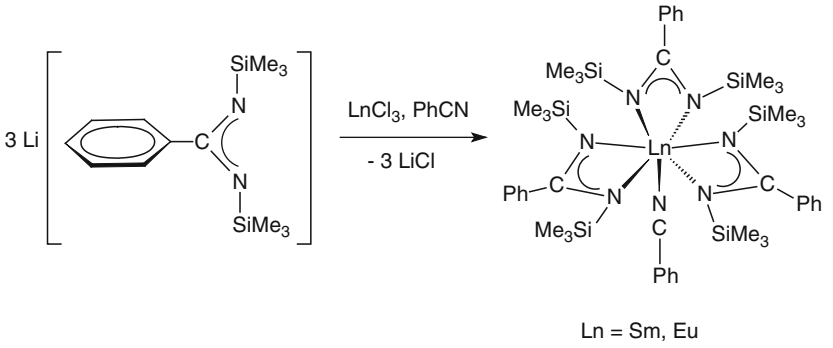

Scheme 15

Shortly after the successful synthesis and characterization of various lanthanide(III) tris(amidinate) derivatives the first disubstituted lanthanide(III) amidinate species were reported. Such compounds appeared to be interesting synthetic targets due to their metallocene-like coordination environment which was expected to allow the isolation and characterization of stable though reactive amide, alkyl, and hydride species. In this respect, the bulky amidinate and guanidinate ligands resemble

even more the substituted cyclopentadienyl ligands such as Cp^*. One of the first representatives of this class of compounds was a sky-blue neodymium complex containing the very bulky nonafluoromesityl-substituted benzamidinate ligand $[2,4,6\text{-}(CF_3)_3C_6H_2C(NSiMe_3)_2]^-$ (Scheme 16) [18].

Retention of LiCl led to formation of an "ate"-complex which is an amidinate analog of the well-known neodymium metallocene complex $Cp^*_2Nd(\mu\text{-}Cl)_2Li(THF)_2$ [3]. While in the case of the large Nd^{3+} ion the use of a sterically bulky amidinate ligand was required, it soon turned out that bis(benzamidinate) lanthanide chlorides could be accessed in a more straightforward manner using scandium and yttrium as smaller central ions [6, 7, 18]. Teuben et al. were able to show that the selective formation of lanthanide bis(amidinates) could be achieved by adjusting the steric requirements of the ligands to the ionic radius of the lanthanide. Metathetical reactions between $ScCl_3(THF)_3$ or $YCl_3(THF)_{3.5}$ with two equivalents of the silyl-substituted amidinate ligands afforded the corresponding bis(amidinato) complexes $[RC_6H_4C(NSiMe_3)_2]_2LnCl(THF)$. A similar approach using yttrium triflate as starting material was used to prepare the first bis(amidinato) lanthanide triflate complexes (Scheme 17) [6, 7, 18].

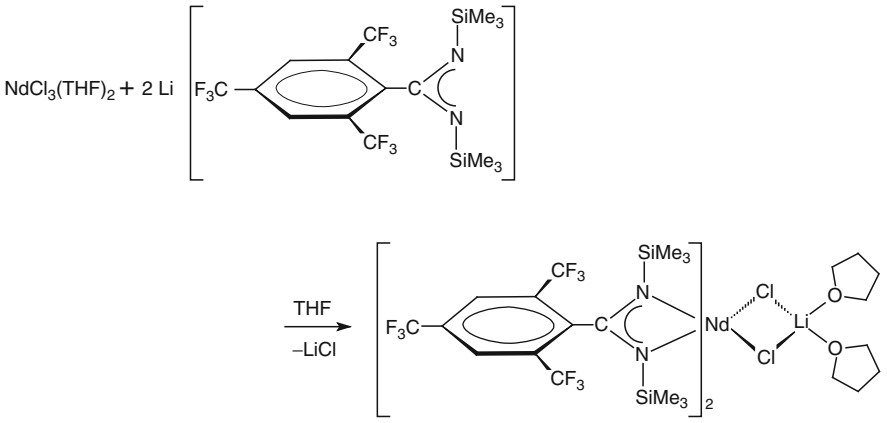

Scheme 16

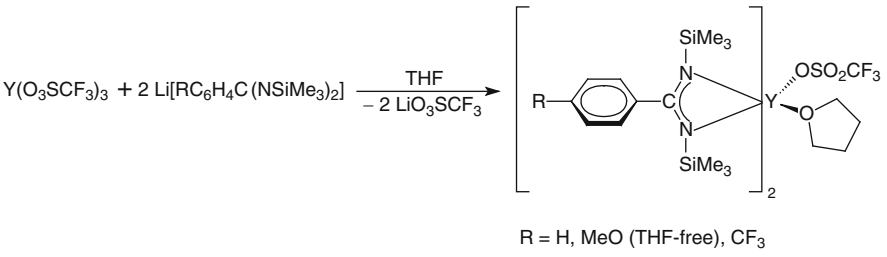

Scheme 17

$$[RC_6H_4C(NSiMe_3)_2]_2YX(THF)_n + LiCH(SiMe_3)_2$$
$$X = Cl,\ n = 1$$
$$X = O_3SCF_3,\ n = 0$$

$$\xrightarrow[-\ LiX]{} [RC_6H_4C(NSiMe_3)_2]_2YCH(SiMe_3)_2$$
$$R = H,\ MeO,\ CF_3$$

Scheme 18

Following the successful isolation of these chloro and triflate precursors, a major synthetic goal was the preparation of reactive alkyl, amide, and hydride species based upon the lanthanide bis(amidinate) moiety. This would further prove the close analogy between lanthanide bis(amidinates) and Cp^*_2Ln-type lanthanide metallocenes. For example, the yttrium(III) benzamidinates $[RC_6H_4C(NSiMe_3)_2]_2YCH(SiMe_3)_2$ are analogs of the metallocene alkyls $Cp^*_2YCH(SiMe_3)_2$. Indeed, it proved possible to employ the same synthetic routes which were well established in lanthanide metallocene chemistry to prepare the corresponding amidinate complexes. For example, alkyl derivatives were found to be easily accessible by alkylation of the corresponding chloride or triflate precursors (Scheme 18). Following their successful syntheses, it was demonstrated that these compounds exhibit comparable catalytic activities, for example, in olefin polymerizations as their metallocene counterparts (cf., Sect. 4.1) [6, 7, 11, 18].

Other σ-alkyl yttrium complexes of this type include $[PhC(NSiMe_3)_2]_2YCH_2Ph(THF)$ and $[PhC(NSiMe_3)_2]_2Y(\mu\text{-}Me)_2Li(TMEDA)$. The *p*-methoxy-substituted derivative $[MeOC_6H_4C(NSiMe_3)_2]_2YCH(SiMe_3)_2$ was characterized by an X-ray structure determination confirming that the bis[*N*,*N*′-bis(trimethylsilyl)-benzamidinate] ligand system sterically resembles more the bulky bis(pentamethylcyclopentadienyl) than the bis(cyclopentadienyl) ligand set. The reactivity of the benzamidinate-stabilized yttrium complexes towards various reagents including hydrogen, ethylene, terminal alkynes, nitriles, and pyridine derivatives was investigated in detail. Hydrogenolysis of the yttrium alkyls in benzene under 4 bar of H_2 afforded the dimeric hydride $[\{RC_6H_4C(NSiMe_3)_2\}_2Y(\mu\text{-}H)]_2$. Both $[PhC(NSiMe_3)_2]_2YCH_2Ph(THF)$ and $[\{RC_6H_4C(NSiMe_3)_2\}_2Y(\mu\text{-}H)]_2$ were modestly active in ethylene polymerization but did not react with propylene and 1-hexene. The alkyls and the hydride were found to react with α-picoline to give an α-picolyl derivative via C–H activation of a methyl group (Scheme 19) [6, 7, 18].

Closely related benzamidinate chemistry has also been investigated with scandium. Due to its small ionic radius, Sc^{3+} forms disubstituted benzamidinate complexes which give rise to interesting derivative chemistry. The main starting material is $[PhC(NSiMe_3)_2]_2ScCl(THF)$ which is available from the reaction of $Na[PhC(NSiMe_3)_2]$ with $ScCl_3(THF)_3$ in THF. The preparation of alkyl and aryl derivatives is illustrated in Scheme 20 (Mes = mesityl) [6, 7, 11, 18].

In the case of the methyllithium reaction the product is a THF solvate while with bulky hydrocarbyls unsolvated complexes were obtained. The compound

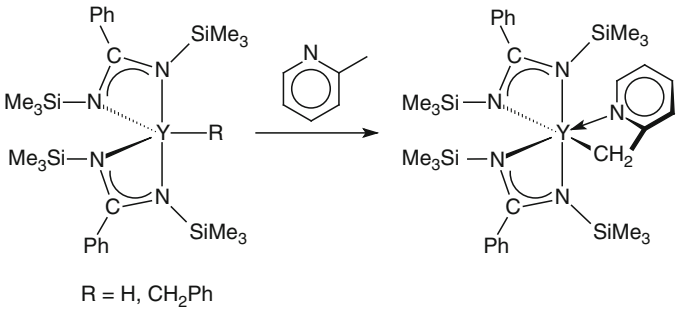

Scheme 19

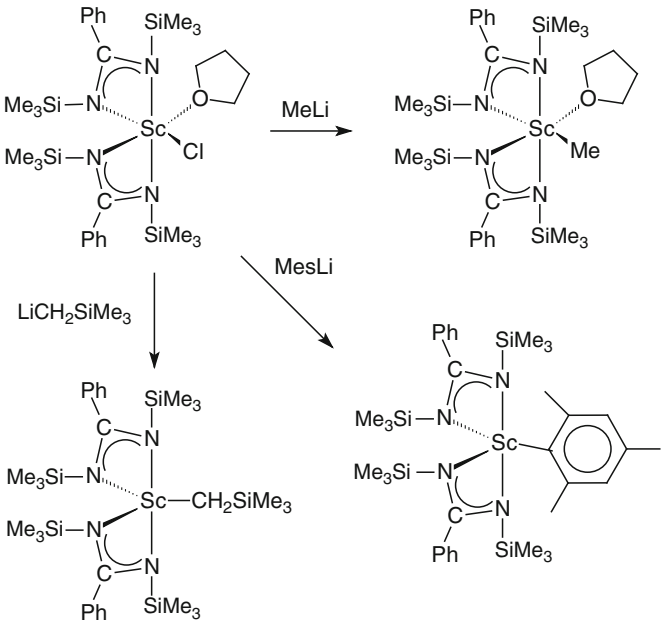

Scheme 20

$[PhC(NSiMe_3)_2]_2ScCH_2SiMe_3$ readily reacts with H_2 to form the dimeric hydride $[\{PhC(NSiMe_3)_2\}_2Sc(\mu\text{-}H)]_2$ [6, 7, 11, 18].

Metathetical routes using bulky lithium guanidinates as starting materials have also been employed to synthesize bis(guanidinato) lanthanide halides (e.g., with lutetium, Scheme 21) as well as reactive alkyls and hydrides [6, 7, 11].

New yttrium and lutetium bis(guanidinate) alkoxides $[(Me_3Si)_2NC(NPr^i)_2]_2LnX$ (X = O^iPr, O^tBu; Ln = Y, Lu) have been synthesized by metathesis reactions of the corresponding bis(guanidinate) chloro-*ate*-complexes $[(Me_3Si)_2NC(NPr^i)_2]_2Ln(\mu\text{-}Cl)_2Li(THF)_2$ (Ln = Y, Lu) with equimolar amounts of potassium *tert*-butoxide or sodium *iso*-propoxide, respectively, in THF at room temperature

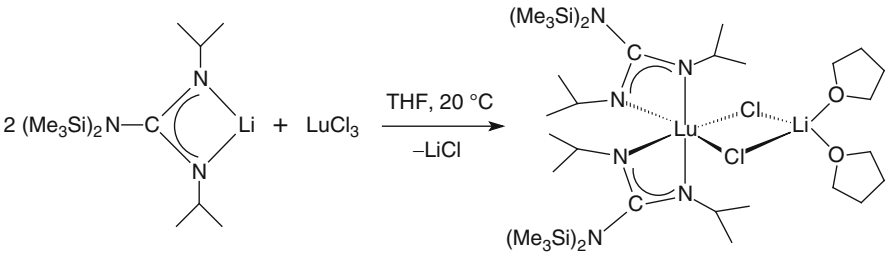

Scheme 21

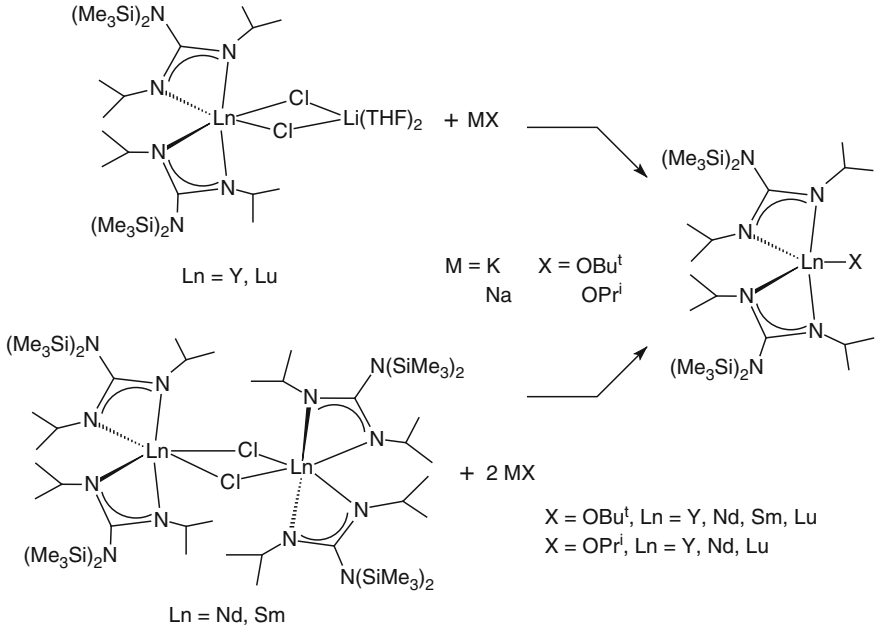

Scheme 22

(Scheme 22). For the preparation of the neodymium- and samarium-containing analogs $[(Me_3Si)_2NC(NPr^i)_2]_2LnX$ (X = O^iPr, O^tBu; Ln = Nd, Sm), the dimeric bis(guanidinate) chloro complexes $[\{(Me_3Si)_2NC(NPr^i)_2\}_2Ln(\mu\text{-}Cl)]_2$ (Ln = Nd, Sm) were treated with a twofold molar excess of MX (M = K, X = OBu^t; M = Na, X = OPr^i) under similar conditions (Scheme 22). The products were obtained after workup in high yields as oxygen- and moisture-sensitive solids which are highly soluble in common organic solvents [32].

Surprisingly, it was found that the bis(guanidinate) *tert*-butoxide and isopropoxide complexes feature remarkably different stabilities. It was found that the *tert*-butoxides are stable in both the solid state and hexane or benzene, since no changes were observed in their ^1H NMR and IR spectra when stored for a long time (over several months) at room temperature. However, the isopropoxides were rather

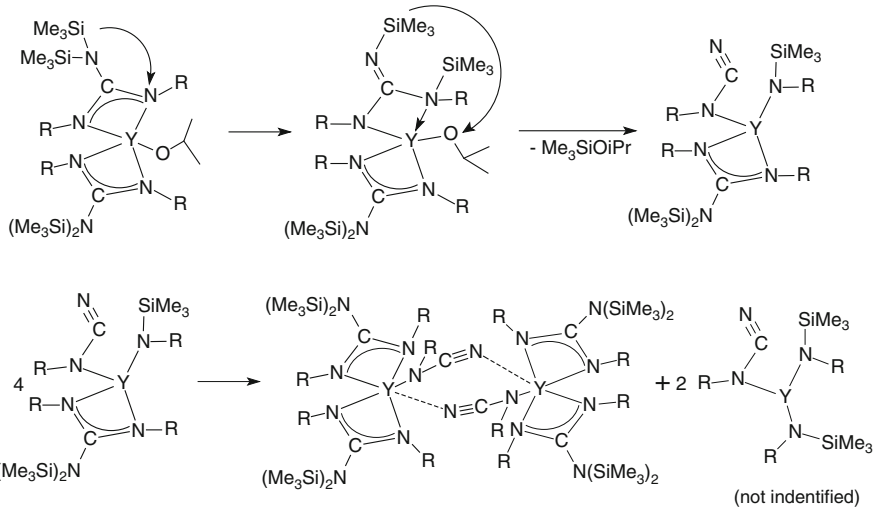

Scheme 23

unstable and slowly decomposed. For example, prolonged storage (2 months) at room temperature of a concentrated hexane solution of the yttrium derivative afforded crystals of the unexpected complex $[\{(Me_3Si)_2NC(NPr^i)_2\}_2Y\{\mu\text{-}N(Pr^i))C{\equiv}N\}]_2$. Apparently, this species resulted from cleavage of two C–N bonds of the guanidinate ligand (Scheme 23). Another type of fragmentation of guanidinate ligands, which includes a 1,3-shift of the Me_3Si group and C–N bond cleavage and which resulted in the formation of the mixed ligand guanidinate amido calcium complex $[\{(Me_3Si)_2NC(NCy)_2\}_2Ca\{\mu\text{-}(Me_3Si)(Cy)N\}]_2$, has been previously reported [32].

Treatment of $[(Me_3Si)_2NC(NPr^i)_2]_2Ln(\mu\text{-}Cl)_2Li(THF)_2$ with methyllithium in the presence of TMEDA afforded the methyl-bridged "ate" complexes $[(Me_3Si)_2NC(NPr^i)_2]_2Ln(\mu\text{-}Me)_2Li(THF)_2$ (Ln = Nd, Yb) which have analogs in Cp^*_2Ln chemistry. With Ln = Y, Nd, and Sm, the unsolvated, chloro-bridged dimers $[\{(Me_3Si)_2NC(NPr^i)_2\}_2Ln(\mu\text{-}Cl)]_2$ were also synthesized. Amidation of these complexes with two equivalents of $LiNPr^i_2$ gave the amido species $[(Me_3Si)_2NC(NPr^i)_2]_2LnNPr^i_2$. The alkyl lanthanide derivatives $[(Me_3Si)_2NC(NPr^i)_2]_2Ln(CH_2SiMe_3)$ (Ln = Y, Nd, Sm, Gd, Yb) were synthesized via a metathesis reaction of the chloro precursors with $LiCH_2SiMe_3$ in toluene. Either the "ate"-complexes or the chloro-bridged dimers can be employed as starting materials for these reactions (Scheme 24) [6, 7, 33, 34].

Treatment of the alkyls with an equimolar amount of $PhSiH_3$ in hexane led to formation of the first known dimeric lanthanide hydrides in a bis(guanidinato) coordination environment (Scheme 25) [6, 7, 33, 34]. These represent a new family of Lewis base free hydrido complexes of the rare earth elements. Single-crystal X-ray and solution NMR studies revealed that these complexes are dimeric in both the

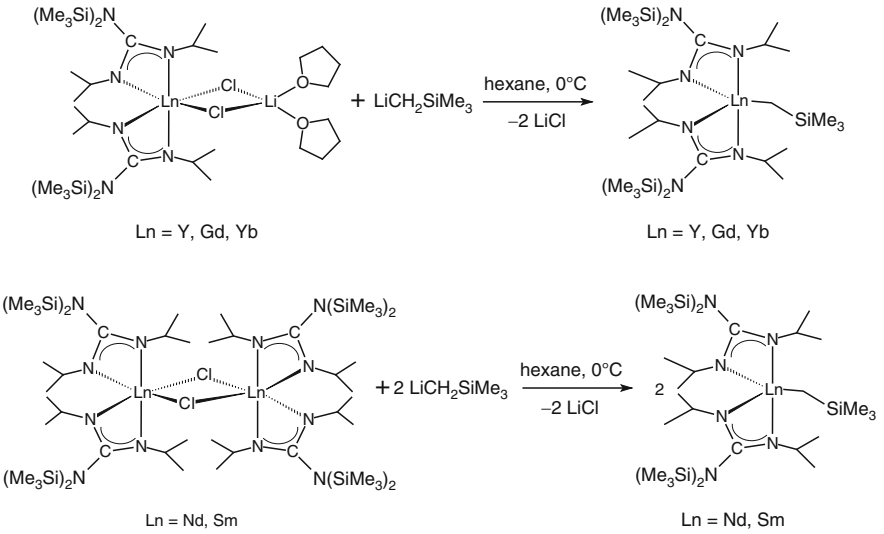

Scheme 24

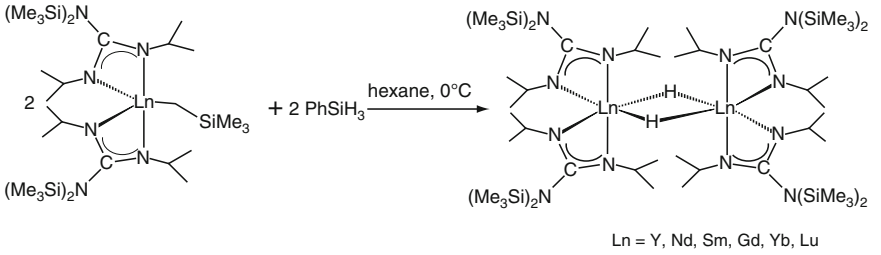

Scheme 25

solid state and in [D_6]benzene. The dimeric hydrido complexes can adopt eclipsed (Nd, Sm, Gd) or staggered (Y, Yb, Lu) conformations depending on the metalatom size [33, 34].

In a similar manner, addition of $N(SiMe_3)_2$ anion equivalents to CyN=C=NCy provided entry to a series of *N*-substituted guanidinate complexes of Sm(III) and Yb(III) with the general formula $[(Me_3Si)_2NC(NCy)_2]_2Ln(\mu\text{-}Cl)_2Li(S)_2$ (Scheme 26, Ln = Sm, Yb; Cy = cyclohexyl; S = Et_2O, 1/2 TMEDA). Substitution of the chloro ligands in these complexes using $LiCH(SiMe_3)_2$ or $LiN(SiMe_3)_2$ yielded solvent-free, monomeric alkyl and amido compounds, respectively (Scheme 26). Definitive evidence for the molecular structures of these products was provided through single-crystal X-ray analysis, and in particular, the results for $[(Me_3Si)_2NC(NCy)_2]_2SmCH(SiMe_3)_2$ and $[(Me_3Si)_2NC(NCy)_2]_2$ – $YbN(SiMe_3)_2$ were presented. These results provided the first reported example of an *organo*lanthanide complex supported by guanidinate ligands [25].

Mutual ligand arrangement in binuclear lanthanide guanidinate complexes of types $[(guanidinate)_2Ln(\mu\text{-}Cl)]_2$, $[(guanidinate)_2Ln(\mu\text{-}H)]_2$, and $(guanidinate)_2$

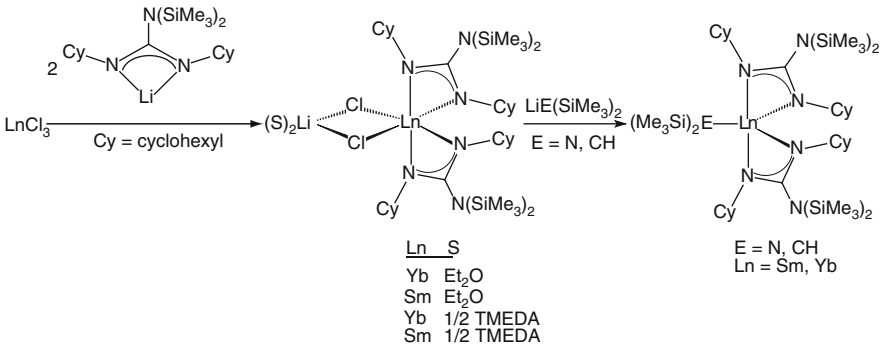

Scheme 26

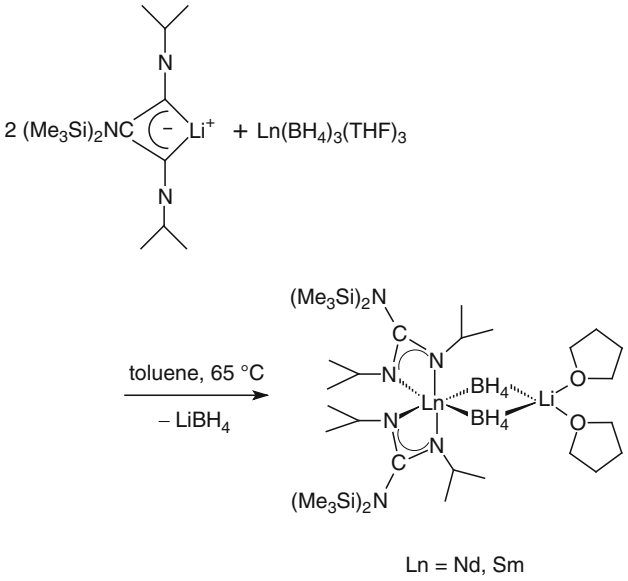

Scheme 27

$Ln(\mu\text{-}Cl)_2Li(THF)_2$ was quantitatively analyzed based on the ligand solid state angle approach. In complexes of the larger early lanthanides Nd, Sm, and Gd, the guanidinate ligands can shield up to 87% of the metal, and the bidentate ligands on opposite metal centers are in an eclipsed arrangement. In complexes of lanthanides with smaller ionic radii such as Y, Yb, and Lu, the guanidinate ligands shield over 88.3% of the metal surface, and their staggered conformation is observed. The same ligand sets, that is, the guanidinate anions $[(Me_3Si)_2NC(NR)_2]^-$ with R = Pr^i and Cy, were utilized to synthesize novel guanidinate borohydride derivatives of lanthanides. For example, the heterobimetallic Ln bis(guanidinate) complexes $[(Me_3Si)_2NC(NPr^i)_2]Ln(\mu\text{-}BH_4)_2Li(THF)_2$ (Ln = Sm, Nd) were obtained according to Scheme 27 by reactions of $Ln(BH_4)_3(THF)_2$ with two equivalents of the corresponding lithium guanidinate [6, 7, 35–37].

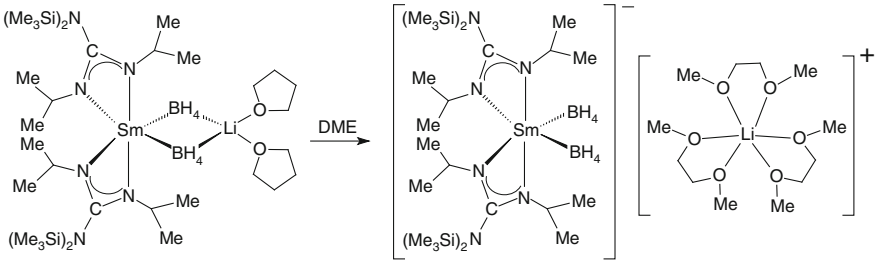

Scheme 28

Subsequent treatment of the bimetallic samarium "ate" complex $[(Me_3Si)_2NC(NPr^i)_2]Sm(\mu\text{-}BH_4)_2Li(THF)_2$, in which Sm and Li are linked by two bridging borohydride ligands, with 1,2-dimethoxyethane (DME) afforded the ionic complex $[Li(DME)_3][\{(Me_3Si)_2NC(NPr^i)_2\}_2Sm(BH_4)_2]$ (Scheme 28). A closely related series of new lanthanide borohydride complexes supported by cyclohexyl-substituted guanidinate ligands $[(Me_3Si)_2NC(NCy)_2]_2Ln(\mu\text{-}BH_4)_2Li(THF)_2$ (Ln = Nd, Sm, Yb) was synthesized by the reaction of related tris(borohydrides) $Ln(BH_4)_3(THF)_2$ with a twofold molar excess of $Li[(Me_3Si)_2NC(NCy)_2]$ in toluene at 65°C. The complexes were isolated after recrystallization from hexane in 66, 64, and 68% yield, respectively. X-ray diffraction studies revealed that all compounds are heterodimetallic complexes that have two borohydride ligands μ-bridging the lanthanide and lithium atoms [37]. The heterobimetallic "ate"-complexes $[(Me_3Si)_2NC(NCy)_2]Ln(\mu\text{-}BH_4)_2Li(THF)_2$ (Ln = Nd, Sm, Yb) were found to catalyze methyl methacrylate and lactide polymerization (cf., Sect. 4.2.1) [6, 7, 35–37].

Bulky formamidinate ligands were also successfully employed to prepare lanthanide bis(amidinates). Reaction of La metal with $Hg(C_6F_5)_2$ and bulky *N*,*N*′-bis(2,6-diisopropylphenyl)formamidine (HDippForm) in THF (Scheme 29) afforded $(DippForm)_2LaF(THF)$ with a rare terminal La–F bond. A novel functionalized formamidine, resulting from ring-opening of THF, was formed as a by-product in this reaction. More recently, these studies have been extended to other lanthanide elements such as Ce, Nd, Sm, Ho, Er, and Yb in order to gain a better understanding of the steric modulation of coordination number and reactivity in the synthesis of lanthanide(III) formamidinates [6, 7].

3.2.3 Lanthanide(III) Mono(Amidinates) and Mono(Guanidinates)

Historically, the last group of lanthanide(III) amidinates and -guanidinates to be synthesized were mono-substituted derivatives. As in cyclopentadienyl-lanthanide chemistry, saturating the coordination sphere of the large lanthanide ions using just one chelating or cyclic ligand proves the most difficult task and often requires careful ligand design. For example, a novel amidinate ligand incorporating a bulky terphenyl group was used to prepare low-coordinate yttrium mono(amidinate) complexes (Scheme 30) [6, 7].

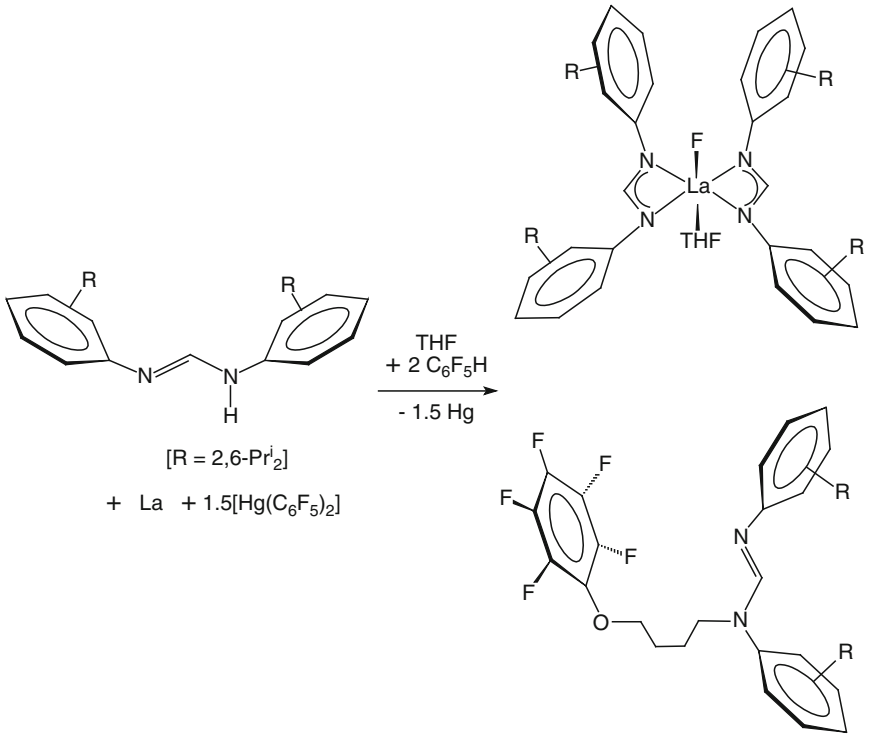

Scheme 29

Especially notable among the most recent developments in lanthanide amidinate chemistry is the successful synthesis of stable mono(amidinate) yttrium dialkyls. The synthetic strategy involved the use of the sterically hindered amidinate ligand $[Bu^tC(NPr^i)_2]^-$. The first complex was prepared by a sequential reaction of $YCl_3(THF)_{3.5}$ with $Li[Bu^tC(NPr^i)_2]$ (one equivalent) and two equivalents of $LiCH(SiMe_3)_2$ followed by pentane extraction. Large crystals of $[Bu^tC(NPr^i)_2]Y[CH(SiMe_3)_2]_2(\mu\text{-Cl})Li(THF)_3$ were isolated in 83% yield and structurally characterized by X-ray methods. Coordination of LiCl to the Y center results in a five-coordinated molecule. Such a retention of alkali metal halides which are formed during the course of reactions is a characteristic phenomenon in organolanthanide chemistry leading to the formation of so-called "ate"-complexes [6, 7]. In a systematic study it was demonstrated that, using a specially designed bulky benzamidinate ligand, it is possible to prepare mono(amidinato) dialkyl complexes over the full size range of the Group 3 and lanthanide metals, that is, from Sc to La (Fig. 4). The synthetic routes leading to the neutral and cationic bis(alkyls) are summarized in Scheme 31 [6, 7].

Mono(guanidinato) complexes of lanthanum and yttrium were synthesized as illustrated in Scheme 32 [6, 7].

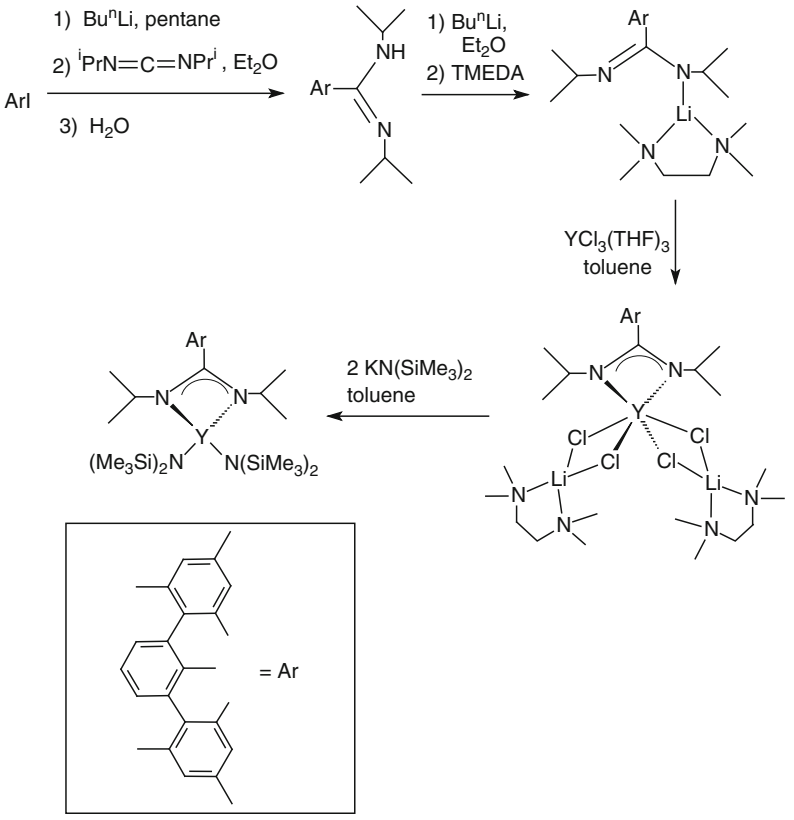

Scheme 30

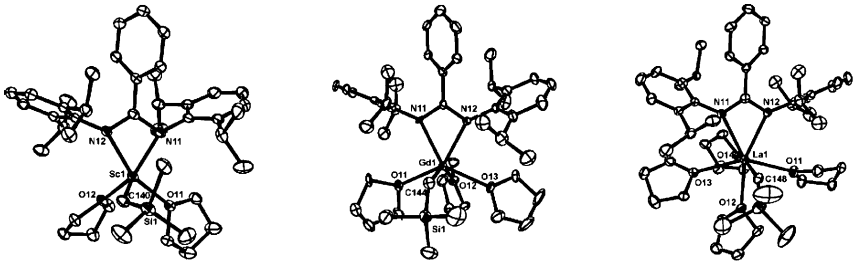

Fig. 4 Molecular structures of $[PhC(NAr)_2]Ln(CH_2SiMe_3)(THF)_n$ cations (Ln = Sc, n = 2; Ln = Gd, n = 3, Ln = La, n = 4)

The La compounds were made starting from $La[N(SiMe_3)_2]_3$ and dicyclohexylcarbodiimide, CyN=C=NCy. Both mono(guanidinate) derivatives are monomeric in the solid state with a four-coordinate La center. In the case of yttrium, it was recently reported that even the less bulky guanidinate ligand $[(Me_3Si)_2NC(NPr^i)_2]^-$ stabilizes mono(guanidinato) complexes. Closely related mono(guanidinato) lanthanide

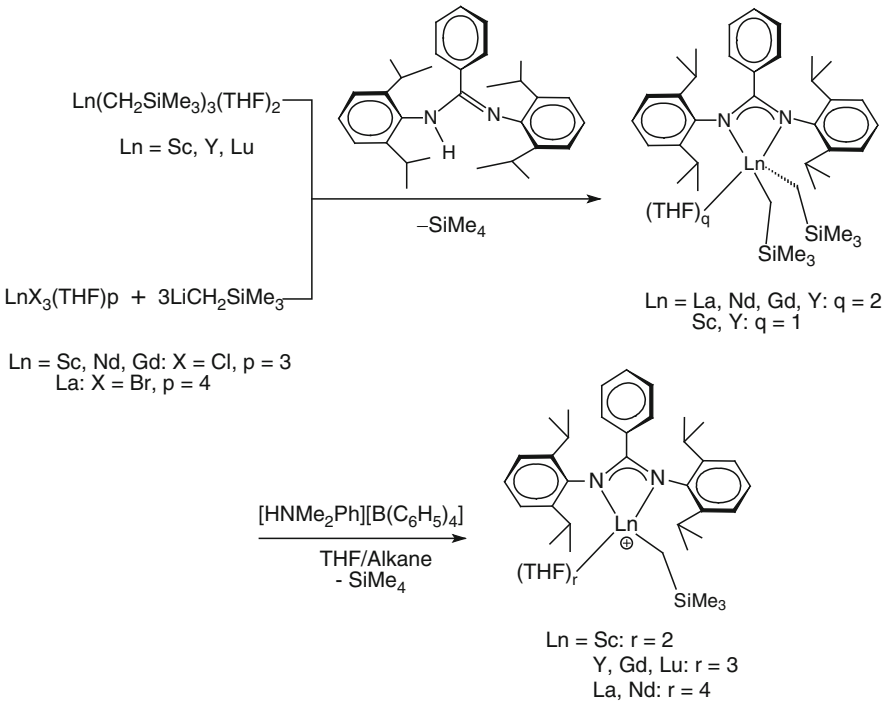

Scheme 31

borohydride complexes of the type $[(Me_3Si)_2NC(NCy)_2]Ln(BH_4)_2(THF)_2$ (Ln = Nd, Sm, Gd, Er, Yb) were prepared by reactions of the corresponding borohydrides $Ln(BH_4)_3(THF)_3$ with the sodium guanidinate $Na[(Me_3Si)_2NC(NCy)_2]$. Scheme 33 illustrates the synthetic route leading to the Gd derivative which was crystallized as an adduct with 1,2-dimethoxyethane (DME) [6, 7, 38].

Bis(phenolate) ligands are present in the lanthanide guanidinate complexes shown in Scheme 34, which were prepared by insertion of *N,N′*-diisopropylcarbodiimide into the Ln–N bonds of appropriate neutral lanthanide amide precursors [6, 7].

Brightly colored mono(benzamidinato) cyclooctatetraenyl lanthanide(III) complexes were prepared by treatment of either $[(C_8H_8)Ln(\mu\text{-}Cl)(THF)_2]_2$ or $[(C_8H_8)Ln(\mu\text{-}O_3SCF_3)(THF)_2]_2$ with $Na[RC_6H_4C(NSiMe_3)_2]$ (R = H, OMe, CF_3) (Schemes 35 and 36). According to X-ray structural analyses of $[PhC(NSiMe_3)_2]Tm(C_8H_8)(THF)$ and $[MeOC_6H_4C(NSiMe_3)_2]Lu(C_8H_8)(THF)$ these compounds are monomeric in the solid state [6, 7, 11].

Insertion of carbodiimides into the Ln–C σ-bond of organolanthanide complexes was also reported to provide a straightforward access to organolanthanide amidinates and guanidinates. The complexes $Cp_2Ln[Bu^nC(NBu^t)_2]$ (Ln = Y, Gd, Er) were prepared this way from Cp_2LnBu^n and *N,N′*-di-*tert*-butylcarbodiimide. The analogous insertion of carbodiimides into Ln–N bonds has been shown to be an effective way of making lanthanide guanidinate

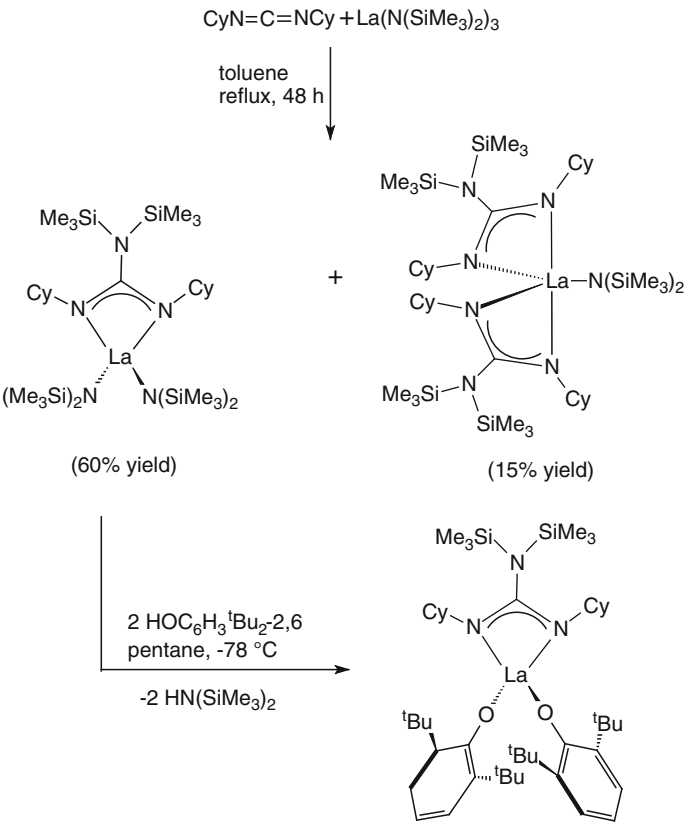

Scheme 32

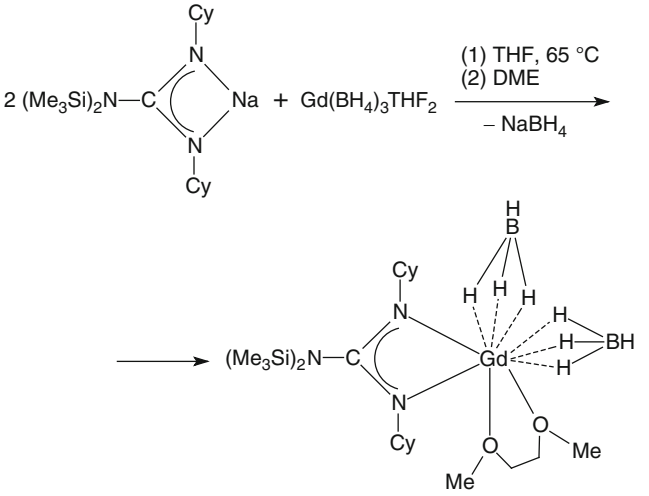

Scheme 33

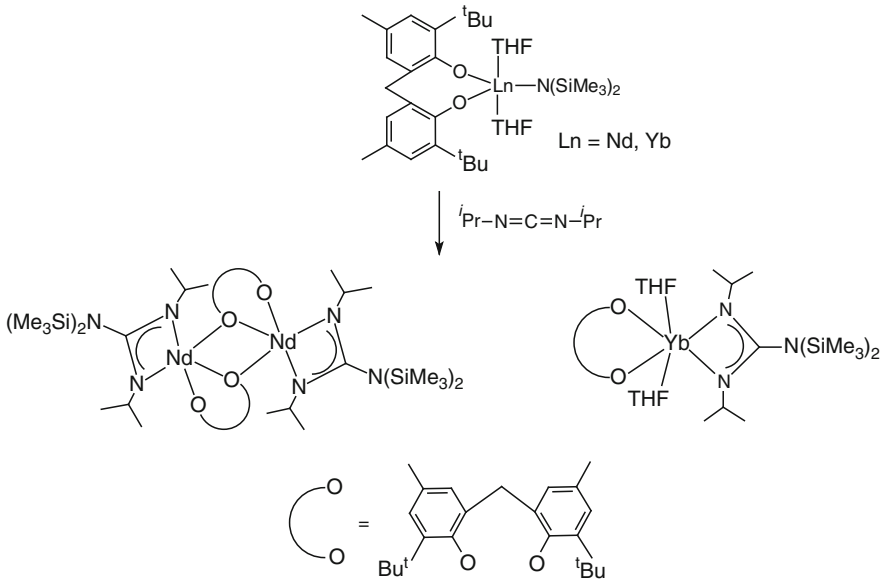

Scheme 34

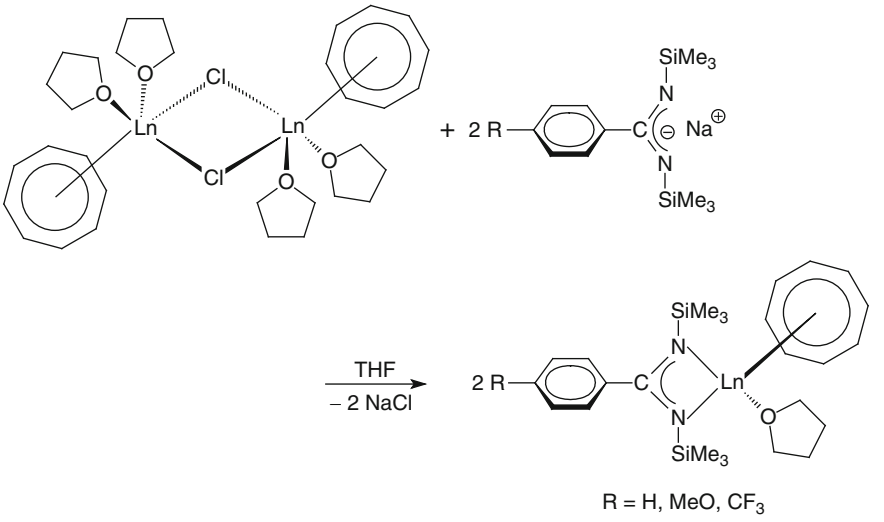

Scheme 35

complexes. For example, insertion of *N,N′*-dicyclohexylcarbodiimide into one of the Y–N bonds of $Y[N(SiMe_3)_2]_3$ afforded the monoguanidinate diamide derivative $[(Me_3Si)_2NC(NCy)_2]Y[N(SiMe_3)_2]_2$. Complexes of the type $Cp_2Ln[Pr^i_2NC(NPr^i)_2]$ (Ln = Y, Gd, Dy, Yb) have been prepared analogously [6, 7, 39, 40]. Scheme 37 illustrates the reaction sequence leading to such metallocene derivatives. [39, 40].

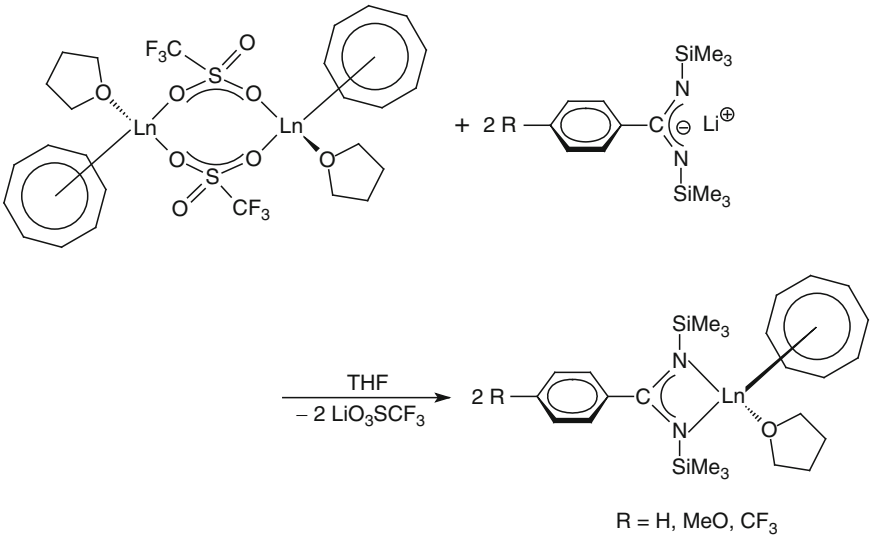

Scheme 36

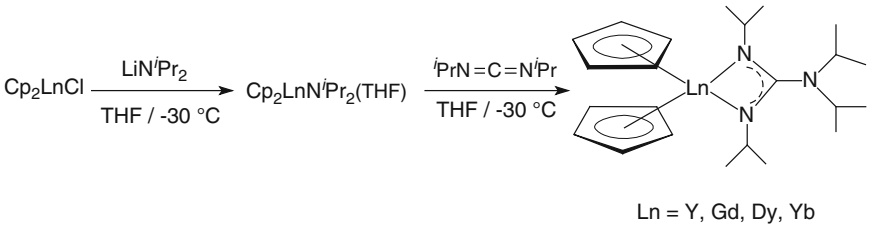

Scheme 37

The related reaction of $CpYCl_2(THF)_3$ with $LiNPr^i_2$ and subsequently with two equivalents of *N,N′*-diisopropylcarbodiimide ($Pr^iN{=}C{=}NPr^i$) in THF gave the organoyttrium guanidinates $[Pr^i_2NC(NPr^i)_2]_3Y$ and $Cp_2Y[Pr^i_2NC(NPr^i)_2]$, which may be rationalized by the rearrangement reaction of the di-insertion product $CpY[Pr^i_2NC(NPr^i)_2]_2$. Treatment of $Pr^iN{=}C{=}NPr^i$ with dimeric lanthanocene primary amides $[Cp_2LnNHR]_2$ (R = Bu^t, Ln = Yb, Er, Dy, Y; R = Ph, Ln = Yb) gave the unexpected products $Cp_2Yb[RNC(NHPr^i)NPr^i]$ (R = Bu^t, Ln = Yb, Er, Dy, Y; R = Ph, Ln = Yb), indicating that a novel isomerization reaction involving a 1,3-hydrogen shift had taken place along with the insertion of carbodiimide into the Ln–N σ-bond (Scheme 38), which provides an efficient synthesis of organolanthanide complexes with asymmetrical guanidinate ligands [40].

In the course of a closely related study, a series of new functionalized amido complexes of ytterbium, $[Cp_2YbNHR]_2$ (R = 8-quinolyl (Qu), 2-pyridyl (Py), 2-aminophenyl, 3-amino-2-pyridyl, and $Cp_2Yb[NHC_6H_4(CH_2NH_2{-}2)]$, have been synthesized by metathesis of Cp_2YbCl and the corresponding amido lithium salts. Their reactivity toward carbodiimides has been investigated, in which multiple N–H

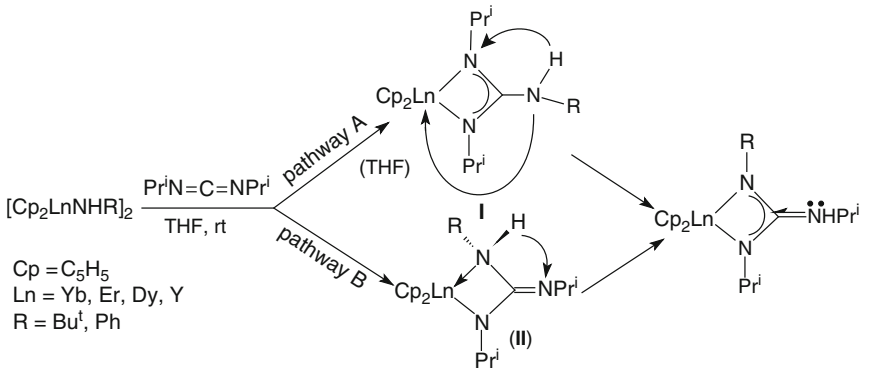

Scheme 38

activation behavior for metal-bound neutral NH_2 and anionic nitrogen-containing fragments, a property that is expressed without dissociation from the lanthanide center, was observed. These results provided an alternative mechanistic insight for the metal-mediated mono- and diguanylation of primary amines and elucidate factors that affect the chemo- and regioselectivities of the addition and protonation steps. Reaction of the 8-quinolyl derivative with two equivalents of RN=C=NR[R = cyclohexyl (Cy), isopropyl (Pr^i)] led to the formal insertion of carbodiimide into the N–H bond of the Yb-bonded amido group to yield $Cp_2Yb[\eta^1:\eta^2\text{-RNC(NHR)NQu}]_2$ (R = Cy, Pr^i). Interestingly, treatment of the 2-pyridyl derivative with RN=C=NR afforded the unexpected products $(Cp_2Yb)_2[\mu\text{–}\eta^2:\eta^2\text{–PyNC(NR)}_2](THF)$(R = Cy, Pr^i), representing the first example of dianionic guanidinate lanthanide complexes. The reaction of the 2-aminophenyl complex with two equivalents of RN=C=NR in THF at room temperature led to the isolation of the single N–H addition products $Cp_2Yb[\eta^1:\eta^2\text{–RNC(NHR)NC}_6H_4NH_2\text{–}2](R = Cy, Pr^i)$ in fairly good yields, while treatment of the same precursor with four equivalents of RN=C=NR under the same conditions gave the double N–H addition products $Cp_2Yb[\eta^1:\eta^2\text{–RNC(NHR)NC}_6H_4\{NC(NHR)_2\text{–}2\}]$ (Scheme 39; R = Cy, Pr^i), via the intraligand proton transfer from chelating NH_2 to the guanidinate group of $Cp_2Yb[\eta^1:\eta^2\text{–RNC(NHR)NC}_6H_4NH_2\text{–}2]$ to give new amido intermediates, followed by a second RN=C=NR insertion into the N–H bond of the resulting amido groups. The complexes $Cp_2Yb[\eta^1:\eta^2\text{–RNC(NHR)NC}_6H_4\{NC(NHR)_2\text{–}2\}]$ can also be obtained by reaction of $Cp_2Yb[\eta^1:\eta^2\text{–RNC(NHR)NC}_6H_4NH_2\text{–}2]$ with one equivalent of RN=C=NR [41].

The double-addition product $Cp_2Yb[\eta^1:\eta^2\text{–CyNC(NHCy)NC}_5H_3N\{NC(NHCy)_2\text{–}3\}]$ could be obtained as red crystals from the 1:4 reaction according to Scheme 40 between $[Cp_2YbNHR]_2$ (R = 3-amino-2-pyridyl) and CyN=C=NCy in 63% yield. Interestingly, this compound can be converted into $(Cp_2Yb)_2[\eta^2:\eta^3\text{–(CyN)}_2CNC_5H_3N\{NC(NHCy)_2\text{–}3\}]$ under reflux in THF and with liberation of a neutral diguanidine, $C_5H_3N(NC(NHCy)_2)$-2,3 (Scheme 40). A preference of the proton transfer to the second carbodiimide insertion into the N–H bond in the formation of $Cp_2Yb[\eta^1:\eta^2\text{–RNC(NHR)NC}_6H_4\{NC(NHR)_2\text{–}2\}]$

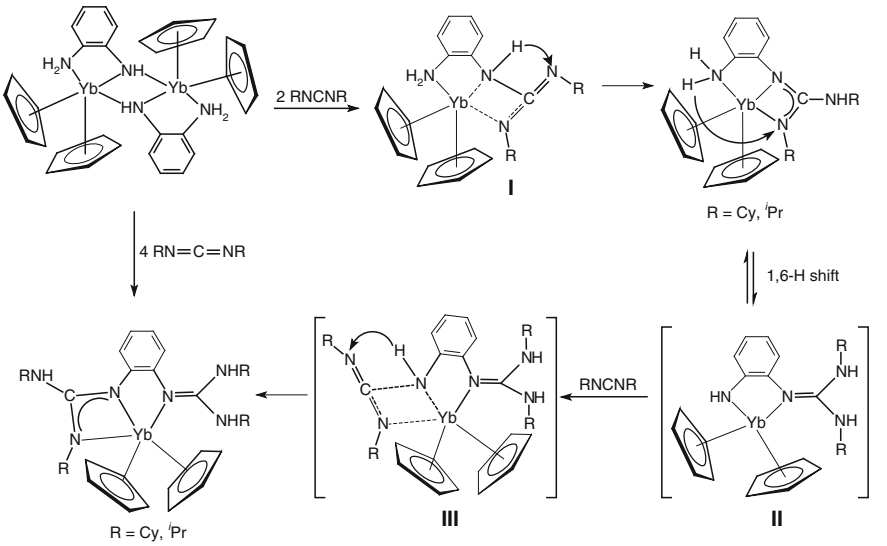

Scheme 39

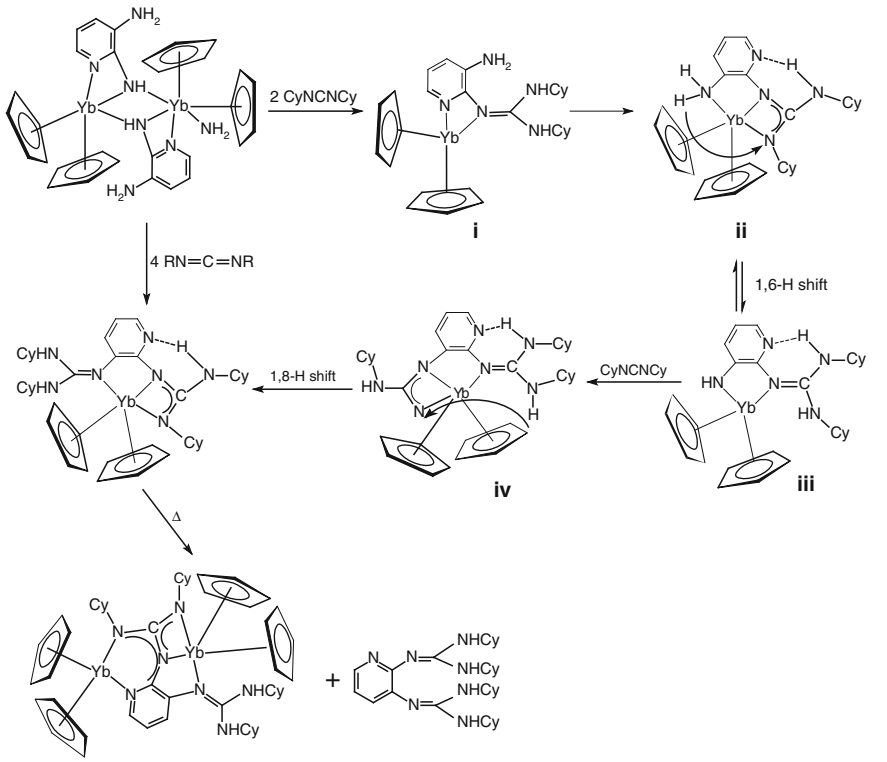

Scheme 40

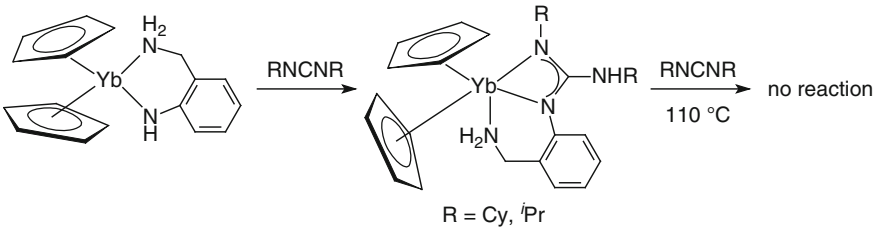

Scheme 41

Scheme 42

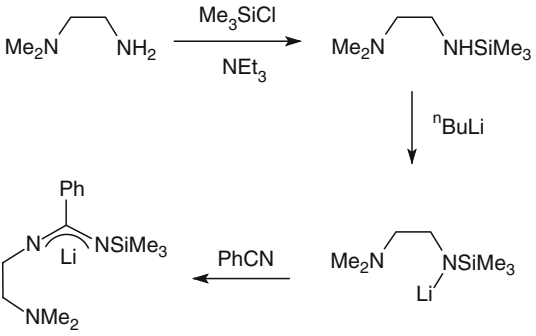

and $Cp_2Yb[\eta^1{:}\eta^2$–CyNC(NHCy)$NC_5H_3N\{NC(NHCy)_2$–3$\}]$ has been confirmed by the fact that treatment of weaker acidic $Cp_2Yb[NHC_6H_4(CH_2NH_2$–2$)]$ with an excess of carbodiimides in THF/toluene, even with prolonged heating, provided only the monoaddition products $Cp_2Yb[\eta^2{:}\eta^1$–RNC(NHR)$NC_6H_4(CH_2NH_2$–2$)]$ (R = Cy, Pr^i) (Scheme 41) [41].

3.2.4 Lanthanide(III) Complexes Containing Functionalized Amidinate Ligands

Pendant-Arm Type Amidinate Ligands

In order to further explore the amidinate/cyclopentadienyl analogy, various amino-functionalized amidinate ligands have been synthesized with the aim of mimicking the well-known pendant-arm half-metallocene catalysts. For example, benzamidinate ligands incorporating a pendant amine functional group were prepared as shown in Scheme 42. Instead of using Me_3SiCl/NEt_3 in the first step, the starting amine can also be converted into the monosilylated derivative by successive reaction with Bu^nLi followed by treatment with Me_3SiCl [6, 7]. Exactly the same synthetic pathway was followed to prepare the corresponding ligand containing a pendant 3-dimethylaminopropyl functionality [42].

Reactions of $Li[Me_3SiNC(Ph)N(CH_2)_3NMe_2]$ (=LiL) with $LnCl_3$ in appropriate stoichiometry led to the dinuclear $[(L)_2Ln(\mu\text{-}Cl)]_2$ (Ln = La, Ce) complexes.

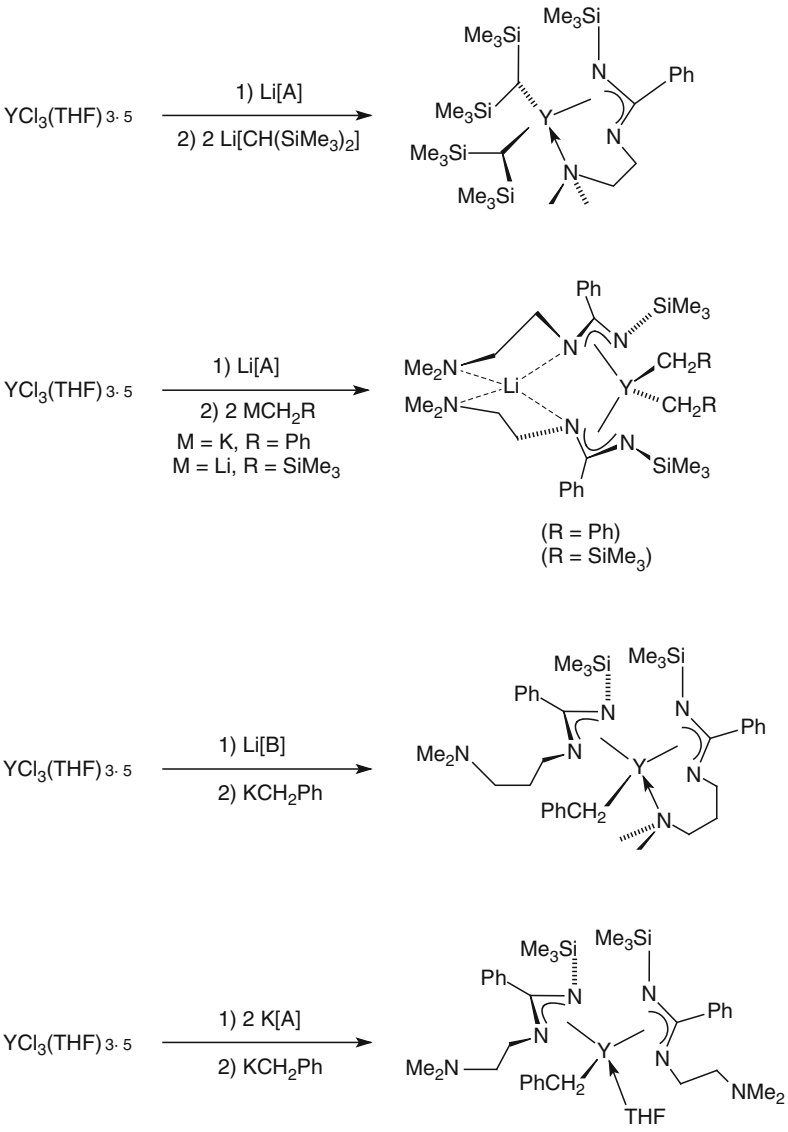

Scheme 43

The potentially tridentate ligands $[Me_3SiNC(Ph)N(CH_2)_nNMe_2]^-$ (Scheme 43, $n = 2$: **A**, $n = 3$: **B**) have also been employed in the synthesis of yttrium alkyl and benzyl complexes [6, 7, 42].

While the dialkyl complexes $[Me_3SiNC(Ph)N(CH_2)_nNMe_2]Y[CH(SiMe_3)_2]_2$ could be isolated salt-free, attempts to prepare analogous benzyl or trimethylsilylmethyl complexes with ligand **A** yielded the ate-complexes $Li[Me_3SiNC(Ph)N(CH_2)_2NMe_2]YR_2$ (R=CH_2Ph, CH_2SiMe_3) in which the Li ion is encapsulated

by two amidinate and two amine nitrogens. The increased spacer length between the amidinate and amine functionalities in ligand **B** prevented encapsulation of the Li ion, but still produced a bis(amidinate) yttrium benzyl complex, $[Me_3SiNC(Ph)N(CH_2)_3NMe_2]_2YCH_2Ph$. In this compound only one of the two NMe_2 functionalities is coordinated to the metal center [6, 7].

Bis(Amidinate) Ligands

Yet another interesting variation of the amidinate theme is the design and use of bis(amidinate) ligands. This can, for example, involve the reductive dimerization of carbodiimides to give oxalamidinate ligands of the type $[C_2N_4R_4]^{2-}$. In the case of lanthanides, the reductive coupling of carbodiimides was achieved with the use of samarium(II) bis(trimethylsilyl)amides. The reaction of $Sm[N(SiMe_3)_2]_2(THF)_2$ with carbodiimides RN=C=NR (R=Cy, $C_6H_3Pr^i_2$–2,6) led to formation of dinuclear Sm(III) complexes. For R=Cy (Scheme 44), the product has an oxalamidinate $[C_2N_4Cy_4]^{2-}$ ligand resulting from coupling of two CyN=C=NCy moieties at the central C atoms. The same product was obtained when the Sm(II) "ate" complex $Na[Sm\{N(SiMe_3)_2\}_3]$ was used as divalent Sm precursor [6, 7].

The dilithium salt of a linked bis(amidinate) dianionic ligand, $Li_2[Me_3SiNC(Ph)N(CH_2)_3NC(Ph)NSiMe_3]$ (=Li_2L) was prepared by reaction of dilithiated *N,N′*-bis(trimethylsilyl)-1,3-diaminopropane with benzonitrile (Scheme 45) [6, 7].

Reaction of the dilithium salt of the linked bis(amidinate) dianionic ligand $[Me_3SiNC(Ph)N(CH_2)_3NC(Ph)NSiMe_3]^{2-}$ (=Li_2L) with $YCl_3(THF)_{3.5}$ gave $[Me_3SiNC(Ph)N(CH_2)_3NC(Ph)NSiMe_3]YCl(THF)_2$, which, by reaction with $LiCH(SiMe_3)_2$, was converted to an alkyl complex (Scheme 46). A structure determination of this compound (Fig. 5) showed that linking together the amidinate functionalities opens up the coordination sphere to allow for the bonding of an

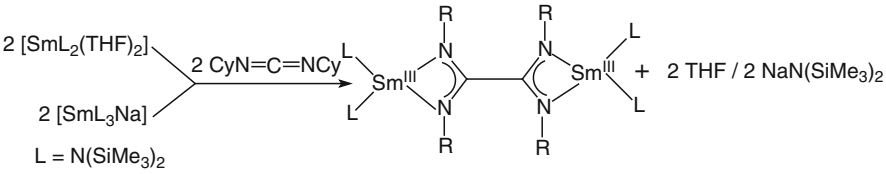

Scheme 44

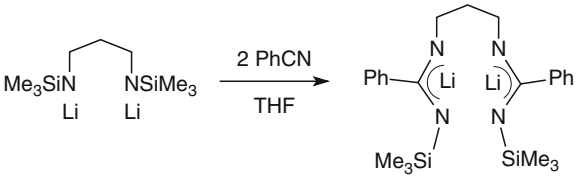

Scheme 45

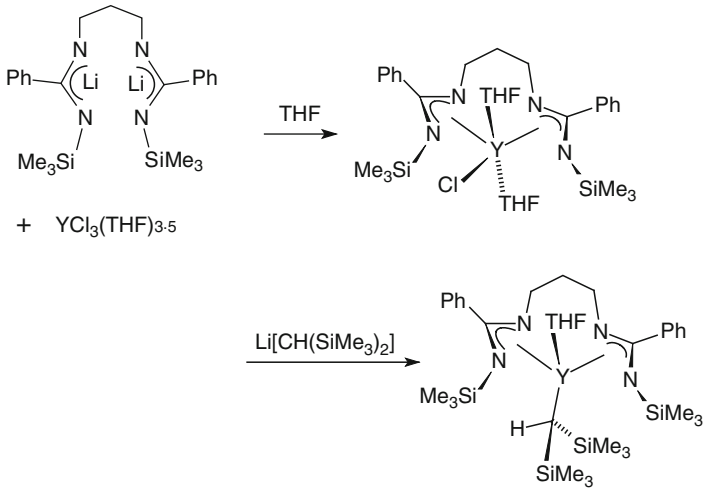

Scheme 46

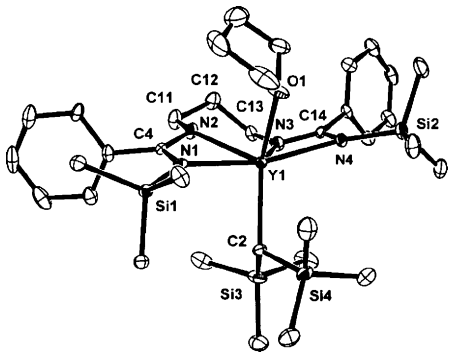

Fig. 5 Molecular structure of $[Me_3SiNC(Ph)N(CH_2)_3NC(Ph)NSiMe_3]Y[CH(SiMe_3)_2](THF)$

additional molecule of THF not present in the unbridged bis(amidinate) analog $[PhC(NSiMe_3)_2]_2Y[CH(SiMe_3)_2]$ [6, 7].

Analogous reaction of $Li_2[Me_3SiNC(Ph)N(CH_2)_3NC(Ph)NSiMe_3]$ ($=Li_2L$) with $YbCl_3$ afforded the linked bis(amidinato) ytterbium chloride $LYb(\mu\text{-}Cl)_2YbL(THF)$. The chloro-bridges in this compound are easily cleaved upon treatment with THF. Further reaction of the resulting monomeric chloro complex with NaCp in DME gave LYbCp(DME) in high yield (Scheme 47, Cp = η^5-cyclopentadienyl) [6, 7, 43].

In an extension of this work, the steric effect of an amide group on the synthesis, molecular structures, and reactivity of ytterbium amides supported by the linked bis(amidinate) ligand was investigated. Reactions of the chloro precursor with sodium arylamides afforded the corresponding monometallic amide complexes in which the linked bis(amidinate) is coordinated to the ytterbium center as a chelating ligand (Scheme 48). In contrast, the reaction with $NaN(SiMe_3)_2$ gave a

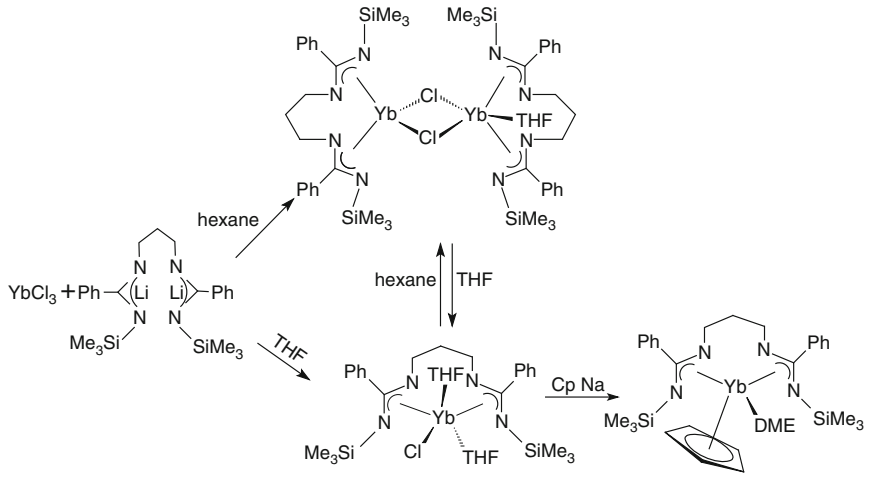

Scheme 47

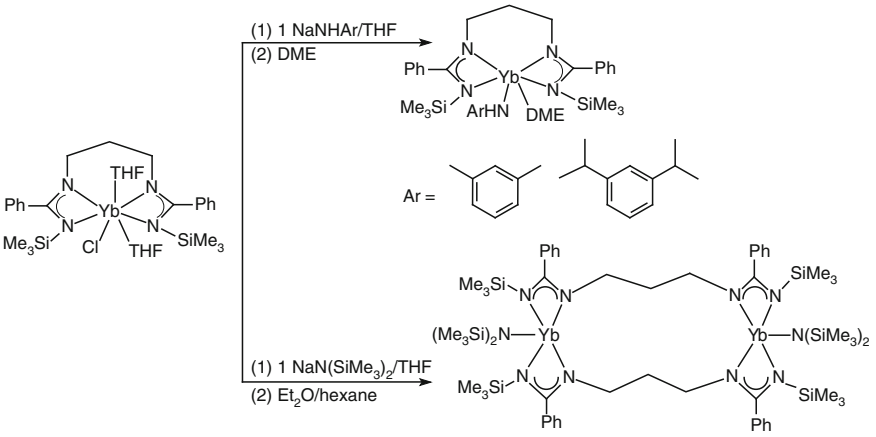

Scheme 48

bimetallic amide complex in which two linked bis(amidinates) act as bridging ancillary ligands connecting two $YbN(SiMe_3)_2$ fragments in one molecule [6, 7, 43].

3.3 Lanthanide(IV) Amidinates

Most recently, it was discovered in our laboratory that benzamidinate ligands are also capable of stabilizing novel cerium(IV) species. Thus, they belong to the limited number of organic ligands which allow the stabilization of lanthanide complexes in all possible oxidation states (+2, +3, and +4). In analogy to the reaction shown in Scheme 10, treatment of anhydrous cerium(III) trichloride with

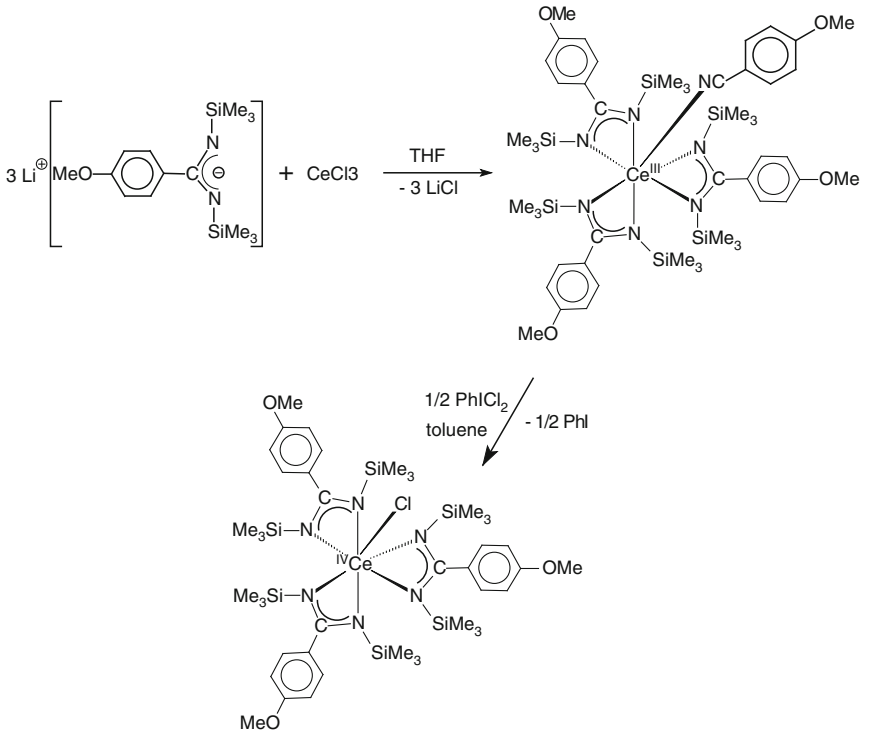

Scheme 49

three equivalents of the lithium amidinate precursor Li[*p*-$MeOC_6H_4C(NSiNe_3)_2$] first afforded the bright yellow *p*-anisonitrile adduct of the homoleptic cerium(III) amidinate (Scheme 49). Oxidation to the corresponding cerium(IV) amidinate [$p-MeOC_6H_4C(NSiMe_3)_2]_3CeCl$ was readily achieved using the reagent phenyliodine(III) dichloride. The advantage of this method is that iodobenzene is formed as the only by-product. This way the almost black cerium(IV) species could be isolated by simple crystallization directly from the concentrated reaction mixture. A single-crystal X-ray analyses clearly established the presence of the first amidinate complex of tetravalent cerium (Fig. 6) [6, 7].

4 Lanthanide Amidinates and Guanidinates in Homogeneous Catalysis

At the time when the first lanthanide amidinate were reported in the early 1990s, these compounds appeared to be just laboratory curiosities for which nobody could envisage any practical uses. This situation changed completely when in 2002 it was discovered that homoleptic lanthanide tris(amidinate) complexes show extremely

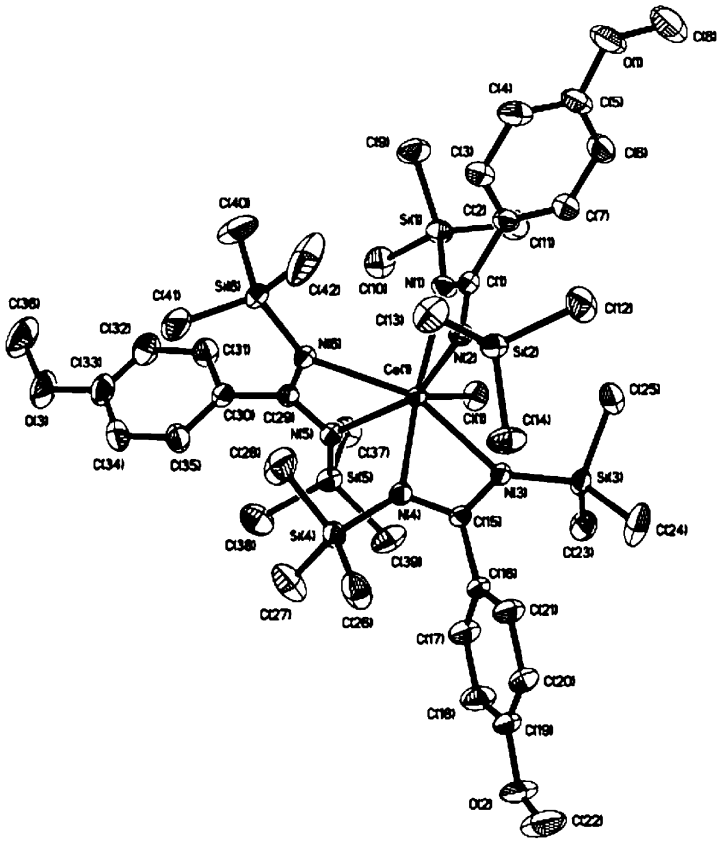

Fig. 6 Molecular structure of $[p\text{-}MeOC_6H_4C(NSiMe_3)_2]_3CeCl$ [6, 7]

high activity for the ROP of CL at room temperature [44]. This was the first time that promising catalytic activity was found for lanthanide amidinates and it stimulated further work in the field. Certain aspects of catalytic applications of lanthanide amidinate complexes have already been summarized in review articles [6, 7, 13, 45].

4.1 Olefin Polymerization Reactions Catalyzed by Lanthanide Amidinates and Guanidinates

The use of amidinato catalyst systems for the polymerization of olefins has first been reported in a patent application by us in cooperation with BASF company [6, 7, 46]. Since then various other patents dealing with the use of amidinato metal complexes as catalysts for olefin polymerizations have appeared. However, the main focus of these studies was on the use of group 4 metal amidinates as these have been found

to exhibit very promising activities as homogeneous polymerization catalysts. This area has recently been compiled in an excellent review article by Eisen et al. [47].

It took several more years until lanthanide amidinates and guanidinates successfully entered catalysis research and proved to be effective catalysts especially for polymerization reactions. The majority of the work published thus far involves the polymerization of polar monomers such as CL, D,L-lactide or methylmethacrylate (MMA) (cf., Sect. 4.2), but promising results have also been achieved with simple olefins. For example, the dimeric bis(guanidinato) lutetium hydride complex $[\{(Me_3Si)_2NC(NPr^i)_2\}_2Lu(\mu\text{-}H)]_2$ was found to catalyze the polymerization of ethylene, propylene, and styrene [33]. Moderate activity in ethylene polymerization was observed with the mono(guanidinato) yttrium dialkyl $[(Me_3Si)_2NC(NPr^i)_2]Y(CH_2SiMe_3)_2(THF)_2$ [6, 7]. More recently the catalytic activity of the $[\{(Me_3Si)_2NC(NPr^i)_2\}_2Ln(\mu\text{-}H)]_2$ complexes shown in Scheme 25 in the polymerization of ethylene, propylene, and styrene has been investigated in a systematic manner. The ethylene polymerization activity of the samarium hydrido complex, 1,268 g mmol^{-1} atm^{-1} h^{-1} was the highest among the tested compounds. By the end of 1 day the complex was still active without loss of the reaction rate. In the case of the yttrium derivative the polymerization process was less rapid (442 g mmol^{-1} atm^{-1} h^{-1}) and the catalyst did not demonstrate loss of the reaction rate during 3 days. Unexpectedly, the neodymium complex had very low activity as a catalyst for the polymerization of ethylene, and after 1 h the reaction stopped. Complexes of gadolinium, ytterbium, and lutetium showed modest catalytic activities (281, 77, and 76 g mmol^{-1} atm^{-1} h^{-1}, respectively). A stoichiometric reaction of the yttrium derivative with ethylene in [D_6]benzene at room temperature under ^{1}H NMR spectroscopic control did not afford an insertion product $[(Me_3Si)_2NC(NPr^i)_2]_2Y(CH_2CH_3)$, but resulted in rapid polyethylene formation [34].

Most of the lanthanide complexes that readily polymerize ethylene are inactive in propylene polymerization [48]. Thus, the complexes $[\{(Me_3Si)_2NC(NPr^i)_2\}_2Ln(\mu\text{-}H)]_2$ (Scheme 25) were also tested in catalysis of propylene and styrene polymerization. The yttrium derivative had low activity in propylene polymerization. Over a period of 2 h the monomer absorption reached 58 mol per mole of catalyst, whereupon the catalytic activity was lost. Complexes with Ln = La, Sm, Dd, and Yb were even less active and became inactive after 15–20 min. In styrene polymerization, only derivatives of smallest lanthanide metals showed catalytic activity. The Lu complex initiated polymerization of styrene (20°C, neat styrene, 5% of Lu complex), and 90% conversion was reached in 6 days. The polystyrene obtained had a high molecular weight (M_n = 811,000 g mol^{-1}, M_w = 1250,000 g mol^{-1}), a narrow molecular-weight distribution (M_w/M_n = 1.54), and a melting temperature of 255–260°C. In the case of Ln = Yb (20°C, neat styrene, 1 mol% of Yb complex, total conversion in 3 days) the obtained polymer had a higher molecular-weight distribution M_w/M_n = 2.6 (M_n = 90,000 g mol^{-1}, M_w = 237,700 g mol^{-1}; melting temperature 289–293°C). The ^{13}C NMR spectra of both polystyrenes indicated their high syndiotacticity [34].

The mono(amidinato) lanthanide alkyls shown in Scheme 31 allowed a comparison of the catalytic performance of cationic group 3 metal and lanthanide alkyls in catalytic ethylene polymerization over the full ion size range of these metals. Ethylene polymerization experiments were performed using the metal dialkyl precursors in combination with the Brønsted activator $[Ph_2NMe_2H][B(C_6F_5)_4]$ and excess isobutyl alumoxane (TIBAO) scavenger. It was found that the catalytic activity of the intermediate cationic alkyl species varies by over 2 orders of magnitude with the size of the metal ion. Thus, the availability of such a large series of homologous precatalysts allows a unique tunability of the catalytic activity [49, 50].

4.2 Polymerization of Polar Monomers Catalyzed by Lanthanide Amidinates and Guanidinates

The strength of lanthanide amidinate and guanidinate complexes in catalysis certainly lies in the field of polymerization reactions of polar monomers. These include acrylic monomers such as MMA and acrylonitrile (AN), but ROP of cyclic esters (β-butyrolactone, CL, lactide, TMC) are also effectively catalyzed by lanthanide amidinates and guanidinates. ROP of cyclic esters promoted by metal initiators have been proven to be the most efficient manner for preparing polyesters with controlled molecular weight and microstructure and narrow molecular-weight distribution. The resulting aliphatic polyesters currently attract growing interest as a promising alternative to synthetic petrochemical-based polymers, since the starting materials for their synthesis can be derived from annually renewable resources. The mechanical and physical properties of polyesters, together with their biodegradable and biocompatible nature, make them perspective thermoplastics with broad commercial applications (e.g., single-use packaging materials, medical sutures, and drug delivery systems) [51–54].

4.2.1 Methylmethacrylate, Acrylonitrile

Thus far, the catalytic polymerization of acrylic monomers such as MMA or AN has mainly been achieved with the use of certain lanthanide mono- and bis(guanidinate) complexes, especially the borohydride derivatives. For example, the mono(guanidinate) lanthanide bis(borohydrides) $[(Me_3Si)_2NC(NCy)_2]Ln(BH_4)_2(THF)_2$ (Ln = Er, Yb) (cf., Scheme 33) were found to display moderate to high catalytic activity for the polymerization of MMA [38]. Both catalysts afforded poly(methylmethacrylate) (PMMA) under mild conditions, with the Er complex being more active than the Yb complex. It is noteworthy that homoleptic guanidinate complexes are completely inert to this polymerization. This demonstrates that the presence of BH_4 groups in the catalyst is crucial for the polymerization. The effect of temperature on polymerization was found to be great. As the temperature increased, the polymerization activity decreased and the molecular weight of PMMA

decreased too. The lower catalytic activity and molecular weight at higher reaction temperatures is due to more facile catalyst deactivation processes at higher temperatures (e.g., backbiting), which is normally found in MMA-polymerization catalyzed by organolanthanide complexes [55, 56]. The reactive lanthanide bis(guanidinate) borohydride derivatives $[(Me_3Si)_2NC(NPr^i)_2]_2Ln(\mu\text{-}BH_4)_2Li(THF)_2$ (Scheme 27, Ln = Nd, Sm) were also reported to be efficient catalysts for the polymerization of MMA [35, 36]. The catalytic activity of the Nd and Sm complexes in polymerization of MMA was studied at room temperature both in a block and in toluene solution. After the addition of the solid complexes (0.2 mol%) to MMA, vigorous exothermic polymerization started. After 10–15 min, the reaction mixture solidified. However, the degree of conversion was at most 50% even after 48 h. Hence, all catalytic experiments were carried out in toluene solution ($C_{MMA} = 4.61\,mol\,L^{-1}$, $C_{cat} = 9.2 \times 10^{-3}\,mol\,L^{-1}$, C_{cat}:C_{MMA} = 1:500). In the reaction with the Sm complex, a degree of conversion of 77% was achieved within 3 h. The resulting polymer had an average molecular weight M_w = 199,900, M_n = 20,100, and a rather high polydispersity index ($M_w/M_n = 9.95$). NMR experiments showed that a heterotactic polymer was formed, with syndiotactic triads slightly predominating. In the presence of the Nd complex, polymerization under analogous conditions proceeded slightly more slowly, and the degree of conversion was 52% after 3 h. The resulting polymer was characterized by a substantially lower molecular weight and a narrower molecular-weight distribution (M_w = 21,400, M_n = 8,500, M_w/M_n = 2.52). The polymer could also be characterized as heterotactic but with a predominance of isotactic triads. Based on the initial region of the kinetic curve of polymerization measured by the dilatometric method (up to the degree of conversion of 20%), the Sm complex exhibited higher activity as compared to the Nd analog [35, 36].

The methyl bridged "ate" complexes $[(Me_3Si)_2NC(NPr^i)_2]_2Ln(\mu\text{-}Me)_2Li(THF)_2$ (Ln = Nd, Yb) (cf., Sect. 3.2.2) were also found to exhibit good catalytic activity for the polymerization of methyl methacrylate [57]. Triad microstructural analysis of the polymers was carried out using ^1H NMR spectra in $CDCl_3$. The catalytic activity increased with increasing polymerization temperature. For example, only a 10% yield was obtained at −78°C, while at 40°C a yield of 82% could be realized. Moreover, this polymerization system gave syndio-rich polymers, and the syndiotacticity decreased with increasing polymerization temperature [57]. The guanidinate lanthanide borohydrides $[Ph_2NC(NCy)_2]Ln(BH_4)_2$ (Ln = Er, Yb), $[(Me_3Si)_2NC(NCy)_2]Ln(BH_4)_2$ (Ln = Er, Yb) and $[(Me_3Si)_2NC(NCy)_2]_2LnBH_4$ (Ln = Er, Yb) have been synthesized and their catalytic performance in the polymerization of MMA studied. It was discovered that the greater the electron donating ability of the guanidinate ligand is, the higher the activity of the corresponding complex becomes. Moreover, it was found that the complexes $[Ph_2NC(NCy)_2]Ln(BH_4)_2$ (Ln = Er, Yb) catalyze the polymerization of AN. Till, this is the first example of AN-polymerization catalyzed by guanidinate lanthanide borohydrides [58].

4.2.2 ROP of Cyclic Esters

As mentioned above, the strength of lanthanide amidinate and guanidinate catalysts lies in the polymerization of polar monomers. ROP of cyclic esters catalyzed by lanthanide amidinates and guanidinates provides an efficient access to polyesters with controlled molecular weight and microstructure as well as narrow molecular-weight distribution. The resulting aliphatic polyesters are attractive biodegradable and biocompatible thermoplastics which are of great current interest, for example, as single-use packaging materials, for use as medical sutures and for drug delivery systems [51–54]. Monomers, which are effectively polymerized in the presence of lanthanide amidinates and/or guanidinates include CL, β-butyrolactone, D,L-lactide, L-lactide, and TMC.

Most of the work in this area has been done with CL as monomer. Metal amidinates and guanidinates, for which high activity in the polymerization of polar monomers such as CL, lactide, and MMA have been reported, include the homoleptic lanthanide amidinates $Ln[RC(NCy)_2]_3(THF)_n$ (R = Me, Ln = Nd, Gd, Yb, $n = 0$; R = Ph, Ln = Y, Nd, Yb, $n = 2$) [35, 36] and the bis(guanidinato) lanthanide amides $[(Me_3Si)_2NC(NPr^i)_2]_2LnN(Pr^i)_2$ (Ln = Y, Nd). The neodymium compound $[MeC(NCy)_2]_3Nd$ was studied by Ephritikhine et al. [59] and compared to the catalytic activity of its uranium(III) counterpart, $[MeC(NCy)_2]_3U$. The Nd complex showed extremely high activity in the ROP of CL. In the presence of 0.5% mol-equivalents of $[MeC(NCy)_2]_3Nd$ in toluene, polymerization of CL was achieved in less than 2 min, giving a viscous gel of poly(ε-caprolactone). It was found that the uranium(III) complex was much less efficient because of its rapid oxidation into U(IV) species [59].

Promising results with respect to the ROP of CL have also been reported for homoleptic lanthanide(III) tris(guanidinates) and lanthanide bis(guanidinate) derivatives [6, 57, 60]. A series of homoleptic lanthanide guanidinates (Scheme 50) was reported to exhibit extremely high activity for the ROP of CL [60].

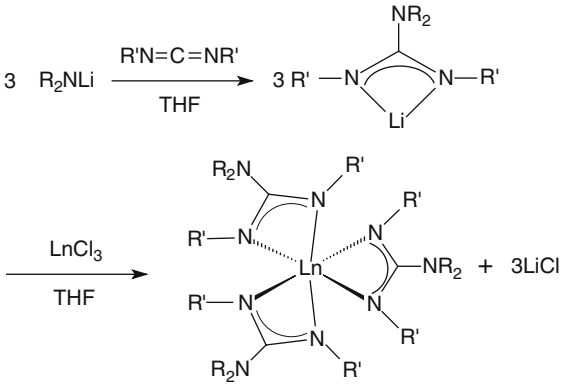

Scheme 50

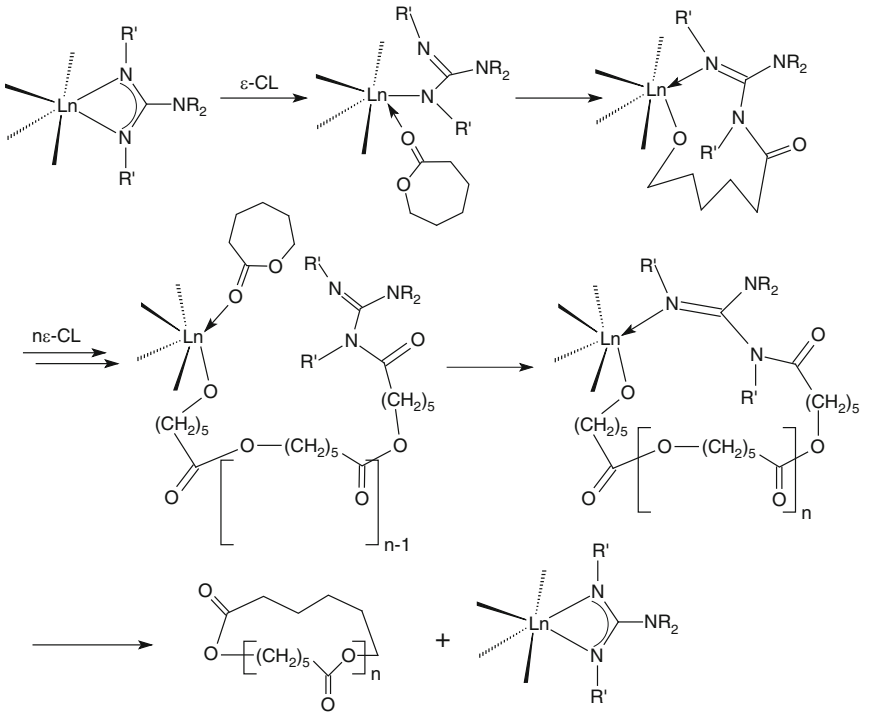

Scheme 51

All these guanidinato lanthanide complexes as an initiator showed extremely high activity in the ROP of CL. For example, the polymerization gave 100% conversion in the case of a monomer/initiator ratio of $[M]/[I] = 2{,}000$ at 35°C for 5 min. The conversion still reaches as high as 80%, even when the amount of $[M]/[I]$ increased to 4,000 under the conditions used. The resulting polymers had high molecular weights and relatively broad molecular-weight distributions ($M_w/M_n = 1.87$–2.51). The different substituents at the guanidinato ligands were found to have great effect on the catalytic activity. The mechanism of the polymerization was also presented (Scheme 51). In the initial step of the polymerization, CL coordinates to the central metal, then a nucleophilic attack by one of the guanidinio-nitrogen atoms at the carbonyl-carbon atom of the lactone takes place, followed by acyl bond cleavage and the formation of an alkoxide complex. The cyclic polymer is then formed through intramolecular attack of the Ln–O bond to the N-bonded acyl carbon atom, and the catalyst is regenerated [60].

The methyl bridged "ate" complexes $[(Me_3Si)_2NC(NPr^i)_2]_2Ln(\mu\text{-}Me)_2Li(THF)_2$ (Ln = Nd, Yb) also exhibit extremely high activity for the ROP of CL to give high molecular-weight polymers [6, 7, 57]. The identity of the central metal atom had a large effect on the catalytic activity. For example, using the Nd complex as a catalyst gave yields as high as 100% in 15 min over $[M]/[I]$ molar ratios

of 500:1 to 1,000:1 at 20°C, while under the same conditions the Yb derivative gave yields of only 27.2–61.2%. The order of reactivity Nd > Yb is in agreement with that found for metallocene-based organolanthanide catalysts [61]. The polymerization systems produced high molecular-weight polymers ($M_n > 10^4$). The molecular mass distributions were broader than those obtained with the homoleptic (phosphoraniminato)lanthanide complexes [62], especially when long reaction times were used. This may be due to a transesterification reaction [57]. Extremely high activity for the polymerization of CL was also achieved with the bis(guanidinato)lanthanide amido derivatives $[(Me_3Si)_2NC(NPr^i)_2]_2LnNPr^i_2$ (Ln = Y, Nd) (cf., Sect. 3.2.2) [63]. The polymerization was completed under mild conditions in toluene solution within minutes. Even if the catalyst amount decreased to 0.04 mol% ($[CL]/[I] = 2{,}500 : 1$), the polymerization still gave yields as high as 80% in the case of the Nd complex as initiator. A significant effect of the central metals on the catalytic activity was observed. The activity order Nd > Y under the used polymerization conditions is in good agreement with the increasing tendency in ionic radii (Nd > Y), which is similar to that found in lanthanocene complex systems [61]. It was proposed that the presence of an Ln–NPr^i_2 σ-bond in $[(Me_3Si)_2NC(NPr^i)_2]_2LnNPr^i_2$ is crucial for the ROP of CL. Further spectroscopic characterization of the oligomer of caprolactone, prepared by the reaction of $[(Me_3Si)_2NC(NPr^i)_2]_2YNPr^i_2$ with CL in a 1:10 molar ratio, showed the presence of a terminal diisopropylamido group. Thus, it was proposed that at the initial stage of the polymerization a nucleophilic attack by the amido nitrogen atom at the lactone carbonyl-carbon atom takes place, followed by acyl-oxygen bond cleavage and the formation of a lanthanide alkoxide. The polymerization mechanism is illustrated in Scheme 52 [63].

The bis(guanidinate) alkoxide complexes $[(Me_3Si)_2NC(NPr^i)_2]_2LnX$ (X = O^iPr, O^tBu; Ln = Y, Nd, Sm, Lu) depicted in Scheme 22 are active catalysts/initiators for the ROP of β-butyrolactone (Scheme 53) under mild conditions to afford syndiotactic poly(hydroxy-3-butyrate) through a chain-end control mechanism [32].

In quest of new single-site catalysts for polymerizations of cyclic esters, a series of mononuclear yttrium(III) complexes were synthesized which are depicted in Scheme 54 [6, 7].

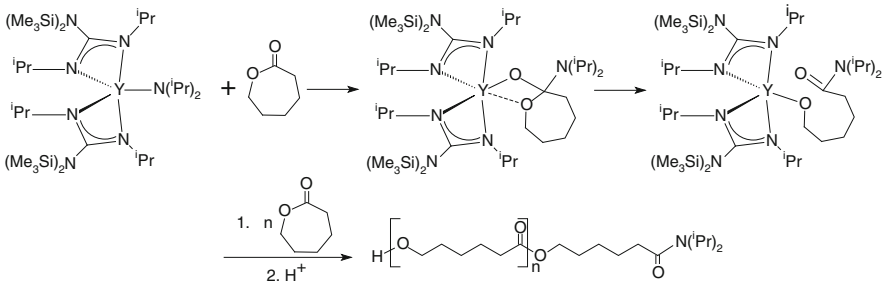

Scheme 52

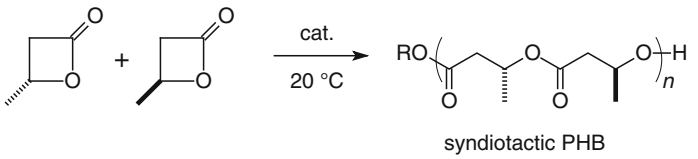

Scheme 53

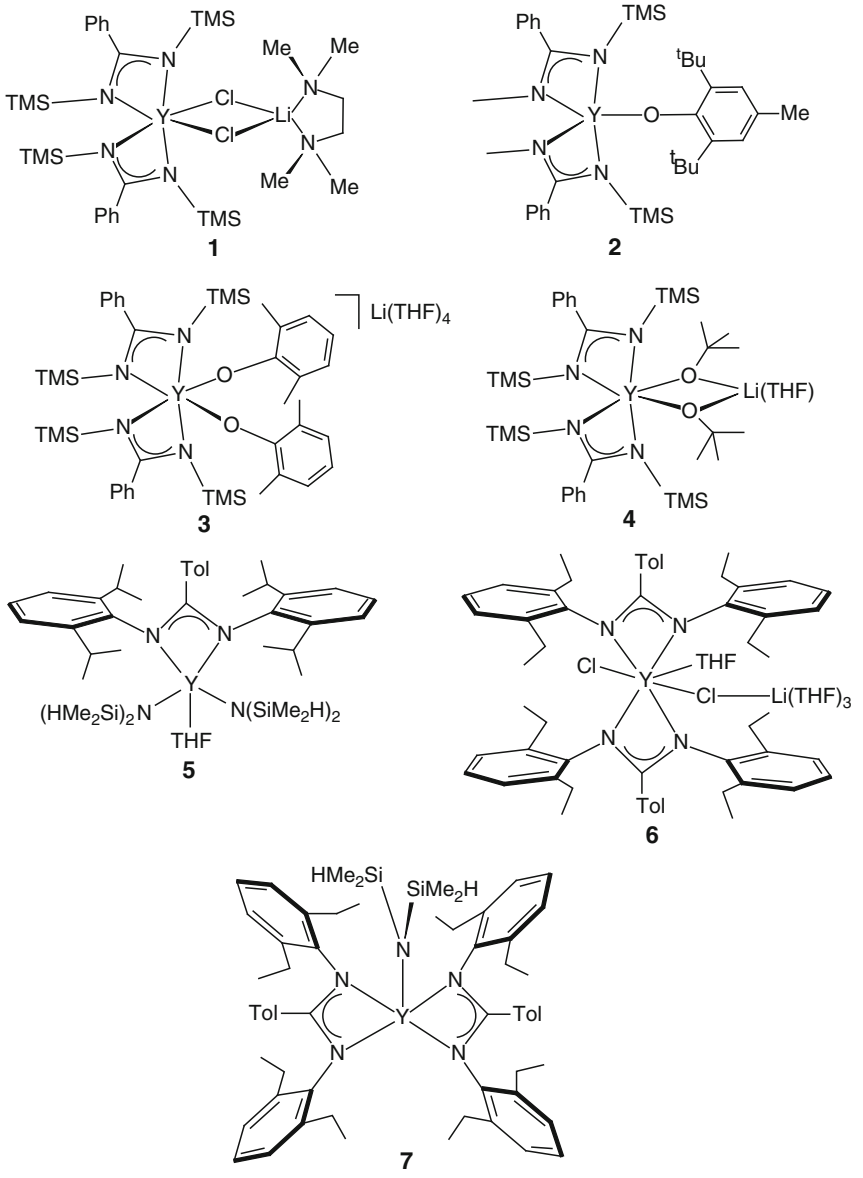

Scheme 54

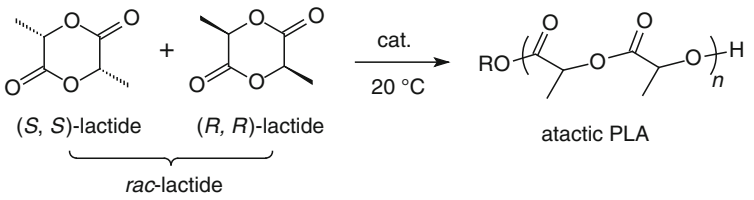

Scheme 55

Coordination numbers ranging from 5 to 7 were observed, and they appeared to be controlled by the steric bulk of the supporting amidinate and coligands. Complexes **2**–**5** and **7** were found to be active catalysts for the polymerization of D,L-lactide (e.g., with **2** and added benzyl alcohol, 1,000 equivalents of D,L-lactide were polymerized at room temperature in less than 1 h). The neutral complexes **2**, **5**, and **7** were more effective than the anionic complexes **3** and **4**. Polymerization of D,L-lactide to polylactide (Scheme 55) was also achieved using the mono(guanidinate) lanthanum complex $[(Me_3Si)_2NC(NCy)_2]La[N(SiMe_3)_2]_2$. Although a high molecular-weight polymer was obtained, polydispersities were broad and no control over the stereochemistry of the polymer was observed [6, 7]. The bis(guanidinate) alkoxide complexes $[(Me_3Si)_2NC(NPr^i)_2]_2LnX$ (X = OPr^i, OBu^t; Ln = Y, Nd, Sm, Lu) shown in Scheme 22 were reported to be active catalysts/initiators for the ROP of *rac*-lactide under mild conditions. Most of these polymerizations proceeded with a significant degree of control. Bis(guanidinate) alkoxides appear to be well suited for achieving immortal polymerization of lactide, through the introduction of large amounts of isopropanol as a chain-transfer agent [32].

Recently, the guanidinate lanthanide borohydrides $[(Me_3Si)_2NC(NCy)_2]Ln(BH_4)_2(THF)_2$ (Ln = Nd, Sm, Er, Yb) and $[(Me_3Si)_2NC(NCy)_2]_2Ln(BH_4)_2Li(THF)_2$ (Ln = Nd, Sm, Yb) were also reported to be promising monoinitiators for the ROP of racemic lactide as well as methyl methacrylate polymerization [6, 7, 37, 59]. These compounds, especially the neodymium derivative $[(Me_3Si)_2NC(NCy)_2]_2Nd(\mu\text{-}BH_4)_2Li(THF)_2$, were found to act as monoinitiators for the ROP of racemic lactide to afford atactic polymers with a good degree of control, that is, controlled molecular weights and relatively narrow polydispersities ($1.09 < M_w/M_n < 1.77$), provided moderate substrate-to-initiator ratios are used [37]. Recently, ytterbium amide complexes stabilized by linked bis(amidinate) ligands (cf., Scheme 48) were reported to be efficient initiators for the polymerization of L-lactide. The catalytic performance was found to be highly dependent on the amido groups and molecular structures [6, 7].

The ROP of TMC using the homoleptic lanthanide amidinate complexes $[RC(NCy)_2]_3Ln$ (R = Me, Ph; Ln = La, Nd, Sm, Yb) as single-component initiators was investigated in detail. It was found that the substituents on the amidinate ligands and the metal centers had a great effect on the catalytic activities of these complexes, that is, Me > Ph, and La > Nd > Sm > Yb. Thus, the lanthanum acetamidinate $[MeC(NCy)_2]_3La$ showed the highest catalytic activity [64].

The ROP of TMC was also achieved using homoleptic lanthanide guanidinate complexes $[Ph'_2NC(NCy)_2]_3Ln$. Here too, the metal centers and the substituents on the guanidinate ligands showed a marked effect on the catalytic activities with $[Ph_2NC(NCy)_2]_3Yb$ being the most active catalyst in this case. Therefore, the activity order under the studied polymerization conditions was Yb > Sm > Nd, which in this particular case is opposite to the order of the ionic radii [28, 65]. The copolymerization of TMC with CL initiated by $[Ph_2NC(NCy)_2]_3Yb$ was also tested [65]. The other members of this series of homoleptic lanthanide(III) guanidinates also exhibited extremely high activity for the ROP of CL giving polymers with high molecular weights. In this case, too, the different substituents at the guanidinate ligands have a great effect on the catalytic activity [6, 7, 65].

Although polymerization catalysis using lanthanide amidinates and guanidinates is still in its infancy, the present results clearly show the great potential this class of rare earth complexes offers. Catalytic activities can be tuned in a wide range by using various group 3 and lanthanide metals and different substituents at the ligand backbone. A major advantage of the amidinates and guanidinates over the established lanthanide metallocene catalysts is their significantly improved air-stability especially in the case of the tris(amidinates).

4.3 Miscellaneous Reactions Catalyzed by Lanthanide Amidinates and Guanidinates

Anionic bridged bis(amidinate) lithium lanthanide complexes have been found to be efficient catalysts for the amidation of aldehydes with amines under mild conditions (Scheme 56). The activity was found to follow the order of yttrium < neodymium < europium ≈ ytterbium. The catalysts are available for the formation of benzamides derived from pyrrolidine, piperidine, and morpholine with good to excellent yields. In comparison with the corresponding neutral complexes, the anionic complexes showed higher activity and a wider range of scope for the amines. A cooperation of the lanthanide and lithium metals in this process was proposed to contribute to the high activity of these catalysts [66, 67].

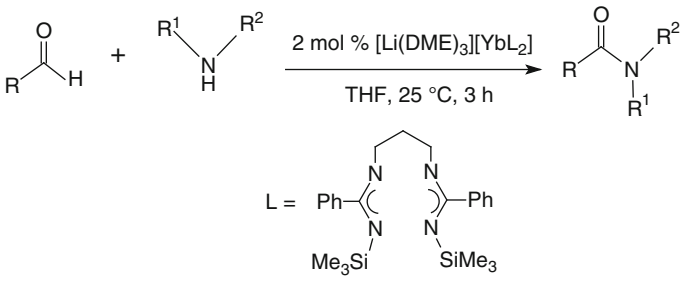

Scheme 56

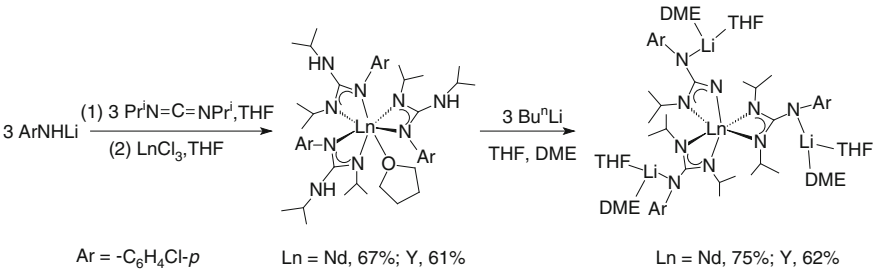

Scheme 57

The amidation of aldehydes with amines has also recently been achieved with the use of the lanthanide tris(guanidinate) complexes shown in Scheme 14 [31]. These complexes were found to be efficient catalysts for amidation of aldehydes with amines under mild conditions with a wide scope of substrates including pyrrolidine, piperidine, and morpholine. In the course of this study, one of the intermediates for this process, the lanthanum amido complex $[\{(Pr^iN)CNHPr^i(NC_6H_4Cl-p)\}_2La(\mu\text{-NHPh})]_2\cdot 3C_7H_8$, was isolated [66]. Most recently, reactions of triguanidinate lanthanide complexes $[(Pr^iN)(NC_6H_4Cl\text{-}p)C(NHPr^i)]_3Ln$ (Ln = Nd, Y) with three equivalents of Bu^nLi according to Scheme 57 gave $[Li(THF)(DME)]_3[Ln[\mu\text{-}\eta^2\text{:}\eta^1\ (Pr^iN)_2C(NC_6H_4Cl\text{-}p)\}_3]$, which represent the first structurally characterized complexes of lanthanide and lithium metals with dianionic guanidinate ligands. The Nd complex was found to be an effective catalyst for amidation of aldehydes with amines under mild conditions with a wide scope of substrates [67].

An interesting organolanthanide-catalyzed reaction which has been studied in recent years is the addition of terminal alkynes to carbodiimides leading to the novel class of *N,N′*-disubstituted propiolamidines. It was found that half-sandwich rare earth metal complexes bearing silylene-linked cyclopentadienyl-amido ligands can act as excellent catalysts in this addition reaction. As illustrated in Scheme 58, a rare earth amidinate species has been confirmed to be a true catalytic species [68].

This organolanthanide-catalyzed reaction provides the first example of efficient preparation of well-defined propiolamidines, a new family of amidines which are difficult to access by other means and may show unique reactivity. A wide range of terminal alkynes could be used for this catalytic cross-coupling reaction which was not affected by either electron-withdrawing or -donating substituents or their positions at the phenyl ring of the aromatic alkyne [68].

More recently, it was demonstrated that this organolanthanide-catalyzed reaction is more general in nature and can be extended to other lanthanide precatalysts as well as the addition of N–H bonds to carbodiimides [69, 70]. For example, the ring-bridged metallocenes $(EBI)LnN(SiMe_3)_2$ (Ln = Y, Sm, Yb; EBI = ethylene-bis(η^5-indenyl)) were found to exhibit versatile catalytic activities with high efficiency toward the addition of the N–H bonds of amines and the C–H bonds of terminal alkynes to carbodiimides, thereby providing access to various substituted guanidines and propiolamidines. Here again, lanthanide guanidinate and

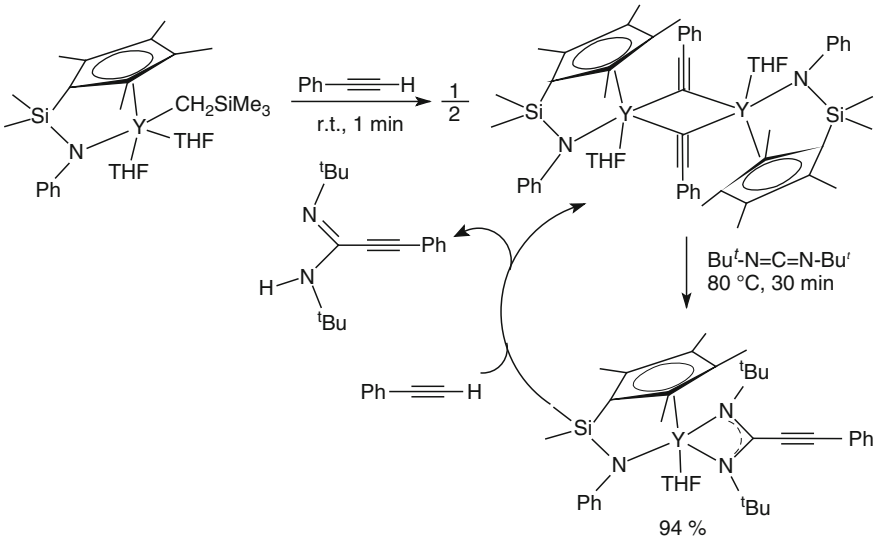

Scheme 58

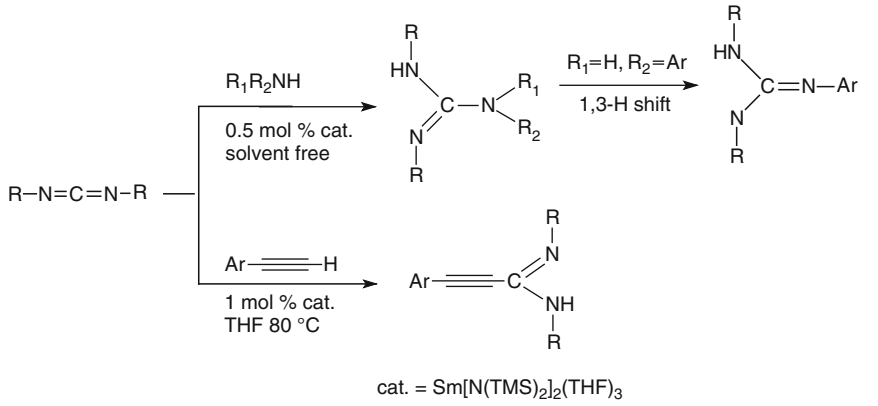

Scheme 59

amidinate species are the key intermediates in the proposed catalytic cycle [69]. Various divalent lanthanide complexes such as $Ln[N(SiMe_3)_2]_2(THF)_3$ (Ln = Sm, Eu, Yb) or $(MeC_5H_4)_2Sm(THF)_2$ were also found to be highly active precatalysts for the addition of N–H and C–H bonds to carbodiimides (Scheme 59) [70, 71]. It was also demonstrated that the cyclopentadienyl-free trivalent lanthanide amides $[(Me_3Si)_2N]_3Ln(\mu\text{-Cl})Li(THF)_3$ (Ln = La, Sm, Eu, Y, Yb) and $Ln[N(SiMe_3)_2]_3$ (Ln = Y, Yb) are highly efficient catalysts for the guanylation of both aromatic and secondary amines with a high activity under mild conditions. It was found that these catalysts are compatible with a wide range of solvents and substrates. In all cases lanthanide amidinates and guanidinates were proposed to be catalytically active intermediates [71].

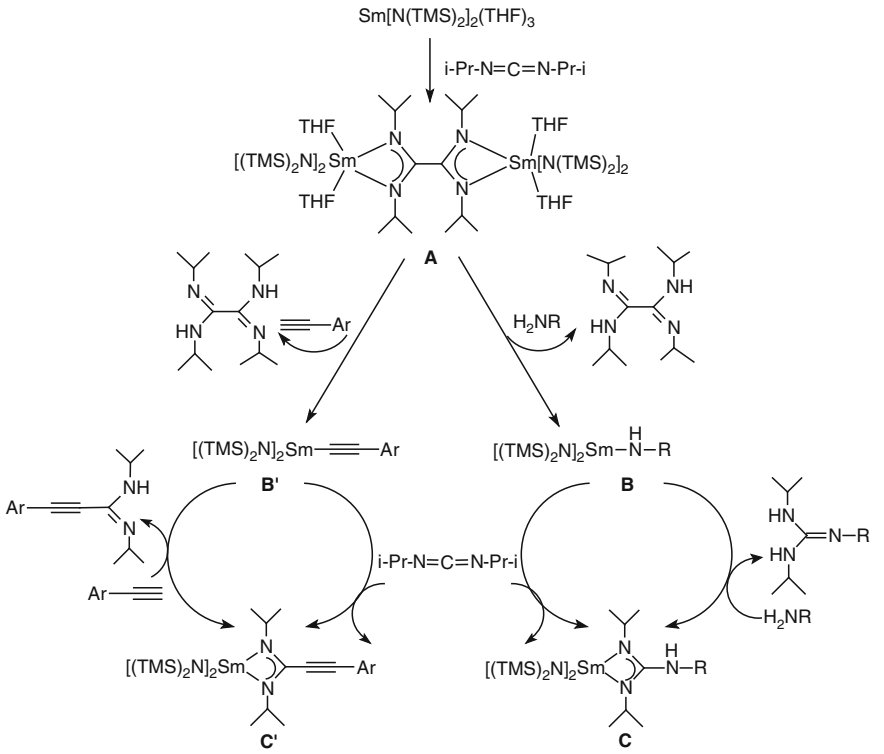

Scheme 60

Scheme 60 illustrates the proposed catalytic cycles for a samarium(II) silylamide precursor. The first step in both reactions is supposed to be the formation of a bimetallic samarium bis(amidinate) species originating from the reductive coupling of carbodiimide promoted by the Ln(II) complex. The active species is proposed to be a samarium guanidinate and a lanthanide amidinate [70].

The catalytic activity of bulky amidinato bis(alkyl) complexes of scandium and yttrium (cf., Sect. 3.2.3) in the intramolecular hydroamination/cyclization of 2,2-dimethyl-4-pentenylamine has also been investigated and compared to the activity of the corresponding cationic mono(alkyl) derivatives. Cyclotrimerization of aryl isocyanates leads to perhydro-1,3,5-triazine-2,4,6-triones (isocyanurates). Another good catalyst for the cyclotrimerization of phenyl isocyanate was found in the organoyttrium amidinate complex $Cp_2Y[Bu^nC(NBu^t)_2]$ [6, 7]. Reaction of the benzylimido–lutetium complex $[Cp'Lu(\mu_3\text{-}NCH_2Ph)]_4$ ($Cp' = \eta^5\text{-}C_5Me_4SiMe$) with four equivalents of benzonitrile at room temperature in toluene gave the benzamidinate dianion complex shown in Scheme 61 in 73% yield after recrystallization from THF [6, 7, 72] X-ray analysis showed that the product has a dimeric structure in which the two Lu atoms are bridged by the ketimido nitrogen atom (Lu–N 2.149(4), 2.326(4) Å), and the amido nitrogen atom is bonded terminally to one

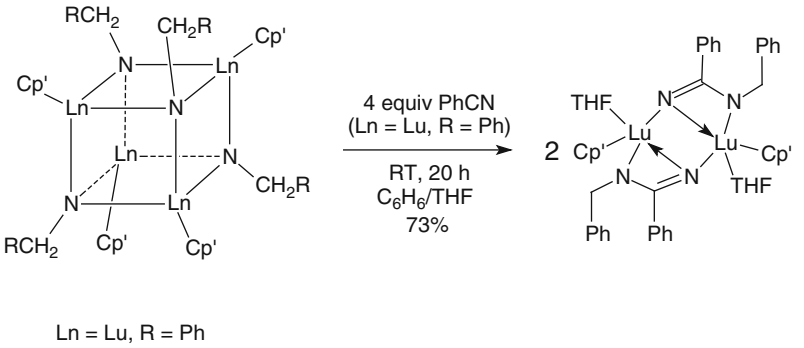

Scheme 61

Lu atom (Lu–N 2.352(4) Å). The formation of the dianion complex apparently proceeds by nucleophilic addition of the imido unit to the C≡N group of benzonitrile, which demonstrates that a lanthanide–imido bond, even in a bridging form, is very reactive. This is in contrast with what was observed previously for bonds between transition metals and bridging imido ligands, which are usually robust and unreactive. Moreover, the resultant product represented the first metal complex of an amidinate dianion, in contrast to the well-known complexes of various metals with amidinate monoanions $[RNC(R')NR]^-$ as ligands [6, 7]. The dianion complex and related complexes derived from imido lanthanide species react with excess of benzonitrile under selective formation of the cyclotrimerization product 2,4,6-triphenyl-1,3,5-triazine [72]

These initial results indicate that lanthanide amidinates and guanidinates may exhibit interesting catalytic activities in reactions other than polymerizations. Clearly, more work in this direction would be highly desirable.

5 Conclusions

This review describes the success story of lanthanide amidinates and guanidinates. First reported 2 decades ago, these compounds have undergone a transition from mere laboratory curiosities to efficient and promising polymerization catalysts in recent years. Thus, this article provides a good example for purely academic research eventually turning out to become the basis for unexpected practical uses. Initial results clearly show that certain lanthanide amidinates and guanidinates show very high catalytic activity in polymerization reactions of olefins and polar monomers. Besides these exciting applications, the synthetic and structural chemistry of lanthanide amidinates is surprisingly diverse and far from being fully exploited. Amidinate and guanidinate ligands rival the ubiquitous cyclopentadienyl ligands in their accessibility and versatility. Important aspects of lanthanide cyclopentadienyl chemistry can now be realized using the amidinate and guanidinate anions as “steric

cyclopentadienyl equivalents". Mono-, di-, and trisubstitution products as well as complexes containing pendant-arm amidinates and bis(amidinate) ligands are available. All three possible oxidation states (+2, +3, and +4) of the lanthanide ions can be stabilized with the use of amidinate ligands. Future preparative work will show if, for example, novel divalent lanthanide amidinate and guanidinate complexes (Nd^{2+}, Eu^{2+}, Dy^{2+}, Tm^{2+}) can be prepared and fully characterized. Further investigation of the recently discovered cerium(IV) benzamidinates is also clearly warranted. It would certainly be of interest to study if these compounds can be employed as oxidation catalysts. Another point worthy of a more thorough investigation would be if and when there is any marked difference in catalytic activities between analogous cyclopentadienyl and amidinate/-guanidinate chemistry. It would be interesting to see if there are examples of compounds belonging to the same class of compounds (e.g., L_2LnX) where the reactivity is different or polymerization is better with one class or other. This could be a good subject for more systematic future studies. In any case it needs no prophet to foresee that the most significant future development in this area lies in the practical exploration of lanthanide amidinates and guanidinates in catalysis but also in materials science and, perhaps, as novel reagents in organic synthesis.

Acknowledgments Financial support of the author's own work on lanthanide amidinates provided by the Deutsche Forschungsgemeinschaft (SPP1166 "Lanthanoid-spezifische Funktionalitäten in Molekül und Material"), the Fonds der Chemischen Industrie, and the Otto-von-Guericke-Universität Magdeburg is most gratefully acknowledged.

References

1. Wilkinson G, Birmingham JM (1954) J Am Chem Soc 76:6210
2. Schumann H (1984) Angew Chem Int Ed 23:474
3. Edelmann FT (2006) Complexes of scandium, yttrium and lanthanide elements. In: Crabtree RH, Mingos DMP (eds) Comprehensive organometallic chemistry III, vol 3, Elsevier, Oxford, p 1
4. Cotton S (2006) Lanthanide and actinide chemistry. Wiley, Chichester, UK
5. Anwander R (1999) In: Kobayashi S (ed) Lanthanides: chemistry and use in organic synthesis, Springer, Berlin, p 1
6. Edelmann FT (2008) Adv Organomet Chem 57:183, and references cited therein
7. Edelmann FT (2009) Chem Soc Rev 38:2253
8. Anwander R (2002) In: Cornils B, Herrmann WA (eds) Applied homogeneous catalysis with organometallic compounds, vol 2. Wiley-VCH, Germany, p 974
9. Hong S, Marks TJ (2004) Acc Chem Res 37:673
10. Edelmann FT (1995) Angew Chem Int Ed 34:2466
11. Edelmann FT, Freckmann DMM, Schumann H (2002) Chem Rev 102:1851
12. Roesky PW (2003) Z Anorg Allg Chem 629:1881
13. Arndt S, Okuda J (2005) Adv Synth Catal 347:339
14. Sanger AR (1973) Inorg Nucl Chem Lett 9:351
15. Boeré RT, Oakley RT, Reed RW (1987) J Organomet Chem 331:161
16. Dehnicke K (1990) Chem-Ztg 114:295
17. Barker J, Kilner M (1994) Coord Chem Rev 13:219

18. Edelmann FT (1994) Coord Chem Rev 137:403, and references cited therein
19. Bailey PJ, Pace S (2001) Coord Chem Rev 214:91
20. Chandra G, Jenkins AD, Lappert MF, Srivastava RC (1970) J Chem Soc:2550
21. Butovskii MV, Tok OL, Wagner FR, Kempe R (2008) Angew Chem Int Ed 47:7246
22. Wedler M, Knösel F, Pieper U, Stalke D, Edelmann FT, Amberger HD (1992) Chem Ber 125:2171
23. Lubben TV, Wolczanski PT, van Duyne GD (1984) Organometallics 3:977
24. Heitmann D, Jones C, Junk PC, Lippert KA, Stasch A (2007) Dalton Trans:187
25. Zhou Y, Yap GPA, Richeson DS (1998) Organometallics 17:4387
26. Päiväsaari J, Dezelah CL, Back D, El-Kaderi HM, Heeg MJ, Putkonen M, Niinistö L, Winter CH (2005) J Mater Chem 15:4224
27. Zhou L, Yao Y, Zhang Y, Sheng H, Xue M, Shen Q (2005) Appl Organomet Chem 19:398
28. Zhou L, Yao Y, Zhang Y, Xue M, Chen J, Shen Q (2004) Eur J Inorg Chem:2167
29. Milanov AP, Fischer RA, Devi A (2008) Inorg Chem 47:11405
30. Chen J, Yao Y, Luo Y, Sheng H, Zhou L, Zhang Y, Shen Q (2004) Huaxue Yanjiu Yu Yingyong 16:253
31. Qian C, Zhang X, Li J, Xu F, Zhang Y, Shen Q (2009) Organometallics 28:3856
32. Ajellal N, Lyubov DM, Sinenkov MA, Fukin, GK, Cherkasov AV, Thomas CM, Carpentier JF, Trifonov AA (2008) Chem Eur J 14:5440
33. Trifonov AA, Fedorova EA, Fukin GK, Bochkarev MN (2004) Eur J Inorg Chem:4396
34. Trifonov AA, Skvortsov GG, Lyubov DM, Skorodumova NA, Fukin GK, Baranov EV, Glushakova VN (2006) Chem Eur J 12:5320
35. Skvortsov GG, Yakovenko MV, Fukin GK, Baranov EV, Kurskii YA, Trifonov AA (2007) Russ Chem Bull Int Ed 56:456
36. Skvortsov GG, Yakovenko MV, Fukin GK, Cherkasov AV, Trifonov AA (2007) Russ Chem Bull Int Ed 56:1742
37. Skvortsov GG, Yakovenko MV, Castro PM, Fukin GK, Cherkasov AV, Carpentier JF, Trifonov AA (2007) Eur J Inorg Chem:3260
38. Yuan F, Zhu Y, Xiong L (2006) J Organomet Chem 691:33770
39. Zhang J, Cai R, Weng L, Zhou X (2003) J Organomet Chem 672:94
40. Zhang J, Cai R, Weng L, Zhou X (2004) Organometallics 23:3303
41. Pi C, Zhang Z, Pang Z, Zhang J, Luo J, Chen Z, Weng L, Zhou X (2007) Organometallics 26:1934
42. Doyle D, Gun'ko YK, Hitchcock PB, Lappert MF (2000) Dalton Trans:4093
43. Wang J, Sun H, Yao Y, Zhang Y, Shen Q (2008) Polyhedron 27:1977
44. Luo Y, Yao Y, Shen Q, Sun J, Weng L (2002) J Organomet Chem 662:144
45. Edelmann FT (1996) Top Curr Chem 179:113, and references cited therein
46. Schlund R, Lux M, Edelmann F, Reissmann, U, Rohde W (1998) US Patent No. US 5707913
47. Smolensky E, Eisen MS (2007) Dalton Trans:5623
48. Jeske G, Lauke H, Mauermann H, Swepston PN, Schumann H, Marks TJ (1985) J Am Chem Soc 107:8091
49. Bambirra S, Bouwkamp MW, Meetsma A, Hessen B (2004) J Am Chem Soc 126:9182
50. Hessen B, Bambirra S (2003) Int Patent No. WO 2004000894
51. Mecking S (2004) Angew Chem Int Ed 43:1078
52. Drumright RE, Gruber PR, Henton DE (2000) Adv Mater 12:1841
53. Auras R, Harte B, Selke S (2004) Macromol Biosci 4:835
54. Ha CS, Gardella JA (2005) Chem Rev 105:4205
55. Yasuda H, Ihara E (1997) Bull Chem Soc Jpn 70:1745
56. Shen Q, Yao Y (2002) J Organomet Chem 647:180
57. Luo Y, Yao Y, Shen Q, Yu K, Weng L (2003) Eur J Inorg Chem:318
58. Yuan FG, Xiong LF, Zhu XH (2007) Suzhou Keji Xueyuan Xuebao, Ziran Kexueban 24:49
59. Villiers C, Thuéry P, Ephritikhine M (2004) Eur J Inorg Chem:4624
60. Chen JL, Yao YM, Luo YJ, Zhou LY, Zhang Y, Shen Q (2004) J Organomet Chem 689:1019
61. Yamashita M, Takemoto Y, Ihara E, Yasuda H (1996) Macromolecules 29:798

62. Gröb T, Seybert G, Massa W, Weller F, Palaniswami R, Greiner A, Dehnicke K (2000) Angew Chem Int Ed 39:4373
63. Yao, Y, Luo Y, Chen J, Zhang Z, Zhang Y, Shen Q (2003) J Organomet Chem 679:229
64. Li C, Wang Y, Zhou L, Sun H, Shen Q (2006) J Appl Polym Sci 102:22
65. Zhou L, Sun H, Chen J, Yao Y, Shen Q (2005) J Appl Polym Sci A Polym Sci 43:1778
66. Wang J, Li J, Xu F, Shen Q (2009) Adv Synth Catal 351: 1363
67. Qian C, Zhang X, Zhang Y, Shen Q (2010) J Organomet Chem 695:747
68. Zhang WX, Nishiura M, Hou Z (2005) J Am Chem Soc 127:16788
69. Zhou S, Wang S, Yang G, Li Q, Zhang L, Yao Z, Zhou Z, Song H (2007) Organometallics 26:3755
70. Du Z, Li W, Zhu X, Xu F, Shen Q (2008) J Org Chem 73:8966
71. Li Q, Wang S, Zhou S, Yang G, Zhu X, Liu Y (2007) J Org Chem 72:6763
72. Cui D, Nishiura M, Hou Z (2005) Angew Chem Int Ed 44:959

Struct Bond (2010) 137: 165–228
DOI:10.1007/430_2010_18

Published online: 18 May 2010

Rare-Earth Metal Postmetallocene Catalysts with Chelating Amido Ligands

Tianshu Li, Jelena Jenter, and Peter W. Roesky

Dedicated to the memory of Professor Herbert Schumann († 2010), a pioneer of organolanthanide chemistry

Abstract This review deals with the synthesis and the catalytic application of noncyclopentadienyl complexes of the rare-earth elements. The main topics of the review are amido metal complexes with chelating bidentate ligands, which show the most similarities to cyclopentadienyl ligands. Benzamidinates and guanidinates will be reviewed in a separate contribution within this book. Beside the synthesis of the complexes, the broad potential of these compounds in homogeneous catalysis is demonstrated. Most of the reviewed catalytic transformations are either C–C multiple bond transformation such as the hydroamination and hydrosilylation or polymerization reaction of polar and nonpolar monomers. In this area, butadiene and isoprene, ethylene, as well as lactides and lactones were mostly used as monomers.

Keywords: Amido ligands · Chelates · Homogeneous catalysis · Rare-earth metals

Contents

T. Li, J. Jenter, and P.W. Roesky (✉)
Institut für Anorganische Chemie, Karlsruhe Institute of Technology (KIT), Geb. 30.45, Engesserstr. 15, 76131 Karlsruhe, Germany
e-mail: roesky@kit.edu

Abbreviations

Ar	Aryl
ATI	Aminotroponiminate
Bu	Butyl
CHO	Cyclohexene oxide
cod	Cyclooctadiene
cot	Cyclooctatetraene
Cp	Cyclopentadienyl, η^5-C_5H_5
Cp*	η^5-C_5Me_5
dep	Deprotonated
DME	Dimethoxyethane
equiv	Equivalent(s)
Et	Ethyl
h	Hour(s)
*i*Bu	*iso*-Butyl
*i*Pr	*iso*-Propyl
Ln	Rare-earth metal
Me	Methyl
min	Minute(s)
MMA	Methyl methacrylate
MMAO	Modified methylalumoxane
NMR	Nuclear magnetic resonance
*n*Pr	*n*-Propyl
Ph	Phenyl
PMMA	Poly(methyl methacrylate)
Py	Pyridine
ROP	Ring-opening polymerization
solv	Solvent
SSIP	Solvent-separated ion pair
*t*Bu	*tert*-butyl
THF	Tetrahydrofuran
TMEDA	Tetramethylethylenediamine

1 Introduction

The use of organometallic compounds of the lanthanides in homogeneous catalysis started in the early 1980s, when Watson and coworkers reported on lanthanide metallocene catalysts for the polymerization of ethylene. These early contributions were already reviewed [1]. Based on the pioneering work of Watson and coworkers, a number of research groups reported on the use of bis(pentamethylcyclopentadienyl) complexes of the general composition [(η^5-$C_5Me_5)_2$LnR] (R = $CH(SiMe_3)_2$, $N(SiMe_3)_2$, H) and their derivatives as catalysts for a number of C–C multiple bond

transformations. The key step in these reactions is the insertion of an Ln–X bond (Ln = Sc, Y, La–Lu; X = H, B, C, N, Si) into a C–C multiple bond [2]. Usually, alkenes and alkynes are thus transformed in hydration [3, 4], hydroboration [5, 6], hydroamination [7, 8], and hydrosilylation reactions [9–12]. In all these transformations, the cyclopentadienyl ligand acts as a spectator ligand, which means that it is not directly involved in the catalytic step. The preparation and the application of lanthanide metallocenes had been reviewed extensively in the previous years [13–15].

Recently, there has been a tremendous development in the noncyclopentadienyl chemistry [16, 17], which sometimes is referred to as "postmetallocene" chemistry [18–20]. The aim of this research is the development of more active and selective catalysts, which in comparison to metallocenes may also lead to a new product spectrum. The basic concept of the postmetallocene chemistry is the formal substitution of the cyclopentadienyl ligands by other anionic ligand systems, which then act as spectator ligands. The general role of the spectator ligand is to control the coordination number and the coordination geometry of the metal and to enable a steric protection of the active site to influence the selectivity [21]. Most efforts in this area were made by the use of anionic nitrogen-based ligand systems. The foundations for the amido metal chemistry of lanthanides were made in the 1970s by Bradley and coworkers [22–24]. First approaches in the new area of postmetallocene chemistry were made by Edelmann and coworkers [2, 25, 26], who used benzamidinate ligands in lanthanide chemistry. Benzamidinates are considered to be sterically equivalent to cyclopentadienyl ligands. In the recent years, the number of contribution to the amido metal chemistry of the lanthanides increased dramatically. Whereas early reviews of this topic could give a comprehensive overview in this area [27, 28], the huge number of publications which are available today forced us to limit the scope of the present review. Therefore, benzamidinates and guanidinates will be reviewed in a separate contribution within this book. We also limited the review to bidentate ligands, which show the most similarities to cyclopentadienyl ligands. The focus of this review lies on the synthesis of catalytic active postmetallocene complexes of the lanthanides. Other amido metal complexes that have not been used for catalytic transformations are not within the scope of this review.

2 Rare-Earth Metal Complexes of *N*,*N*-Bidentate Ligands

2.1 Monoanionic Ligands

2.1.1 Aminopyridinato Ligands

Aminopyridinato ligands are an important group of asymmetric *N*,*N*-bidentate ligands and derived from deprotonation of 2-aminopyridines. The flexibility of binding modes of aminopyridinato ligands can be explained by two resonance forms: the amidopyridine and the aminopyridinato. The anionic function is localized at either

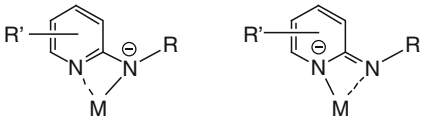

Scheme 1

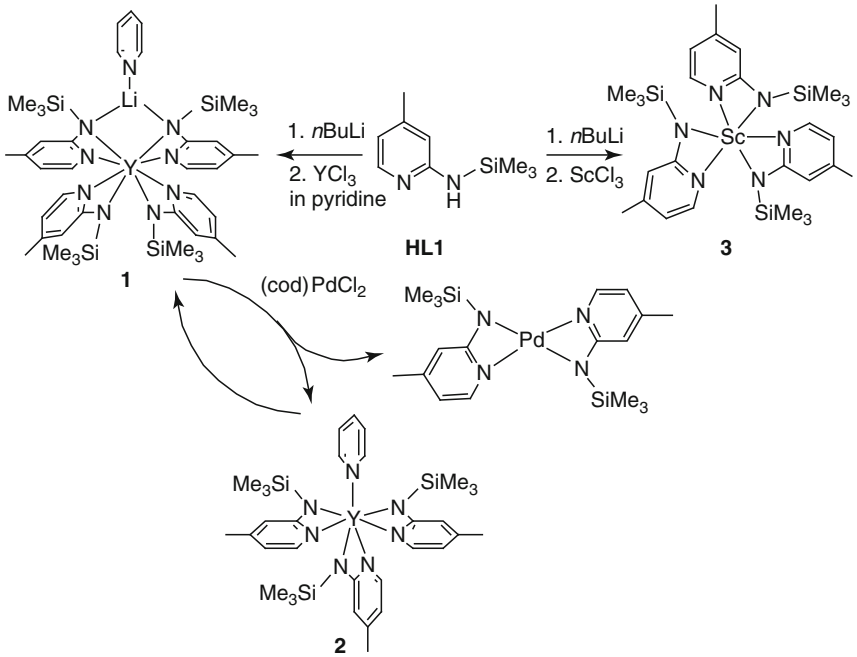

Scheme 2

the amido nitrogen atom (amidopyridine) or the pyridine nitrogen atom (aminopyridinate) (Scheme 1). The two resonance forms are indicated by metal and nitrogen bond distances. Coordination chemistry of rare-earth metals with aminopyridinato ligands has been extensively studied by Kempe and coworkers [29–32]. In general, the lanthanide aminopyridinato complexes were found to have longer bond distances between metal and pyridine nitrogen atoms [33].

In 1998, Kempe and coworkers [34] reported the first aminopyridinato rare-earth metal complexes. 4-Methyl-2-[(trimethylsilyl)amino]pyridine (**HL1**) was utilized in this complex. The reaction of lithiated **L1** and YCl_3 in ether and pyridine led to the "ate" complex $[Y(\mathbf{L1})_4(LiPy)]$ (Py = pyridine) (**1**). The complex **1** catalytically mediated a ligand transfer reaction to form $[Pd(\mathbf{L1})_2]$ and $[Y(\mathbf{L1})_3(py)]$ (**2**) from $[Pd(cod)Cl_2]$ (cod = cyclooctadiene). The **L1** ligand transfer from yttrium to palladium and the regeneration of **1** are significant in the efficient synthesis of the very strained amido palladium complexes (Scheme 2). Lithiated **L1** underwent a salt metathesis reaction with $ScCl_3$, at low temperature in THF, to yield the homoleptic complex $[Sc(\mathbf{L1})_3]$ (**3**) (Scheme 2). **3** is the first reported scandium aminopyridinato complex [35].

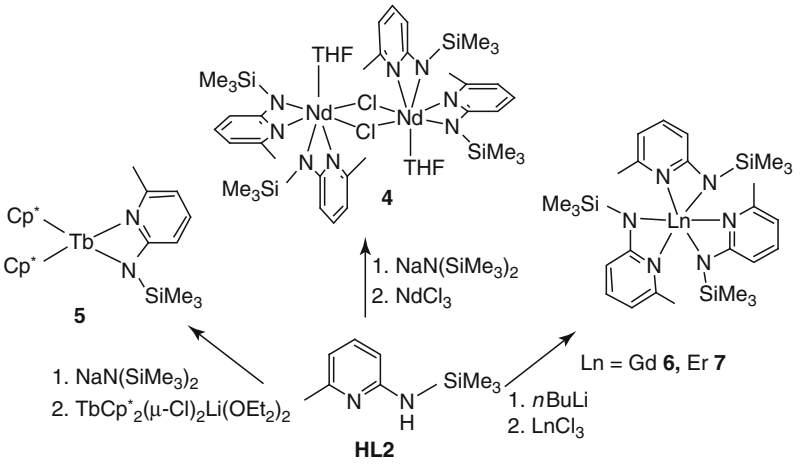

Scheme 3

L1 is a relatively small aminopyridinato ligand, resulting in a low steric demand at the metal center and leading to the formation of "ate" complexes. In 2003, Junk and coworkers characterized the first none "ate" heteroleptic lanthanide complexes containing an amidopyridinato ligand with a methyl substituent at the 6-position of pyridine ring, 6-methyl-2-[(trimethylsilyl)amino]pyridine (**HL2**) [36, 37]. The polymeric sodium amidopyridine species $[Na(\mathbf{L2})(THF)_{0.5}]_n$ reacted with $NdCl_3$ and $[TbCp^*_2(\mu\text{-}Cl)_2Li(OEt_2)_2]$ ($Cp^* = C_5Me_5$) to afford dimeric $[Nd(\mathbf{L2})_2(THF)(\mu\text{-}Cl)]_2$ (**4**) and monomeric $[TbCp^*_2(\mathbf{L2})]$ (**5**). **5** is the first terbium Cp^* compound structurally characterized. Similarly to $[Sc(\mathbf{L1})_3]$ (**3**), the reaction of $LnCl_3$ and lithiated **L2** led to the homoleptic tris-amido complexes $[Ln(\mathbf{L2})_3]$ (Ln = Gd (**6**), Er (**7**)) (Scheme 3).

In 2004, Kempe and coworkers designed bulkier aminopyridinato ligands by introducing alkylphenyl substituents at the amido N atom as well as the 6-position of the pyridine ring. Steric demanding aminopyridine ligands were efficiently synthesized by Grignard coupling and palladium-catalyzed aryl amination methods [38]. The reaction of $[Y(CH_2SiMe_3)_3(THF)_2]$ with (2, 6-diisopropylphenyl)-[6-(2,4,6-triisopropylphenyl)pyridin-2-yl]amine (**HL3**), (2,4,6 -trimethylphenyl)[6-(2,4,6-triisopropylphenyl)pyridin-2-yl]amine (**HL4**), and (2,6-diisopropylphenyl)-[6-(2,6-dimethylphenyl)pyridin-2-yl]amine (**HL5**) led to the monoaminopyridinate yttrium complexes, $[Y(CH_2SiMe_3)_2(\mathbf{L3})]$ (**8**), $[Y(CH_2SiMe_3)_2(\mathbf{L4})]$ (**9**), and $[Y(CH_2SiMe_3)_2(\mathbf{L5})]$ (**10**), correspondingly. The cationic yttrium complexes, $[Y(CH_2SiMe_3)(THF)_3(\mathbf{L3})][BPh_4]$ (**11**), $[Y(CH_2SiMe_3)(THF)_3(\mathbf{L4})][BPh_4]$ (**12**), and $[Y(CH_2SiMe_3)(THF)_3(\mathbf{L5})][BPh_4]$ (**13**) were obtained by abstraction of one alkyl using the anilinium borate $[C_6H_5NH(CH_3)_2][BPh_4]$ (Scheme 4). These cationic complexes **11**, **12**, and **13** exhibited high catalytic activity in the polymerization of ethylene in the presence of aluminum alkyl compounds. Reversible polyethylene chain transfer between the organoyttrium cations and the aluminum compounds was observed. Al-terminated polyethylene

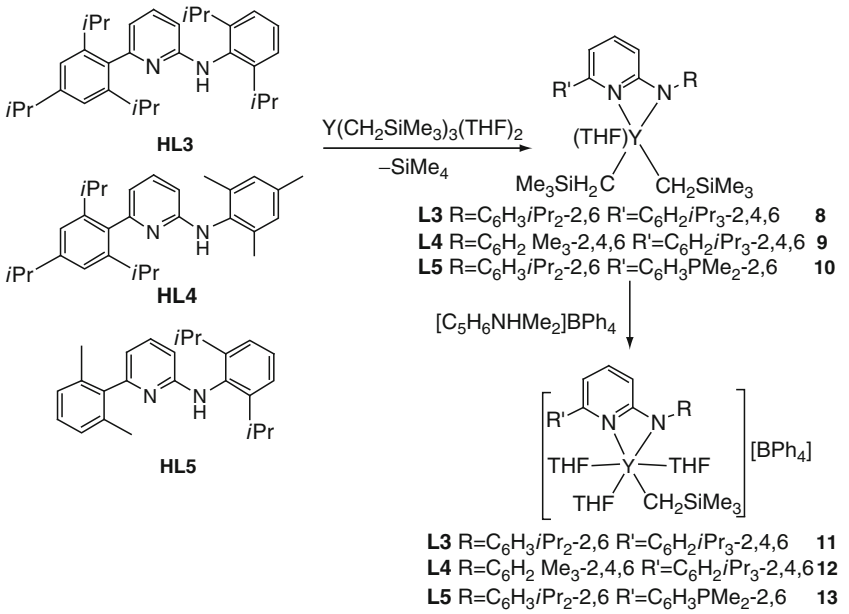

Scheme 4

with high molecular weight and narrow molecular weight distribution was reported. The bulkier aminopyridinate ligand complex **11** provided a better catalytic activity and was about twice more active than **12**. The coordination study by Kempe and coworkers revealed that the less bulky ligand **L5** had the tendency to form bis-aminopyridinato complexes (Scheme 6) [39]. Such complexes do not initiate the polyethylene chain growth [40].

HL3 and **HL4** were also reacted with $[Ln\{N(SiHMe_2)_2\}_3(THF)_2]$ via amine elimination to form the corresponding mono(aminopyridinato) complexes (Ln = Y (**14** and **15**), La (**16** and **17**)). Complexes **14–17** are not active for the polymerization of ethylene in the presence of alkylaluminium compounds. The reactions of the mono(aminopyridinato) complexes with aluminum compounds $AlEt_3$ or $AlHiBu_2$ showed a fast aminopyridinato ligand transfer to the aluminum atom. The products of the transfer reaction are aminopyridinato-stabilized dialkylaluminium compounds. The catalytic activity was believed to be prohibited by the ligand transfer reaction (Scheme 5) [41].

Deprotonation of **HL5** with KH led to polymeric **KL5**. The reaction of $LnCl_3$ with 2 equiv of **KL5** in THF afforded the bis-aminopyridinato complexes $[Ln(\mathbf{L5})_2Cl(THF)]$ (Ln = Y (**18**), Nd (**19**)). Alkylation of the yttrium complex **18** with 1 equiv of $LiCH_2SiMe_3$ gave the alkylyttrium complex $[Y(\mathbf{L5})_2(\mathbf{CH_2SiMe_3})(\mathbf{THF})]$ (**20**). In addition, the five-coordinated silylamide $[Nd(\mathbf{L5})_2\{N(SiMe_3)_2\}]$ (**21**) was obtained by the reaction of **19** with 1 equiv of $K\{N(SiMe_3)_2\}$ [39]. The attempt of forming a novel aminopyridinato rare-earth metal hydrido complex by treating **20** with $PhSiH_3$ unexpectedly led to the product

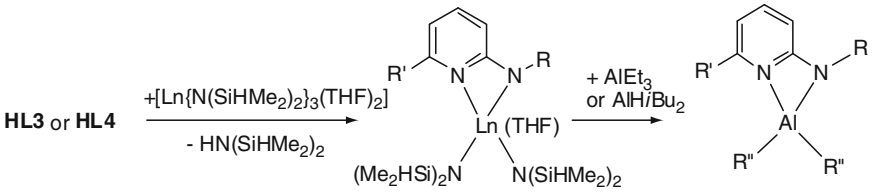

Scheme 5

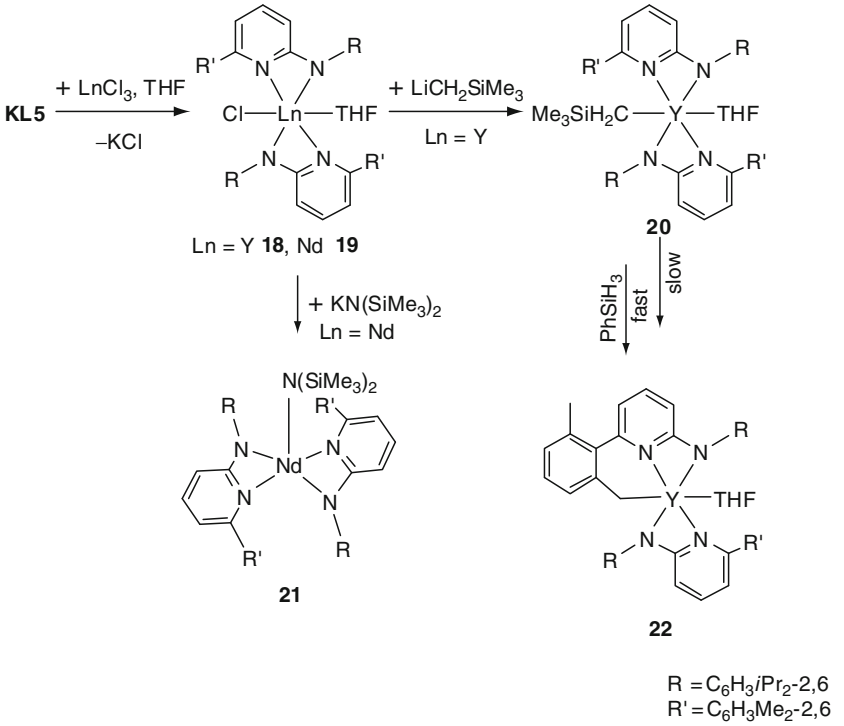

Scheme 6

of intramolecular sp^3-hybridized C–H bond activation, [Y(**L5**)(**L5**-H)(THF)] (**22**). **22** was also produced slowly after keeping the complex at room temperature for 2 weeks without $PhSiH_3$ (Scheme 6). Yttrium hydride was believed to be generated by the reaction of the alkyl with $PhSiH_3$, and reacted rapidly with a methyl group on the phenyl ring to form **22** [42].

KL3 and **KL5** underwent clean salt metathesis with $NdCl_3$ in THF to form a dinuclear mono(aminopyridinato) complex, $[Nd(\mathbf{L3})Cl_2(THF)_2]_2$ (**23**) (Scheme 7) and a mononuclear bis-aminopyridinato complex, $[Nd(\mathbf{L5})_2Cl(THF)]$ (**19**) (Scheme 6), respectively. The steric effect of bulky ligand **L3** favors the

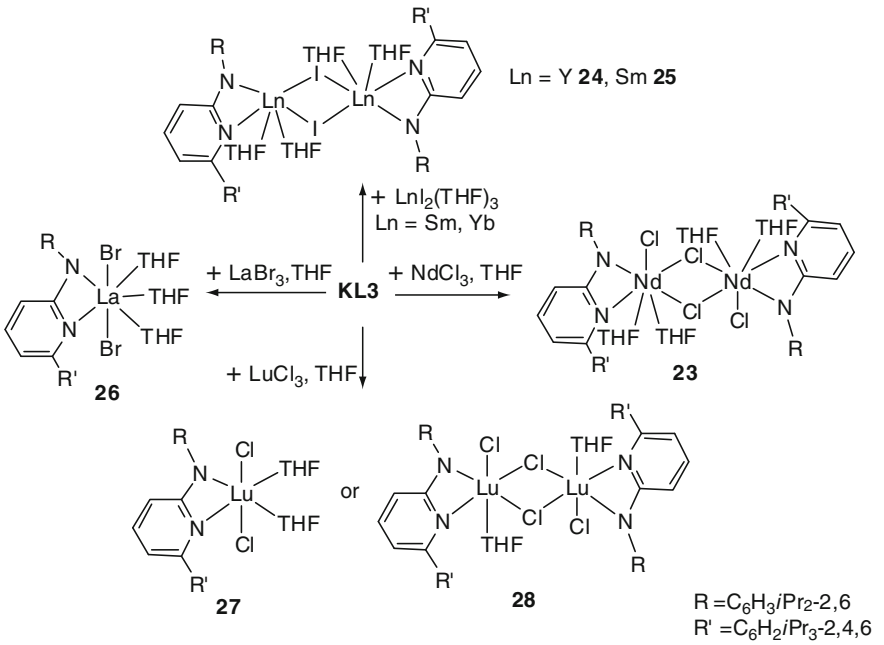

Scheme 7

formation of mono(aminopyridinato) complex **23**. Ethylene polymerization activity of the neutral complexes **23** and **19** was studied and compared with those of the cationic complexes **11** and **12**. Based on the same ligand on the metal center, with the same condition, **23** was ~20 times less active than **11**, and **19** was ~10 times less active than **12** [40]. The effects of the metal ion and oxidation state of rare-earth metal aminopyridinate complexes on ε-caprolactone polymerization were studied by Kempe and Guillaume [43]. Heteroleptic amido complexes of divalent lanthanides could be stabilized by deprotonated **L3**. Reacting **KL3** with divalent $LnI_2(THF)_3$ in THF led to the dinuclear complexes $[Ln(\mathbf{L3})I(THF)_2]_2$ (Ln = Yb (**24**), Sm (**25**)) [39]. The seven-coordinated complex $[La(\mathbf{L3})Br_2(THF)_3]$ (**26**) was prepared by the reaction of **KL3** and $LaBr_3$ in THF [44]. The reaction of **KL3** and $LuCl_3$ afforded the monoaminopyridinate complex $[Lu(\mathbf{L3})Cl_2(THF)_2]$ (**27**). Recrystallization of **27** formed dinuclear $[Lu(\mathbf{L3})Cl_2(THF)_2]_2$ (**28**) (Scheme 7) [43].

In the presence of $NaBH_4$, **24**, **26**, and **27** were efficient initiators for the ring-opening polymerization (ROP) of ε-caprolactone to produce α,ω-dihydroxytelechelic polymers in high yield with high molar mass and moderate molar mass distributions (Scheme 8). NMR evidence indicated that Ln–BH_4 complex was the active site of coordination insertion of ε-caprolactone subsequently polymerized by an Ln–O active species [43].

The aminopyridinato ligand complexes remain of great interest and challenge to synthetic chemists to introduce new substituents (including chiral groups) on pyridine or (and) amido nitrogen and to provide new opportunities for catalytic studies.

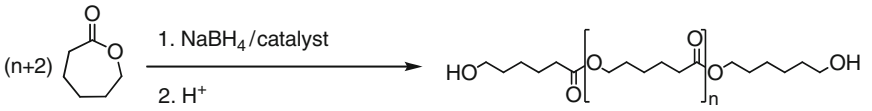

Scheme 8 Polymerization of ε-caprolactone to produce α,ω-dihydroxytelechelic polymers

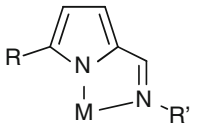

Scheme 9

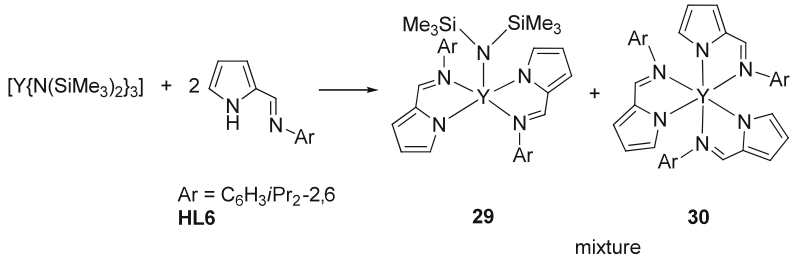

Scheme 10

2.1.2 Pyrrolyl Ligands

Similarly to aminopyridinato ligands, pyrrolyl ligands (also known as iminopyrrole ligands) belong to asymmetric *N*,*N*-bidentate ligands. One of the differences between these two ligand systems is the size of chelating ring in the metal complexes: the pyrrolyl ligand forms a five-membered ring, while the aminopyridinato ligand forms a four-membered ring. Bidentate pyrrolyl ligands can be conveniently prepared by the condensation reaction of 2-formylpyrrole with amines. The electronic and steric properties of the pyrrolyl ligands can be easily tuned by altering the R group on the pyrrole ring and R′ group on the imine (Scheme 9). A variety of metal complexes bearing pyrrolyl ligands have been synthesized and explored as active polymerization catalysts [45].

The first rare-earth metal complexes containing pyrrolyl ligands were reported by Mashima and coworkers [46] in 2001. The reaction of $[Y\{N(SiMe_3)_2\}_3]$ with 2 equiv of the pyrrolyl ligand **HL6** bearing *N*-aryl substituent (R′ = Ar = $C_6H_3iPr_2$-2, 6) led to a mixture of bis-pyrrolyl complex $[Y(\mathbf{L6})_2\{N(SiMe_3)_2\}]$ (**29**) and tris-pyrrolyl complex $[Y(\mathbf{L6})_3]$ (**30**). Only the homoleptic complex **30** was obtained by treating $[Y\{N(SiMe_3)_2\}_3]$ with 3 equiv of **HL6** (Scheme 10) [46].

In 2003, Arnold and coworkers developed a series of bis-pyrrolyl Sm and Y complexes by using the steric more demanding pyrrolyl ligand **L7**. Compared with **L6**, **L7** has a *t*Bu group at 5-position of the pyrrole ring. $[Sm(\mathbf{L7})_2Cl(THF)]$ (**31**) was

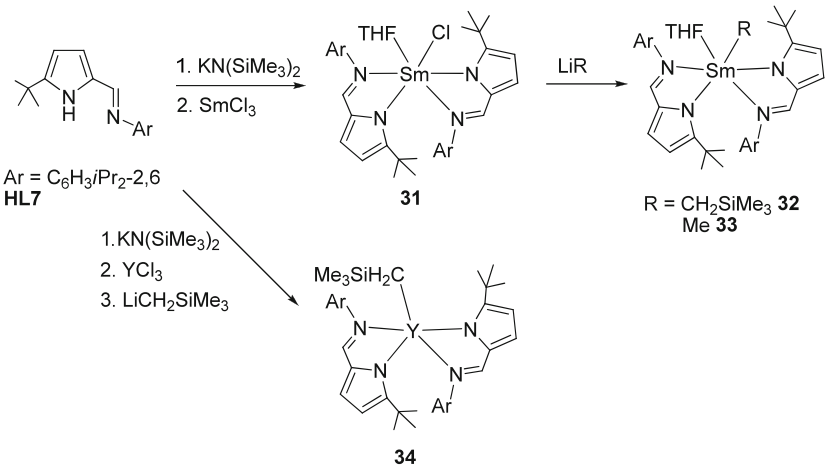

Scheme 11

prepared by the reaction of **KL7** with $SmCl_3$ in THF. The corresponding Sm alkyl complexes [Sm(**L7**)$_2$(THF)(R)] (R = CH_2SiMe_3 (**32**), Me (**33**)) were prepared by the treatment of **31** with LiR in toluene. The yttrium complex [Y(**L7**)$_2$(CH_2SiMe_3)] (**34**) was prepared by using the same method without the isolation of the yttrium chloro complex [Y(**L7**)$_2$Cl(THF)] (Scheme 11) [47].

The alkyl complexes **32–34** were investigated as catalysts for the polymerization of methyl methacrylate (Scheme 12). The samarium complex **32** exhibited high catalytic activity and excellent stereoselectivity in the polymerization at ambient temperature. The bulk polymerization catalyzed by **32** produced significantly high molecular weight isotactic PMMA ($M_n = 1.41 \times 10^6$, $M_w/M_n = 1.31$). The triad contents in PMMA were determined by ^{1}H NMR. The *mm* triad content in the range of 91.3–97.8% was obtained at a wide temperature range (−40 to 65°C). The yttrium complex **34** showed high catalytic activity and relatively low stereoselectivity, while **33** was inactive. The ^{1}H NMR study of **33** showed that the dissociation rate of coordinated THF was too slow to allow the formation of an active enolate species with methyl methacrylate (MMA). In addition, the methyl group in **33** may directly attack the MMA carbonyl to deactivate the initiator [47].

Recently, Cui and coworkers prepared many other rare-earth metal complexes containing **L6** (Scheme 13) and an analogous ligand **L8** bearing *N*-aryl substituent (R′ = Ar = $C_6H_3Me_2$-2, 6) (Scheme 13). The catalytic activity of the complexes in the polymerization of lactides or isoprene was investigated [48, 49]. In the reaction of [Y(CH_2SiMe_3)$_3$(THF)$_2$] with 1 equiv of **HL6**, the pyrrolyl ligand was deprotonated by –CH_2SiMe_3 and its C=N was reduced to C–N by intramolecular alkylation, generating a THF-coordinated bimetallic yttrium complex **35** that was bridged by two dianionic pyrrolylaldiminate ligands, in which the pyrrolyl ring acted as a heterocyclopentadienyl ligand. The reaction of [Ln(CH_2SiMe_3)$_3$(THF)$_2$] (Ln = Sc, Y, and Lu) with 2 equiv of **HL6** led to the monomeric bis-pyrrolyl

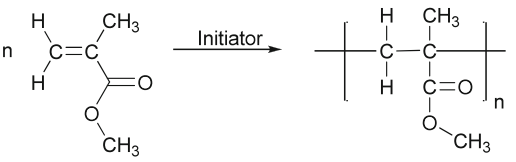

Scheme 12 Polymerization of methyl methacrylate

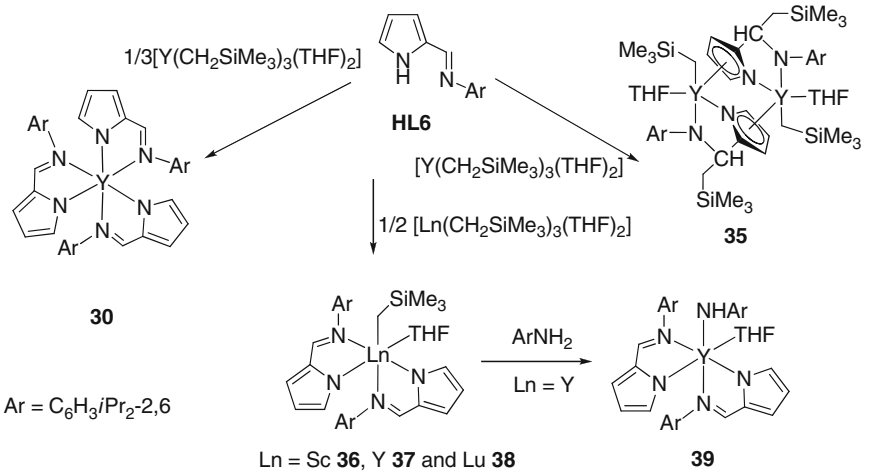

Scheme 13

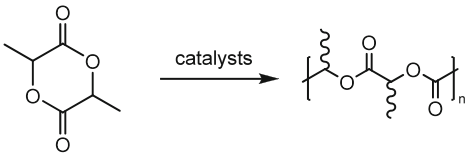

Scheme 14 Polymerization of lactide

complexes [Ln(**L6**)$_2$(CH$_2$SiMe$_3$)] (Ln = Sc (**36**), Y (**37**), Lu (**38**)), respectively. The reaction of [Ln(CH$_2$SiMe$_3$)$_3$(THF)$_2$] (Ln = Sc, Lu) with even 1 equiv of **HL6** selectively formed bis-pyrrolyl complexes **36** and **38**. Amination of **37** with 2,6-diisopropylaniline gave the corresponding yttrium amido complex **39**. The previously reported [46] tris-pyrrolyl yttrium complex **30** could also be prepared by reacting **HL6** with [Y(CH$_2$SiMe$_3$)$_3$(THF)$_2$] in 3:1 molar ratio (Scheme 13) [48, 49]. **35**, **37**, **39**, and **30** were investigated for the polymerization of D,L-lactide (Scheme 14). Atactic polylactides with high molecular weight and narrow molecular weight distribution were obtained in the polymerization catalyzed by **35**, **37**, and **39**. Compared with the dinuclear complex **35**, **37** and **39** were real "single-site" catalysts and exhibited higher catalytic activity and more controllable polymerization.

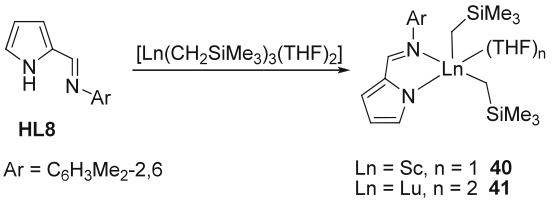

Scheme 15

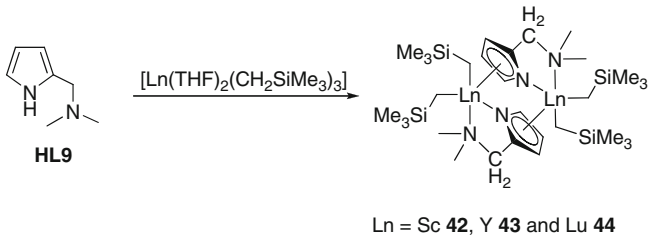

Scheme 16

30 is not an active catalyst for the polymerization of lactide. This fact might be due to the less active chelating Y–N initiator in **30** than Y–C initiator in **35**, **37**, and **39** [48].

Monopyrrolyl ligand complexes [Ln(**L8**)$(CH_2SiMe_3)_2(THF)_n$] (Ln = Sc, n = 1 (**40**); Ln = Lu, n = 2 (**41**)) were prepared by the reaction of [Ln$(CH_2SiMe_3)_3(THF)_2$] (Ln = Sc, Lu) with 1 equiv of **HL8**, respectively (Scheme 15) [49].

Pyrrolyl-like ligand 2,2-dimethyl-aminomethylpyrrole **HL9** was used by Cui and coworkers to synthesize aminomethylpyrrole ligand complexes [Ln(μ-**L9**)$(CH_2SiMe_3)_2]_2$ (Ln = Sc (**42**), Y (**43**), Lu (**44**)). **42–44** were prepared by reacting [Ln$(CH_2SiMe_3)_3(THF)_2$] (Ln = Sc, Y, Lu) with 1 equiv of **HL9**, respectively, and showed a similar structure to **35** (Scheme 16).

In the presence of $AlEt_3$ and $[Ph_3C][B(C_6F_5)_4]$, **40**, **41**, and **43** showed catalytic activity for isoprene polymerization (Scheme 17). The resulting polyisoprene had a predominant *cis*- or *trans*-configuration. The Sc metal center of **40** with the smaller ionic radius and five coordination ligands around is electronically more positive than the Lu metal center in **41**. As a result, **40** is more accessible to the insertion of the nonpolar monomer isoprene and is a more active catalyst than **41** and **43** [49].

2.1.3 Indolide-Imine Ligands

Similarly to aminopyridinato and pyrrolyl ligands, indolide-imine ligands are asymmetric *N*,*N*-bidentate ligands. They form a six-membered chelating ring around the metal center. In 2008, Cui and coworkers [50] initiated the investigation of rare-earth metal complexes containing indolide-imine ligands.

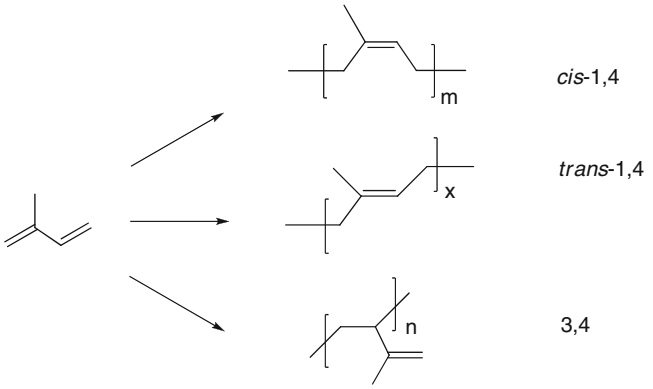

Scheme 17 Polymerization of isoprene

Two indolide-imine ligands **L10** and **L11** were introduced into a series of scandium and lutetium complexes. The reaction of **HL10** or **HL11** with $[Ln(CH_2SiMe_3)_3(THF)_2]$ (Ln = Sc, Lu) led to monoligand bis-alkyl complexes $[Ln(\mathbf{L})(CH_2SiMe_3)_2(THF)]$ (**L** = **L10**, Ln = Sc (**45**) and Lu (**46**); **L** = **L11**, Ln = Sc (**47**) and Lu (**48**)) or bis-ligand mono-alkyl complex $[Lu(\mathbf{L11})_2(CH_2SiMe_3)]$ (**49**). Lutetium amidinate complexes $[Lu(\mathbf{L10})\{i\,Pr_2NC(CH_2SiMe_3)N i\,Pr_2\}_2]$ (**50**) and $[Lu(\mathbf{L11})_2\{i\,Pr_2NC(CH_2SiMe_3)N i\,Pr_2\}]$ (**51**) were prepared by the reaction of *N*,*N*′-diisopropylcarbodiimide with **46** and **49**, respectively (Scheme 18).

All the complexes in Scheme 18 were investigated as catalysts for isoprene polymerization (Scheme 17). **45–48** or **51** together with aluminum alkyl and borate as cocatalysts generated a homogeneous single-site catalytic system, showed high *cis*-1,4-selectivity, and produced high molecular weight polyisoprene with narrow molecular weight distribution. Scandium complexes **45** and **47** exhibited higher activity than lutetium complexes **46** and **48**. This fact proved that the Lewis-acidic scandium metal center was in favor of the insertion of monomer. By the fact that the lower activity of the amidinate complexes **50** and **51** compared with the alkyl complexes **45–48**, Ln-η^3-NCN was less accessible than Ln–C to the monomer insertion. The *cis*-1,4-selectivity of this catalytic system was highly affected by the steric effect from the *ortho*-substituent of *N*-aryl ring on the ligand. The bulkier substituent generated the greater steric effect around the metal center and led to the high *cis*-1, 4-selectivity. Additionally, the choice of aluminum alkyl and borate, and polymerization temperatures have large influence on both the catalytic activity and the regioselectivity [50].

2.1.4 Anilido-Phosphinimine Ligands

Anilido-phosphinimines are another group of asymmetric monoanionic bidentate ligands, similar to anilido-imine ligands deriving from aniline-imines **I** (Scheme 19) [51]. Anilido-phosphinimines are obtained by deprotonation of the corresponding

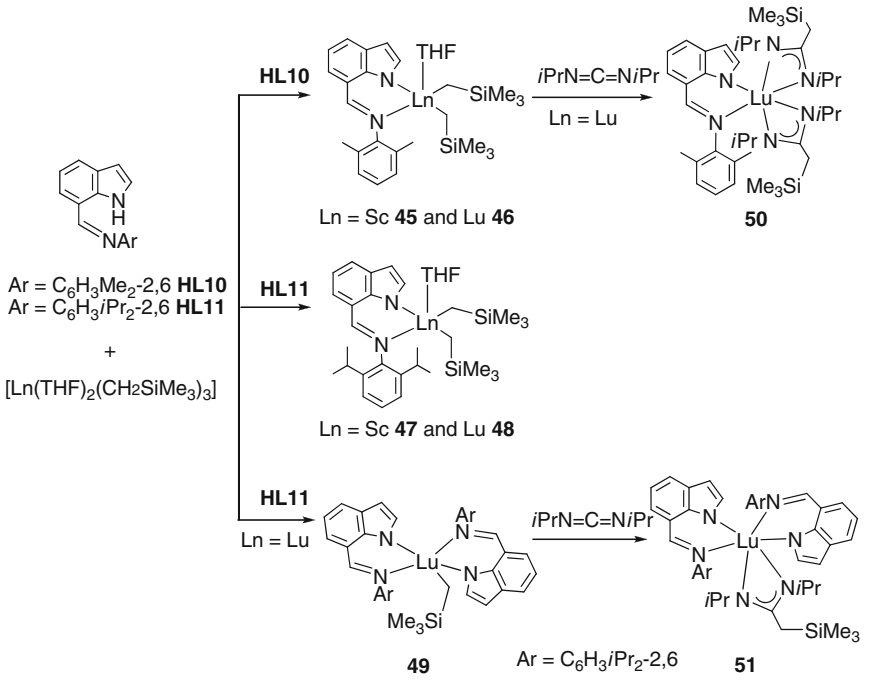

Scheme 18

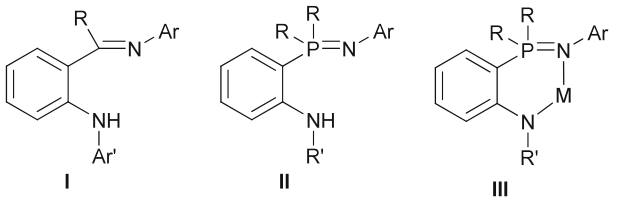

Scheme 19

aniline-phosphinimines **II** and form six-membered metallacycles **III** upon coordination of the nitrogen atoms on a metal center (Scheme 19). Only a few examples of anilido-phosphinimine rare-earth metal complexes have been reported in the literature. Anilido-phosphinimine ligands were used by Piers and coworkers [52] for stabilizing organoyttrium cations.

Investigation of the catalytic activity of anilido-phosphinimine rare-earth metal complexes was exclusively reported by Cui and coworkers. Various anilido-phosphinimine rare-earth metal complexes were synthesized by deprotonation of aniline-phosphinimines **II-A** with $[Ln(CH_2SiMe_3)_3(THF)_2]$ [53]. Interestingly, the deprotonation of **II-A** was followed by intramolecular C–H activation of the phenyl group on the phosphine moiety to generate dianionic ligands which coordinated to the metal center in a *C*,*N*,*N*-tridentate mode. The resulting complexes

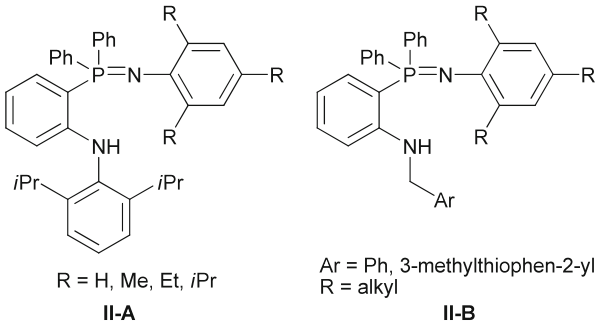

Scheme 20

showed high activity in the ROP of D,L-lactide (Scheme 14) [53]. There was no such C–H activation observed by using aniline-phosphinimines **II-B** (Scheme 20). Deprotonation of **II-B** with $[Ln(CH_2SiMe_3)_3(THF)_2]$ led to monoanionic ligands which coordinated to the metal center in a *N*,*N*-bidentate mode [54].

By using type **II-B** aniline-phosphinimines (Scheme 20), various bisalkyl rare-earth metal complexes were synthesized. All complexes **52–58** were obtained by the reaction of the corresponding aniline-phosphinimines **HL12–HL15** with $[Ln(CH_2SiMe_3)_3(THF)_2]$ (Ln = Sc, Y, Lu) in toluene via alkyl elimination (Scheme 21) [54].

The catalytic activity of complexes **52–58** in the presence of various cocatalysts composed of aluminum alkyls and borates or boranes was investigated for the polymerization of butadiene (Scheme 17) [54]. The catalytic activity was strongly influenced by the type of aluminum alkyls, in the sequence $AlEt_3 \geq Al\mathit{i}Bu_3 > AlMe_3$. The *trans*-1,4-selectivity was strongly affected by the bulkiness of aluminum alkyls, in the sequence $Al\mathit{i}Bu_3$ (91%) > $AlEt_3$ (89%) > $AlMe_3$ (82%). Both the catalytic activity and the *trans*-1,4-selectivity were only slightly affected by the type of borates and boranes. Investigation of the metal center effect with scandium, lutetium, and yttrium complexes **54**, **55**, and **56** showed the catalytic activity in the sequence of Y > Sc > Lu and the *trans*-1,4-selectivity in the sequence of Sc > Lu > Y. The catalytic activity was strongly influenced by the bulkiness of the *ortho*-substituents on the *N*-aryl ring of the ligand. With increasing the bulkiness, the catalytic activity decreased. The same behavior was observed for the *trans*-1,4-selectivity. **52** bearing *ortho*-methyl substituents and **54** bearing *ortho*-ethyl substituents exhibited a *trans*-1,4-selectivity of 91%. With the higher bulkiness of the *ortho*-substituents in **57** bearing *iso*-propyl groups, the *trans*-1,4-selectivity decreased (81%). The influence of the thiophenyl group of the ligands was investigated by comparison of the activity of **58** bearing a phenyl substituent, with the scandium analogous **52**, **54**, and **57** bearing the thiophenyl moiety. **58** showed the highest activity and a *trans*-1,4-selectivity (84%) similar to that of **57** (81%), but lower than that of **52** (91%) and **54** (91%). In summary, all complexes **52–58** showed moderate activity and predominant *trans*-1,4-selectivity for the polymerization of butadiene.

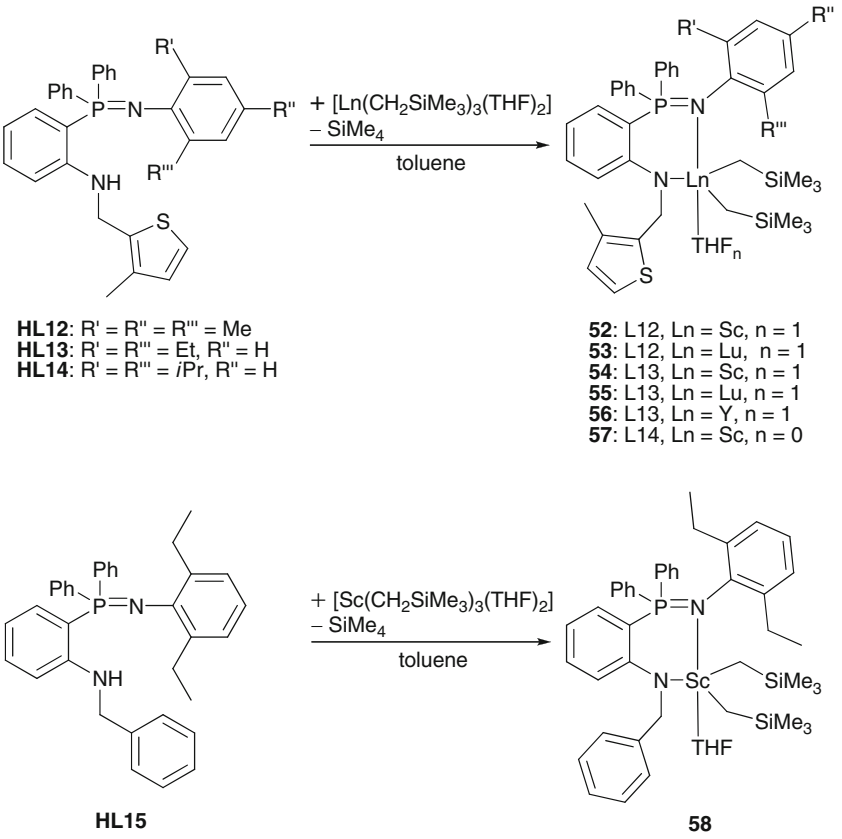

Scheme 21

2.1.5 β-Diketiminato Ligands

The β-diketiminato derivatives have been widely used in inorganic and organometallic chemistry due to their strong metal–ligand bonds and simple synthetic modifications to fine-tune steric and electronic effects by altering substituents on the ligand. In many cases, β-diketiminato are a group of symmetric *N*,*N*-bidentate ligands. Numerous β-diketiminate metal complexes were found to be effective catalysts for the polymerization reactions and organic transformations [55].

Most commonly, β-diketimines are prepared by the condensation reaction of a primary amine with either a β-diketone or a 1,1,3,3-tetraethoxypropane. Two categories **A** and **B** of β-diketiminato ligands distinguished by their electronic and steric properties are shown in Scheme 22. Category **A** ligands restrain *N*-substituent R^1 and R^2 as $SiMe_3$ group and are varied by altering aryl or alkyl groups as R^3 and R^4 substituent. Alternatively, category **B** ligands are varied by varying aryl groups as R^1 and R^2 substituent and alkyl groups as R^3 and R^4 substituent [56].

In 2002, a comprehensive review by Lappert and coworkers [55] described the preparation and the characterization of β-diketiminato ligands and their metal

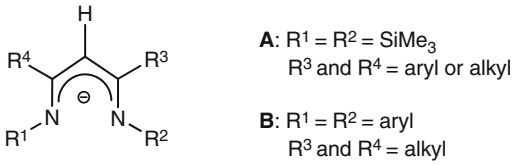

Scheme 22

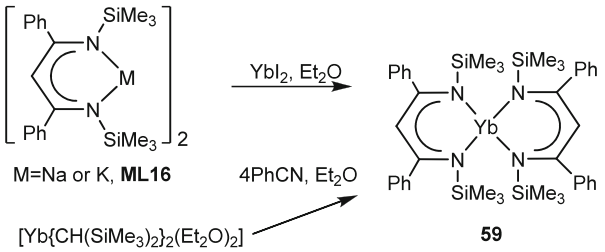

Scheme 23

complexes. Rare-earth metal β-diketiminato complexes and their catalytic activities were briefly mentioned in other reviews as well [28, 57–62].

In 1994, the first rare-earth metal β-diketiminato complexes were reported by Lappert and coworkers for a category **A** complex and by Drees and Magull for category **B** complexes [63, 64]. Ytterbium(II) bis-β-diketiminato complex **59** was obtained by treating YbI_2 with a potassium or sodium salt of β-diketiminate **ML16** (category **A**). Alternatively, **59** also could be prepared by 4 equiv of α-hydrogen-free nitrile (PhCN) insertion into Yb–C bond in $[Yb\{CH(SiMe_3)_2\}_2(Et_2O)_2]$ (Scheme 23) [63].

Followed by the early discoveries of **59**, Lappert and coworkers extended **L16** to many other lanthanide bis-β-diketiminato complexes, that is, trivalent complexes, [Ce(**L16**)$_2$Cl] (**60**), [Pr(**L16**)$_2$Cl] (**61**), [Nd(**L16**)$_2$Cl] (**62**), [Sm(**L16**)$_2$Cl] (**63**), [Yb(**L16**)$_2$Cl] (**64**), [Tm(**L16**)$_2$I] (**65**), and divalent complexes [Sm(**L16**)$_2$(THF)$_2$] (**66**) and [Yb(**L16**)$_2$(THF)$_2$] (**67**). The crystal structure of [Nd(**L16**)$_2$Cl] (**62**) disclosed that the metal center was well shielded and not accessible, as a result of the extreme sterical hinderal of ligand **L16**. The effort of replacing the chloride from [Ce(**L16**)$_2$Cl] (**60**) with the bulky alkyl $\{CH(SiMe_3)_2\}^-$ led to the mono-β-diketiminato complex [Ce(**L16**)$(CH(SiMe_3)_2)_2$] (**68**) (Scheme 24) [65].

In addition to the homoleptic Yb(II) complex **59**, Lappert and coworkers synthesized a series of mononuclear Yb(II) complexes (**69–72**) via salt elimination by using a variety of categories **A** ligands (**L17–L20**) (Scheme 25) [66]. The X-ray crystal structures of complexes **59**, **69**, and **71** were obtained and showed a distorted tetrahedral geometry. NMR experiments indicated that two isomers with similar structures were present for **71** and **72** with the asymmetric ligands **L19** and **L20** [65, 66]. Although [Zr(**L20**)Cl_3] was patented as an active catalyst for olefin polymerization [55], none of the rare-earth metal complexes with category **A** ligands have been reported as active catalysts.

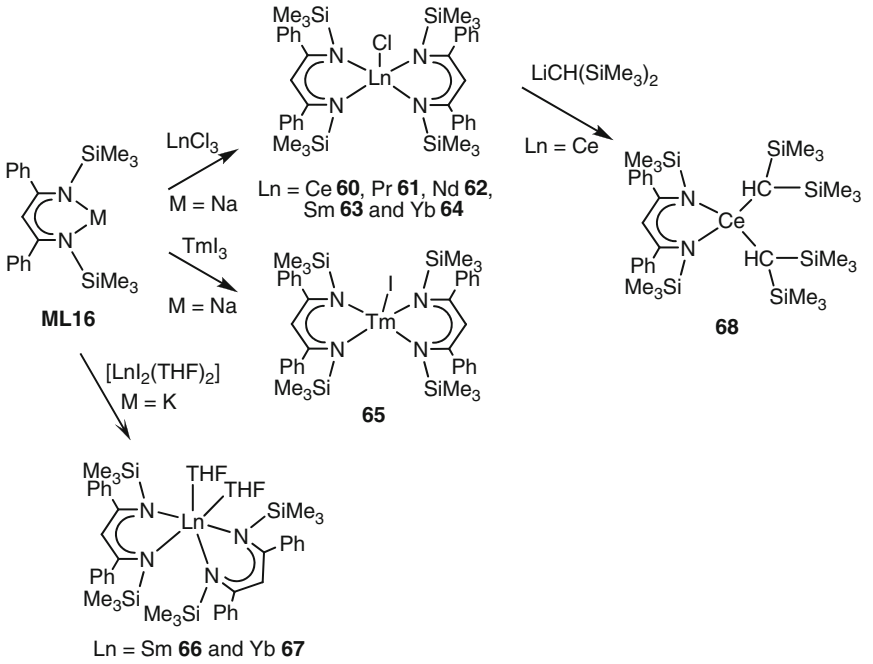

Scheme 24

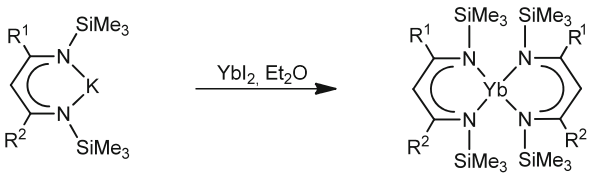

KL16	$R^1 = R^2$ = Ph	**59**
KL17	$R^1 = R^2 = C_6H_4$Ph-4	**69**
KL18	$R^1 = R^2 = C_6H_4$Me-4	**70**
KL19	$R^1 = C_6H_4$Me-4, R^2 = 1-adamantyl	**71**
KL20	R^1 = Ph, R^2 = *t*Bu	**72**

Scheme 25

In 1994, Drees and Magull prepared mono-, bis-, and tris-β-diketiminato ligand lanthanide (samarium(III) and gadolinium(III)) complexes via salt metathesis by using lithium salts of β-diketiminate, **LiL21** (category **B**). The reaction of **LiL21** with $GdBr_3$ led to a monoligand complex [Gd(**L21**)Br_2(THF)$_2$] (**73**). On the contrary, a tris-ligand complex [Sm(**L21**)$_3$] (**74**) was prepared by the reaction of **LiL21** and SmI_2 via disproportionation of an unstable intermediate Sm(II) complex [Sm(**L21**)$_3$]$^-$. Sm metal was a byproduct of the disproportionation reaction. The similar complex [Gd(**L21**)$_3$] (**75**) could be formed from the reaction of [Gd(OC_6H_3tBu$_2$-2, 6)$_3$] and **LiL21** in a 1:3 ratio (Scheme 26) [64, 67].

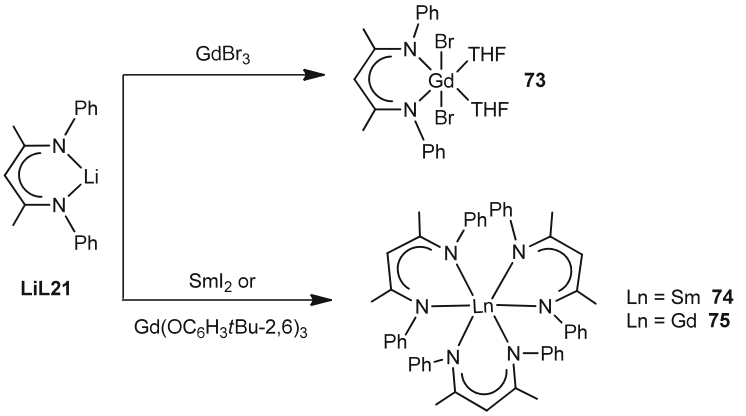

Scheme 26

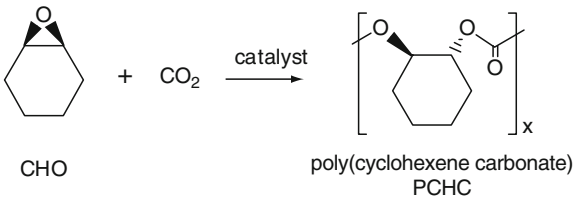

Scheme 27 Polymerization of cyclohexene oxide (CHO) and CO_2 to produce polycarbonates

Zr complexes of **L21** showed catalytic activity for ethylene polymerization [68, 69]. In addition, Coates and coworkers discovered that the β-diketiminate Zn alkoxide bridging complexes have surprisingly high catalytic activity for cyclohexene oxide (CHO) and CO_2 polymerization to produce polycarbonates under mild conditions (Scheme 27) [70].

Hultzsch and coworkers employed **L21** and another similar ligand **L22** with modified *N*-aryl substituents in lanthanum and yttrium and presented the first homogeneous rare-earth metal catalysts for CHO and CO_2 copolymerization. [Y(**L21**)$_2${N(SiHMe$_2$)$_2$}] (**76**), [Y(**L21**)$_3$] (**77**), and [Y(C$_5$Me$_5$)(**L21**){N(SiHMe$_2$)$_2$}] (**78**) were prepared via amine elimination by reacting **HL21** with [Y{N(SiHMe$_2$)$_2$}$_3$(THF)$_2$] and [Y(C$_5$Me$_5$){N(SiHMe$_2$)$_2$}$_2$(THF)], respectively (Scheme 28). [Ln(**L22**){N(SiHMe$_2$)$_2$}$_2$] (Ln = La (**79**), Y (**80**)) and [La(**L22**){N(SiMe$_3$)$_2$}$_2$] (**81**) were prepared by reacting **HL22** with [Ln{N(SiHMe$_2$)$_2$}$_3$(THF)$_2$] or [La{N(SiMe$_3$)$_2$}$_3$] (Scheme 29). **76**, **78**, and **79–81** exhibited moderate catalytic activity in the copolymerization of CHO and CO_2 [71, 72].

In 2008, Cui and coworkers isolated [Lu(**L21**)(CH$_2$SiMe$_3$)$_2$(THF)] (**82**) and [Ln(**L22**)(CH$_2$SiMe$_3$)$_2$(THF)] (Ln = Y (**83**), Lu (**84**)) from the reaction of **HL21** or **HL22** with [Lu(CH$_2$SiMe$_3$)$_3$(THF)$_2$] via alkane elimination (Scheme 30). **82–84** were active catalysts for the copolymerization of CHO and

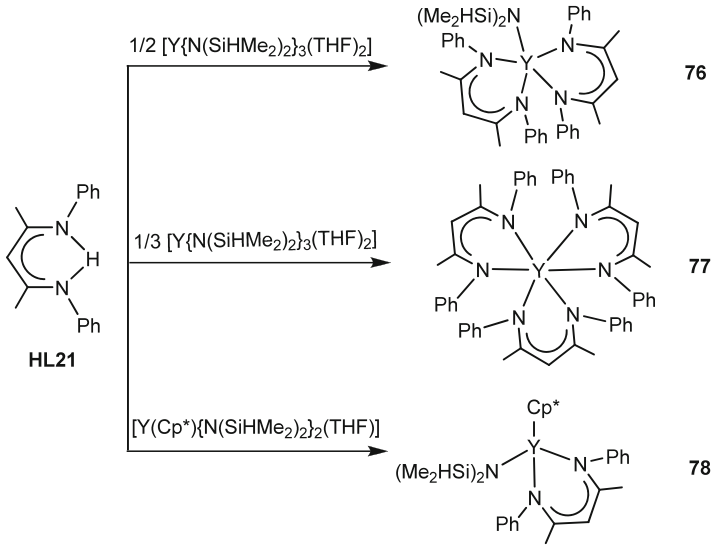

Scheme 28

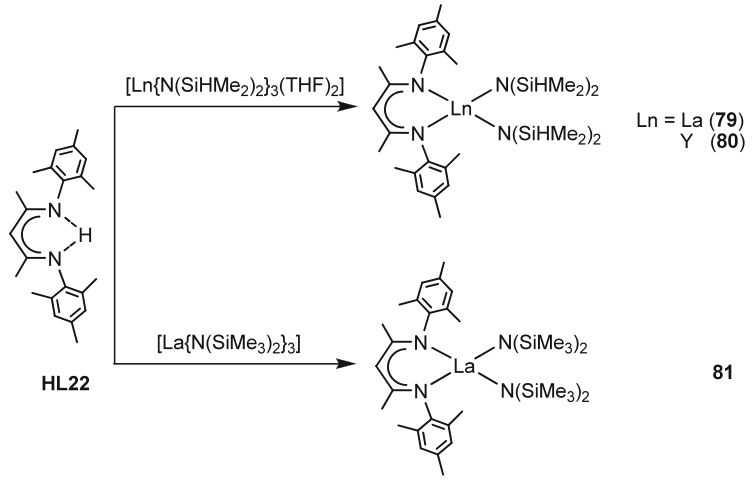

Scheme 29

CO_2 as single-component catalysts. After systematic investigation of a series of β-diketiminate rare-earth metal complexes, they suggested that the center metal with larger ionic radius and less steric hinder was beneficial for the copolymerization of CHO and CO_2 [73].

Category **B** ligand **L23** is a very similar ligand to **L22** with modified *N*-aryl substituents (Ar = $C_6H_2Me_2$-2,6). Lanthanide dichloride complexes [Ln(**L23**)Cl_2(THF)$_2$] (Ln = Yb (**85**), Nd (**86**)) were prepared by the metathesis reaction of **LiL23** with anhydrous $LnCl_3$ in THF at room temperature.

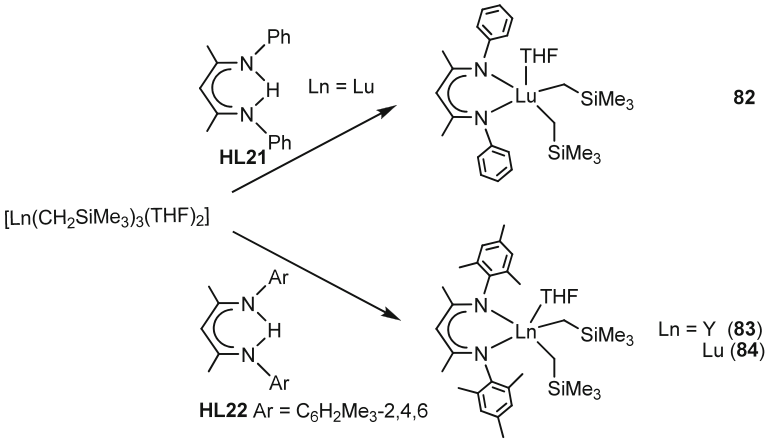

Scheme 30

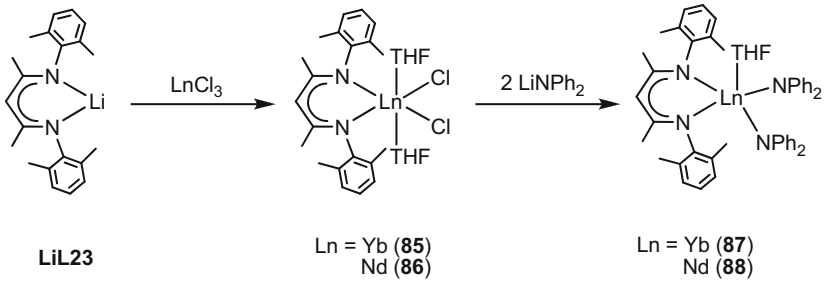

Scheme 31

The reaction of **85** or **86** with 2 equiv of $LiNPh_2$ in THF led to the salt-free complexes [Ln(**L23**)$(NPh_2)_2$(THF)] [Ln = Yb (**87**), Nd (**88**)] (Scheme 31). Both **87** and **88** showed good catalytic activity for the polymerization of acrylonitrile to form polyacrylonitrile. The catalytic activity was affected by catalyst concentration, solvent, and temperature, while the molecular weight of resulting polymer was independent of temperature. **87** and **88** exhibited high catalytic activity for the ROP of ε-caprolactone to produce α,ω-dihydroxytelechelic polymers at room temperature (Scheme 8). The catalytic system yielded high molecular weight polymers ($M_n > 10^4$) with relatively narrow molecular weight distributions (M_w/M_n = 1.35–1.90). The order of catalytic activity **88** > **87** was observed, which was in agreement with the trend of ionic radius $Nd^{3+} > Yb^{3+}$ [74].

Compared to ligands **L22** and **L23**, **L24** is a bulkier β-diketiminate ligand by altering methyl with *iso*-propyl on *N*-aryl substituents on **L23**. **L24** has been broadly used in rare-earth metal chemistry and many interesting complexes have been studied.

The triple chloro bridging dinuclear β-diketiminate ytterbium complex [Yb(**L24**)Cl(μ-Cl)$_3$Yb(**L24**)(THF)] (**89**) was an unexpected product from

recrystallization in toluene of the complex [Yb(**L24**)$(THF)_2(Cl)_2$] (**90**), which resulted from the reaction of **LiL24** and $YbCl_3$ [75]. Chloro bridges in **89** could be cleaved by donor solvents, such as DME, to produce the monomeric complex [Yb(**L24**)Cl_2(DME)] (**91**), which is a versatile precursor for the preparation of β-diketiminate ytterbium monoamido complexes. Reacting **91** with 1 equiv of Li*N*iPr_2 in THF led to the anionic β-diketiminate ytterbium amido complex [Yb(**L24**)(N*i*Pr_2)(μ-Cl)$_2$Li$(THF)_2$] (**92**), while the similar reaction of **91** with $LiNPh_2$ led to the neutral complex [Yb(**L24**)(NPh_2)Cl(THF)] (**93**). Recrystallization of **92** from toluene at elevated temperature resulted in the neutral chloro bridging β-diketiminate amido complex [Yb(**L24**)(N*i*Pr_2)(μ-Cl)]$_2$ (**94**), which also can be prepared by the reaction of **91** with 1 equiv of Li*N*iPr_2 in toluene directly. $LiNC_5H_{10}$ reacted with **91** in toluene to prepare the neutral β-diketiminate amido complexes [Yb(**L24**)(NC_5H_{10})(THF)(μ-Cl)]$_2$ (**95**). Synthetic routes for **89–95** are shown in Scheme 32 [76].

93–95 exhibited good catalytic activity for the polymerization of MMA to form PMMA (Scheme 12). The amido group had a significant influence on the catalytic

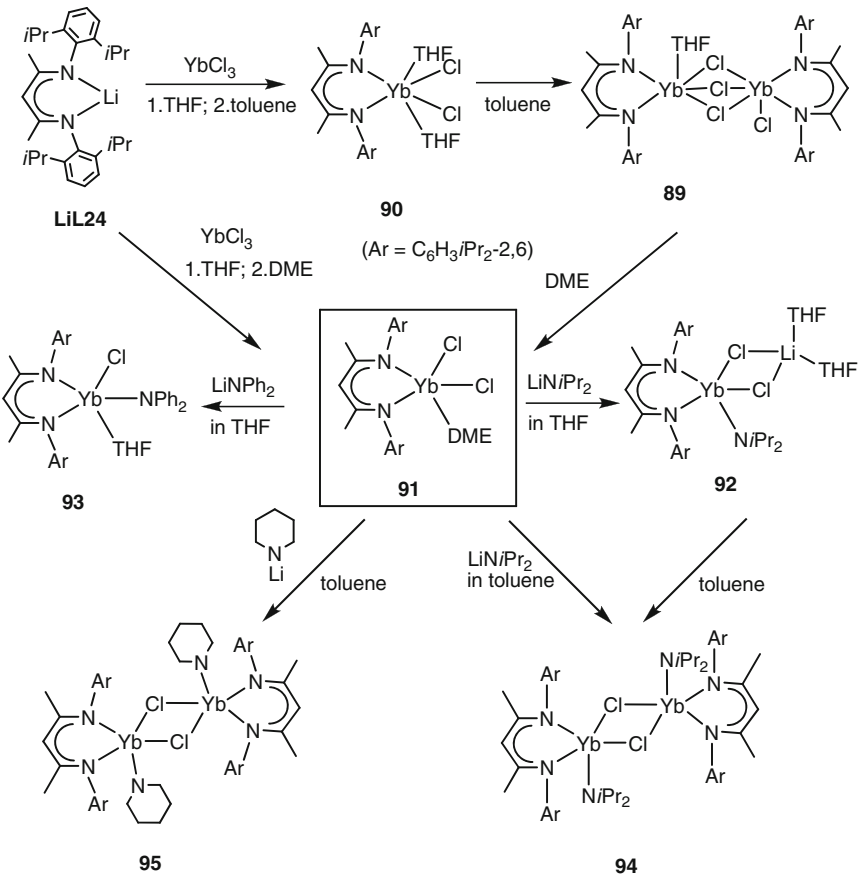

Scheme 32

activity. The activity order for the complexes was observed as **93** < **94** < **95** or $NPh_2 < NiPr_2 < NC_5H_{10}$, which was contrary to the order of the Yb–N (amido) bond lengths. However, the activity of these complexes was still lower than that of lanthanocene amido complexes. **93–95** proved to be more efficient catalysts than lanthanocene amido complexes for the ROP of ε-caprolactone (Scheme 8). The fact of stronger electron-donating ability of β-diketiminate ligand than that of cyclopentadienyl ligand suggested that increasing electron density of the ligand around the metal center might be beneficial to the catalytic activity for polymerization of ε-caprolactone. However, the molecular weight distribution of the resultant polymers was relatively broad ($M_w/M_n = 1.43$–1.71). The intramolecular transesterification caused by the metal complexes might be responsible for the low molecular weight and broad molecular weight distribution [76].

Tris(η^3-allyl) complexes [La(η^3-allyl)$_3$(dioxane)]$_2$(μ-dioxane) and [Ln(η^3-allyl)$_3$(μ-dioxane)] (Ln = Y, Sm, Nd) were prepared by the one-pot reaction of $LnCl_3(THF)_n$ (Ln = La, $n = 4$; Ln = Y, Sm, Nd, $n = 3$) with 3 equiv of allyl-MgCl in THF/1,4-dioxane followed by crystallization in 1,4-dioxane/toluene. The reaction of tris-ally complexes with the β-diketimine **HL24** in THF at 60°C led to [Ln(η^3-allyl)$_2$(**L24**)] (Ln = La (**96**), Y (**97**), Sm (**98**), Nd (**99**)) (Scheme 33). They are the first isolated mixed-ligand lanthanide allyl complexes [77].

All complexes mentioned above were highly effective single-component catalysts for the ROPs of ε-caprolactone (Scheme 8) and rac-lactide (Scheme 14) without the need of an activator. The metal radius was influential to the catalytic activity. Both polymerization catalysis rates decreased in the trend of **96** > **99** > **98** > **97**, in agreement with the decrease in metal ion radii (La > Nd > Sm > Y). The investigation of polymer end group showed that the polymer chain growth was initiated by allyl transfer to monomer [77].

Following the exploration of many catalytic applications in the rare-earth metal complexes containing **L24**, Lappert and coworkers recently described the

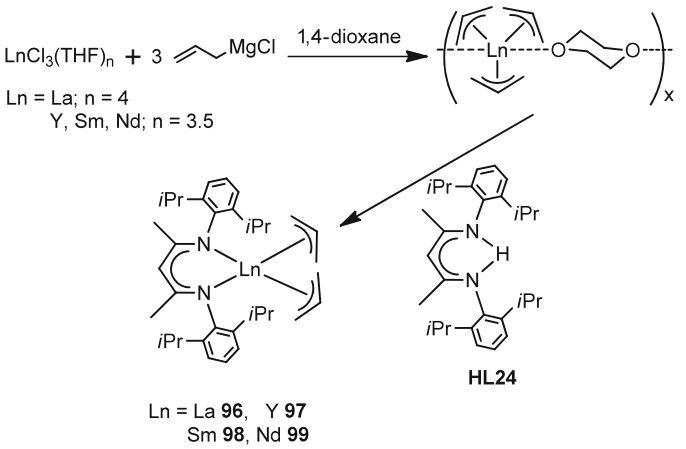

Scheme 33

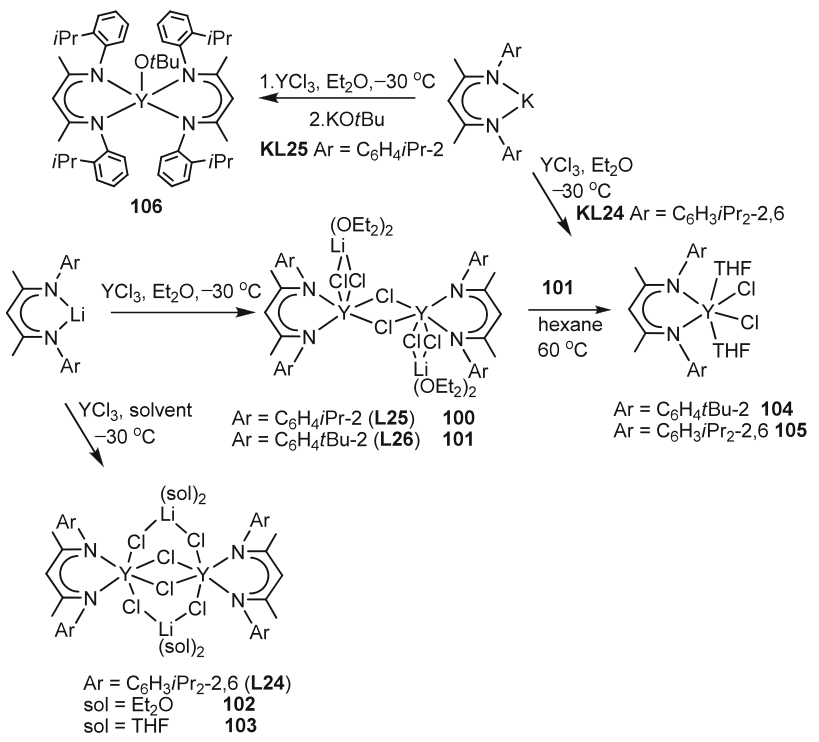

Scheme 34

synthesis of a series of β-diketiminate yttrium complexes **100–106** stabilized by **L24**, and other two similar category **B** ligands **L25** and **L26**. The reaction of 1 equiv of lithium salts of **L25** or **L26** and YCl_3 in Et_2O under mild conditions led to $[Y(\mu\text{-Cl})(\mathbf{L})(\mu\text{-Cl})_2Li(OEt_2)_2]_2$ (**L** = **L25** (**100**) or **L26** (**101**)) and $[Y(\mu\text{-Cl})(\mathbf{L24})(\mu\text{-Cl})Li(solv)_2(\mu\text{-Cl})]_2$ (sol = Et_2O (**102**), THF (**103**)). Each of the $Li(OEt_2)_2Cl_2$ moieties is bonded in a terminal (**100** and **101**) or bridging (**102** and **103**) mode with respect to the two yttrium atoms; the structural difference could be caused by the greater steric effect of **L24** than that of **L25** or **L26**. Recrystallization of **101** in hexane at 60°C gave the mononuclear yttrium complex $[Y(\mathbf{L26})Cl_2(THF)_2]$ (**104**). The similar complex **105** was directly synthesized from YCl_3 and **KL24**. The first bis-β-diketiminate rare-earth metal alkoxide, $[Y(\mathbf{L25})_2(O\mathit{t}Bu)]$ (**106**) was prepared by reacting 2 equiv of **KL25** with YCl_3 and KO*t*Bu at −30°C (Scheme 34) [78].

For comparison of category **A** ligand **L16** and category **B** ligand **L24**, Yb(II) complexes were performed by Lappert and coworkers. Dinuclear heteroleptic Yb(II) iodo complexes (**107** and **108**) were prepared via salt elimination or ligand redistribution (Scheme 35) [56].

Reactivity studies of **107** and **108**, which stabilized by **L16** (category **A**) and **L24** (category **B**) ligands, demonstrated that category **B** ligands are more versatile. The studies discovered many synthetic routes to novel heteroleptic

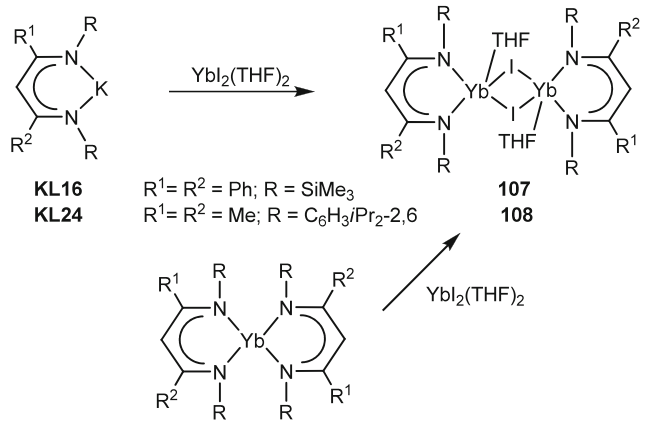

Scheme 35

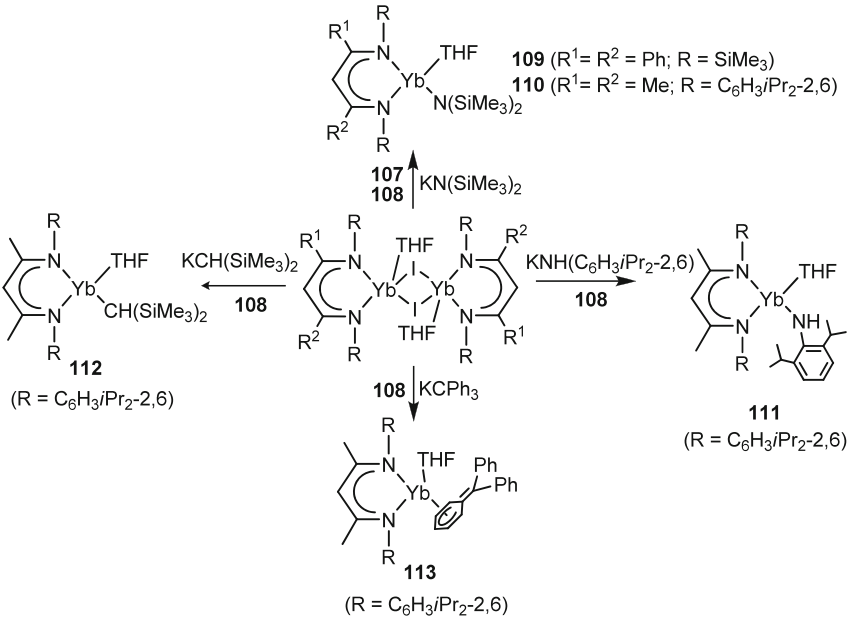

Scheme 36

Yb(II) β-diketiminato complexes (**109–113**). The reaction of **107** or **108** with $KN(SiMe_3)_2$ yielded the mononuclear amido complex [Yb(**L**){$N(SiMe_3)_2$}(THF)] (**L** = **L16** (**109**) or **L24** (**110**)). **108** with K{$NH(C_6H_3iPr_2$–2,6)} resulted in [Yb(**L24**){$NH(C_6H_3iPr_2$-2,6)}(THF)] (**111**). The treatment of **108** with slightly less than 1 equiv of K{$CH(SiMe_3)_2$} afforded [Yb(**L24**){$CH(SiMe_3)_2$}(THF)] (**112**). **108** reacted with $KCPh_3$ in THF yielding [Yb(**L24**)($C_6H_5CPh_2$)(THF)] (**113**) (Scheme 36) [56].

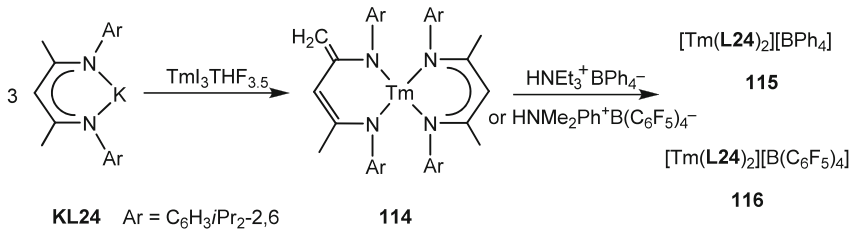

Scheme 37

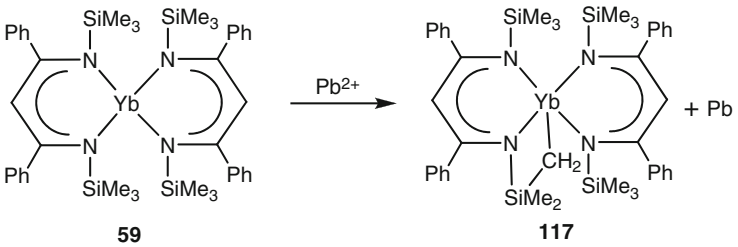

Scheme 38

Attempted synthesis of sterically demanding bis- or tris-β-diketiminato ligand (**L24**) complexes of thulium resulted in a ligand deprotonation product **114**, including both a normal and a deprotonated ligand. Protonation of **114** led to the first cationic β-diketiminato lanthanide complexes **115** and **116**, remarkable for containing a potentially highly electrophilic cation (Scheme 37).

A similar complex [Yb(**L16**)(**L16**^{dep})] (**117**) was prepared by oxidation of **59** with Pb^{2+} (Scheme 38). The single crystal X-ray structure of **117** revealed that **L16**^{dep} is the *C*,*N*,*N*-tridentate bicyclic ligand as a result of C–H activation on silane [79].

Since Piers and coworkers [80] reported the first scandium β-diketiminate complexes by using category **B** ligands in 1999, a few scandium β-diketiminate complexes have been revealed to be highly active catalysts for the polymerization of ethylene and the intramolecular hydroamination [81, 82].

The reaction of $ScCl_3(THF)_3$ with the lithium salts of the ligands ArNC(R)CHC(R)NAr (Ar = C_6H_3iPr-2,6R = Me (**L24**), *t*Bu (**L27**)) afforded [Sc(**L24**)Cl_2(THF)] (**118**) and [Sc(**L27**)Cl_2] (**119**). [Sc(**L24**)Me_2] (**120**) and [Sc(**L27**)Me_2] (**121**) could be prepared by alkylation with methyllithium (Scheme 39) [80].

The base-free dimethyl Sc complex **121** was a highly active catalyst precursor for ethylene polymerization under $B(C_6F_5)_3$, trityl borate, or methylaluminoxane (MAO)-type activation. The catalytic activity of **121** was similar to those observed of Group 4 metallocene complexes [81]. Generally, cationic scandium complexes are believed to be the active species. Activation of the catalyst was studied by reacting **120** and **121** with various equivalences of $B(C_6F_5)_3$. The monomeric bulky *t*Bu-substituted dimethyl complex **121** reacted with 1 equiv of $B(C_6F_5)_3$

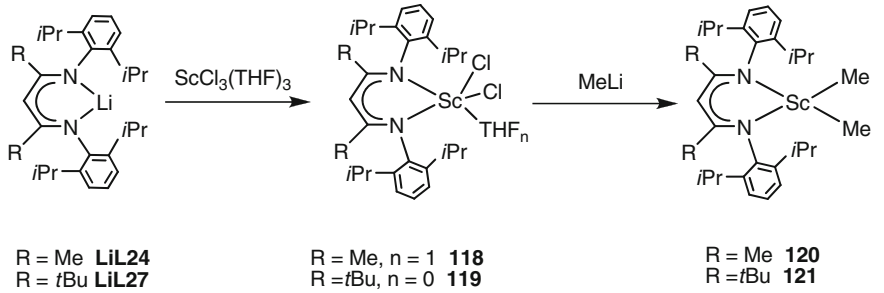

Scheme 39

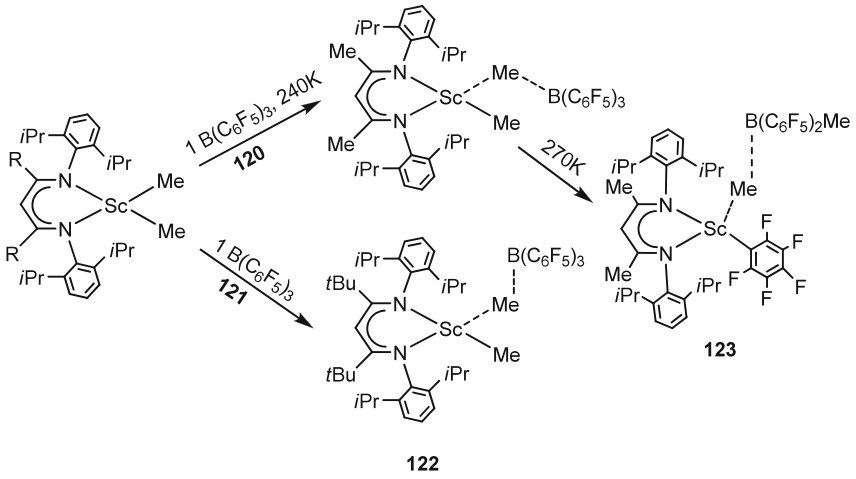

Scheme 40

to give a well-characterized contact ion pair (CIP) **122** which is a highly active catalyst. The less sterically hinderal Me-substituted **120** activated by $B(C_6F_5)_3$ produced a similar CIP at 240 K. Upon the temperature increasing to 270 K, rapid C_6F_5 transfer from the borate counterion to scandium center resulted in a CIP [Sc(**L24**)(C_6F_5)][MeB(C_6F_5)$_2$Me] (**123**) (Scheme 40). **123** was not known for its catalytic activity, which suggested that C_6F_5 back transfer on **120** with lower steric effect might be related to the inert behavior in the polymerization of ethylene [60, 83, 84].

The trityl borate $[Ph_3C][B(C_6F_5)_4]$ did not cause C_6F_5 back transfer. However, if the coordination site on Sc had sufficient open, the solvent molecules would coordinate to the metal center to form solvent-separated ion pairs (SSIPs), which were inactive in catalysis of polymerizations. A series of scandium methyl SSIPs **124**–**128** stabilized by the relatively less steric effect β-diketiminato **L24** were prepared by reacting **120** with $[Ph_3C][B(C_6F_5)_4]$ in an arene solvent. The synthetic route is shown in Scheme 41 and the complexes were studied for the relevance to propagation processes in the polymerization of alkene. Competition

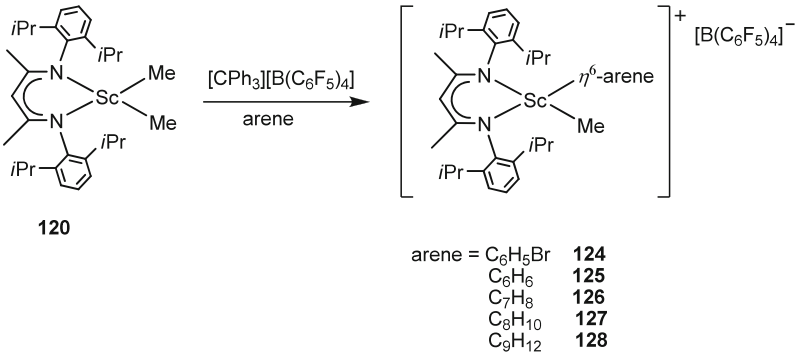

Scheme 41

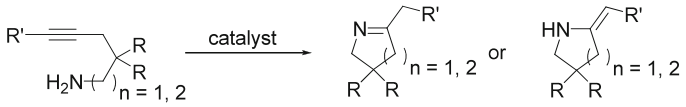

Scheme 42 The intramolecular hydroamination of alkynes

experiments revealed that the order of arene coordination in this series of SSIPs was $C_7H_8 > C_9H_{12} > C_6H_6 > C_6H_5Br$. When the polymerization of ethylene was performed in toluene, ethylene was unable to compete with toluene. Thus, no catalytic activity was observed [84, 85].

Additional catalytic investigation of β-diketiminate scandium complexes by Piers and coworkers showed that well-characterized complexes **121** and **122** with the bulky ligand **L27** were highly active catalysts for intramolecular hydroamination to form nitrogen heterocycles. The catalytic reaction was monitored by determining starting material and product with ^{1}H NMR. Both the neutral complex **121** and the CIP complex **122** are effective catalysts (10 mol%) for the intramolecular hydroamination of 5-phenyl-4-pentyl-1-amine (R = H, R′ = Ph, $n = 1$ in Scheme 42). However, they are not active catalysts for the potential application to the intermolecular hydroamination of 1-hexyne with alkylamines [82].

121 and **122** were studied for the intramolecular alkene hydroamination of 2,2-diphenyl-4-pentenylamine (R = Ph, $n = 1$ in Scheme 43) to the desired cyclic amine product. They both catalyzed the alkene hydroamination to five-membered ring cyclic amine, pyrrolidine at room temperature. Pyrrolidine product was obtained with >95% yield by using 5 mol% **122** for 2 h or >80% yield by using 10 mol% **121** at room temperature for 135 h. The cationic complex **122** is not only much more efficient than the neutral complex **121**, but also catalyzes the hydroamination to form six-membered ring cyclic amine piperidine product ($n = 2$ in Scheme 43) with >90% yield at elevated temperature (65°C) for 24 h [82].

Stoichiometric reaction of the cationic catalyst **122** with 2,2-diphenyl-4-pentenylamine afforded the cationic amido complex **129** characterized by NMR (Scheme 44). The catalytic studies suggested that **129** was an active catalyst for the hydroamination of alkenes [82].

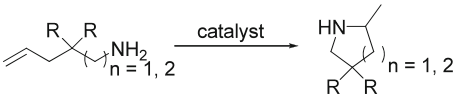

Scheme 43 The intramolecular hydroamination of alkenes

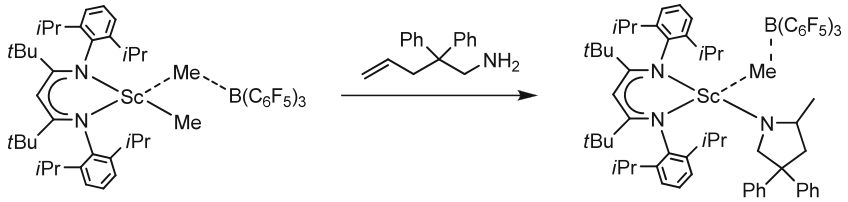

122 **129**

Scheme 44

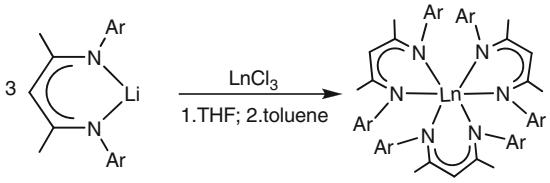

Ar = Ph, **LiL21** Ln = Nd **133**

Ar = C_6H_4Me-4, **LiL28** Ln = Nd **134**

Ar = C_6H_4Cl-4, **LiL29** Ln = Pr **130**, Nd **131**, Sm **132**

Scheme 45

Only a few tris-β-diketiminato rare-earth metal complexes (**74**, **75**, and **77**) were prepared [64,71,72] and no catalytic activities were reported until Shen and coworkers' very recent discovery on synthesis and catalytic applications of such complexes [86]. To compare the electronic effects of ligands on the reactivity of their lanthanide complexes, **L21** and its derivatives **L28** (a methyl electron-donating group at the *para*-position on the phenyl) and **L29** (a chloro electron-withdrawing group at the *para*-position on the phenyl) were used in the study. $LnCl_3$ (Ln = Pr, Nd, Sm) and lithium salt of **L29** via salt elimination led to [Ln(**L29**)$_3$] (Ln = Pr (**130**), Nd (**131**), Sm (**132**)). [Nd(**L21**)$_3$] (**133**) and [Nd(**L28**)$_3$] (**134**) were prepared by the same method shown in Scheme 45.

All tris-β-diketiminato complexes **130–134** exhibited high catalytic activity for the ROP of ε-caprolactone and L-lactide. α,ω-dihydroxytelechelic polymers in high yield with high molar mass and moderate molar mass distributions (M_w/M_n = 1.38–1.89) were produced from the ROP of ε-caprolactone (Scheme 8) catalyzed by **130–134**. **130–134** are highly active catalysts for the ROP of L-lactide to produce polylactide (Scheme 14). The electronic factor of the β-diketiminate ligand largely affects the catalytic activity of the complexes. **131** containing an

electron-withdrawing group Cl on the ligand showed the highest catalytic activity, whereas **134** bearing an electron-donating group Me on the ligand exhibited the lowest catalytic activity, which is consistent with the electron deficiency of the ligand. Hence, an increase in the electron density of the ligand (**L29** < **L21** < **L28**) around the metal center will decrease the catalytic activity (**131** > **133** > **134**) for both polymerization procedures in the present systems. This can be explained by the fact that the electron-withdrawing substituents on the ligand create the central metal electron deficiency which accelerates the initiation of monomer. The catalytic activity also depended strongly on the size of the center metal: a decrease in the ionic radii of the metal (Pr > Nd > Sm) resulted in a remarkable decrease in the catalytic activity **130** > **131** > **132**. The same trend was also previously observed when **96–99** were used as the catalysts for lactide polymerization [77].

2.1.6 Bis(phosphinimino)methanide Ligands

Besides attracting much attention in main-group and transition-metal chemistry, ligands that contain P–N units have become more and more popular in rare-earth metal chemistry [87–94]. This section focuses on bis(phosphinimino)methanides as a bidentate *N*,*N*-ligand system which proved to be very suitable in stabilizing rare-earth metal complexes. The rare-earth metal complexes containing these ligands showed interesting coordination modes as well as good catalytic activities in hydroamination and hydrosilylation reactions and in the polymerization of MMA and ε-caprolactone [95–99]. The bis(phosphinimino)methanide framework can be formally built up by replacing two carbon atoms of the well-known β-diketiminato framework with two phosphorus atoms (Scheme 46). Those two ligand systems exhibit a topological relationship which appears among others in similarities in donor identity and steric demands. However, bis(phosphinimino)methanide ligands show a more localized negative charge on the methanide carbon atom. Therefore, this carbon atom can act as a third coordination site by building a long bonding interaction with the metal center. The resulting metallacycles show as a typical structural feature the pseudoboat conformation (Scheme 47).

Furthermore, in contrast to β-diketiminato ligands, the methanide group of bis(phosphinimino)methanides can be deprotonated again to give bis(phosphinimino)methandiides which act as dianionic *N*,*N*-ligand systems. As shown by Cavell et al., this ligand forms a "pincer" carbene-type complex with samarium, which exhibits a

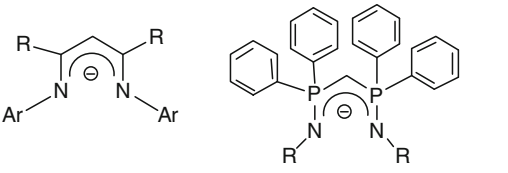

β-diketiminates bis(phosphinimino)methanides

Scheme 46

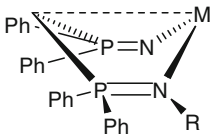

Scheme 47

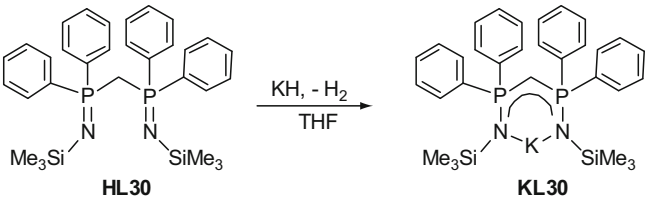

Scheme 48

short bonding distance between the metal center and the methandiide carbon atom [100, 101]. To study the catalytic activity of the rare-earth metal complexes, we will only discuss monoanionic bis(phosphinimino)methanide ligand systems. Although bis(phosphinimino)methanides with different substituents (R = aryl, Mes, $SiMe_3$) were reported [102], to the best of our knowledge, catalytic applications in rare-earth metal chemistry have been restricted to the trimethylsilyl-substituted species. According to this, we focus on the $\{CH(PPh_2NSiMe_3)_2\}^-$ ligand (**L30**) and on the corresponding rare-earth metal complexes.

The bis(phosphinimino)methanide rare-earth metal complexes are prepared by two general methods: salt and amine eliminations. The salt elimination method is more established. To avoid the problem of occlusion of solvated lithium chloride in salt methasesis reactions, the potassium bis(phosphinimino)methanide complex **KL30** was used as a ligand transfer reagent. The solvent-free complex **KL30** can be easily accessed by the reaction of bis(phosphinimino)methane **HL30** with an excess of KH in THF (Scheme 48) [103].

Ln(III) Complexes

*Complexes of Composition [Ln(**L30**)X_2] (X Represents a Leaving Group)*

The dimeric rare-earth metal dichloride complexes $[Ln(\mathbf{L30})Cl_2]_2$ (Ln = Y (**135**), Sm (**136**), Dy (**137**), Er (**138**), Yb (**139**), Lu (**140**)) were obtained from the salt metathesis reaction of potassium bis(phosphinimino)methanide **KL30** with anhydrous yttrium or lanthanide trichlorides (Scheme 49) [104]. When the metal center is larger than samarium, bis(phosphinimino)methanide lanthanide dichloride complexes could not be obtained.

In the solid state, the complexes **135–140** are dimeric compounds, in which the metal centers are asymmetrically bridged by two μ-chlorine atoms. With regard

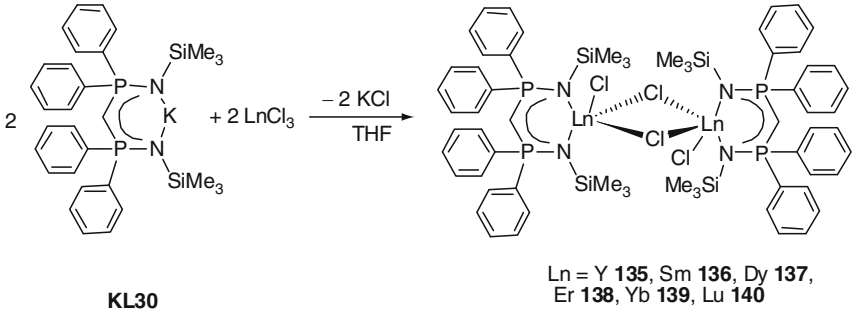

Scheme 49

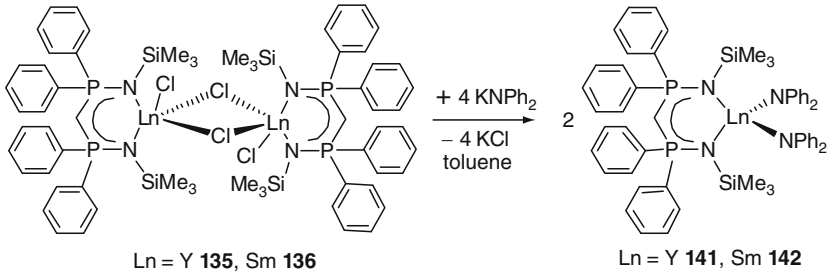

Scheme 50

to the catalytic activity of the complexes, we were searching for a ligand that can act as a leaving group. A small ligand such as CH_3^- or Cl^- leads to unreactive metalate complexes or dimeric compounds. A bulky ligand will not coordinate twice to the metal center. The amido ligand $(NPh_2)^-$ is a medium-sized group and may act as a good leaving group. To investigate the catalytic activity, we synthesized bis(phosphinimino)methanide complexes containing $(NPh_2)^-$. The reaction of the chloro complex **135** or **136** with $KNPh_2$ afforded the corresponding compound [Ln(**L30**)$(NPh_2)_2$] (Ln = Y (**141**) or Sm (**142**)) (Scheme 50) [104].

The bis(amido) complexes **141** and **142** showed no catalytic activity in inter- or intramolecular hydroamination reactions. Because of the low basicity of the Ph_2N^- group, it cannot be protonated by aliphatic amines RNH_2 or R_2NH. Therefore, the initial step of the catalysis failed and these complexes do not serve as catalysts for inter- or intramolecular hydroamination.

To overcome this problem, the more basic $\{N(SiHMe_2)_2\}^-$ ligand was used to synthesize catalytically active bis(phosphinimino)methanide complexes. Scheme 51 shows the three different pathways for the synthesis of the bis(amide) complexes [Ln(**L30**)$\{N(SiHMe_2)_2\}_2$] (Ln = Y (**143**), La (**144**), Sm (**145**), Ho (**146**), Lu (**147**)) [105, 106]: 1) **HL30** and [Ln$\{N(SiHMe_2)_2\}_3(THF)_2$] (Ln = Y, La, Sm, Ho, Lu) (Anwander Amides) [107] reacted via amine elimination in boiling toluene to give the complexes **143**–**147** in high yields and as pure products. 2) The salt metathesis reaction of the corresponding chloro complexes **135** or **136** and $KN(SiHMe_2)_2$

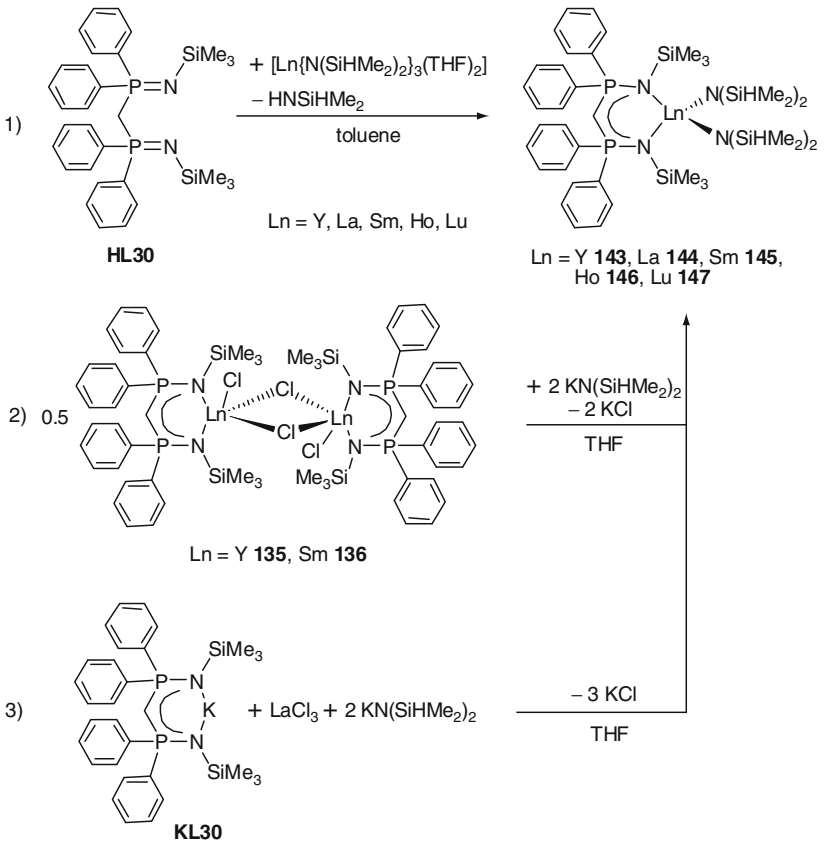

Scheme 51

in THF led to the bis(amide) complexes **143** or **145**. 3) The most convenient approach is a one-pot reaction of **KL30** with anhydrous lanthanum trichloride and $KN(SiHMe_2)_2$ in THF, which afforded the desired product **144**. Disadvantages of pathway 3) are the existence of impurities in the product and the low yields.

Compounds **143**–**147** exhibited characteristic features of catalytically active species. The bis(phosphinimino)methanide ligand acted as a spectator ligand. In contrast, the $N(SiHMe_2)_2^-$ ligand was expected to act as a leaving group and to be replaced by the substrate in the initial step of the catalysis. According to this, the catalytic activity of complexes [Ln(**L30**){$N(SiHMe_2)_2$}$_2$] (Ln = Y (**143**), La (**144**), Sm (**145**), Ho (**146**), Lu (**147**)) was investigated for intramolecular hydroamination/cyclization, hydrosilylation, and sequential hydroamination/hydrosilylation reactions [106]. The rate dependence on the ionic radius of the center metal was investigated by using one of the most reactive aminoalkenes, 1-(prop-2-enyl)-cyclohexanemethanamine (Scheme 52), as test substrate in hydroamination/cyclization reactions.

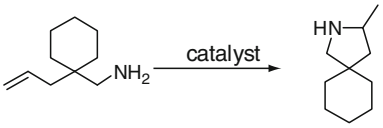

Scheme 52 The intramolecular hydroamination of 1-(prop-2-enyl)-cyclohexanemethanamine

The kinetic studies were carried out with a constant catalyst concentration of 2 mol% and monitored by in situ ^{1}H NMR spectroscopy. The reaction rate increased with increasing ionic radius and the lanthanum compound **144** showed the highest catalytic activity. To investigate the rate law, further kinetic studies were undertaken by using the same substrate in Scheme 52 and the yttrium complex **143**. The rate law, $\nu = k[\text{substrate}]^0[\text{catalyst}]^1$, was determined and is identical to that of the hydroamination/cyclization reactions catalyzed by the lanthanide metallocene complexes [108]. In addition, the catalytic reaction was monitored by ^{31}P{^{1}H} NMR spectroscopy. No signal of the free ligand was observed and the monitored signal remained in the region of the complex **143** ($\delta = 17.1$ ppm). This indicated that during the catalytic reaction, **L30** stayed attached to the metal center. To explore the reaction scope and the substrate selectivity in hydroamination/cyclization reactions, the most active catalyst **144** was used for further reactions with nonactivated aminoalkynes (Scheme 42) and aminoalkenes (Scheme 43).

The aminoalkynes with bulky geminal substituents in β-position to the amino group (Thorpe–Ingold effect) were converted rapidly to their cyclic products at room temperature by using low concentrations (1–2 mol%) of the catalyst. Other aminoalkynes could also be cyclized quickly at 60 or 100°C with 1–2 mol% catalyst/activator loadings. All reactions of the aminoalkynes led to the cyclic imines shown in Scheme 42. It is well known that, compared to the hydroamination of aminoalkynes, the cyclization of aminoalkenes remains significantly lower turnover frequencies. Most aminoalkenes could be converted into the cyclic products at 60°C. Similarly to the aminoalkynes, the aminoalkenes bearing bulky geminal substituents in β-position to the amino group were more reactive and could be rapidly cyclized at 60°C within 1.5–3 h by using 1–2 mol% of the catalyst only. Furthermore, a six-member-ring cyclic amine could be formed at 60°C within 22 h. It showed that the rate of cyclization followed the order of the ring size $5 > 6$, which is consistent with classical stereoelectronically controlled cyclization processes. In comparison to the metallocene complexes, the catalytic rates of **143**–**147** for the hydroamination are lower. However, **143–147** are easily accessible in a one-step procedure and are more robust toward moisture and air. In summary, all substrates were converted into the cyclic products under moderate reaction conditions in high yields and the reactions proceeded regiospecifically.

Moreover, the catalytic activity of **143**–**145** and **147** for the intermolecular hydrosilylation reactions has been explored (Scheme 53).

The rate dependence on the ionic radius of the center metal was investigated. As previously observed for the hydroamination reaction, the reaction rate increased with increasing ionic radius, so that the lanthanum complex **144** was proved to be

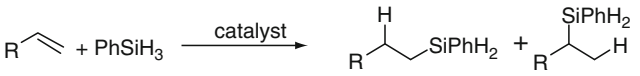

Scheme 53 Intermolecular hydrosilylation reaction

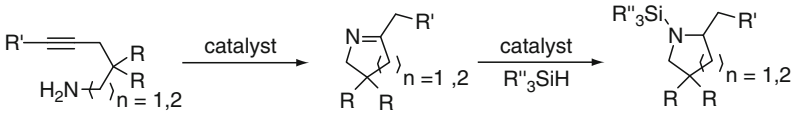

Scheme 54 The sequential hydroamination/hydrosilylation reaction

the most active catalyst. For this reason, **144** was used in further studies. In a full screening of **144**, different terminal olefins and one diene were used in the reaction with phenylsilane. All experiments were carried out with a low catalyst/activator loading of 1.5 mol% at room temperature to give quantitative yields. The catalytic reaction of the aliphatic substrates led to the corresponding anti-Markovnikov products with very high regioselectivity. Only the reaction of styrene produced a product mixture. Furthermore, the cyclization/silylation of hexa-1,5-diene afforded the corresponding cyclic species in quantitative yield. The catalytic activity of the lanthanum complex **144** in hydrosilylation reaction is comparable to that reported for the metallocene catalysts.

The sequential hydroamination/hydrosilylation reaction (Scheme 54) catalyzed by **143** and **144** was also investigated. In the first step, aminoalkynes were converted to cyclic imines by hydroamination reaction and the subsequent hydrosilylation led to the corresponding silicon species. Hydrolysis of the products gave cyclic amines similar to the ones obtained from the hydroamination of aminoalkenes. However, the starting materials in the sequential hydroamination/hydrosilylation reaction were aminoalkynes. Therefore, the reactions are faster and easier to perform.

Different aminoalkynes and phenylsilane were studied as substrates. The reactions were performed in one-pot sequences by mixing the catalyst and the aminoalkyne at the first step, followed by adding phenylsilane to the reaction mixture when the cyclic amines reached complete conversion. All reactions were undertaken with catalyst loadings of 2 mol% and led selectively to the corresponding products. As observed for the individual reaction, the lanthanum compound **144** was more active than the yttrium compound **143** and the hydroamination was always the slower step. In the hydroamination reaction, the substrates with bulky substituents in β-position to the amino group could be cyclized at room temperature rapidly, whereas the reactions of other substrates required elevated temperature (60 or 100°C). The hydrosilylation reactions were completed after 4 h at room temperature and gave the corresponding five- or six-membered ring products. **143** and **144** are the first rare-earth metal catalysts reported for the sequential hydroamination/hydrosilylation reaction.

In summary, [Ln(**L30**){$N(SiHMe_2)_2$}$_2$] (Ln = Y (**143**), La (**144**), Sm (**145**), Ho (**146**), Lu (**147**)) are catalytically active systems for hydroamination, hydrosilylation, and the sequential hydroamination/hydrosilylation reactions. Due to the rate

dependence on the ionic radius of the center metal, the lanthanum complex **144** is the most active catalyst. All reactions afforded the products in high yields and good reaction times [105, 106].

*Complexes of Composition [Ln(**L30**)X]*

Alternatively to cyclopentadienyl ligands, we successfully introduced cyclooctatetraene as a ligand in bis(phosphinimino)methanide rare-earth metal complexes [96]. The corresponding complexes [Ln(**L30**)(η^8-C_8H_8)] (Ln = Y (**148**), Sm (**149**), Er (**150**), Yb (**151**), Lu (**152**)) could be obtained in a one-pot reaction by treating **KL30** with anhydrous lanthanide trichlorides in THF followed by subsequent addition of a freshly prepared solution of $K_2C_8H_8$ in THF (Scheme 55) [96]. Two additional pathways have been established for the synthesis of the samarium complex **149** (Scheme 55). The treatment of the chloro complex **136** with $K_2C_8H_8$ in THF afforded the desired product **149**. The target complex **149** also could be obtained by the reaction of **KL30** with [(η^8-C_8H_8)SmI(THF)$_3$] in THF [109].

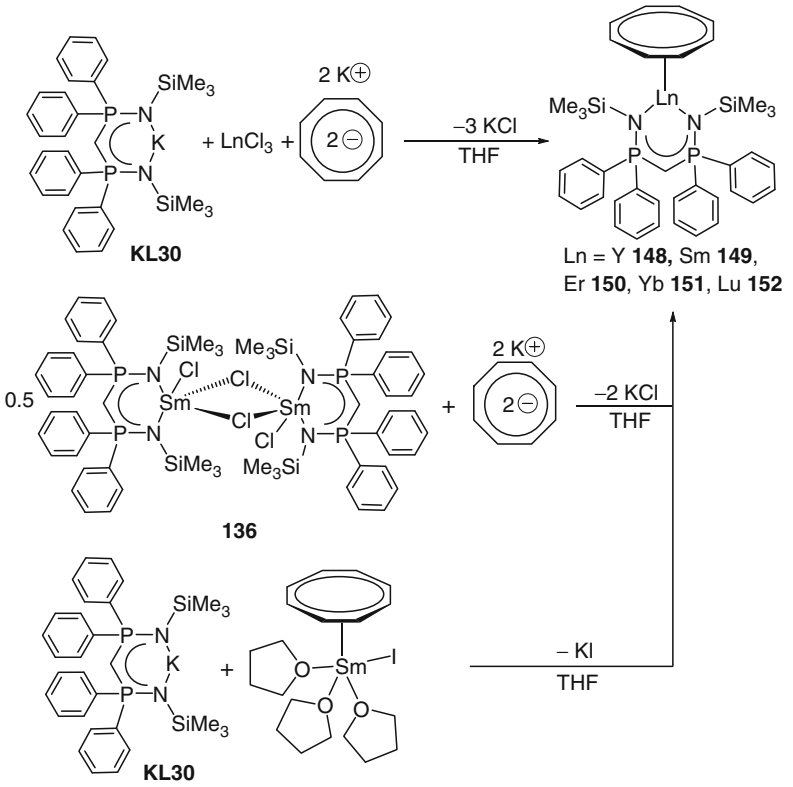

Scheme 55

Mechanistic studies of the lanthanide metallocene-catalyzed hydroamination/cyclization reaction suggested that the leaving group was replaced by the substrate in the initial step [110]. Bis(phosphinimino)methanide complexes **148–152** contain no obvious leaving groups. To discover new mechanistic aspects, the catalytic activity of compounds **148–152** in the hydroamination/cyclization reaction was explored. Various aminoalkynes and aminoalkenes were used as substrates for the intramolecular hydroamination reaction (Schemes 42 and 43). A moderate activity could be observed at elevated temperatures only. The reaction scope was limited to five-membered ring formation. The aminoalkynes were quantitatively converted to the corresponding cyclic imines at elevated temperatures with a catalyst loading of 2 mol%. The aminoalkenes are less reactive than the aminoalkynes. Only the substrates bearing bulky substituents at the β-position of the amino group could be cyclized. The reaction rate depended on the ionic radii of the center metal. 5-phenyl-4-pentyn-1-amine (R = H, R′ = Ph, n = 1 in Scheme 42) was used as a substrate in kinetic studies of **148** and **149**. The samarium complex **149** proved to be the more active catalyst. Kinetic studies of both reactions indicate zero-order kinetics in substrate concentration. Further ^{1}H and ^{31}P{^{1}H} NMR experiments with **149** showed that neither the bis(phosphinimino)methanide nor the cyclooctatetraene ligand was dissociated from the metal center during the catalytic reaction. Even though complexes [Ln(**L30**)(η^8-C_8H_8)] (**148–152**) could not compete with metallocene catalysts, kinetic studies showed a new mechanistic pathway of the hydroamination/cyclization reaction.

*Complexes of Composition [Ln(**L30**)XX′]*

Former works have shown that certain lanthanide complexes bearing PN ligands in the coordination sphere could be used as catalysts for ε-caprolactone polymerization [90, 111, 112]. For this reason, asymmetrically substituted bis(phosphinimino)methanide rare-earth metal complexes were synthesized by our group and have been tested toward their catalytic activity in polymerization reactions [99]. Initially, the chloro complexes [Ln(**L30**)Cl{N(PPh_2)$_2$}] (Ln = Y (**153**), La (**154**), Nd (**155**), Yb (**156**)) containing the N(PPh_2)$_2^-$ ligand that is bulky enough to coordinate only once onto the metal center were prepared. The chloro atom is small enough to fit between the two bulky spectator ligands and was not replaced by a second N(PPh_2)$_2^-$ ligand. There are three different synthetic pathways to obtain the compounds **153–156** (Scheme 56): 1) The reaction of **KL30** and [Ln{(PPh_2)$_2$N}Cl_2(THF)$_3$] (Ln = Y, La) [89] in THF gave **153** and **154**. 2) The reaction of chloro complexes **135** and **139** with KN(PPh_2)$_2$ in THF afforded **153** and **156**. 3) The most convenient approach was the one-pot reaction of **KL30**, anhydrous lanthanide trichlorides, and KN(PPh_2)$_2$ in THF. As described in Scheme 56, this reaction pathway is applicable for rare-earth metals with different ionic radii. Further studies focused on the lanthanum complex **154** which showed the best catalytic activity of **153–156** for polymerization reactions. To have a different leaving group in the catalytic reactions, the remaining chloro ligand in **154** was replaced by the {NPh_2}$^-$ ligand. The lanthanum compound [La(**L30**){NPh_2}{N(PPh_2)$_2$}] **157**

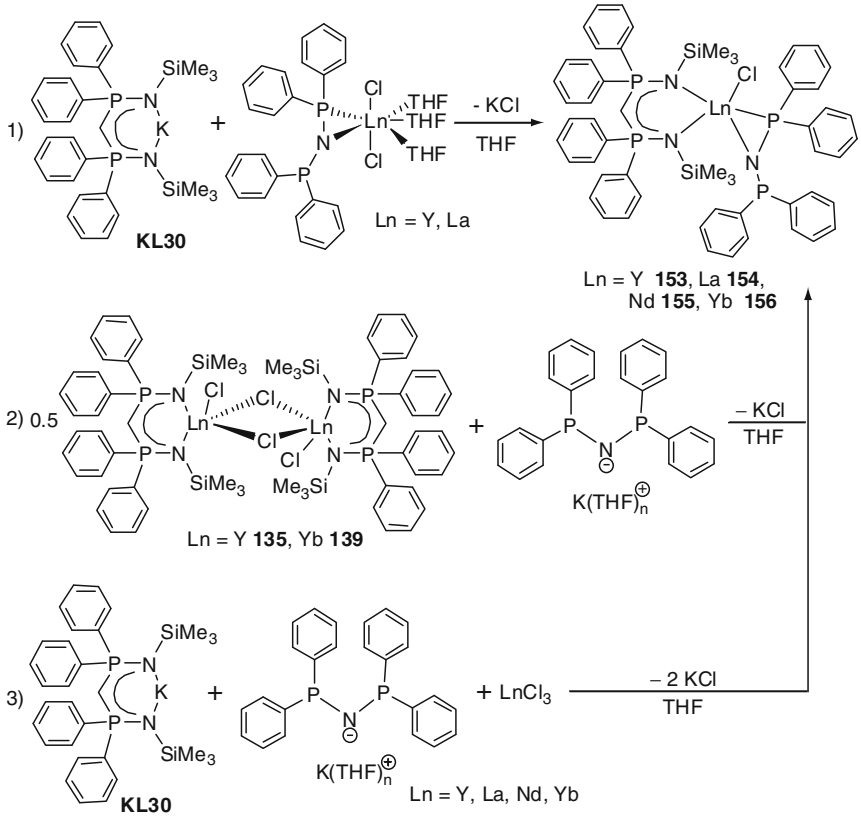

Scheme 56

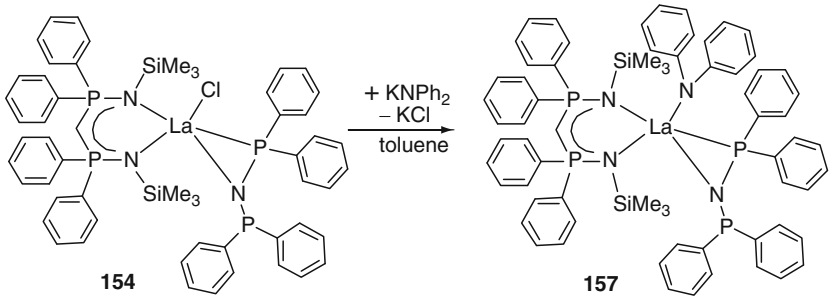

Scheme 57

was synthesized by the treatment of [La(**L30**)Cl{N(PPh$_2$)$_2$}] **154** with KNPh$_2$ in toluene (Scheme 57).

The catalytic activity of **153–157** was investigated for the polymerization reactions of polar monomers such as ε-caprolactone and methyl methacrylate [99].

Compounds **153–157** are highly active catalysts for ε-caprolactone polymerization reactions (Scheme 8). Using molar monomer and initiator ratios of 240–440:1 at room temperature gave the polymers in good reaction times and yields. The rate dependence on the ionic radius of the center metal was observed. The catalytic reactions with the lanthanum and the neodymium complexes **154** and **155** without any cocatalyst afforded the corresponding polycaprolactones within 5 min. The amido compound **157** showed slightly lower activity than the chloro complex **154**. Unfortunately, the resulting polycaprolactones exhibited high polydispersities regardless of the catalyst used in the reactions.

Better results were obtained in the methyl methacrylate polymerization reactions (Scheme 12). **153–156** showed high catalytic activity with a strong dependence on the ionic radius of the center metal. The lanthanum complex **154** was the most active catalyst and initiated the polymerization without any cocatalyst. Addition of small amounts of $AlEt_3$ as cocatalyst increased the yield significantly. Polymerization initiated by **154** depended on the temperature and a low temperature (−78°C) was required to afford almost quantitative yields. The resulting polymers were basically syndiotactic and exhibited high molar masses and narrow polydispersities. The catalytic reaction with the lanthanum compound **157** showed no increase of catalytic activity but led to a larger fraction of atactic poly(methyl methacrylate). Moreover, the catalytic activity of all utilized initiators was solvent dependent. **153**, **155**, and **156** only showed catalytic activity by the addition of a cocatalyst. **153** afforded lower yield after changing the solvent from toluene into THF.

Ln(II) Complexes

Previous works showed that divalent lanthanide complexes such as $[Sm(\eta^5\text{-}C_5Me_5)_2(THF)_2]$ [113], $[Sm(\eta^5\text{-}C_5H_5)_2]$ [114], and $[Yb(\eta^5\text{-indenyl})_2(THF)_2]$ [115] are efficient catalysts for the polymerization of ε-caprolactone. Furthermore, divalent samarocenes exhibited good catalytic activity in hydroamination reactions [116]. Marks and coworkers established the mechanism of the hydroamination/cyclization reaction catalyzed by lanthanide metallocene [110]. They showed that divalent samarium complexes act as precatalysts, but the catalytically active species are trivalent complexes generated in situ by oxidation of the samarocenes. According to this, divalent lanthanide complexes containing **L30** instead of cyclopentadienyl ligands were synthesized. The bis(phosphinimino)methanide lanthanide iodo complexes **158–160** were prepared by the reaction of **KL30** with anhydrous lanthanide diiodides in THF [95,98]. As shown in Scheme 58, the ytterbium complex **160** showed a monomeric structure $[Yb(\mathbf{L30})I(THF)_2]$ in solid state, whereas the europium and the samarium compounds formed dimeric complexes $[Ln(\mathbf{L30})I(THF)]_2$ (Ln = Eu (**158**), Sm (**159**)) because of their larger ionic radii.

Further reactions of iodo complexes **158** and **160** with $KN(PPh_2)$ in THF led to heteroleptic compounds $[Ln(\mathbf{L30})\{N(PPh_2)\}(THF)]$ (Ln = Eu (**161**), Yb (**162**)) [95]. An alternative reaction pathway (Scheme 59) started from the trivalent ytterbium complex **156** which already contained both ligands: **L30** and the

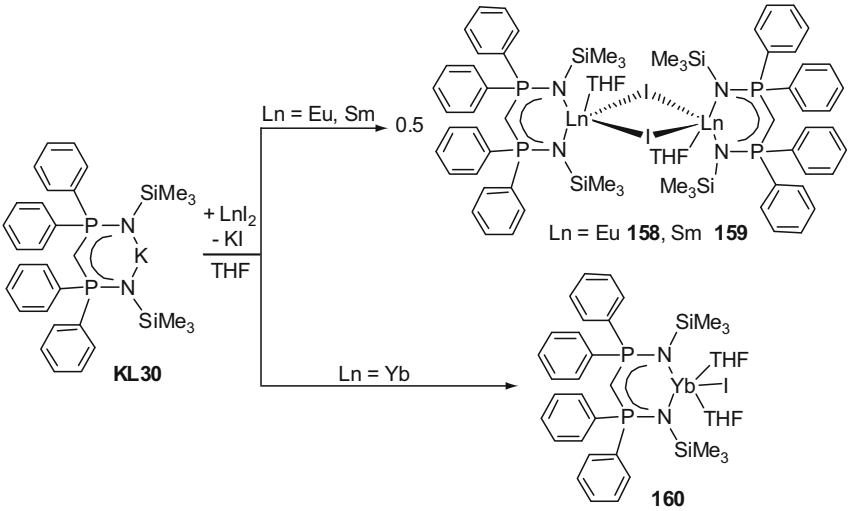

Scheme 58

$N(PPh_2)^-$ ligand. Reduction with elemental potassium in refluxing THF also gave the divalent ytterbium complex **162**.

Further treatment of [Sm(**L30**)I(THF)]$_2$ (**159**) with $KNPh_2$ in THF afforded the dimeric compound [(Sm(**L30**)$_2$)$_2$(μ-I)(μ-NPh_2)] (**163**). The reaction of **159** with potassium bis(phosphinimino)methanide **KL30** resulted in the homoleptic compound **164** (Scheme 60).

Catalytic applications were investigated for samarium and ytterbium iodo complexes **159** and **160**.

The divalent ytterbium complex **160** was studied as precatalyst for the intramolecular hydroamination/cyclization reaction [95]. Various aminoalkynes (Scheme 42) and aminoalkenes (Scheme 43) were used as substrates. There was no reaction observed at room temperature, but at elevated temperature a moderate activity was observed. The reaction scope was limited to five-membered ring formation. The aminoalkynes were converted to the corresponding cyclic imines at elevated temperatures with a catalyst loading of 1.4–5.3 mol% in quantitative yields. Aminoalkenes, which are less reactive than aminoalkynes, could be cyclized only if they contain bulky substituents in the β-position of the amino group. By using 1-(prop-2-enyl)-cyclohexanemethanamine (Scheme 52) as substrate, the cyclic product could be obtained in good yield at elevated temperature. Kinetic studies of the cyclization of 5-phenyl-4-pentyn-1-amine indicate zero-order kinetics in substrate concentration. The change of color from red to yellow during the experiment indicates an in situ oxidation reaction of **160**.

The divalent samarium complex **159** was studied as an initiator in the polymerization of ε-caprolactone (Scheme 8) [98]. The catalytic reactions at room temperature within 1 h afforded the corresponding polycaprolactones in high yields (92–95%). A strong dependence of the polymer molecular weights on the concentration of

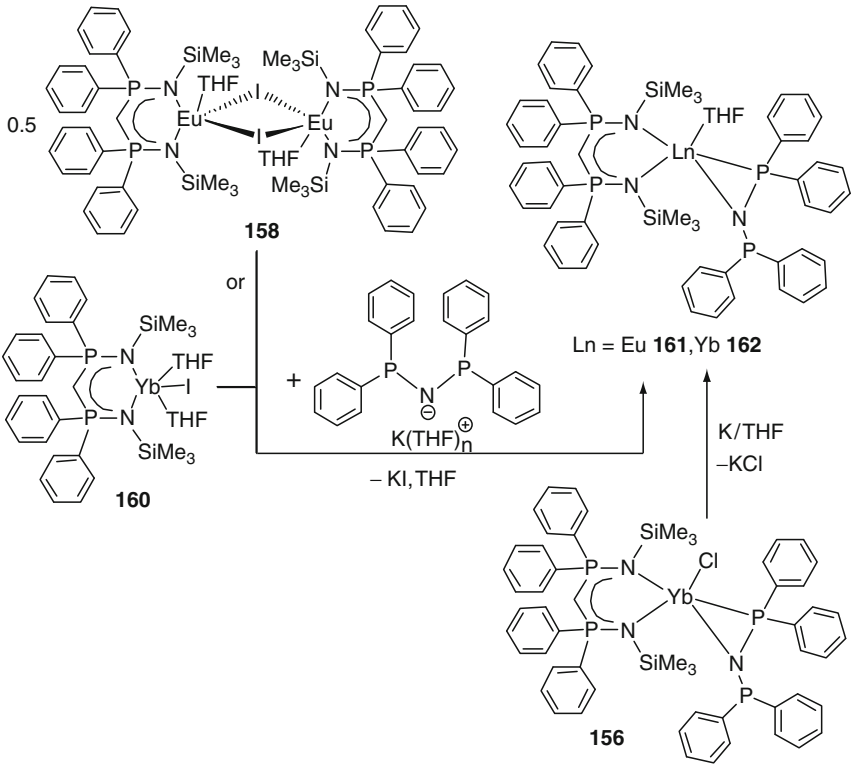

Scheme 59

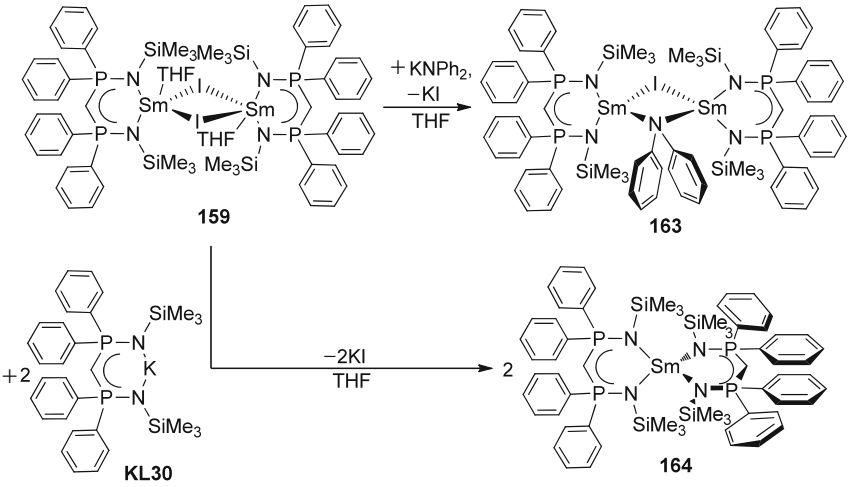

Scheme 60

initiator was observed. At elevated temperature, the polymer molecular weights decreased. **159** showed high activity in the polymerization of ε-caprolactone and led to high molecular weight polymers in good yields and with moderate polydispersities [98].

2.1.7 Aminotroponiminate Ligands

Alternative to cyclopentadienyl ligands, aminotroponiminates ($\{(R)_2ATI\}^-$) **I** (Scheme 61) were introduced into rare-earth metal chemistry in 1997 [117]. Aminotroponiminates are bidentate monoanionic ligands, containing a seven-membered ring backbone, forming five-membered metallacycles upon coordination to a metal atom. The nearly planar ligand framework exhibits a delocalized ten π-electron system and therefore shows low reactivity toward most nucleophiles and electrophiles. In addition, mono-bridged bisaminotroponiminates **II** [118–122] and double-bridged bisaminotroponiminates(tropocoronands) **III** [123–125] are known (Scheme 61). These ligands are tetradentate dianionic ligands, and the resulting metal complexes are similar to *ansa*-metallocenes. Type **III** ligands are not established in the rare-earth metal chemistry. However, various rare-earth metal complexes containing type **II** ligands were synthesized [118–121]. This section mainly focuses on aminotroponiminates and presents one mono-bridged bisaminotroponiminate complex. Those rare-earth metal complexes with reported catalytic activities will be discussed here. These complexes have been investigated only for hydroamination reactions.

Aminotroponiminates ($\{(i\text{Pr})_2ATI\}^-$)

In rare-earth metal chemistry, mostly the *N*,*N*-diisopropyl-substituted aminotroponiminate ligand ($\{(i\text{Pr})_2ATI\}^-$) has been used. To avoid occlusion of solvated lithium chloride in the salt methasesis reactions, the potassium aminotroponiminate complex **KL31** was used as a ligand transfer reagent. The solvent-free complex **KL31** can be easily accessed by the treatment of $H\{(i\text{Pr})_2ATI\}$ **HL31** with an excess of KH in THF (Scheme 62) [117].

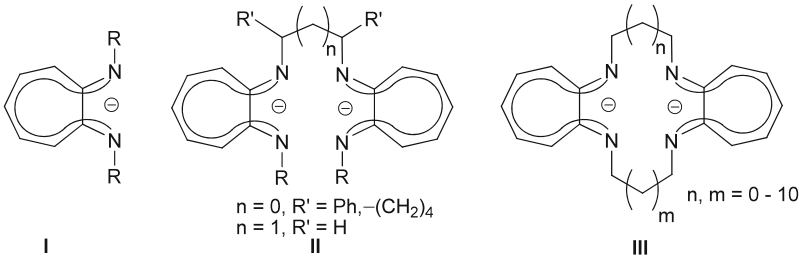

Scheme 61

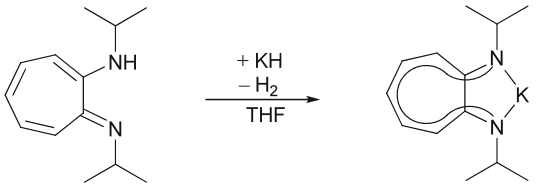

HL31 KL31

Scheme 62

In 1998, the catalytic activity of aminotroponiminate rare-earth metal complexes was investigated for the first time in the hydroamination/cyclization reactions of aminoalkynes [126]. The aminotroponiminate yttrium amide complexes [Y(**L31**){N(SiMe$_3$)$_2$}$_2$] (**166**) and [Y(**L31**)$_2${N(SiMe$_3$)$_2$}] (**168**) were synthesized via the salt metathesis reactions shown in Scheme 63 [126]. Treating **KL31** with 1 equiv of anhydrous yttrium trichloride in THF afforded the dimeric complex [Y(**L31**)Cl$_2$]$_2$ (**165**). The reaction of **165** with KN(SiMe$_3$)$_2$ in toluene led to the monoaminotroponiminate yttrium bis(amido) complex **166**. The reaction of 2 equiv of **KL31** with 1 equiv of anhydrous yttrium trichloride in THF afforded the bis-aminotroponiminate yttrium chloro complex **167** and traces of **165** and the homoleptic complex [Y(**L31**)$_3$]. The attempt of purifying the product by recrystallization failed and only increased the ratio of **165**. Using a 10% excess of **KL31**, the desired product **167** and [Y(**L31**)$_3$] were obtained. The crude product was able to be purified by recrystallization to give the pure bis-aminotroponiminate yttrium chloro complex **167**. Further reaction of **167** with KN(SiMe$_3$)$_2$ in toluene afforded the corresponding bis-aminotroponiminate yttrium amido complex **168**.

The catalytic activity of **166** and **168** was investigated for the intramolecular hydroamination/cyclization of aminoalkynes and an aminoalkene [126]. Compounds **166** and **168** exhibited characteristic features of active catalysts. The aminotroponiminate ligand acted as a spectator ligand by staying attached to the metal center during the catalytic cycle. The N(SiMe$_3$)$_2^-$ ligand acted as a leaving group and were replaced by the substrate in the initial step of the catalysis. Nonactivated aminoalkynes and aminoalkenes without bulky geminal substituents in β-position to the amino group were used in catalysis (Schemes 42 and 43). The aminoalkene was not converted into the corresponding cyclic amine by using **166** and **168** as catalysts. Both complexes showed good catalytic activity in the hydroamination/cyclization of aminoalkynes. All substrates were quickly converted into the corresponding cyclic imines at room temperature. The bis-aminotroponiminate complex **168** showed a higher catalytic activity than the monoaminotroponiminate complex **166**. Similarly to the well-established analogous lanthanocene catalyst [Y{Cp*}$_2${CH(SiMe$_3$)$_2$}] [127, 128], kinetic studies of both **168** and **166** indicated zero-order kinetics in substrate concentration. Although the catalytic activity of **168** was about 5–7 times lower than the activity of the lanthanocene catalyst, **168** and **166** are the first reported noncyclopentadienyl organolanthanide catalysts for hydroamination/cyclization reactions.

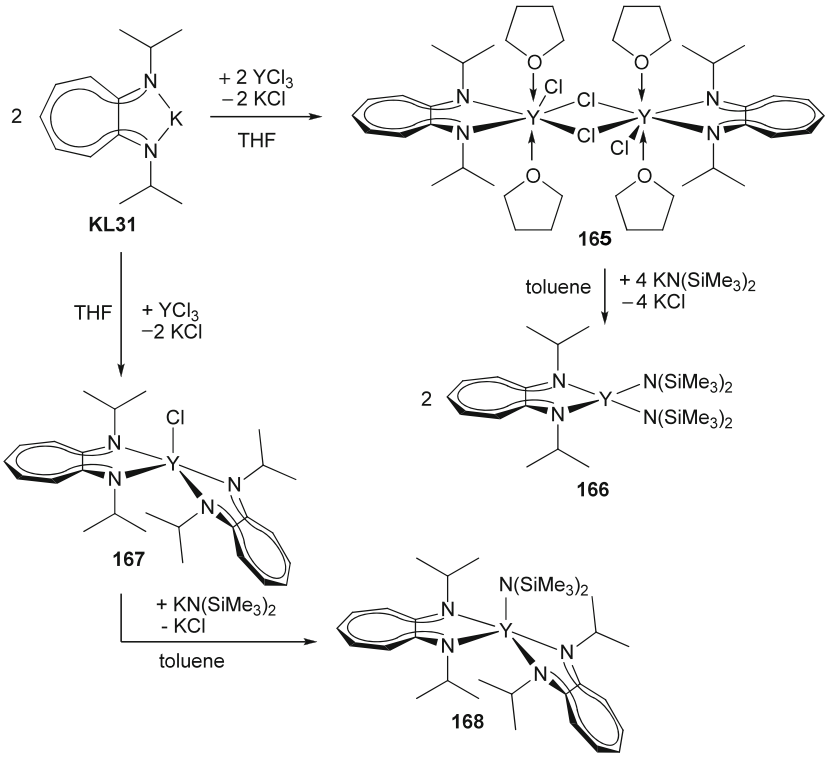

Scheme 63

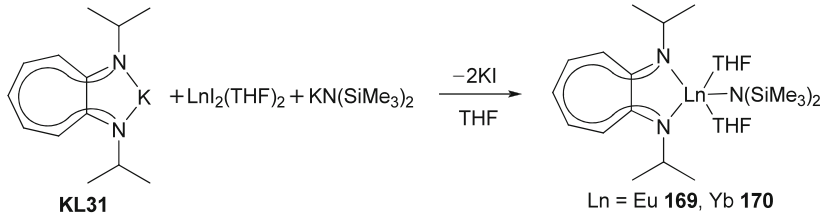

Scheme 64

Recently, aminotroponiminate complexes of divalent lanthanides were prepared for the first time [129]. With regard to catalytic applications, amido complexes of europium and ytterbium were synthesized. The preparation of compounds **169** and **170** was undertaken in a one-pot reaction of **KL31**, anhydrous lanthanide diiodides and $KN(SiMe_3)_2$ in THF at room temperature (Scheme 64).

The catalytic activity of the ytterbium complex **170** was investigated in the hydroamination/cyclization reactions of aminoalkenes. Various nonactivated aminoalkenes were used as substrates (Scheme 43). The reaction scope is limited to five-membered ring formation. The aminoalkenes bearing bulky geminal substituents in β-position to the amino group are more reactive and could be

rapidly cyclized at room temperature within 0.25–5.5 h by using 2–5 mol% of the catalyst. The aminoalkenes without bulky substituents reacted with significantly lower rates and yields. For the substrate 1-aminopent-4-ene, no reaction occurred even at elevated temperatures. In comparison with the well-established corresponding calcium complex [Ca(**L31**){N(SiMe$_3$)$_2$}] [130], the catalytic scope of **170** was limited, but the rate was substrate dependent. Based on the established mechanism of the hydroamination/cyclization reactions catalyzed by divalent samarocenes [110], the precatalyst **170** was oxidized in situ during the catalytic conversion and the catalytically active species might be a trivalent ytterbium complex. Therefore, a comparison with the divalent calcium complex is restricted to the rates.

Mono-Bridged Bisaminotroponiminate

The only mono-bridged bisaminotroponiminate investigated for catalytic reactions is the recently reported chiral-bridged bisaminotroponiminate lutetium complex **174**. Scheme 65 shows the two reaction pathways leading to the desired product **174**: 1) The chiral-bridged aminotroponimine (*S*, *S*)-H$_2${(*i*PrATI)$_2$diph} (**171**) treated with potassium hydride in THF gave the dipotassium salt [(*S*, *S*)-K$_2${(*i*PrATI)$_2$ diph}] (**172**). The salt metathesis reaction of **172** with anhydrous lutetium trichloride in THF afforded [(*S*, *S*)-Lu{(*i*PrATI)$_2$diph}Cl(THF)] (**173**) which was an enantiomerically pure complex. The chiral alkyl complex [(*S*, *S*)-Lu{(*i*PrATI)$_2$diph}

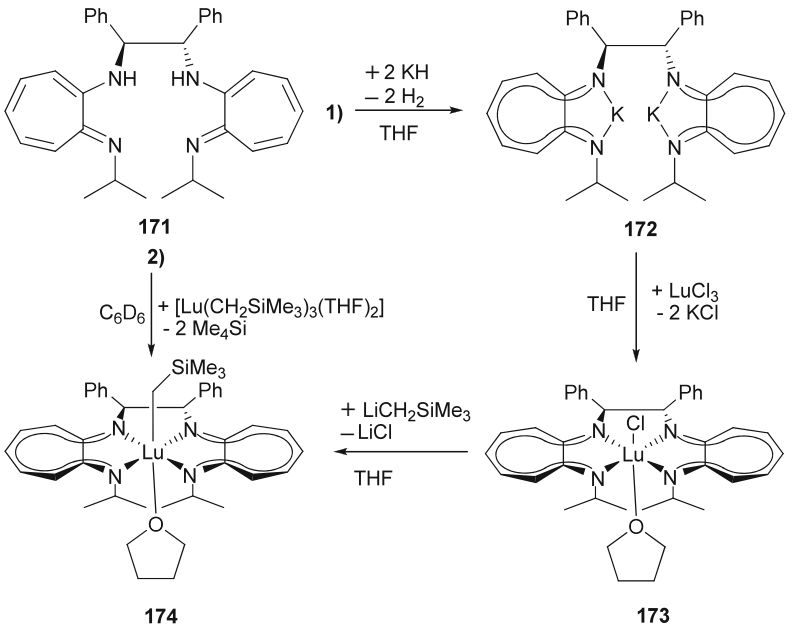

Scheme 65

$(CH_2SiMe_3)(THF)]$ (**174**) was obtained by the treatment of **173** with $LiCH_2SiMe_3$ in THF. 2) In an NMR-scale reaction of aminotroponimine (*S*, *S*)-H_2\{(*i*PrATI)$_2$diph\} (**171**) with $[Lu(CH_2SiMe_3)_3(THF)_2]$ in C_6D_6 the desired alkyl complex **174** was obtained. **174** is extremely moisture and temperature sensitive, therefore difficult to store. For this reason, the second reaction pathway was used to prepare **174** in situ for catalytic studies [120]. The catalytic activity of the lutetium complex **174** was studied in the hydroamination/cyclization of aminoalkenes [120]. Various non-activated aminoalkenes were used as substrates (Scheme 43). All substrates were converted into the corresponding cyclic imines at room temperature or elevated temperature in high yields by using 5 mol% of the catalyst. Kinetic studies indicated zero-order kinetics in substrate concentration. Aminoalkenes bearing bulky geminal substituents in β-position to the amino group are more reactive and were rapidly converted at room temperature and 60°C. In addition, a six-membered ring cyclic imine was formed by using **174** as a catalyst. The reaction rate followed the order $5 > 6$, which is consistent with classical stereoelectronically controlled cyclization processes. Moderate enantioselectivities were obtained [120].

2.1.8 Bisoxazolinate Ligands

Bisoxazolinates are widely used ligands in main-group, transition, and rare-earth metal chemistry [131]. In general, bisoxazoline ligands with one carbon atom linking two oxazoline rings were the most frequently used (Scheme 66). The bidentate *N*,*N*-ligand system is similar to β-diketiminato ligands and exhibits a delocalized π-electron system. Bisoxazolinates **V** were generated by deprotonation of bisoxazolines **IV** (Scheme 66). The ligand framework incorporates stereogenic centers which are usually located on C_4 and (or) C_5 position, and thus chiral bisoxazolinate ligands can be generated. The corresponding chiral bisoxazolinate metal complexes are of particular importance for asymmetric catalysis. This section focuses on the synthesis of bisoxazolinate rare-earth metal complexes and their catalytic applications in polymerization and hydroamination reactions.

In 1999, Anwander et al. synthesized the first rare-earth metal complexes containing bisoxazolinate ligands [132]. Yttrium and lanthanum were chosen as examples for small and large rare-earth metal centers to show the high scope of the synthesis. Both types of complexes, mono-bisoxazolinates and bis-bisoxazolinates,

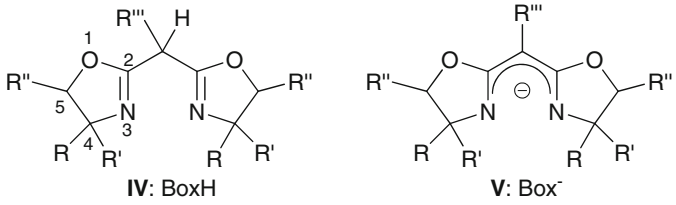

Scheme 66

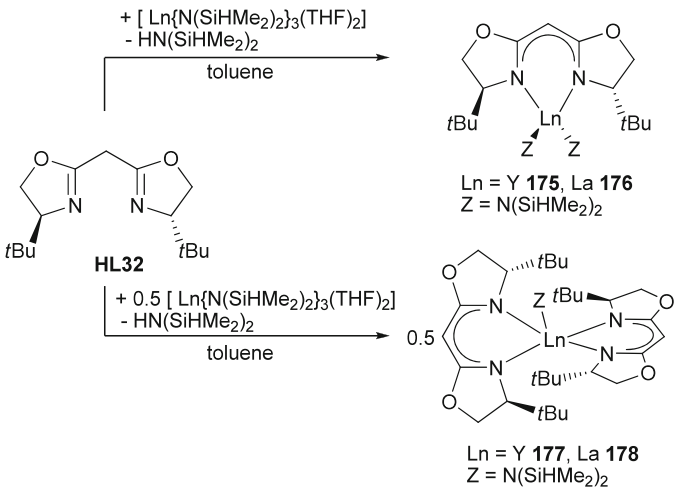

Scheme 67

were prepared by amine elimination shown in Scheme 67. The reaction of 1 equiv of bisoxazoline **HL32** with 1 equiv $[Ln\{N(SiHMe_2)_2\}_3(THF)_2]$ (Ln = Y, La) in toluene afforded mono-bisoxazolinate complexes **175** and **176**. The reaction of 2 equiv of bisoxazoline **HL32** with 1 equiv of $[Ln\{N(SiHMe_2)_2\}_3(THF)_2]$ (Ln = Y, La) in toluene led to bis-bisoxazolinates complexes **177** and **178**. Both types of complexes contained a chiral bisoxazolinate ligand as the spectator ligand and $N(SiHMe_2)_2^-$ ligand as the leaving group. Catalytic applications were investigated by Anwander et al. for heterogeneous catalysis [133]. **177** was grafted on mesoporous silica and used as a catalyst in the asymmetric hetero-Diels-Alder cyclization reaction.

In addition to bis-bisoxazolinate complexes **177** and **178**, chiral and nonchiral bis-bisoxazolinate rare-earth metal complexes were synthesized to investigate their catalytic activity for ROP of D,L-lactide and D,L-β-butyrolactone [134]. By using the same synthetic pathway as for compounds **177** and **178**, bis-bisoxazolinate complexes **179–182** were obtained via the amine elimination reactions of 2 equiv of the corresponding bisoxazolines **HL33–HL35** with 1 equiv of $[Ln\{N(SiHMe_2)_2\}_3(THF)_2]$ (Ln = Y, La) in benzene or toluene (Scheme 68).

All complexes **177–182** showed high catalytic activity in the ROP of D,L-lactide (Scheme 14) and D,L-β-butyrolactone (Scheme 69) [134]. The polymerization reactions proceeded at room temperature with turnover frequencies of up to $31,200\ h^{-1}$ and turnover numbers of up to 2,400. The reactions occurred in a controlled fashion, giving polymers with relatively narrow polydispersities (M_w/M_n = 1.08–1.44). However, the chiral bis-bisoxazolinate complexes did not lead to stereoselective products and only atactic polymers were produced.

In 2003, Marks et al. investigated the catalytic activity of various chiral bisoxazolinate rare-earth metal complexes in intramolecular hydroamination/cyclization reactions [135]. Several examples of bisoxazolines used in the

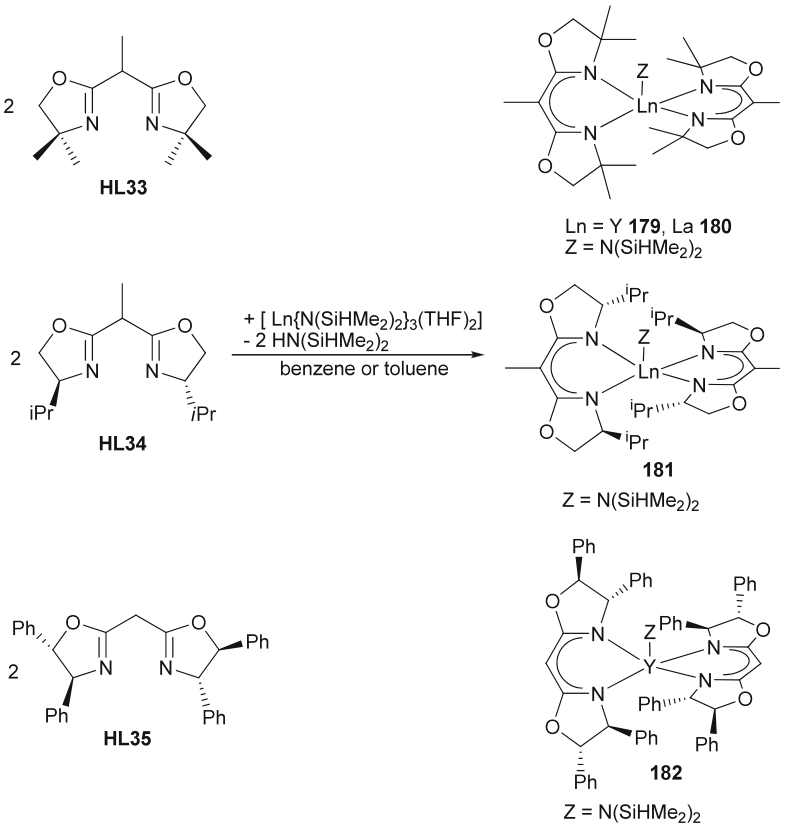

Scheme 68

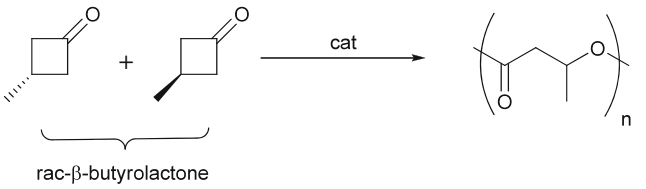

Scheme 69 Ring-opening polymerization of D,L-β-butyrolactone

catalytic screening study are shown in Scheme 70. The complexes were synthesized in situ in the NMR-scale reactions from the metal precursors $[Ln\{N(SiMe_3)_2\}_3]$ or $[Ln\{CH(SiMe_3)_2\}_3]$ (Ln = La, Nd, Sm, Y, Lu) and 1.2 equiv of the corresponding oxazolines **HL** in C_6D_6 (Scheme 70) and directly used in the catalytic study of hydroamination without isolation. The synthesis of samarium and lanthanum complexes **183** and **184** (Scheme 70) was monitored by ^1H NMR spectroscopy that showed the feasibility of the amine elimination route leading to mono-bisoxazolinate rare-earth metal complexes. The NMR results supported

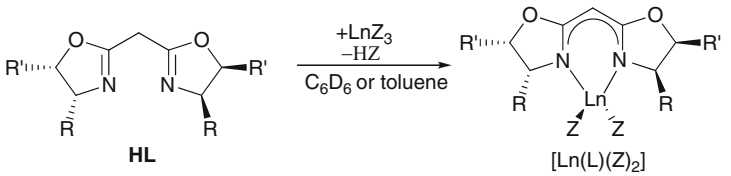

R = *S*-*t*Bu,R' = H *S*-**HL32**
R = *S*-*i*Pr,R' = H *S*-**HL34**
R = *S*-Ph,R' = *R*-Ph 4*R*,5*S*-**HL35**
R = *S*-Ph,R' = H
R = *S*-Ph,R' = Me_2
R = *S*-C_6H_4*t*Bu-4,R' = *R*-C_6H_4*t*Bu-4

Z = $N(SiMe_3)_2$, $CH(SiMe_3)_2$
Ln = La, Nd,Sm,Y, Lu
R,R' = alkyl, aryl, phenyl, H

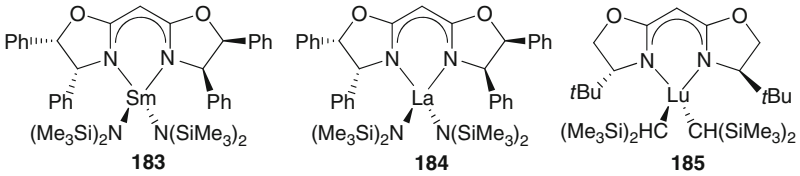

183 **184** **185**

Scheme 70

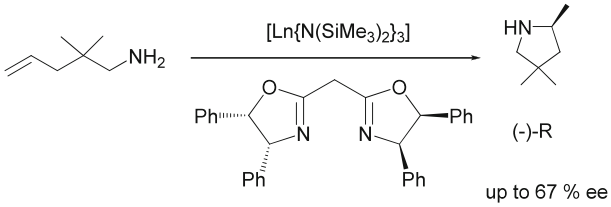

Scheme 71

the proposed structure of **183** and **184**, each coordinating one bisoxazolinate and two bistrimethylsilylamido ligands. Furthermore, to prove the proposed structure of the complexes, the lutetium complex **185** (Scheme 70) was characterized by X-ray diffraction. **185** was generated via alkane elimination by the treatment of $[Lu\{CH(SiMe_3)_2\}_3]$ with oxazoline **L32** in toluene. Single crystals were obtained by recrystallization from pentane and the solid state structure showed the expected mono-bisoxazolinate bis-alkyl complex **185**.

The catalytic activity of the chiral complexes [Ln(**L**)$\mathbf{Z}_2$] shown in Scheme 70 was investigated in NMR-scale intramolecular hydroamination/cyclization reactions [135]. The rate dependence on the ionic radii of the center metal was studied by using 5 mol% bisoxazoline **L32** and $[Ln\{N(SiMe_3)_2\}_3]$ as precatalysts and 2,2-dimethyl-4-penten-1-amine as substrate (Scheme 71). The reaction rate as well as the enantioselectivities increased with increasing radius of the center metal. Therefore, the lanthanum compound **184** was the most active catalyst among the investigated complexes.

Furthermore, a screening study of the different bisoxazolinate ligands **HL** rare-earth metal complexes was undertaken by using [La{N(SiMe$_3$)$_2$}$_3$] and various bisoxazolines as catalysts in cyclization reactions of substrate 2,2-dimethyl-4-penten-1-amine. It showed that aryl stereodirecting groups at C_4 position and additional substitutions at C_5 position of the oxazoline ring led to high turnover frequencies and good enantioselectivities. The best result was again obtained by using **184** as a catalyst. This reaction gave a turnover frequency of 25 h^{-1} and an enantiomeric excess of 67%. With increasing the amount of bisoxazoline ligand from one to two equivalents to form bis-bisoxazolinate complexes, the reaction rate of the catalysis decreased, while the enantiomeric excesses of the products were similar to those obtained with mono-bisoxazolinate complexes [Ln(L)Z$_2$]. The catalytic reaction scope was explored by using the optimized precatalyst **184** in the hydroamination reactions of various aminoalkenes and aminodienes in forming five- or six-membered ring products. All substrates were rapidly converted into the corresponding cyclic products at room temperature or 60°C. As expected, the aminoalkenes bearing bulky geminal substituents in β-position to the amino group were more reactive and showed higher turnover frequencies. No obvious correlation was found between the substrate steric bulk and the enantiomeric excesses of cyclization. Consistent with classical stereoelectronically controlled cyclization processes, the formation of the six-membered rings was slower than that of the five-membered rings. Kinetic studies of hydroamination of 2,2-dimethyl-4-penten-1-amine (Scheme 71) indicated zero-order in substrate concentration and first order in catalyst concentration, which is common in organolanthanide-catalyzed hydroamination/cyclization reactions. In summary, the chiral bisoxazolinate complex **184** showed high catalytic activity and enantioselectivities, comparable to or greater than those achieved with chiral organolanthanocene catalysts [136].

2.2 Dianionic Ligands

2.2.1 Diamide Ligands

N,*N*-Chelating diamide ligands are a group of dianionic ligands and they are formed by double deprotonation of diamines. The generic structure for a diamide ligand coordinated to a metal is shown in Scheme 72. The coordination of dianionic ligands may increase the electrophilicity of the metal center and create a different steric property in the complexes [137–142]. The electronic and steric properties of diamide ligands can be modified by variation of the bridging unit X and the R substituent of the amide. Due to the flexibility of the linking unit X, a large variety of diamide ligands and their metal complexes were prepared and characterized [139, 143–147]. Many diamide ligands introduced here are based on C_2 symmetric biphenyl and binaphthyl frameworks. The diamide metal complexes have been widely applied as catalysts for polymerization reactions and organic transformations [28, 142, 144, 146, 148, 149].

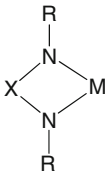

Scheme 72

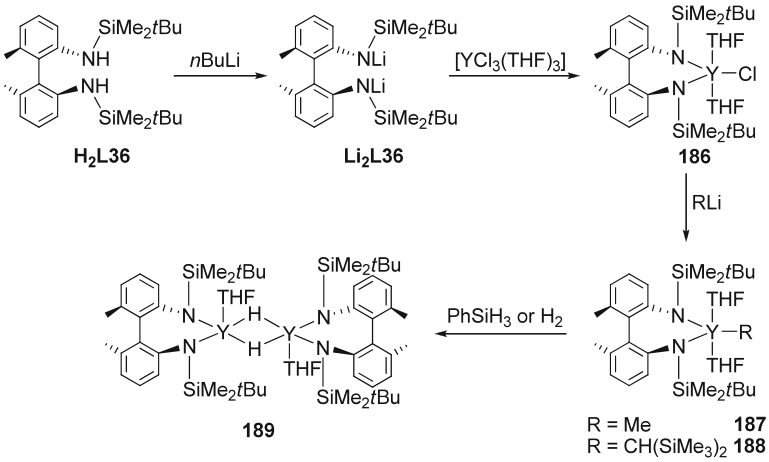

Scheme 73

Biaryl Diamides

In 1999, Gountchev and Tilley prepared a series of alkyl and hydride yttrium complexes containing an axially chiral bis(silylamido)biphenyl ligand **L36**. The lithium salt **Li$_2$L36** was obtained from the lithiation of the bis(silylamine)biphenyl with *n*BuLi. The reaction of **Li$_2$L36** and [YCl$_3$(THF)$_3$] in refluxing THF produced the yttrium chloride complex [Y(**L36**)Cl(THF)$_2$] (**186**). The reaction of **186** and LiR (R = Me or CH(SiMe$_3$)$_2$) led to alkylyttrium complexes [Y(**L36**)R(THF)$_2$] (R = Me (**187**) and CH(SiMe$_3$)$_2$ (**188**)). The dinuclear hydride complex [Y(THF)H(**L36**)]$_2$ (**189**) was obtained by exposure of **187** or **188** to H_2 gas or by the reaction of **187** or **188** with PhSiH$_3$ (Scheme 73). **187**–**189** showed lack of catalytic activity for the polymerization of ethylene or silane [150].

Although **187**–**189** were not active catalysts for polymerization process, **187** and **189** proved to be active olefin hydrosilylation catalysts, presumably **187** first reacted with a silane to form a reactive metal hydride species. They are the first examples of d^0 metal complexes with non-Cp ligands in the catalytic hydrosilylation of olefins. The mechanism was believed to be consistent with that of other d^0 metallocene-based catalysts and included two steps 1) fast olefin insertion into the metal hydride bond and 2) a slow metathesis reaction with the silane. The catalysts exhibited a high regioselective preference for terminal addition in the case of aliphatic olefins

and a lower preference for 2,1 addition in the case of aromatic olefins. When enantiomerically pure catalyst *S*-**187** was used in the hydrosilylation of norbornene, a remarkable 90% ee in favor of the (1*S*)-enantiomer was obtained [151].

In 1994, Marks and coworkers synthesized the lanthanide metallocene complexes as the first enantioselective catalysts for hydroamination [152]. After the simple lanthanide tris(amide) complexes $[Ln\{N(SiMe_3)_2\}_3]$ were discovered as efficient catalysts for hydroamination, Livinghouse and coworkers showed that the catalytic activity was dramatically increased by introducing a chelating diamide ligand to $[Ln\{N(SiMe_3)_2\}_3]$ [153]. Many rare-earth metal diamide complexes have been prepared and studied for hydroamination in particular [148, 154, 155]. $[Ln(diamide)\{N(SiMe_3)_2\}]$ were prepared via amine elimination in NMR tubes by reacting $[Ln\{N(SiMe_3)_2\}_3]$ with various diamines (Scheme 74). The resulting complexes were not isolated and their catalytic activity for the hydroamination of alkenes was screened. The study showed that 1) all modified diamide complexes exhibited higher catalytic activity than $[Ln\{N(SiMe_3)_2\}_3]$ and 2) the complexes supported by sterically hindered chelating diamides offered better catalytic activity and improved stereoselectivity in intramolecular alkene hydroamination (Scheme 43) [156–158].

In 2003, O'Shaughnessy and Scott reported the first example of rare-earth metal complexes supported by biaryl diamide ligands as the catalysts for the hydroamination reactions [159]. A series of C_2 symmetric secondary diamine proligands **L37–L40** were prepared by arylations of (*R*)-2,2′-diamino-6,6′-dimethybiphenyl under palladium catalysis. **L37** reacted with complexes $[Ln\{N(SiHMe_2)_2\}_3(THF)_2]$ to form the biaryl diamide complexes [Ln(**L37**) $\{N(SiHMe_2)_2\}(THF)_2]$ (Ln = Y (**190**), La (**191**), Sm (**192**)). Deprotonation

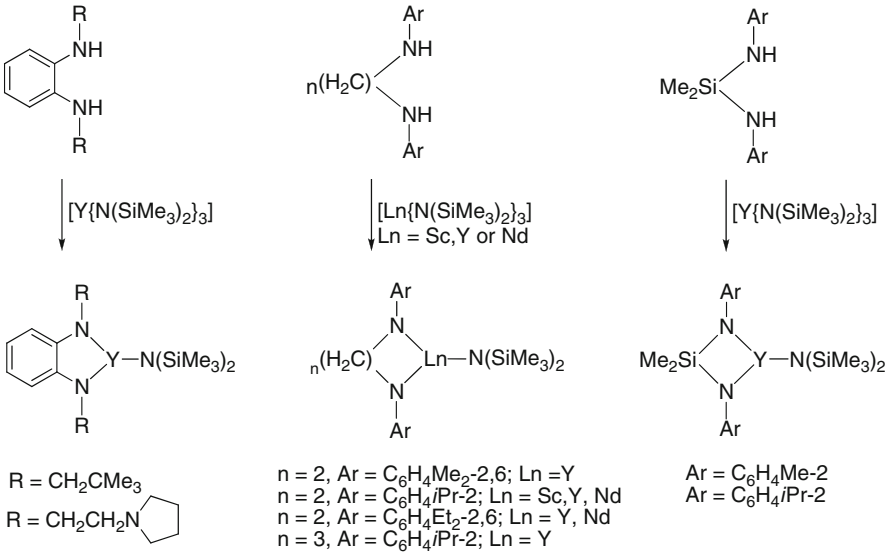

Scheme 74

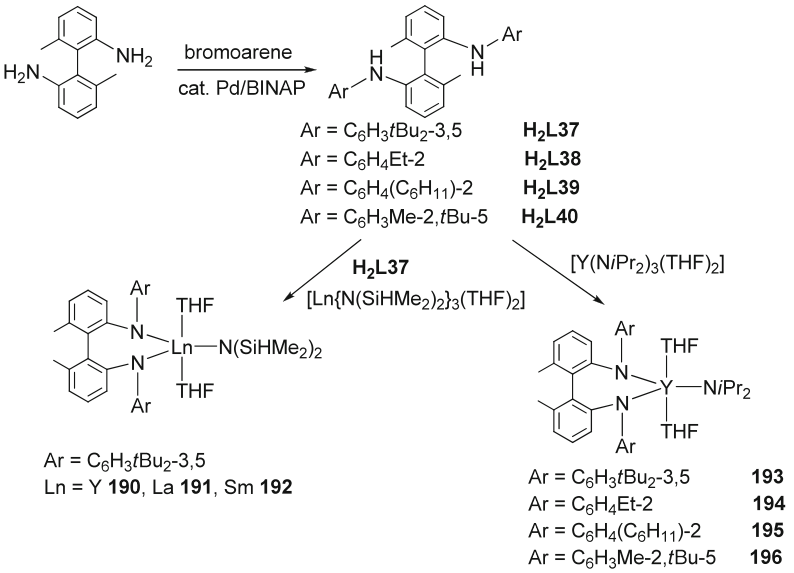

Scheme 75

of more sterically hindered ligands **L38–L40** proceeded very slowly with $[Ln\{N(SiHMe_2)_2\}_3(THF)_2]$. However, the reaction of the diamide ligands with alkylamide $[Y(NiPr_2)_3(THF)_2]$ conveniently led to the corresponding complexes $[Y(diamide)(NiPr_2)(THF)_2]$ (diamide = **L37–L40**, (**193**–**196**)) (Scheme 75). **193**–**196** were formed without isolation and directly tested as catalysts for hydroamination. None of above biaryl diamide complexes was structurally defined. All complexes catalyzed the cyclization of aminoalkene to completion with ee up to 50% with 3% catalyst loading. The reaction rate increased in the order of Y < Sm < La, while ee decreased in the same order. These results suggest that the metal ion with the largest radius shows the highest rate and its coordination sphere related to the chiral environment is the most difficult to control. The yttrium silylamide complex **190** was a significant slower catalyst than the yttrium alkylamide complex **193**. This result can be explained by the relative basicities difference between the leaving groups silylamide $[N(SiHMe_2)_2]^-$ and alkylamide $[NiPr_2]^-$. Given that the silylamides are expected to be more basic than the alkyl amides, the alkyl amides will be more easily protonated by the substrate at the first step of the catalytic cycle [159].

In the same year, the first structurally defined biaryl diamide complexes as enantioselective intramolecular hydroamination catalysts were reported by Schulz and coworkers. They are the first example of lanthanide catalysts supported by a binaphthyl diamide ligand. 2 equiv of the lithium salt of the binaphthyl diamide ligand $\mathbf{Li_2L41}$ and anhydrous $LnCl_3$ in THF at ambient temperature generated "ate" complexes $[Li(THF)_4][Ln(\mathbf{L41})_2]$ (Ln = Sm **197** and Yb **198**) via salt elimination (Scheme 76).

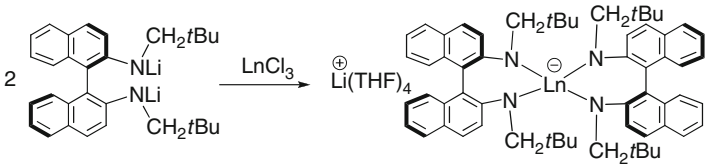

Scheme 76

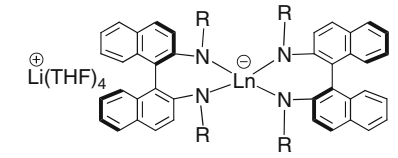

R = CH_2tBu	**L41**	Ln = Sm **197**,Yb **198**, Nd **199**, Lu **200**
R = CH_2iPr	**L42**	Ln = Yb **201**
R = CH_2Ph	**L43**	Ln = Yb **202**
R = *i*Pr	**L44**	Ln = Y **203**, Yb **204**
R = cyclohexyl	**L45**	Ln = Yb **205**, Lu **206**
R = Ph	**L46**	Ln = Y **207**
R = cyclopentyl	**L47**	Ln = Y **208**, Yb **209**

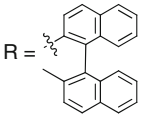

L48 Ln = Yb **210**

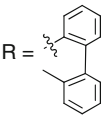

L49 Ln = Yb **211**

Scheme 77

Compared with [Sm{N(SiMe$_3$)$_2$}$_3$], **197** and **198** proved to be more efficient catalysts for the hydroamination of 1-(aminomethyl)-1-allylcyclohexane to produce a five-membered-ring cyclic amine (spiropyrrolidine) with an ee up to 53% (Scheme 52). **198** is a more active and selective catalyst than **197**.

Schulz and coworkers followed the same synthetic route shown in Scheme 76 and prepared a series of binaphthyl diamide ate complexes **199–211** (Scheme 77) by modifying the metal center or the substituent on the binaphthyl nitrogen atom [160–164]. All "ate" complexes have been investigated as the catalysts for hydroamination. With the exception of the yttrium complex **207** bearing phenyl groups on the nitrogen atom, all "ate" complexes were efficient catalysts for the asymmetric hydroamination of the aminopentene derivatives. The catalysts **197–201** supported by the same diamide ligand **L41** were studied for the metal center effect on the catalytic hydroamination of 1-(aminomethyl)-1-allylcyclohexane (Scheme 52). Ytterbium complex **198** was the most active and selective catalyst among them. The catalytic activity of ytterbium complexes bearing different diamide ligands demonstrated that

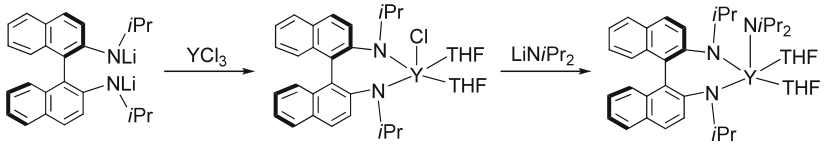

Li_2L44 212 213

Scheme 78

the more sterically hindered diamide complexes afforded higher enantioselectivity, but lower catalytic rate. In this series of complexes, the ytterbium complex **209** bearing diamide ligand **L47** exhibited the highest ee (up to 87%) for the hydroamination of 1-(aminomethyl)-1-allylcyclohexane, while the yttrium complex **208** bearing the same ligand was slightly more active. **210** and **211** with additional chiral moieties on the diamide ligands did not increase the ee of the transformation. The ytterbium complex **198** proved to be the most active catalyst of this series and even successfully catalyzed the hydroamination of aminopentenes with internal double bonds [148, 154, 160–164].

To understand the function of the ionic "ate" complexes in the catalytic hydroamination reactions, the neutral yttrium chloro complex **212** containing diamide ligand **L44** was prepared by the reaction of YCl_3 with 1 equiv of **Li_2L44** to compare with the "ate" complexes. The neutral yttrium amido complex **213** was obtained from reacting **212** with LiN*i*Pr_2 in THF (Scheme 78).

Complexes **213** and **203** bearing the same enantiopure binaphthyldiamide ligand were compared for the catalysis of several hydroamination reactions with various substrates. The comparison showed differences in activity and/or selectivity in two catalytic systems. The results indicate that different active species are involved. Both complexes produce pyrrolidines and piperidines with moderate to high enantioselectivity and their catalytic activity are comparable [162].

To optimize the enantioselectivity of the hydroamination reaction, the diamide ligand **L47** that supported the ytterbium complex **209** exhibiting the highest ee was selected for the preparation of ytterbium and yttrium alkyl complexes. The "ate" diamide alkyl lanthanide complexes [Ln(**L47**)(μ-Me)$_2$Li(THF)$_2$(μ-Me)Li(THF)] (Ln = Y (**214**), Yb (**215**)) and [Ln(**L47**)(μ-Me)$_2$Li(TMEDA)(μ-Me)Li(OEt$_2$)] (Ln = Y (**216**), Yb (**217**)) were prepared from a one-pot procedure of combining $LnCl_3$, diamine **H_2L47** and 4 equiv of MeLi in THF or Et_2O/TMEDA (Scheme 79). The neutral alkyl complexes [Ln(**L47**){CH_2SiMe_3}(THF)$_2$] (Ln = Y (**218**), Yb (**219**)) were obtained from the reaction of equimolar amount of **H_2L47** and isolated [Ln(CH_2SiMe_3)$_3$(THF)$_2$] or from a one-pot procedure of combining [$LnCl_3$(THF)$_{3.5}$], 3 equiv of Li(CH_2SiMe_3)$_3$, and **H_2L47** in hexane. [Y(**L47**){CH_2SiMe_3}(DME)] (**220**) was obtained from recrystallization of **218** in DME (Scheme 80) [165].

214–220 are the first examples of fully characterized alkyl amido neutral or anionic complexes that are prepared in a one-pot procedure from commercially available rare-earth metal halides, an alkyllithium reagent, and a chiral diamide

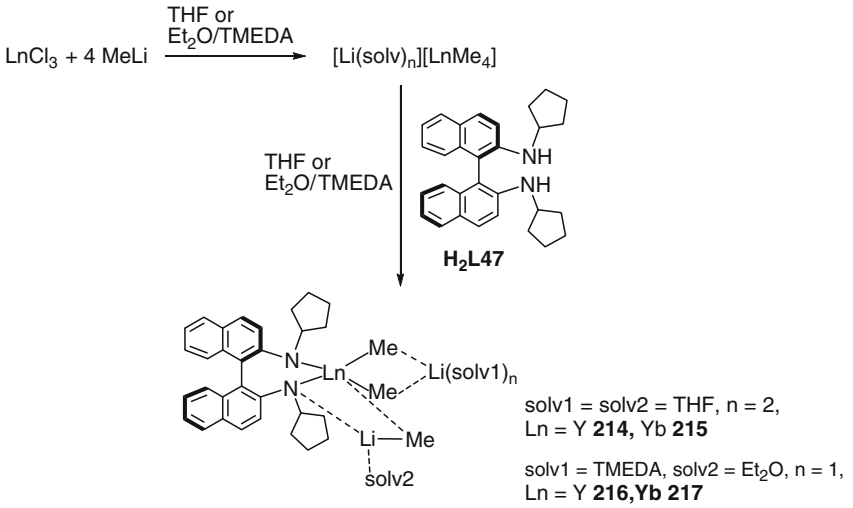

Scheme 79

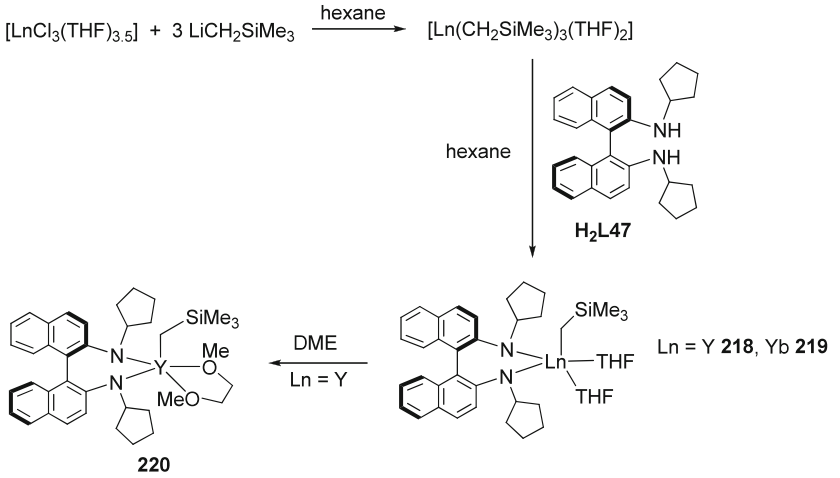

Scheme 80

ligand. All the complexes were proved to be highly active catalysts for the hydroamination of various substrates to form five- or six-membered rings. Up to 83% ee could be reached in producing 2,4,4-trimethylpyrrolidine (Scheme 71) by using ytterbium alkyl "ate" complex **215** as a catalyst. In both neutral and anionic cases, yttrium alkyl complexes are greatly more active but slightly less selective than ytterbium alkyl complexes. This might be a result of the lower stability of ytterbium alkyl precatalysts [165].

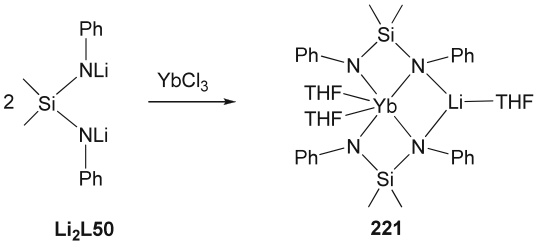

Li_2L50 **221**

Scheme 81

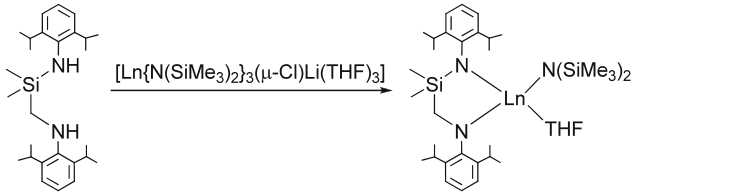

H_2L51 Ln = Y **222**, Nd **223**, Sm **224**, Dy **225**, and Yb **226**

Scheme 82

Silylene-Bridged Diamides

The lithium salt of the silylene-bridged diamide ligand **L50** reacted with $YbCl_3$ to form the "ate" diamide complex [Yb(**L50**)$_2$(THF)$_2$Li(THF)] (**221**) (Scheme 81). This complex showed moderate catalytic activity for the polymerization of MMA at room temperature. Syndiotactic-rich polymers with high molecular weights ($M_n > 10^4$) and relatively narrow molecular weight distributions ($M_w/M_n = 1.45$) were obtained (Scheme 12) [166].

Wu and coworkers prepared a new diamide ligand **L51** with a CH_2SiMe_2 bridging unit and a series of rare-earth metal complexes supported by **L51**. Diamide complexes [Ln(**L51**){N(SiMe$_3$)$_2$}(THF)] (Ln = Y (**222**), Nd (**223**), Sm (**224**), Dy (**225**), Yb (**226**)) were obtained from the reaction of **H_2L51** with 1 equiv of corresponding rare-earth metal amide complexes [Ln{N(SiMe$_3$)$_2$}$_3$(μ-Cl)Li(THF)$_3$] in toluene (Scheme 82) [167].

The complexes **222–226** exhibited a high catalytic activity on the cyclotrimerization of aromatic isocyanates to produce triaryl isocyanurates (Scheme 83). They are the first reported Cp-free rare-earth metal complexes showing high activity and selectivity on the cyclotrimerization of aryl isocyanates. For comparison, the starting trisamide complex [Yb{N(SiMe$_3$)$_2$}$_3$(μ-Cl)Li(THF)$_3$] was studied for the catalysis and showed a catalytic activity comparable with those of the new complexes **222–226**. All the complexes showed no catalytic activity on the cyclotrimerization of 4-nitrophenylisocyanate and exhibited a relatively low catalytic activity on the cyclotrimerization of aliphatic isocyanates [167].

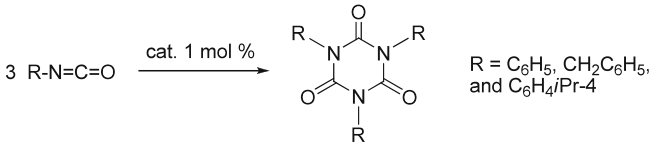

Scheme 83

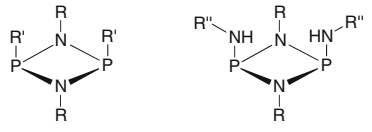

Scheme 84

Bis(amido)cyclodiphosph(III)azane Ligands

Substituted cyclodiphosph(III)azanes are well established as ligands in main-group [168–170] and transition-metal chemistry [171, 172]. Cyclodiphosph(III)azanes are usually synthesized by the reaction of PCl_3 with an excess of the corresponding amine to give chlorocyclodiphosph(III)azanes $[RNPCl]_2$ (R = alkyl, aryl) [173]. The chlorine atoms can be replaced by various alkoxy, arylalkoxy, alkyl, and amino substituents (R′) leading to $[RNPR']_2$ (**I**) shown in Scheme 84 [168, 171, 174]. The amino-substituted cyclodiphosph(III)azanes **II** (Scheme 84) can be deprotonated twice to give bis(amido)cyclodiphosph(III)azanes which are known as dianionic bidentate ligands in main-group [170] and early-transition-metal chemistry [175–180]. Recently, a bis(amido)cyclodiphosph(III)azane was introduced to rare-earth metal chemistry by our group and the first cyclodiphosph(III)azane complexes of yttrium and the lanthanides have been synthesized [181].

The dilithium salt **Li_2L52** was used as a ligand transfer reagent for the dianionic *cis*-bis(amido)cyclodiphosph(III)azane ligand. **Li_2L52** was easily accessed by the treatment of *cis*-bis(amino)cyclodiphosph(III)azane **H_2L52** with 2 equiv of *n*BuLi in THF (Scheme 85) [168].

The reaction of **Li_2L52** with anhydrous $LnCl_3$ in THF led to "ate" complexes with occluded lithium chloride. In rare-earth metal chemistry, potassium salts of the ligands are used to avoid the formation of "ate" complexes. Unfortunately, the attempts to generate the dipotassium salt of **L52** failed. To obtain the neutral chloro complexes **227–230**, the in situ generated "ate" complexes were heated in toluene to extrude lithium chloride (Scheme 86).

Neodymium-based Ziegler–Natta systems play a major role in the industrial polymerization of 1,3-butadiene to poly-*cis*-1,4-butadiene [182–184]. Therefore, the catalytic activity of the neodymium complex **229** was investigated for the polymerization of 1,3-butadiene [181]. The observed catalytic

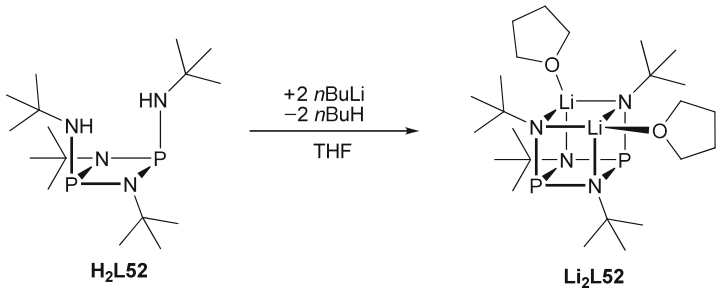

Scheme 85

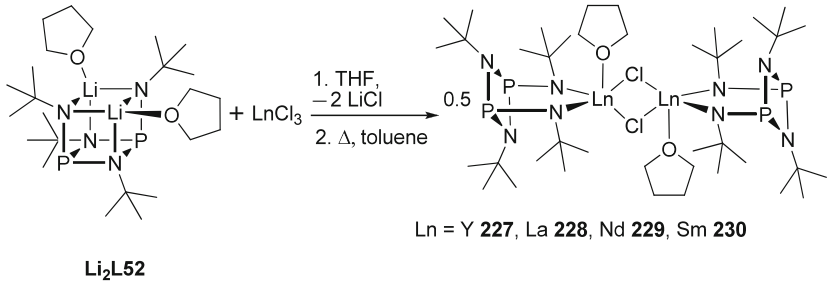

Scheme 86

activity was strongly dependent on the nature of the cocatalyst. **229** and cocatalyst mixtures of $AlEt_3/B(C_6F_5)_3$ (7200:96), $AlMe_3/B(C_6F_5)_3$ (7200:96), $AlEt_3/[Ph_3C][B(C_6F_5)_4]$ (7200:96), or $AlEt_3/[PhNMe_2H][B(C_6F_5)_4]$ (7200:86) showed low activity and resulted in low yields. For these runs, the microstructure of the products was not established. By using modified methylalumoxane comprised of trimethylaluminium and triisobutylaluminium (MMAO-3A) as the cocatalyst, the catalytic system showed very high activity and resulted in a *cis*-selectivity of 94%. The best result for the catalytic activity of **229** was obtained with a mixture of $AlMe_3/[R_2(Ph)NH][B(C_6F_5)_4]$ (R = octadecyl) (7.2:93.2) as the cocatalyst. A very high turnover rate and a *cis*-selectivity of 93% were observed and polymers with high molecular masses and moderate polydispersities were obtained.

3 Conclusions

Within the past 10 years, several classes of postmetallocenes of the lanthanides, especially the monoanionic amido metal complexes, were developed as homogeneous catalysts. These compounds were basically used in two fields, C–C multibond transformations and the polymerization catalysis. In the area of multibond transformations, the hydroamination and the hydrosilylation reaction were most intensely

studied, whereas in the area of polymerization butadiene and isoprene, ethylene, as well as lactides and lactones were mostly used as monomers. This review was focused on the synthesis of the catalysts. Other chapters within this book are reviewing the mentioned catalytic transformations in more detail. In general, lanthanide catalysts combine several favorable features, which are high catalytic activities and in some cases also high selectivities. In comparison to the well-established platinum metal catalysts, lanthanide-based systems are less expensive and show a low toxicity, which makes them applicable for drug synthesis. As result of the lanthanide contraction, the 4f-elements catalysts have the unique property in the periodic chart to be optimized by tuning the ion radius without altering the ligand sphere or the reaction conditions.

Based on the present development, we expect that the rapid development of new postmetallocene catalysts of the lanthanides will continue in the near future.

Acknowledgment We thank the DFG (SPP 1166 "Lanthanide specific functionalities in molecules and materials") for financial support of our work related to the topic of this contribution.

References

1. Watson PL, Parshall GW (2002) Acc Chem Res 18:51
2. Edelmann FT (1996) Top Curr Chem 179:113
3. Evans WJ, Bloom I, Hunter WE, Atwood JL (1983) J Am Chem Soc 103:1401
4. Jeske G, Lauke H, Mauermann H, Schumann H, Marks TJ (1985) J Am Chem Soc 107:8111
5. Harrison KN, Marks TJ (1992) J Am Chem Soc 114:9220
6. Bijpost EA, Duchateau R, Teuben JH (1995) J Mol Catal 95:121
7. Gagné MR, Marks TJ (2002) J Am Chem Soc 111:4108
8. Arredondo VM, McDonald FE, Marks TJ (1998) J Am Chem Soc 120:4871
9. Fu P-F, Brard L, Li Y, Marks TJ (2002) J Am Chem Soc 117:7157
10. Castillo I, Tilley TD (2000) Organometallics 19:4733
11. Molander GA, Winterfeld J (1996) J Organomet Chem 524:275
12. Schumann H, Keitsch MR, Winterfeld J, Mühle S, Molander GA (1998) J Organomet Chem 559:181
13. Edelmann FT (2007) In: Crabtree RH, Mingos DMP (eds) Comprehensive organometallic chemisty III, Pergamon, Oxford
14. Schumann H (1984) Angew Chem Int Ed 96:475
15. Edelmann FT (1996) Top Curr Chem 179:247
16. Edelmann FT (1995) Angew Chem Int Ed 34:2466
17. Edelmann FT, Freckmann DMM, Schumann H (2002) Chem Rev 102:1851
18. Bryliakov KP (2007) Russ Chem Rev 76:253
19. Busico V, Cipullo R, Romanelli V, Ronca S, Togrou M (2005) J Am Chem Soc 127:1608
20. Trifonov AA, Skvortsov GG, Lyubov DM, Skorodumova NA, Fukin GK, Baranov EV, Glushakova VN (2006) Chem Eur J 12:5320
21. Britovsek GJP, Gibson VC, Wass DF (1999) Angew Chem Int Ed 38:428
22. Bradley DC, Ghotra JS, Hart FA (1973) J Chem Soc Dalton Trans 1021
23. Bradley DC, Ghotra JS, Hart FA (1972) J Chem Soc Chem Commun 349
24. Alyea EC, Bradley DC, Copperthwaite RG (1972) J Chem Soc Dalton Trans 1580
25. Edelmann FT (2008) Adv Organomet Chem 57:183
26. Edelmann FT (2009) Chem Soc Rev 38:2253

27. Kempe R (2000) Angew Chem Int Ed 39:468
28. Piers WE, Emslie DJH (2002) Coord Chem Rev 233–234:131
29. Kempe R, Noss H, Irrgang T (2002) J Organomet Chem 647:12
30. Kempe R, Oberthür M, Hillebrand G, Spannenberg A, Fuhrmann H (1998) Polimery (Warsaw) 43:96
31. Schareina T, Kempe R (2002) Synth Methods Organomet Inorg Chem 10:1
32. Kempe R (2003) Eur J Inorg Chem 791
33. Deeken S, Motz G, Kempe R (2007) Z Anorg Allg Chem 633:320
34. Spannenberg A, Arndt P, Kempe R (1998) Angew Chem Int Ed 37:832
35. Glatz G, Demeshko S, Motz G, Kempe R (2009) Eur J Inorg Chem: 1385
36. Baldamus J, Cole ML, Helmstedt U, Hey-Hawkins E-M, Jones C, Junk PC, Lange F, Smithies NA (2003) J Organomet Chem 665:33
37. Cole ML, Junk PC (2003) New J Chem 27:1032
38. Scott NM, Schareina T, Tok O, Kempe R (2004) Eur J Inorg Chem: 3297
39. Scott NM, Kempe R (2005) Eur J Inorg Chem: 1319
40. Kretschmer WP, Meetsma A, Hessen B, Schmalz T, Qayyum S, Kempe R (2006) Chem Eur J 12:8969
41. Döring C, Kempe R (2009) Eur J Inorg Chem: 412
42. Skvortsov GG, Fukin GK, Trifonov AA, Noor A, Döring C, Kempe R (2007) Organometallics 26:5770
43. Guillaume SM, Schappacher M, Scott NM, Kempe R (2007) J Polym Sci A Polym Chem 45:3611
44. Kretschmer WP, Meetsma A, Hessen B, Scott NM, Qayyum S, Kempe R (2006) Z Anorg Allg Chem 632:1936
45. Mashima K, Tsurugi H (2005) J Organomet Chem 690:4414
46. Matsuo Y, Mashima K, Tani K (2001) Organometallics 20:3510
47. Cui C, Shafir A, Reeder CL, Arnold J (2003) Organometallics 22:3357
48. Yang Y, Li S, Cui D, Chen X, Jing X (2007) Organometallics 26:671
49. Yang Y, Liu B, Lv K, Gao W, Cui D, Chen X, Jing X (2007) Organometallics 26:4575
50. Yang Y, Wang Q, Cui D (2008) J Polym Sci A Polym Chem 46:5251
51. Hayes PG, Welch GC, Emslie DJH, Noack CL, Piers WE, Parvez M (2003) Organometallics 22:1577
52. Conroy KD, Piers WE, Parvez M (2008) J Organomet Chem 693:834
53. Liu B, Cui D, Ma J, Chen X, Jing X (2007) Chem Eur J 13:834
54. Wang D, Li S, Liu X, Gao W, Cui D (2008) Organometallics 27:6531
55. Bourget-Merle L, Lappert MF, Severn JR (2002) Chem Rev 102:3031
56. Hitchcock PB, Khvostov AV, Lappert MF, Protchenko AV (2009) Dalton Trans 2383
57. Hitchcock PB, Hulkes AG, Khvostov AV, Lappert MF, Protchenko AV (2003) Spec Publ R Soc Chem 287:86
58. Lappert MF (2000) J Organomet Chem 600:144
59. Hitchcock PB, Hu J, Lappert MF, Layh M, Liu D-S, Severn JR, Shun T (1996) An Quim Int Ed 92:186
60. Zeimentz PM, Arndt S, Elvidge BR, Okuda J (2006) Chem Rev 106:2404
61. Arndt S, Okuda J (2005) Adv Synth Catal 347:339
62. Cassani CM, Gun'ko YK, Hitchcock PB, Hulkes AG, Khvostov AV, Lappert MF, Protchenko AV (2002) J Organomet Chem 647:71
63. Hitchcock PB, Holmes SA, Lappert MF, Tian S (1994) J Chem Soc Chem Commun 2691
64. Drees D, Magull J (1994) Z Anorg Allg Chem 620:814
65. Hitchcock PB, Lappert MF, Tian S (1997) J Chem Soc Dalton Trans 1945
66. Avent AG, Hitchcock PB, Khvostov AV, Lappert MF, Protchenko AV (2003) Dalton Trans 1070
67. Drees D, Magull J (1995) Z Anorg Allg Chem 621:948
68. Rahim M, Taylor NJ, Xin S, Collins S (1998) Organometallics 17:1315
69. Vollmerhaus R, Rahim M, Tomaszewski R, Xin S, Taylor NJ, Collins S (2000) Organometallics 19:2161

70. Moore DR, Cheng M, Lobkovsky EB, Coates GW (2002) Angew Chem Int Ed 41:2599
71. Vitanova DV, Hampel F, Hultzsch KC (2005) J Organomet Chem 690:5182
72. Lazarov BB, Hampel F, Hultzsch KC (2007) Z Anorg Allg Chem 633:2367
73. Zhang Z, Cui D, Liu X (2008) J Polym Sci A Polym Chem 46:6810
74. Xue M, Yao Y, Shen Q, Zhang Y (2005) J Organomet Chem 690:4685
75. Yao Y, Zhang Y, Shen Q, Yu K (2002) Organometallics 21:819
76. Yao Y, Zhang Z, Peng H, Zhang Y, Shen Q, Lin J (2006) Inorg Chem 45:2175
77. Sanchez-Barba LF, Hughes DL, Humphrey SM, Bochmann M (2005) Organometallics 24:3792
78. Wei X, Cheng Y, Hitchcock PB, Lappert MF (2008) Dalton Trans 5235
79. Hitchcock PB, Lappert MF, Protchenko AV (2005) Chem Commun 951
80. Lee LWM, Piers WE, Elsegood MRJ, Clegg W, Parvez M (1999) Organometallics 18:2947
81. Hayes PG, Piers WE, McDonald R (2002) J Am Chem Soc 124:2132
82. Lauterwasser F, Hayes PG, Bräse S, Piers WE, Schafer LL (2004) Organometallics 23:2234
83. Hayes PG, Piers WE, Parvez M (2005) Organometallics 24:1173
84. Hayes PG, Piers WE, Parvez M (2003) J Am Chem Soc 125:5622
85. Hayes PG, Piers WE, Parvez M (2007) Chem Eur J 13:2632
86. Xue M, Jiao R, Zhang Y, Yao Y, Shen Q (2009) Eur J Inorg Chem 4110
87. Gamer MT, Canseco-Melchor G, Roesky PW (2003) Z Anorg Allg Chem 629:2113
88. Gamer MT, Roesky PW (2004) Inorg Chem 43:4903
89. Roesky PW, Gamer MT, Marinos N (2004) Chem Eur J 10:3537
90. Roesky PW, Gamer MT, Puchner M, Greiner A (2002) Chem Eur J 8:5265
91. Recknagel A, Steiner A, Noltemeyer M, Brooker S, Stalke D, Edelmann FT (1991) J Organomet Chem 414:327
92. Reißmann U, Poremba P, Noltemeyer M, Schmidt H-G, Edelmann FT (2000) Inorg Chim Acta 303:156
93. Wetzel TG, Dehnen S, Roesky PW (1999) Angew Chem 111:1155
94. Wingerter S, Pfeiffer M, Baier F, Stey T, Stalke D (2000) Z Anorg Allg Chem 626:1121
95. Panda TK, Zulys A, Gamer MT, Roesky PW (2005) J Organomet Chem 690:5078
96. Panda TK, Zulys A, Gamer MT, Roesky PW (2005) Organometallics 24:2197
97. Roesky PW (2006) Z Anorg Allg Chem 632:1918
98. Wiecko M, Roesky PW, Burlakov VV, Spannenberg A (2007) Eur J Inorg Chem 876
99. Gamer MT, Rastätter M, Roesky PW, Steffens A, Glanz M (2005) Chem Eur J 11:3165
100. Aparna K, Ferguson M, Cavell RG (2000) J Am Chem Soc 122:726
101. Cavell RG, Kamalesh Babu RP, Aparna K (2001) J Organomet Chem 617–618:158
102. Panda TK, Roesky PW (2009) Chem Soc Rev 38:2782
103. Gamer MT, Roesky PW (2001) Z Anorg Allg Chem 627:877
104. Gamer MT, Dehnen S, Roesky PW (2001) Organometallics 20:4230
105. Rastätter M, Zulys A, Roesky PW (2006) Chem Commun 874
106. Rastätter M, Zulys A, Roesky PW (2007) Chem Eur J 13:3606
107. Anwander R, Runte O, Eppinger J, Gerstberger G, Herdtweck E, Spiegler M (1998) J Chem Soc, Dalton Trans 847
108. Giardello MA, Conticello VP, Brard L, Gagné MR, Marks TJ (1994) J Am Chem Soc 116:10241
109. Mashima K, Nakayama Y, Nakamura A, Kanehisa N, Kai Y, Takaya H (1994) J Organomet Chem 473:85
110. Hong S, Marks TJ (2004) Acc Chem. Res 37:673
111. Gröb T, Seybert G, Massa W, Weller F, Palaniswami R, Greiner A, Dehnicke K (2000) Angew Chem 112:4542
112. Ravi P, Gröb T, Dehnicke K, Greiner A (2001) Macromolecules 34:8649
113. Evans WJ, Katsumata H (1994) Macromolecules 27:2330
114. Agarwal S, Brandukova-Szmikowski NE, Greiner A (1999) Macromol Rap Commun 20:274
115. Cui D, Tang T, Cheng J, Hu N, Chen W, Huang B (2002) J Organomet Chem 650:84
116. Gagné MR, Nolan SP, Marks TJ (1990) Organometallics 9:1716
117. Roesky PW (1997) Chem Ber/Recl 130:859

118. Roesky PW (2000) Chem Soc Rev 29:335
119. Roesky PW (2003) Z Anorg Allg Chem 629:1881
120. Meyer N, Zulys A, Roesky PW (2006) Organometallics 25:4179
121. Meyer N, Roesky PW (2007) Dalton Trans 2652
122. Meyer N, Roesky PW (2009) Organometallics 28:306
123. Franz KJ, Doerrer LH, Spingler B, Lippard SJ (2001) Inorg Chem 40:3774
124. Franz KJ, Lippard SJ (2000) Inorg Chem 39:3722
125. Franz KJ, Lippard SJ (1998) J Am Chem Soc 120:9034
126. Bürgstein MR, Berberich H, Roesky PW (1998) Organometallics 17:1452
127. Den Haan KH, De Boer JL, Teuben JH, Spek AL, Kojic-Prodic B, Hays GR, Huis R (1986) Organometallics 5:1726
128. Gagné MR, Stern CL, Marks TJ (1992) J Am Chem Soc 114:275
129. Datta S, Gamer MT, Roesky PW (2008) Organometallics 27:1207
130. Datta S, Roesky PW, Blechert S (2007) Organometallics 26:4392
131. Dagorne S, Bellemin-Laponnaz S, Maisse-François A (2007) Eur J Inorg Chem 913
132. Görlitzer HW, Spiegler M, Anwander R (1999) J Chem Soc, Dalton Trans 4287
133. Gerstberger G, Anwander R (2001) Microporous Mesoporous Mater 44–45:303
134. Alaaeddine A, Amgoune A, Thomas CM, Dagorne S, Bellemin-Laponnaz S, Carpentier J-F (2006) Eur J Inorg Chem 3652
135. Hong S, Tian S, Metz MV, Marks TJ (2003) J Am Chem Soc 125:14768
136. Gagné MR, Brard L, Conticello VP, Giardello MA, Stern CL, Marks TJ (1992) Organometallics 11:2003
137. van der Linden A, Schaverien CJ, Meijboom N, Ganter C, Orpen AG (1995) J Am Chem Soc 117:3008
138. Duchateau R, van Wee CT, Teuben JH (1996) Organometallics 15:2291
139. Duchateau R, van Wee CT, Meetsma A, van Duijnen PT, Teuben JH (1996) Organometallics 15:2279
140. Duchateau R, Tuinstra T, Brussee EAC, Meetsma A, van Duijnen PT, Teuben JH (1997) Organometallics 16:3511
141. Duchateau R, Brussee EAC, Meetsma A, Teuben JH (1997) Organometallics 16:5506
142. Baumann R, Davis WM, Schrock RR (1997) J Am Chem Soc 119:3830
143. Scollard JD, McConville DH, Vittal JJ (1995) Organometallics 14:5478
144. Scollard JD, McConville DH, Payne NC, Vittal JJ (1996) Macromolecules 29:5241
145. Long DP, Bianconi PA (1996) J Am Chem Soc 118:12453
146. Horton AD, de With J, van der Linden AJ, van de Weg H (1996) Organometallics 15:2672
147. Guerin F, McConville DH, Payne NC (1996) Organometallics 15:5085
148. Zi G (2009) Dalton Trans 9101
149. Konkol M, Okuda J (2008) Coord Chem Rev 252:1577
150. Gountchev TI, Tilley TD (1999) Organometallics 18:2896
151. Gountchev TI, Tilley TD (1999) Organometallics 18:5661
152. Giardello MA, Conticello VP, Brard L, Sabat M, Rheingold AL, Stern CL, Marks TJ (1994) J Am Chem Soc 116:10212
153. Kim YK, Livinghouse T, Bercaw JE (2001) Tetrahedron Lett 42:2933
154. Aillaud I, Collin J, Hannedouche J, Schulz E (2007) Dalton Trans 5105
155. Hultzsch KC (2005) Org Biomol Chem 3:1819
156. Kim H, Livinghouse T, Shim JH, Lee SG, Lee PH (2006) Adv Synth Catal 348:701
157. Kim JY, Livinghouse T (2005) Org Lett 7:4391
158. Kim YK, Livinghouse T (2002) Angew Chem, Int Ed 41:3645
159. O'Shaughnessy PN, Scott P (2003) Tetrahedron Asymmetry 14:1979
160. Aillaud I, Wright K, Collin J, Schulz E, Mazaleyrat J-P (2008) Tetrahedron Asymmetry 19:82
161. Aillaud I, Collin J, Duhayon C, Guillot R, Lyubov D, Schulz E, Trifonov A (2008) Chem Eur J 14:2189
162. Riegert D, Collin J, Daran J-C, Fillebeen T, Schulz E, Lyubov D, Fukin G, Trifonov A (2007) Eur J Inorg Chem 1159

163. Riegert D, Collin J, Meddour A, Schulz E, Trifonov A (2006) J Org Chem 71:2514
164. Collin J, Daran J-C, Jacquet O, Schulz E, Trifonov A (2005) Chem Eur J 11:3455
165. Aillaud I, Lyubov D, Collin J, Guillot R, Hannedouche J, Schulz E, Trifonov A (2008) Organometallics 27:5929
166. Zhou L, Yao Y, Li C, Zhang Y, Shen Q (2006) Organometallics 25:2880
167. Wu Y, Wang S, Zhu X, Yang G, Wei Y, Zhang L, Song H-b (2008) Inorg Chem 47:5503
168. Schranz I, Stahl L, Staples RJ (1998) Inorg Chem 37:1493
169. Schranz I, Moser DF, Stahl L, Staples RJ (1999) Inorg Chem 38:5814
170. Stahl L (2000) Coord Chem Rev 210:203
171. Balakrishna MS, Reddy VS, Krishnamurthy SS, Nixon JF, Burckett St Laurent JCTR (1994) Coord Chem Rev 129:1
172. Balakrishna MS, Chandrasekaran P, Venkateswaran R (2007) J Organomet Chem 692:2642
173. Holmes RR (1961) J Am Chem Soc 83:1334
174. Hill TG, Haltiwanger RC, Thompson ML, Katz SA, Norman AD (1994) Inorg Chem 33:1770
175. Grocholl L, Stahl L, Staples RJ (1997) Chem Commun 1465
176. Moser DF, Carrow CJ, Stahl L, Staples RJ (2001) J Chem Soc, Dalton Trans 1246
177. Axenov KV, Klinga M, Leskela M, Repo T (2005) Organometallics 24:1336
178. Axenov KV, Klinga M, Leskelae M, Kotov V, Repo T (2004) Eur J Inorg Chem 4702
179. Axenov KV, Kotov VV, Klinga M, Leskelae M, Repo T (2004) Eur J Inorg Chem 695
180. Moser DF, Grocholl L, Stahl L, Staples RJ (2003) Dalton Trans 1402
181. Rastätter M, Muterle RB, Roesky PW, Thiele SK-H (2009) Chem Eur J 15:474
182. Taube R, Sylvester G (1996) In: Cornils B, Herrmann WA (eds) Applied homogeneous catalysis with organometallic compounds, VCH, Weinheim, Germany, p 280
183. Wilson DJ (1996) Polym Int 39:235
184. Witte J (1981) Angew Makromol Chem 94:119

Index